PB92-143064

REPORT NO.
UCB/EERC-89/09
SEPTEMBER 1989

EARTHQUAKE ENGINEERING RESEARCH CENTER

FEASIBILITY AND PERFORMANCE STUDIES ON IMPROVING THE EARTHQUAKE RESISTANCE OF NEW AND EXISTING BUILDINGS USING THE FRICTION PENDULUM SYSTEM

by

VICTOR ZAYAS
STANLEY LOW
LUIS BOZZO
STEPHEN MAHIN

Report to the National Science Foundation

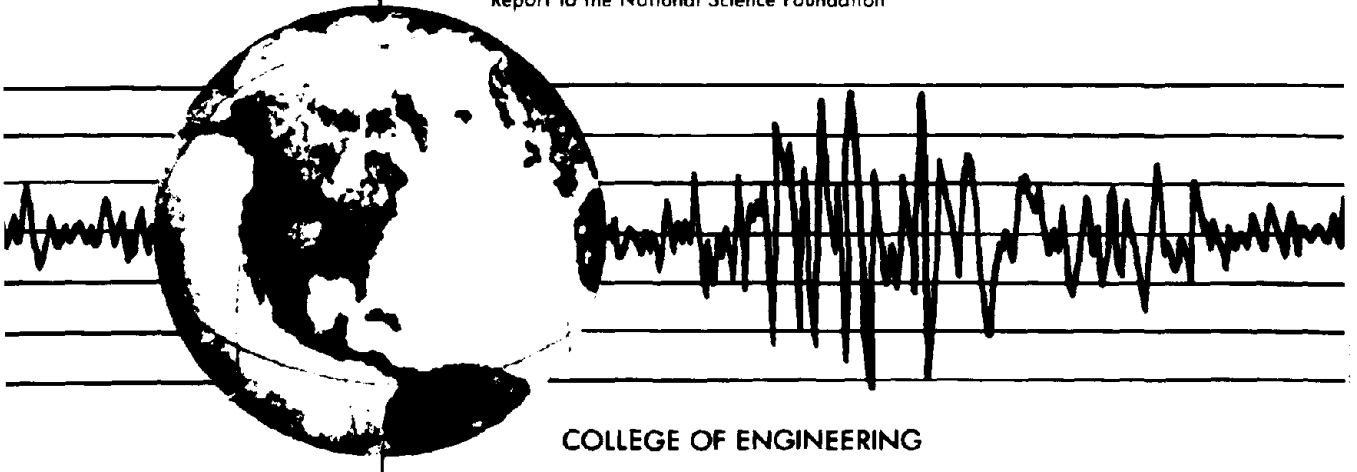

COLLEGE OF ENGINEERING

UNIVERSITY OF CALIFORNIA AT BERKELEY

For sale by the National Technical Information Service, U.S. Department of Commerce, Springfield, Virginia 22161

See back of report for up to date listing of EERC reports.

50272-101

REPORT DOCUMENTATION PAGE	1. REPORT NO. NSF/ENG-89026	2.	3. PB92-143064

4. Title and Subtitle
Feasibility and Performance Studies on Improving the Earthquake Resistance of New and Existing Buildings Using the Friction Pendulum System

5. Report Date
September 1989

6.

7. Author(s)
V. Zayas, S. Low, L. Bozzo, S. Mahin

8. Performing Organization Rept. No.
UCB/EERC-89/09

9. Performing Organization Name and Address
Earthquake Engineering Research Center
University of California, Berkeley
1301 S 46th St.
Richmond, CA 94804

10. Project/Task/Work Unit No.

11. Contract(C) or Grant(G) No.
(C)
(G) ISI-8860953

12. Sponsoring Organization Name and Address
National Science Foundation
1800 G. St. NW
Washington, DC 20550

13. Type of Report & Period Covered

14.

15. Supplementary Notes

16. Abstract (Limit: 200 words) The Friction Pendulum System (FPS) is an innovative technique for improving the earthquake resistance of buildings, which uses steel connections to isolate seismically a building by means of small amplitude pendulum motions. The anticipated seismic performance of building structures using the FPS steel connections was investigated analytically and experimentally. Buildings designed to have approximately equivalent construction costs as conventional building designs were studied. The earthquake responses of the FPS supported buildings were compared with those of conventional code design.

The FPS was assessed to be feasible and cost effective for improving the seismic resistance of new buildings. The flexibility to select any isolator period makes the approach suitable for a wide range of applications. The compact size and high strength of the FPS isolators permit a versatility in installation details that helps to achieve construction which is cost equivalent to non-isolated buildings, yet provides substantially improved seismic resistance. A cost equivalent example building, designed with the FPS and a reduced seismic design load of 50%, demonstrated 86% less building damage during severe earthquakes as compared with the full strength design without the FPS.

The FPS was also assessed to be a feasible and attractive technique to improve the seismic resistance of existing hazardous buildings. The flexibility to achieve relatively long isolator periods of 3 to 4 seconds offered improved performance for the cases of weak buildings studied. The compact size and high strength of the FPS isolators also offered advantages in retrofit details.

17. Document Analysis a. Descriptors

b. Identifiers/Open-Ended Terms

c. COSATI Field/Group

18. Availability Statement:
Release unlimited

19. Security Class (This Report)
unclassified

20. Security Class (This Page)
unclassified

21. [illegible]

22. [illegible]

(See ANSI-Z39.18) *See Instructions on Reverse*

OPTIONAL FORM 272 (4-77)
(Formerly NTIS-35)
Department of Commerce

FEASIBILITY AND PERFORMANCE STUDIES ON IMPROVING THE EARTHQUAKE RESISTANCE OF NEW AND EXISTING BUILDINGS USING THE FRICTION PENDULUM SYSTEM

by

Victor Zayas

Stanley Low

Luis Bozzo

and

Stephen Mahin

A Report to Sponsor:
National Science Foundation

Report No. UCB/EERC-89/09
Earthquake Engineering Research Center
College of Engineering
University of California, Berkeley
California

September 1989

ABSTRACT

The feasibility of using an innovative earthquake resistant construction technique to improve the earthquake resistance of buildings was investigated. The technique, called the Friction Pendulum System (FPS), uses steel connections to seismically isolate the buildings using small amplitude pendulum motions. The anticipated seismic performance of building structures using the FPS steel connections was investigated using analytical and experimental studies. Buildings designed to have approximately equivalent construction costs as conventional building designs were studied. The earthquake response of the FPS supported buildings were compared to those of conventional code design.

The FPS was assessed to be a feasible and cost effective construction technique for improving the seismic resistance of new buildings. The flexibility to select any isolator period makes the approach suitable to a wide range of applications. The compact size and high strength of the FPS isolators, permits a versatility of installation details which helps to achieve construction which is cost equivalent to non-isolated buildings, yet provides substantially improved seismic resistance. A cost equivalent example building, designed with the FPS and a reduced seismic design load of 50%, demonstrated 86% less building damage during severe earthquakes as compared to the full strength design without the FPS.

The FPS was also assessed to be a feasible and attractive technique to improve the seismic resistance of existing hazardous buildings. The flexibility to achieve relatively long isolator periods of 3 to 4 seconds offered improved performance for the cases of weak buildings studied. The compact size and high strength of the FPS isolators also offered advantages in retrofit details.

Model size FPS isolators were tested at velocities up to 20 inches/second, and at varied pressure loads. They consistently achieved ideal linear stiffnesses and dynamic friction coefficients of less than 5%. Analytical studies of example building cases showed that the shear loads, story drifts, ductility demands, and structure inelastic energy dissipation in FPS supported structures were substantially reduced as compared to similar structures without the FPS. The studies showed that the torsion motions occurring in asymmetrical structures with large mass eccentricities can be substantially reduced using the FPS. The FPS offers the potential to improve the seismic performance for a wide variety of structures.

ACKNOWLEDGMENTS

This research was funded by the National Science Foundation, Small Business Innovation Research Program, under SBIR Phase I grant No. ISI-8860953. The NSF program official for this grant is A. J. Eggenberger. The SBIR Program manager is Ritchie B. Coryell.

The support of the National Science Foundation in funding this research, and the advice of Dr. Eggenberger and Mr. Coryell, are greatly appreciated. The opinions, findings, conclusions and recommendations expressed in this report, however, are those of the authors and do not necessarily reflect the views of the National Science Foundation.

The research work reported was a cooperative research effort by Earthquake Protection Systems, San Francisco, and the Department of Civil Engineering, University of California, Berkeley. The collaborative research effort was made possible by the NSF Small Business Innovation Research Program, the University of California Earthquake Engineering Research Center, and Earthquake Protection Systems, which encourage joint industry and academic research.

TABLE OF CONTENTS

CHAPTER 1

SUMMARY OF THE PHASE I RESEARCH

SECTIONS

1.1 Introduction

The Friction Pendulum System (FPS) is an innovative approach for improving the earthquake resistance of structures. Structures supported on FPS connections respond to earthquake ground motions as would a simple pendulum. These simple pendulum motions are easy to control and predict. The feasibility of using the FPS approach to improve the earthquake performance of buildings is examined in this report.

The feasibility of using the FPS in new building construction in a cost effective manner is examined in Chapter 2. The feasibility of using the FPS approach to improve the seismic resistance of existing hazardous buildings is examined in Chapter 3. The feasibility assessments are based on the technical performance evaluations presented in Chapters 4 through 8. In each of these chapters a specific technical issue is investigated. The conclusions, references, and figures pertinent to the issue are presented at the end of each chapter.

This report summarizes the results of the Phase I research sponsored by the National Science Foundation, Small Business Innovation Research Program. Consistent with the feasibility assessment objectives of the Phase I program, simple examples and laboratory tests, and simplified analytical models are used to assess the overall performance characteristics of the FPS. The simple building examples, tests and analytical models have the benefit of being both instructional and illustrative of the anticipated overall behavior of buildings supported on FPS isolators. More detailed investigations of different building types, localized structural behavior, and the response to varied earthquake loadings are planned for the Phase II program.

1.2 Identification Of The Need

It has been estimated that a major earthquake occurring in a large metropolitan area in the U.S. could result in upwards of 70 billion dollars in damages and in tens of thousands of fatalities. Even more moderate seismic events can cause collapse of existing hazardous buildings, damage to new buildings, business interruptions, and disruptions of vital public services, all of which have been proven to have profound long-term impacts on the economic and social well-being of the affected communities. Because of this, considerable research has been performed to develop reliable techniques to design and analyze earthquake resistant structures.

Studies by the U.S. Geological Survey (USGS) have indicated that earthquake shaking can produce forces in structures 10 to 20 times higher than those currently used in building design. Economic considerations have lead to a design approach for conventional buildings which relies on inelastic energy dissipation, rather than strength, as the means of resisting the effects of such large earthquakes. As a result, properly designed and constructed buildings would remain standing following a major earthquake, but substantial damage to the structure and to contents would be anticipated. Research on these types of structures has shown the need for costly details and construction practices in order to achieve the desired behavior.

During the past decade, greater focus has been placed on developing design strategies which reduce the need for costly structural details while providing greater protection against damage to the structure and contents. With this in mind, a variety of seismic isolation systems has been proposed in which the structure is supported on components or devices which preferentially modify the dynamic characteristics of the supported structure and/or limit the amplitude of forces which can be transmitted from the ground into the structure. By reducing the dynamic response of the structure, lower design forces may be considered, seismically induced deformations and damages can be reduced, and critical contents (such as those involving toxic chemical or biological operations, data processing and telecommunications equipment, and high technology manufacturing facilities) may be economically protected from earthquake damage.

An important application of the seismic isolation approach relates to the mitigation of hazards posed by structures built prior to the development of modern design and construction practices. Reduction of seismic deficiencies in such structures using conventional means, is not only technically difficult and costly but is highly disruptive to the building occupants. The applicability of seismic isolation techniques to existing seismically hazardous buildings appears promising due to the possible reduction in design forces and the localization of the structural modifications to one floor level. However, improved methods for earthquake resistant construction of new or existing buildings which increase the cost of construction are not widely used in the building industry.

1.3 Background

The Friction Pendulum System (FPS) is an innovative seismic isolation system which appears to offer improvements in strength, longevity, versatility, ease of installation, and cost as compared to previous systems. Moreover, the approach adds several inherent performance benefits not available before. The FPS is based on

well known engineering principles and is constructed of conventional materials with demonstrated longevity and resistance to environmental deterioration. The desirable isolation characteristics exhibited by FPS components hold the promise of an economical and effective system for significantly increasing the seismic resistance of new structures and for substantially reducing the earthquake hazards posed by existing structures. In order to achieve the potential benefits of this and other innovative systems, careful attention must be placed on economic, architectural and construction aspects as well as on the more traditional technical issues.

The Friction Pendulum System (FPS) offers a simple approach for increasing a structure's earthquake resistance. A cross section view of an FPS steel connection is shown in Figure 1.1. The FPS concept is based on an innovative way of achieving a pendulum motion. Fig. 1.2 schematically illustrates how the FPS achieves a pendulum response for a supported building. The building responds to earthquake motions with small amplitude pendulum motions. Friction damping effectively absorbs the earthquake's energy. The result is a simple, predictable, and stable earthquake response. Examples of the FPS hysteretic loops are shown in Fig. 1.3.

The connections can be installed at the bottoms or tops of lower story columns, or between the building and its foundation. The operation of the connection is the same whether the concave surface is facing up or down. Fig. 1.4 illustrates the operation of the connection when installed at the top of a column, with the concave surface facing downward.

Previous research by the investigators has addressed how the FPS connections behave under simulated earthquake conditions (Ref. 1.1). The FPS connections serve as shear links which absorb the damaging earthquake motions and energies. When the earthquake forces are below the threshold level, the building responds like a conventional structure. Once the threshold is exceeded the buildings ductility response and energy absorption are controlled by the FPS connections.

The lateral restoring stiffness of the activated FPS connection is:

$$k = \left(\frac{W}{r} \right)$$

where W is the supported weight and r is the length of the radius of curvature of the concave surface. This is the same as the stiffness of a simple pendulum.

The weight proportional stiffness is a unique property of the FPS which greatly reduces the torsion response of a structure. The center of lateral stiffness of the FPS connections coincides with the center of mass. Since the friction force is also proportional to the supported weight, the center of rigidity of the connections acting as a group always coincides with the center of mass of the building. This property makes the FPS connections particularly effective at minimizing adverse torsional motions which would otherwise occur in asymmetrical buildings.

The FPS connections also serve as seismic isolators. Seismic isolation is achieved by shifting the response of the structure to a range where the lateral loads are reduced. The extent of the period shift is controlled by the radius of curvature of the concave surface.

The natural period of vibration of a rigid mass supported on FPS connections is determined from the pendulum equations and is:

$$T = 2\pi\sqrt{\frac{r}{g}}$$

where g is the acceleration of gravity. This is the sliding period of the isolators. It is also the sliding or activated period for a short and relatively stiff building.

The fact that the period is independent of the structure mass is another unique property of the FPS which can have advantages in controlling the response of a building. The desired structure period can be selected by simply choosing the radius of curvature of the concave surface. The period does not change if the structure weight changes or is different than assumed.

Another unique property of the FPS connections, as compared to other sliding supports, is the design of the articulated slider. The semi-spherical design of the slider results in uniform contact pressures between the slider and the concave surface for any combination of lateral and vertical loads. This avoids edge gouging, and reduces high frequency stick-slip motions which occur with other sliding support systems.

Seismic isolation is an emerging technology which has been receiving increasing attention in recent years by researchers and design professionals. The research presented herein builds on previous research on the FPS concept by Zayas, Low and Mahin (Ref. 1.1). During this previous research effort simple building models with FPS connections were tested on the University of California Berkeley shake table. The research presented also builds on extensive worldwide research on seismic isolation by other

investigators. These include work on sliding isolation systems by Kelly (Ref. 1.4), Mostaghel (Ref. 1.5), and Constantinou (Ref. 1.6); and isolation systems with displacement restraints by Kelly (Ref. 1.7); and related research efforts by other investigators in the U.S. (Refs. 1.8 and 1.9), Japan (Ref. 1.10), France (Ref. 1.11), China (Ref. 1.12) and New Zealand.

One of the potential advantages offered by the FPS approach, compared to other available techniques, is the cost of installation. The connection size, strength, materials and versatility should make the approach easier and less expensive to install. Potential reductions in other construction costs could completely compensate for the cost of installing the FPS, thereby achieving a cost-equivalent but more earthquake resistant building.

The need for cost effective ways to mitigate seismic hazards of existing buildings has recently been recognized by many municipal governments in California. California Senate Bill 547 (Ref. 1.2), which was passed in 1986, requires that California cities adopt a program by Jan. 1, 1990, to reduce the hazards from unreinforced masonry buildings. Cities have begun to identify seismically hazardous buildings and to notify the owners. Many building owners have resisted city efforts to require seismic upgrades because of occupant disturbance and cost issues.

Cost is also a primary factor affecting the implementation of improved seismic resisting methods in new buildings. Technologies that increase the earthquake resistance of new buildings but also increase the construction costs have not been widely used. The Structural Engineers Association of Northern California (SEAONC) has developed Tentative Seismic Isolation Design Requirements (Ref. 1.3) which would permit reductions in the cost of seismically isolated buildings. These or other equivalent criteria are likely to be adopted into the Uniform Building Code by 1991, which should stimulate commercial applications of the seismic isolation approach for buildings.

1.4 Phase I Research Objectives

The primary objectives of the Phase I research are to assess the technical feasibility of using the FPS to improve the seismic performance of new and existing buildings. The following technical and engineering issues were investigated:

1. The feasibility of achieving significant increases in the earthquake resistance of new buildings without increasing the construction costs.

2. The feasibility of applying the FPS to existing hazardous buildings, thereby helping to protect these buildings from damage and collapse.

3. The interrelationships between the FPS design parameters (friction coefficient, radius of curvature and displacement travel) and the building design parameters (period and strength) for earthquakes of different strengths.

4. The ability of FPS components to achieve dynamic coefficients of friction which are less than 5%, for relative sliding velocities which are representative of earthquake loadings.

5. Investigations of building parameters which control the structure's torsional response, and to estimate the potential for reductions in damaging torsion motions for asymmetrical buildings using the FPS approach.

The research work and principal findings are summarized below.

1.5 Summary of the Research and Findings

The feasibility of applying the FPS to new building construction is examined in Chapter 2. Details which could be used for the installation of the FPS isolators are proposed. An example building was selected and redesigned using the FPS. The example building was a steel moment frame building, a common type of construction used for commercial and institutional buildings. The FPS offered the versatility of installation details which helped achieve an isolated building which was cost equivalent to the non-isolated building, and yet had significantly improved earthquake performance. Analyses results indicated that seismic damage during a severe earthquake would be reduced by 89%.

The feasibility of using the FPS to retrofit existing hazardous buildings is examined in Chapter 3. Considerations for applying the technique to the different types of existing hazardous buildings are examined. The seismic performance of the FPS is assessed for a case study of a structurally weak building.

Preliminary design considerations were proposed on the selection of FPS parameters suitable to weak buildings. When properly designed, the FPS was found to reduce ductility demand by 86%. Analyses results indicated that the expected performance would be better than conventional strengthening techniques used alone. However, it was unclear if the anticipated reductions in earthquake forces and ductility demands alone, would be sufficient to prevent collapse of weak hazardous buildings. Strengthening of portions of the building may also be required.

The feasibility assessments put forward in Chapters 2 and 3 are based on studies of the technical properties and performance of the FPS which are presented in Chapters 4 to 8. Results from tests of individual FPS isolators are reported in Chapter 4. Low friction FPS assemblies were tested at high sliding velocities of up to 20 inches/second. The dynamic coefficients of friction of the low

friction assemblies were found to be less than 5%. These dynamic friction values were considered suitable for seismic retrofits or cost equivalent new building construction. The hysteretic loops were observed to have an ideal bi-linear response with linear lateral stiffness throughout the displacement travel. The lateral stiffness was directly proportional to the vertical load, and exactly matched the theoretically predicted pendulum stiffness. The loops were observed to be stable and non-degrading over many cycles of loading at varied vertical loads.

Analytical studies on the torsion response of FPS supported structures are presented in Chapter 5. Analytical models are developed and found to compare well with experimental results. The weight proportional stiffness properties of the FPS reduced the torsion motions of asymmetrical structures. The weight proportional stiffness directly compensated for the effects of mass eccentricities. The reductions in torsional motions of up to 80% were observed, as compared to linear elastic structures with equivalent eccentricities. Parameter studies indicated that the reduction of torsion motions would be substantial for a wide variety of building configurations. The unique ability of the FPS to reduce torsion motions is one of the most attractive aspects of the approach.

Investigations on the effects of engaging the lateral displacement restraint of the FPS are presented in Chapter 6. Engagement of the lateral displacement restraints occurs when the seismic loading demand exceeds the lateral displacement capacity of the FPS. Analytical models were developed which could simulate the effects of engaging the displacement restraints, and were found to agree well with experimental results. Time history analyses of nonlinear models of the example building, including the displacement restraint model, were used to assess the effects on this type of building. The displacement restraint was found to break up the modes of vibration, preventing resonant dynamic responses from building up in any one set of modes. When displacement loading demand exceeded displacement capacity by 50%, the FPS retained 85% of its effectiveness in reducing inelastic ductility demand, 95% of its effectiveness in reducing structural inelastic energy dissipation, and 80% of its effectiveness in reducing first story drift.

The inelastic responses of multistory structures supported on the FPS isolators are presented in Chapter 7. Bi-linear elastic plastic models of the building structures are used to investigate the relationship between the primary building and FPS properties, and to assess the relationship between yielding in the structure and response of the FPS. The analytical model of the example building presented in Chapter 2 is used as a basic case. The structure strengths and structure periods are varied to simulate other building cases. Nine different cases were considered, and

the responses with and without the FPS were compared. The responses for total displacements, structure ductility demand, structure story drift, and structure energy dissipation were assessed and compared. The total lateral displacement at the roof level of the FPS isolated structures was found to be less than, or approximately equal to, the roof displacements occurring in the same structures without the FPS. The structure ductility demand, structure story drift, and structure energy dissipation was found to be always less than, and usually substantially less than, those occurring in the same structure without the FPS. For structures with periods less than 0.86 sec., ductility and drift values in FPS supported structures were found to be of similar magnitudes to those occurring in equivalent non-isolated structures with four times the strengths. Weak structures representative of existing hazardous buildings were given particular attention. Lengthening the period and lowering the friction coefficient of the FPS was found to reduce the yielding and ductility demands in these structures.

Whereas example building cases and responses to particular earthquake motions were studied in Chapters 2 through 7, a broader and more theoretical approach was taken in Chapter 8. Equivalent single degree of freedom models representing elastic structures supported on FPS isolators were developed. The equations of motion for the equivalent system were formulated and used to investigate the interrelationships of the FPS parameters of period and friction coefficient, to the period and strength of the structure, and the strength of the ground motion. A systematic study of the responses of the equivalent system to ten different ground motions was undertaken, and the results for each of the individual motions, as well as the means and coefficients of variation of the responses are reported. The strength required to maintain an elastic response in the building was identified, as well as the base shear and displacement responses.

When the structural period was greater than 0.5 sec., the total displacements of the equivalent systems relative to the ground were found to be approximately equivalent to the total displacement in elastic structures without the FPS. The total drift displacement for these cases could be estimated from displacement response spectra. Once the total drift was known, the sliding displacement in the FPS and drift displacement in the structure could be calculated from the basic relationship between the FPS period, friction coefficient, and building period. The total drift was relatively independent of the selection of FPS period and friction coefficient. The selection of longer FPS periods and lower friction coefficients was found to reduce the drift displacement in the structure, while increasing the drift displacement in the FPS by a comparable amount. For structures with periods less than 0.5 sec., total displacements in the FPS supported structures were greater than those of the elastic structures without the FPS, and the total displacement was affected by the selection of the FPS period and friction coefficient. The structural drifts and forces in the FPS supported structures were always less than those in the elastic structures without the FPS.

1.6 Technical Feasibility Conclusions

The FPS was assessed to be a feasible and cost effective construction technique for improving the seismic resistance of new buildings. The flexibility to select any isolator period makes the approach suitable to a wide range of applications. The compact size, high strength, and articulated joint of the FPS, permits a versatility of installation details which helps to achieve construction which is cost equivalent to non-isolated buildings, yet provides substantially improved seismic resistance. The cost equivalent example building investigated, designed with the FPS and a reduced seismic design load of 50%, demonstrated 86% less building damage during severe earthquakes as compared to the full strength design without the FPS.

The FPS was also assessed to be a feasible and attractive technique to improve the seismic resistance of existing hazardous buildings. The flexibility to achieve relatively long isolator periods of 3 to 4 seconds offered improved performance for the cases of weak buildings studied. The the compact size and high strength of the FPS isolators also offered advantages in retrofit details. The approach also offered reduced disturbance of building occupants as compared to conventional strengthening techniques.

It is possible to manufacture low friction FPS assemblies with dynamic frictions of less than 5% at earthquake velocities. Model size FPS bearings were tested at relative sliding velocities up to 20 inches/second, and at varied pressure loads. They consistently achieved ideal linear stiffnesses and dynamic friction coefficients of less than 5%. The attainment of these low dynamic friction values is important for applications to existing hazardous buildings and cost equivalent construction of new buildings.

The shear loads, story drifts, ductility demands, and structure inelastic energy dissipation in FPS supported structures were always reduced as compared to similar structures without the FPS. Using longer periods and lower friction coefficients in the FPS isolators reduce the drift deformations in the structural frames, while maintaining approximately the same total roof drift displacement.

Limited yielding and ductility response may be permitted in FPS supported structures. When the seismic loading demands exceeded displacement travel capacity, the FPS retained a large percentage of its effectiveness to reduce building damage, demonstrating the robustness of the approach.

The torsion motions occurring in asymmetrical structures with large mass can be substantially reduced using the FPS. Single degree of freedom response spectra can be used for design purposes to give reasonable estimates of the total displacements, base shears and structure drifts occurring in FPS supported structures.

The FPS offers the potential to improve the seismic performance for a wide variety of structures.

1.7 Potential Applications

Because of the inherent simplicity, versatility, stability and durability of the FPS concept, it should become a major tool for the seismically resistant design of buildings once the engineering design and detailing issues are resolved, and simple yet reliable design procedures are developed. Reduction of the seismic hazards in new and existing buildings is a problem of national importance and one which is expected to become increasingly critical in the years to come. The development of a reliable, economical and practical FPS seismic isolation system is expected to significantly increase seismic safety. In addition, the FPS will provide an effective method for mitigating damages to non-structural components and building contents, and for overcoming difficult structural problems such as those as associated with inelastic torsional response. Illustrations of possible applications to buildings are shown in Figs. 1.5 to 1.7.

In addition, the versatility of this system has yet to be explored. Innovative applications of this system with high potential include very irregular or unusual structures (Fig. 1.8), or industrial, manufacturing or chemical processing facilities, critical structures with stringent performance requirements, bridges, and supported equipment (Figs. 1.9 to 1.13). Development of a feasible and economical FPS solution for conventional buildings will naturally lead to these other applications.

1.8 Future Research Needs

The Phase I research established the ability of the FPS to improve the overall seismic performance of new or existing buildings. Consistent with the Phase I objectives and limitations, the investigations used simple analytical models to assess the response of limited building types (ie: moment resisting frames), to a few representative earthquake loadings.

Additional research and engineering evaluations are needed to answer a substantial number of engineering questions on the effects and performance of the FPS within buildings. Investigations are needed to assess the performance of the FPS when applied to different building types, including braced frames, shear walls, and bearing wall structures. Since the lateral forces in the FPS are proportional to the supported weight, this changes the distributions of forces and stresses within structures. Thus, the local effects on individual structural members and standard structural details and design practice need to be addressed.

Experimental investigations of the responses of realistic multistory building models subjected to shake table tests are needed. The dynamic responses of low friction FPS isolators under shake table tests need to be investigated. The effects of higher mode responses need to be assessed, examining the differences between FPS supported structures and conventional structures. The influences of friction coefficients and FPS periods on the higher mode responses need to be investigated, as well as design methods and installation approaches which may influence and control higher mode responses. Also, for buildings with sensitive equipment the occurrence of high frequency vibrations and in-structure response needs to be investigated.

Shake table tests are also needed on the responses of weak and non-ductile buildings supported on FPS isolators, with attention to the interactions between the responses of the buildings and the FPS.

There is also the need to investigate the effects of varied and diverse ground motions on all the response characteristics. Moreover, before the FPS technique can be accepted and applied within the industry, there is the need to develop simple yet reliable design guidelines and procedures. A thorough investigation of these important engineering considerations is required to insure the safety of the public in the application of the proposed new construction methods. These investigations are planned for the Phase II research program.

1.9 References - Chapter 1

1.1. Zayas V. A., Low S. S., and Mahin S.A.,"The FPS Earthquake Resisting System: Experimental Report," Report No. UCB/EERC-87/01, Earthquake Engineering Research Center, University of California, Berkeley, June 1987.

1.2. State of California Seismic Safety Commission, "Guidebook: To Identify and Mitigate Seismic Hazards in Buildings," Report No. SSC 87-03, December 1987.

1.3. Structural Engineers Association of Northern California, "Tentative Seismic Isolation Design Requirements," September 1986.

1.4. Kelly J. M. and Chalhoub M. S., "Sliders and Tension Controlled Reinforced Elastomeric Bearings Combined for Earthquake Isolation," Earthquake Engineering Research Center, University of California, Berkeley, 1988.

1.5. Mostaghel N. and Tanbakuchi J., "Response of Sliding Structures to Earthquake Support Motion," Earthquake Engineering and Structural Dynamics, Vol. 11, 729-748, 1983.

1.6. Constantinou M.C. and Tadjbakhsh I. G., "The Optimum Design of a Base Isolation System With Frictional Elements," Earthquake Engineering and Structural Dynamics, Vol. 12, 203-214, 1984.

1.7. Kelly J. M., Griffith M., and Aiken I., "A Tension Restraint for Uplift Control," Report No. UCB/EERC-87/03, Earthquake Engineering Research Center, University of California, Berkeley, 1987.

1.8. Tarics A. G., Kelly J. M., Way D., "The Seismic Rehabilitation of Existing Buildings Using Base Isolation," Joint Report Reid and Tarics Associates and Earthquake Engineering Research Center, University of California, Berkeley,

1.9. Mayes R. L., Jones L. R., Kelly T. E., and Button M. R., "Design Guidelines for Base-Isolated Buildings with Energy Dissipators," Earthquake Spectra, Vol. 1, No. 1, November 1984.

1.10. Kitagawa Y., "Base Isolated Building Structures in Japan," International Organization for the Development of Concrete, Prestressing and Related Materials and Techniques, New Zealand, August 1987.

1.11. Jolivet F. and Richli M., "Aseismic Foundation System for Nuclear Power Stations," Departements Genie Civil, Spie-Batignoles, France, 1977.

1.12. Li L., "Advances in Base Isolation in China," Presented at the 3rd International Conference on Soil Dynamics and Earthquake Engineering., Princeton University, USA, June 1987.

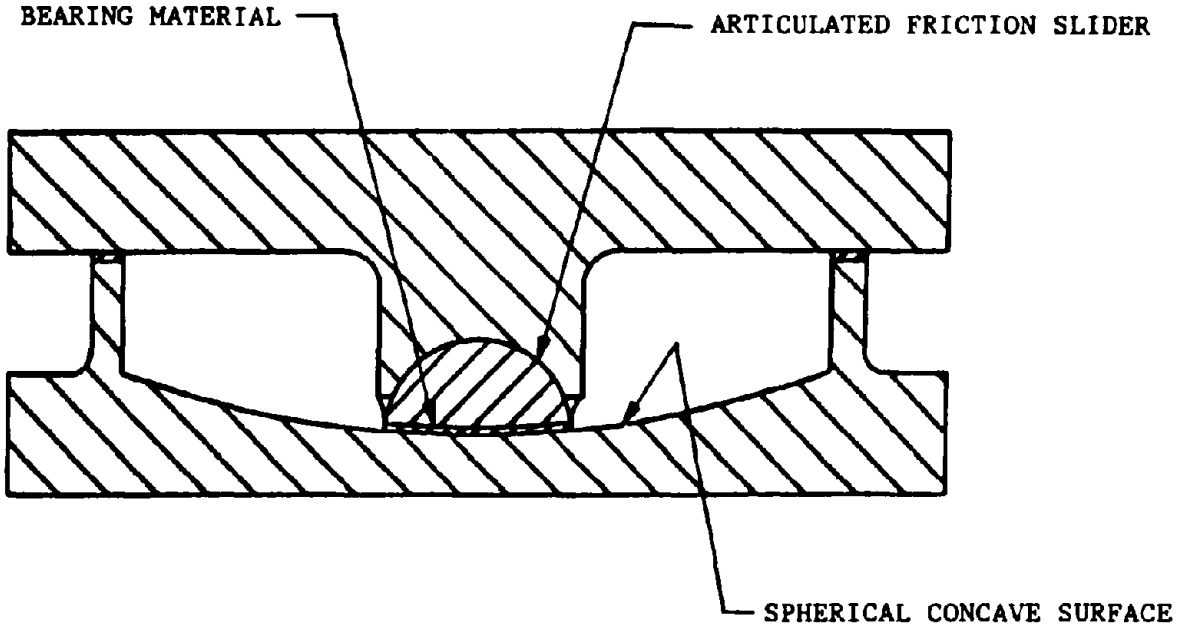

Fig. 1.1 FPS Isolator Section

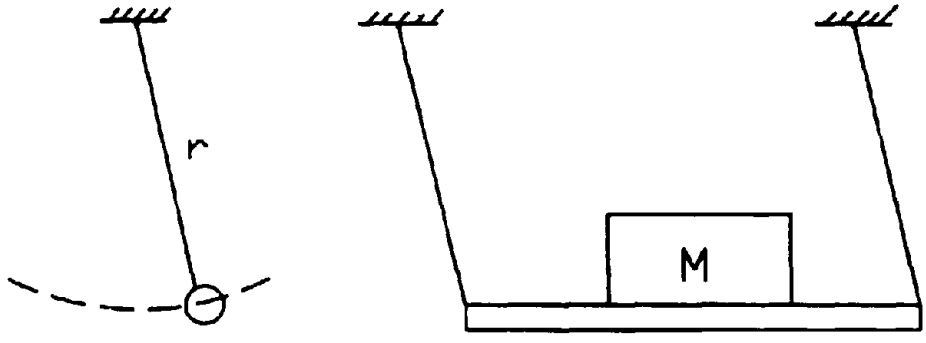

PENDULUM MOTION

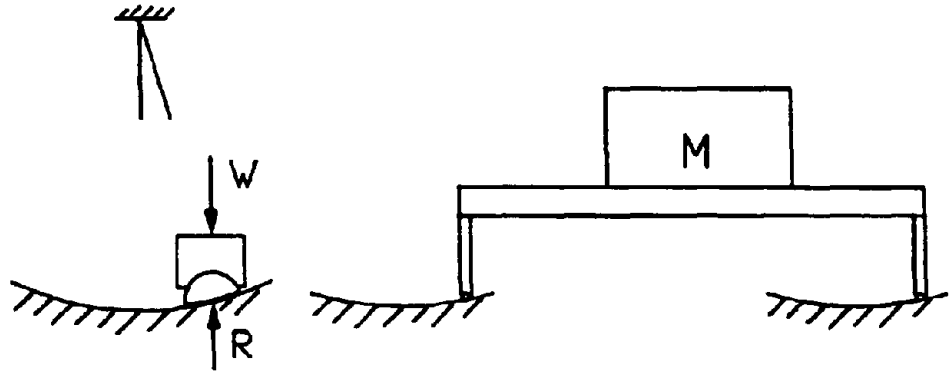

SLIDING PENDULUM MOTION

EQUATIONS: PERIOD $T = 2\pi\sqrt{r/g}$

STIFFNESS $k = W/r$

W = WEIGHT
r = RADIUS OF CURVATURE

Fig. 1.2 Basic Principles

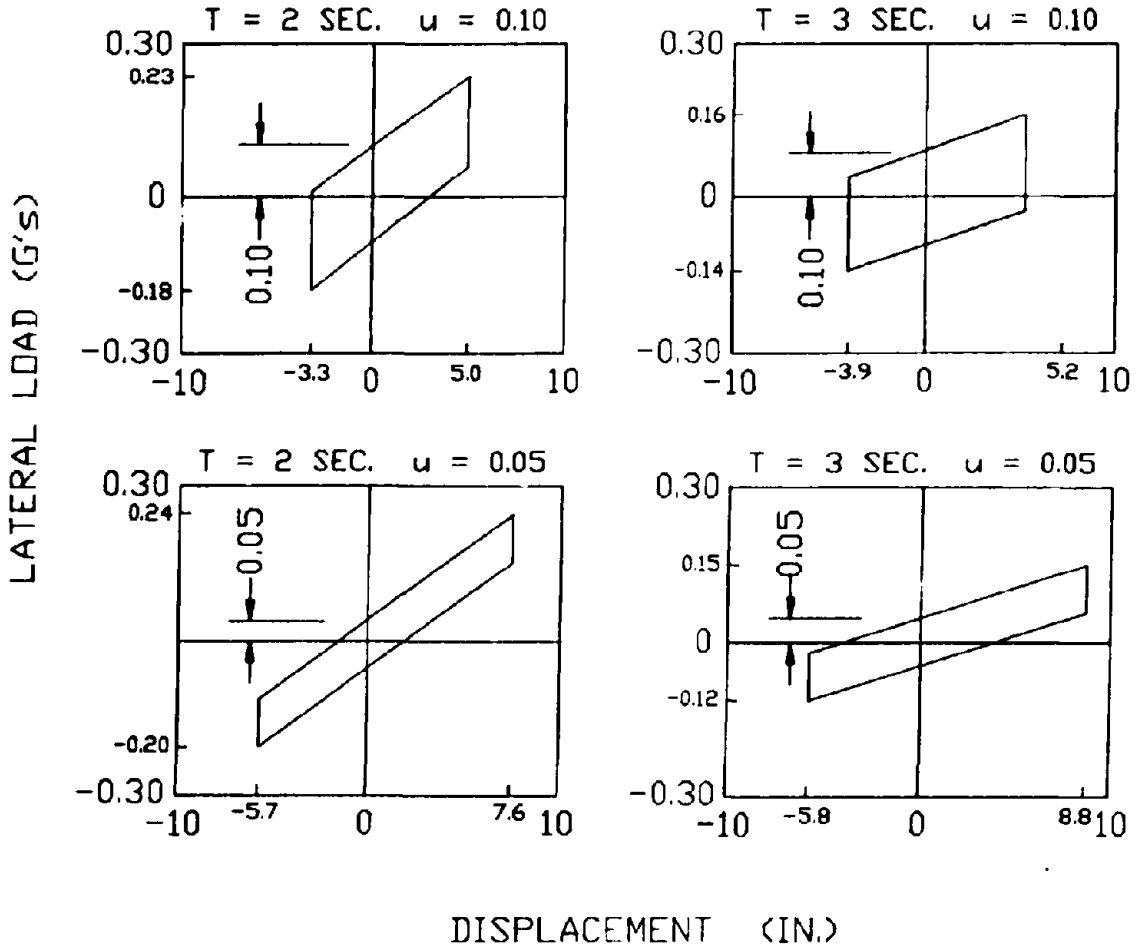

HYSTERETIC RESPONSES TO THE 2 x EL CENTRO EARTHQUAKE

Fig. 1.3 FPS Hysteretic Loops

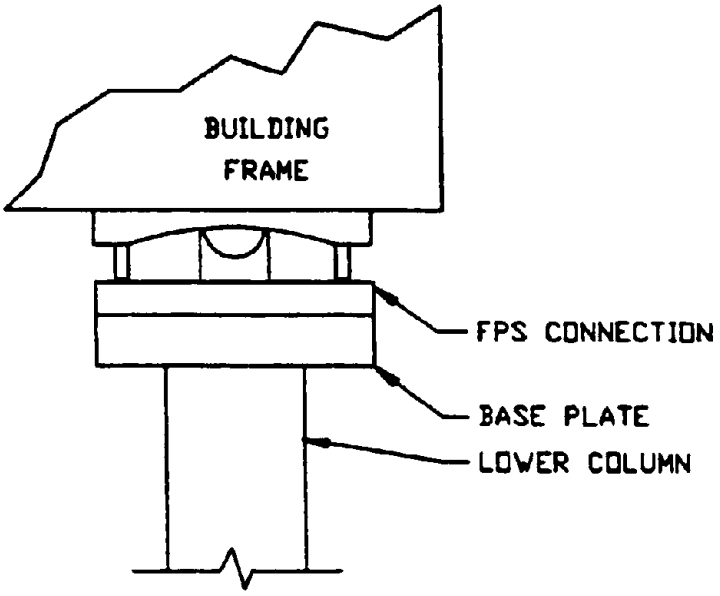

Fig. 1.4 FPS Operation

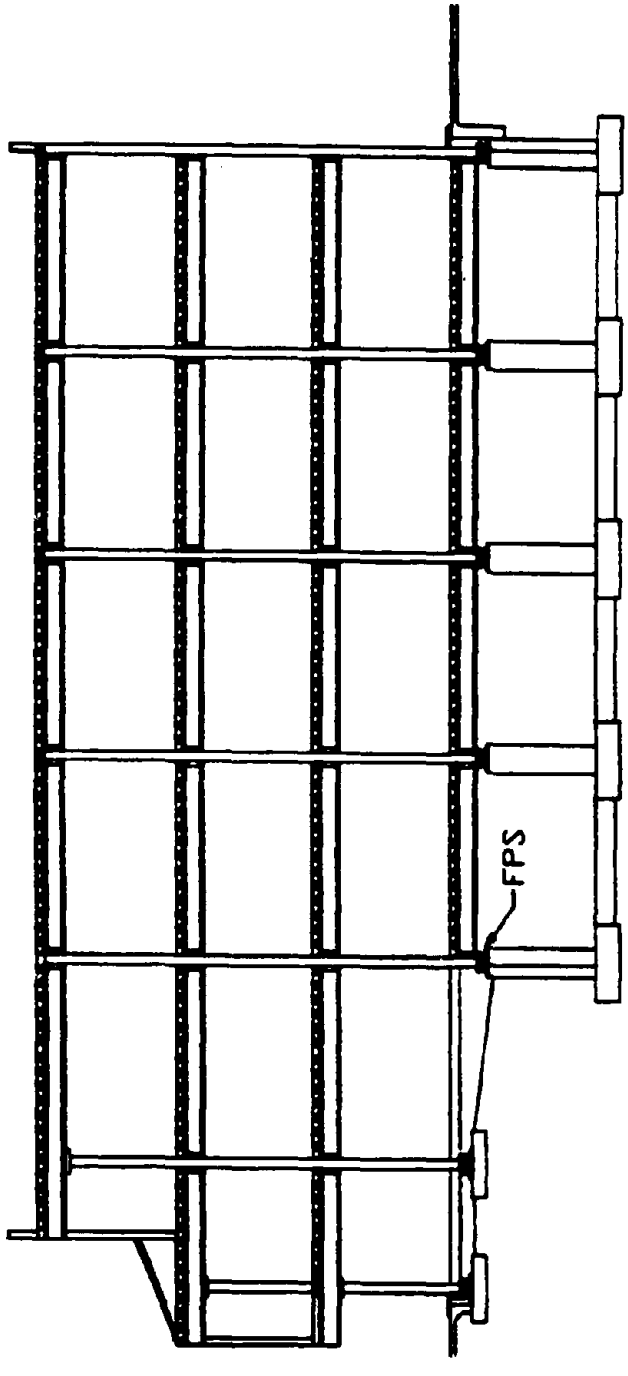

Fig. 1.5 Low Rise Building

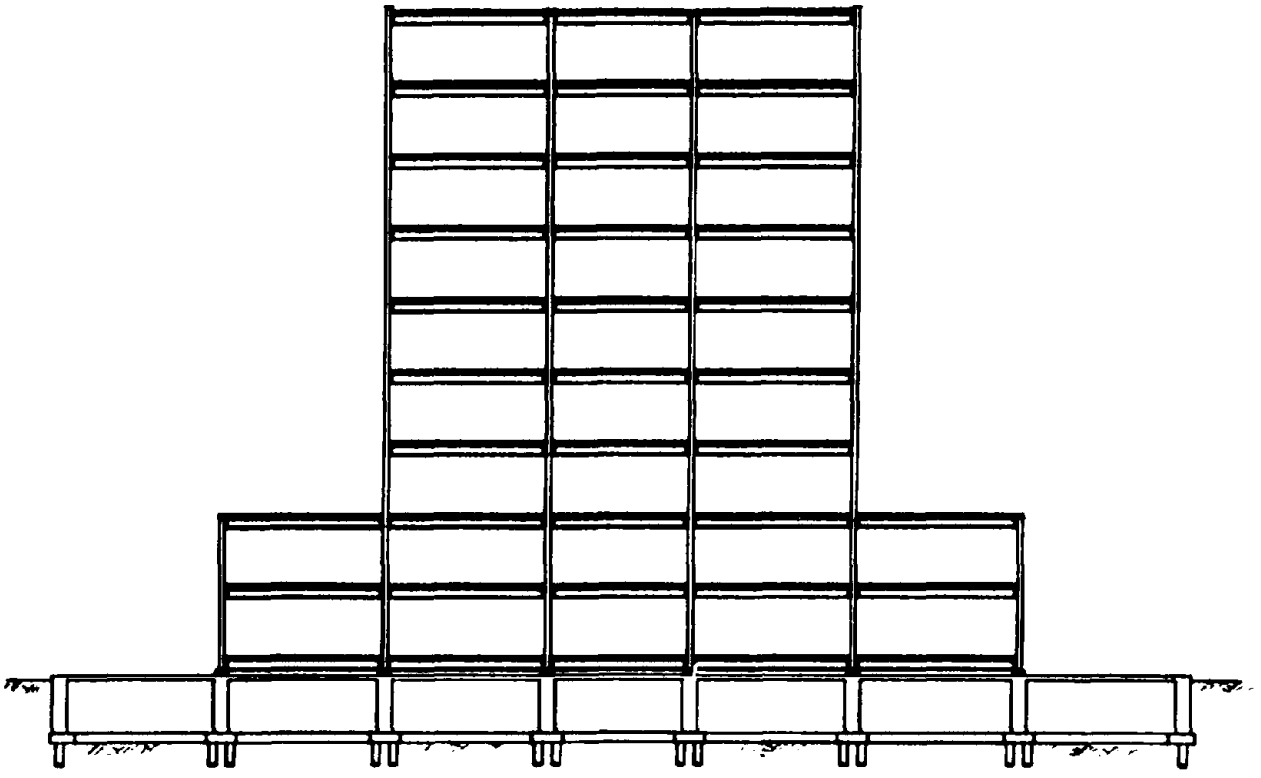

Fig. 1.6 Office Building

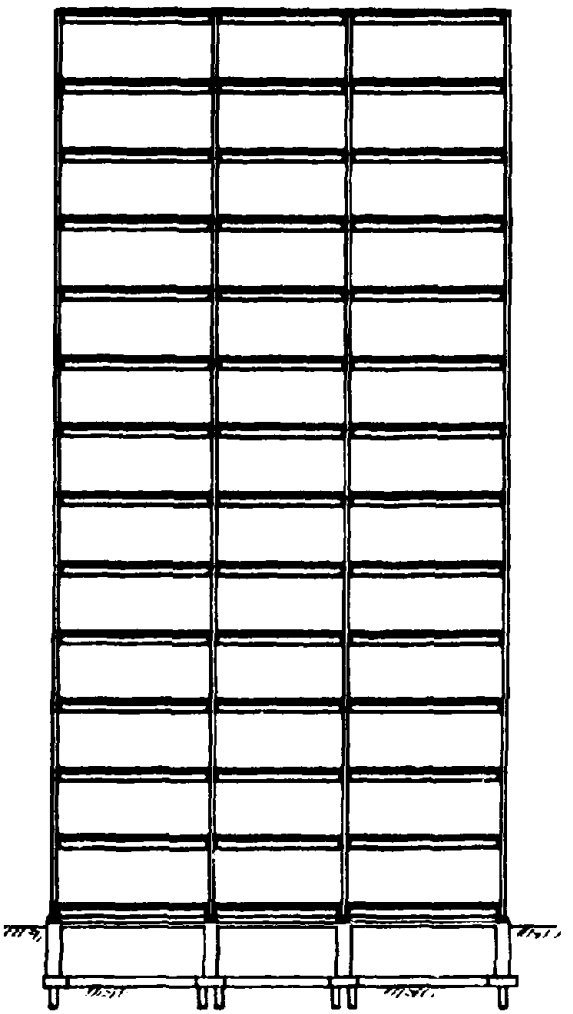

Fig. 1.7 Symmetrical Building

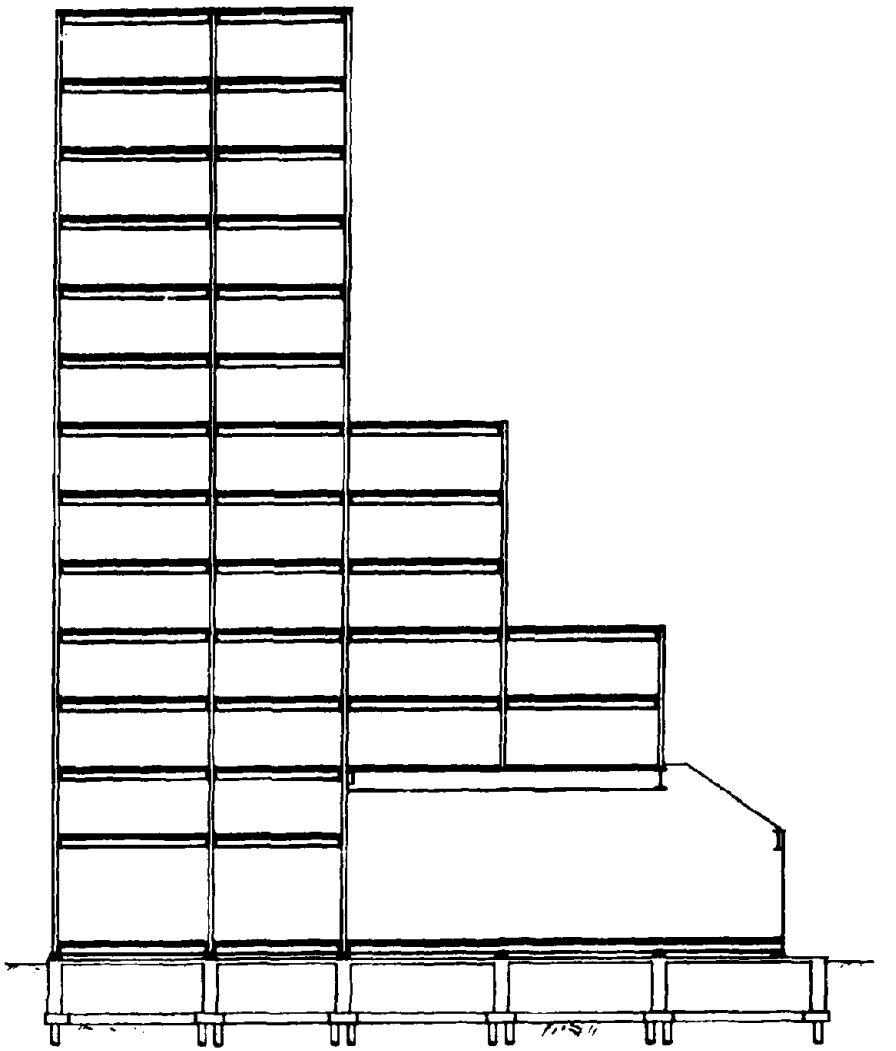

Fig. 1.8 Asymmetrical Building

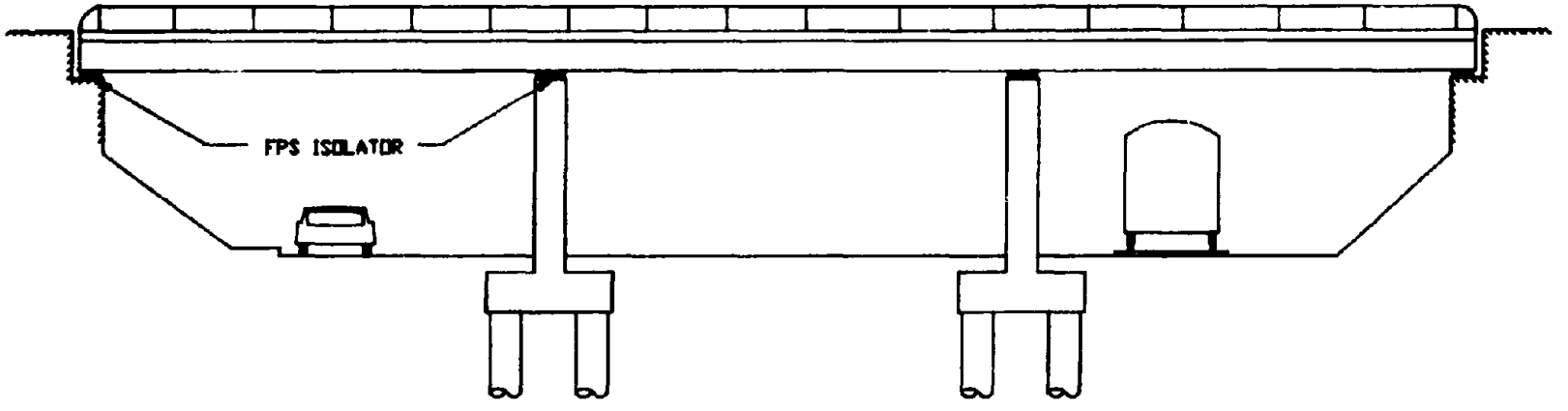

Fig. 1.9 Highway Bridge

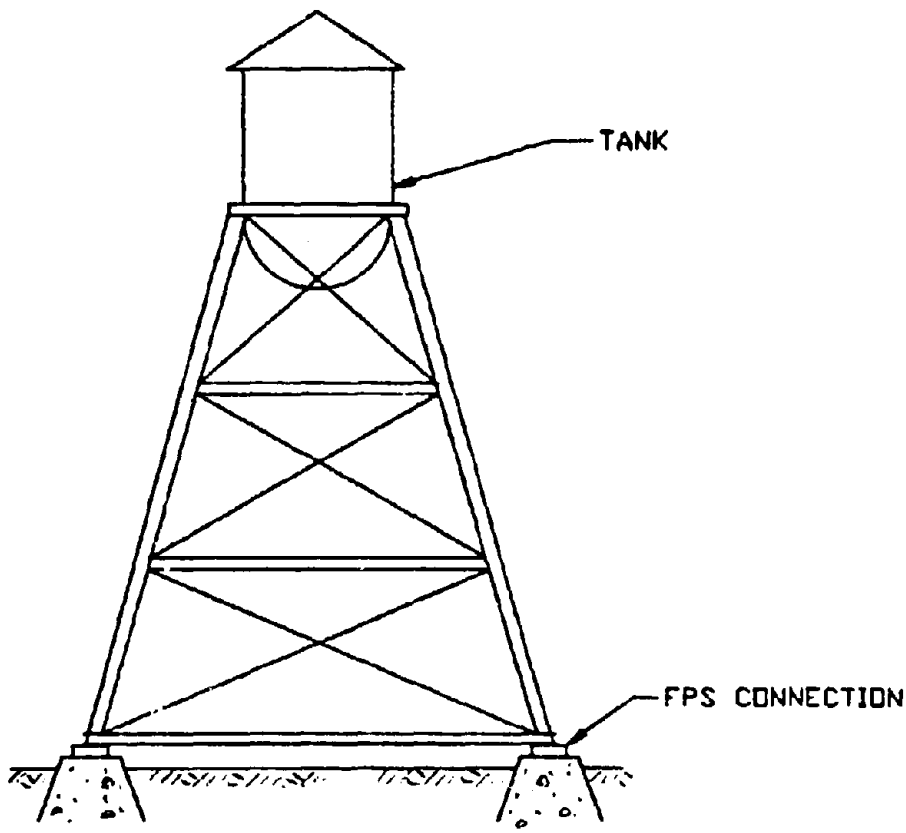

Fig. 1.10 Water Tank

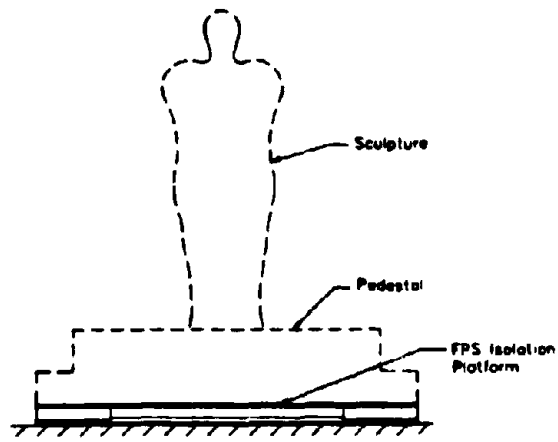

Fig. 1.11 Museum Sculpture

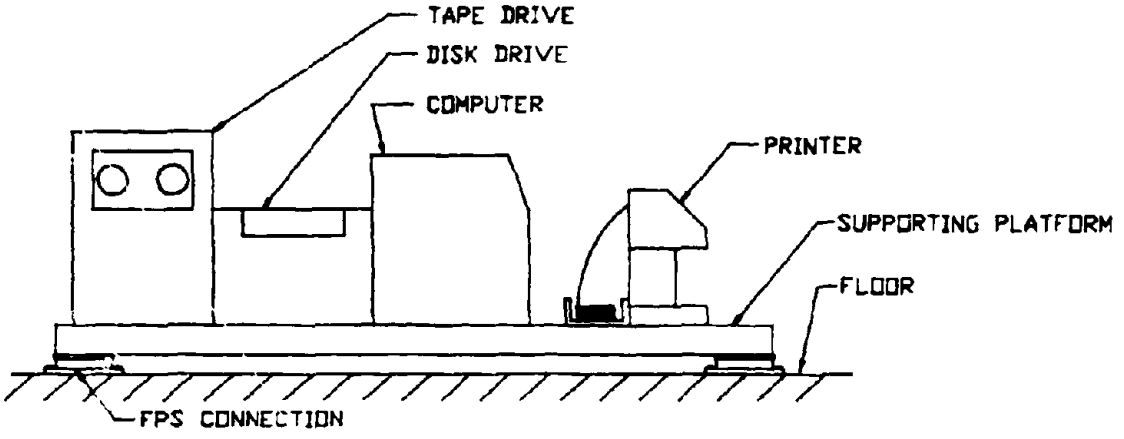

Fig. 1.12 Computer Equipment

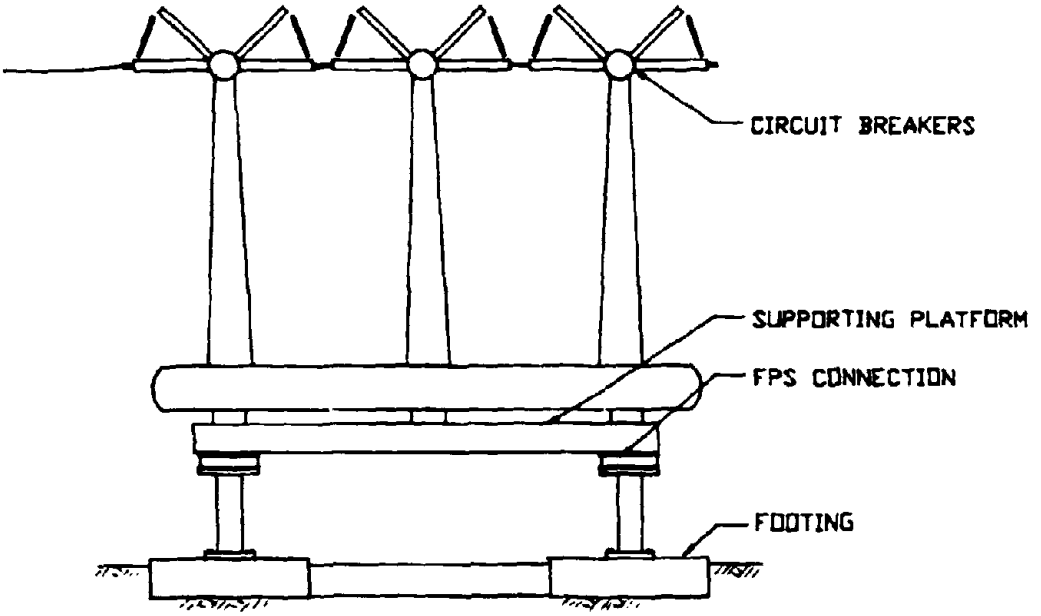

Fig. 1.13 Electrical Circuit Breakers

CHAPTER 2

FEASIBILITY OF THE FPS FOR NEW BUILDING CONSTRUCTION

by

Victor Zayas

and

Stanley Low

SECTIONS

2.1 Installation Details

The application of the FPS technique to new buildings requires the development of practical installation details which are compatible with existing construction practices. Details which could be used for the installation of FPS isolators within building frames are shown in Figs. 2.1 through 2.6.

Example details for installing the FPS connections within a building frame are illustrated in Fig. 2.1. Installation of the isolators between the foundation and first floor is the approach which has been used in completed installations of rubber bearing seismic isolators. This approach offers the advantage of simplified architectural and structural details to accommodate the seismic movements. The steel girders directly above the isolators can resist the P-Delta moments which occur in the rubber isolators because of the eccentricity of the gravity loads during earthquake movements. However, for buildings which do not otherwise require a crawl space, the addition of this partial story can be expensive.

For many buildings, it would appear that installation of seismic isolators at the tops or bottoms of the first story columns could be a more cost effective way of incorporating seismic isolation. The design and size of the FPS isolators appears to be well suited for this installation approach. The steel components of the FPS facilitates the fabrication of high strength, relatively compact isolators, which could readily fit at the top or bottoms of columns. The steel cylinder which encloses the articulated slider, provides an inherently redundant mechanism for carrying lateral and vertical loads. When located at the top of a column, the FPS connection can be installed with the concave surface facing downward. In this orientation the articulated slider remains at the centerline of the column during earthquake movements. This avoids P-Delta moments in the columns caused by eccentric gravity loads from seismic movements of the building. When installed at the bottom of a column with the concave surface facing upward, the gravity loads remain concentric on the column. A disadvantage of installing the isolators at the tops or bottoms of columns, as compared to the crawl space approach, is that additional seismic gap details for architectural components which cross the seismic gap are required.

A possible combination of the bottoms of columns approach, and the between the foundation and first floor approach, is illustrated in Fig. 2.2. Placing the FPS isolators at the bottoms of the first story columns, and using a concrete flat slab for the first floor directly above the isolators, can reduce the structural costs of the crawl space approach, and reduce the architectural detail costs associated with the bottoms of columns approach.

In some installation applications it may be desirable to include an uplift restraint detail as part of the FPS connection. An illustration of a possible uplift restraint detail is shown in Fig. 2.3. The tension rods would be able to carry tension loads and

limit uplift displacements, while permitting lateral seismic movements within the isolators.

Details which could be used to accommodate seismic movements for elevators and stairs which cross the seismic gap are shown in Fig. 2.4.

The versatility of the FPS isolators to accommodate different installation details, and any desired isolator period, can facilitate the application of seismic isolation to buildings. Illustrations of possible building applications are shown in Figs. 2.5 and 2.6. Because the FPS can absorb torsional mass eccentricities as well as the seismic deformations, the asymmetrical building shown in Fig. 2.6 could achieve seismic resistance capabilities which exceed those of a symmetrical building which relies only on ductility detailing.

2.2 Example Building

In order to investigate the technical feasibility of applying the FPS technique to new buildings, an example building was selected and redesigned using the FPS approach. The example building was used to illustrate the possible design approaches and the potential benefits. The comparative earthquake performances and construction costs are evaluated.

Earthquake Protection Systems asked Cygna Consulting Engineers of San Francisco to provide an example case of an actual building which had been designed according to the conventional building code approach. Cygna offered an example case of a three story steel moment frame building which the owner considered critical for business operations. Cygna engineers had recently designed this important "Operations Building" according to the 1985 Uniform Building Code (UBC) earthquake criteria. Since the ability to continue operations of the building after an earthquake was important, at the request of the owner, the building had been designed as an "Essential Facility" according to UBC procedures. An importance factor I of 1.5 was used, resulting in a design base shear coefficient of 0.14. The layout and details of the building's structural frame as designed by Cygna are shown in Figs. 2.7 to 2.10. Additional details on the building's design are provided in Appendix A- Sections 1 and 5.

As is common in commercial buildings of this type, the architectural design included a first story which was taller than the upper stories. The building also had relatively long girder spans of 28 ft. to 32 ft. As usually occurs in such buildings, the tall first story was more flexible than the upper stories. The UBC seismic design was controlled by drift, not strength, as is generally the case for steel moment frames. In order to control the first story drift, the design engineer was forced to use special square tubular steel columns, and imbed these columns into the foundation grade beams to create a fixed-base connection. The special tubular columns and foundation connections were high cost

structural items in the non-isolated design. The resulting seismic drifts at a base shear loading of 0.14W, were the maximum permitted by code.

The elastic and plastic strengths of the building were calculated based on the actual member sizes, and included structural redundancy effects (Appendix A - Section 5). The elastic strength was computed to be 0.31W, and the ultimate plastic strength was 0.45W. These calculated strengths are consistent with test results of the building frames, which typically show ultimate lateral strengths of 3 to 5 times the design loads.

The building site was located approximately 8 miles from the San Andreas Fault. Fig. 2.11 shows the U.S.G.S. average response spectra for magnitude 5, 6, and 7 earthquakes for a stiff soil site at a distance of 8 miles from the fault (Ref. 2.1). The UBC required design strength for a moment frame, designed with an importance factor of 1.5 is also shown. The average magnitude 7 earthquake was noted to be 5 to 10 times stronger than the required UBC design strength.

A magnitude 7 or stronger earthquake was considered to be a realistic event to expect during the life of the building. The steel frame was considered to have sufficient strength and ductility capacity to withstand the seismic deformations of a magnitude 7 earthquake with light to moderate structural damage. However, large drift deformations, substantially exceeding code allowables, and high accelerations would be expected to cause significant damage to the non-structural components and operational equipment items within the building. Such damage could render the building incapable of functioning after a severe earthquake. For these reasons, the Cygna engineers believed the application of the FPS technique would be of particular value for this type of building. The objective was to determine the extent to which the FPS isolators could reduce the estimated damage caused by large drifts occurring during severe seismic events. Cygna engineers worked together with Earthquake Protection System engineers to devise the isolation approach, and review the comparative performance and costs.

2.3 FPS Isolation Approach

Different schemes for installing the FPS isolators in the example building were considered. The advantages and disadvantages of the different schemes were considered to be as follows:

1. Tops of Lower Level Columns. Advantages: Least impact on existing design concept; and most cost effective. Disadvantage: Seismic gap details required for stairs and architectural components which cross the FPS level.

2. Bottoms of Lower Level Columns. Advantages: Small impact on existing design concept; and the design and details are similar to a standard base plate connection. Disadvantages: Special details

would be required for stairs and and architectural components to accommodate the seismic gap at FPS level; and the pinned column base would require strong and stiff tubular columns with equal stiffness in both the x and y axes to control the deflections of the lower story.

3. Between Foundation and First Floor. Advantages: Simple details for stairs and and architectural components; and the accelerations of the first story floor would also be reduced. Disadvantages: Configuration and expensive construction changes would be required to add the isolation story; including deeper excavation for the foundation and the added structural floor framing.

After comparing the alternatives, the design with the FPS on top of the lower level columns was considered the preferred isolation scheme for this building. This approach was the most cost effective, and also minimized the need for design and configuration changes. The structural frame and isolator details using the FPS at tops of the lower level columns are shown in Figs. 2.12 to 2.15. Architectural details to accommodate the seismic movements are shown in Figs. 2.16 to 2.19.

Based on dynamic analyses results (Appendix A, Sections 5 to 8), a sliding period of 2.25 secs., a dynamic friction coefficient of 10%, and a lateral sliding capacity of 6.5 inches were selected for the design of the FPS isolators. The dynamic analyses predicted an isolator sliding displacement of 4.7 inches for the magnitude 7 earthquake loading. The required lateral displacement capacity according to Section B of the Tentative Seismic Isolation Design Requirements (Ref. 2.2) was computed to be 4 inches (Appendix A, Section 3). The isolator design exceeded the minimum requirements of the SEAOC guidelines because the magnitude 7 earthquake loading exceeded the seismic loading used to develop the minimum criteria of the SEAOC guidelines.

Placement of the FPS isolators at the tops of the lower level columns resulted in a hinge connection at this joint. The columns below the FPS were changed from special steel columns to reinforced concrete columns which were integral with the foundation. The higher section modulus of the concrete columns reduces the drift at the first level, and results in equal column stiffness in the two loading directions. Since the FPS isolators would provide the necessary deformation and ductility capacity, the lower ductility capacity of the concrete columns versus the steel columns was not considered a disadvantage for the isolated design.

Two different structural design criteria for the isolated building were examined. In the first, the strength and stiffness of the structural frame were assumed to be the same as the original non-isolated design ("Full Strength Isolated Design"). In the second, the sizes of the structural members were reduced to the degree that the structural savings could offset the cost of adding the FPS isolators ("Cost Equivalent Isolated Design"). The redesigned structural frame of the cost equivalent design is shown in Figs. 2.12 to 2.14, and is discussed below. The full strength

isolated design was assumed to have the same structural configuration as the cost equivalent design, but with the strength and stiffness of the structural members equal to those of the original non-isolated design.

2.4 Cost Equivalent Design

The "Cost Equivalent" isolated building design was used to determine the feasibility of achieving increased earthquake resistance capacity without increasing construction costs. The design base shear coefficient was 0.067, as compared to 0.14 for the original non-isolated design. This 50% reduction in the design base shear permitted enough savings in the structural frame to offset the added structural and architectural costs associated with the isolated design. The base shear coefficient of 0.067 is the calculated design base shear required by the 1985 UBC if the isolator sliding period of 2.25 secs. is used as the building period in the UBC formulas. The cost equivalent isolated design was also checked against the "Tentative Seismic Isolation Design Requirements" of SEAONC [Ref. 2.2], and also complied with these guidelines. Additional details on the checks with the UBC and SEAOC design criteria are provided in Appendix A.

As was the case for the non-isolated design, the seismic design of the cost equivalent building was controlled by interstory drift. The resulting seismic drifts at a base shear loading of 0.067 were the maximum permitted by code. The elastic and plastic strengths of the cost equivalent design were calculated based on the reduced member sizes, including structural redundancy effects. The elastic strength was computed to be 0.14W, and the ultimate plastic strength 0.31W (Appendix A - Section 5).

The savings in the structural steel and foundation details permitted by use of the isolation approach was estimated to offset the cost of the 32 FPS isolators and the architectural and structural details required for the seismic gap. A summary of the estimated structural savings and isolation costs is given in Table 2.1. Thus, the estimated construction cost of the isolated design was approximately equal to the cost of the non-isolated design. The construction cost of the full strength isolated design was estimated to be approximately 1.8% greater than the non-isolated design. Additional details on the redesign details and cost estimates are provided in Appendix A, Section 4.

2.5 Comparison of Building Performance With and Without the FPS

Time history dynamic analyses were used to compare the earthquake performance of the isolated designs to the original design. To do this comparison, scaled earthquake loadings representing magnitude 5, 6 and 7 earthquakes were used in the non-linear analysis program Dynin (Ref. 2.3).

The Dynin models of the non-isolated and isolated structures

are shown in Appendix A, Section 5. A stick model was used with nodal masses representing the second floor, third floor, and roof. The structures were analyzed as elastic upper structures on non-linear FPS isolators. The stiffness of each building level was derived from the section properties of the corresponding structure. The nonlinear properties of the FPS isolators were included in the modeling of the first level. Analyses results for seismic drifts occurring within the structural frame were used to estimate damage to the building.

Additional analyses of this building, including inelastic modeling of the upper structure, are presented in Chapters 6 and 7. As discussed in Chapters 7 and 8, for a building in this period range, the total seismic drifts which occur are approximately the same whether the building is isolated or not, and whether the upper structure remains elastic or is permitted to yield. The primary effect of the isolators is that a reduced percentage of the total drift occurs within the structural frame. Similarly with an inelastic model of the upper structure, it is primarily the distribution of drifts among stories which is affected by the inelastic response, not the total drift. The elastic upper structure model was, therefore, considered sufficient for design development, and for non-structural damage estimates which are based on total drift. The non-isolated building would not be capable of achieving the story shears predicted by the elastic upper structure model. However, the predicted elastic shears are a measure of the earthquake loading demand on the structural frame. Analyses results for the ductility demand, energy absorption demand, and inelastic structural drifts using inelastic structural models of the upper structure are presented in Chapters 6 and 7. The inelastic analyses results presented in Chapters 6 and 7 confirm the overall results and conclusions drawn from the analyses of the elastic models presented in this Chapter.

The input earthquake loadings were scaled to approximately represent the average spectra for magnitude 5, 6, and 7 earthquakes at a distance of 8 miles from the site. Values obtained for base shear, story shears and story drifts were used to compare the response of the isolated and non-isolated buildings. Comparisons of the base shear responses for the simulations of the three different magnitude events are shown in Fig. 2.20.

The earthquake loading used to represent a magnitude 5 earthquake was the El Centro earthquake scaled to a PGA of 0.15g and the time scale compressed to one-half. The response spectra plots and the tabulated analytical results are given in Appendix A, Section 6. This low intensity earthquake shaking is of comparable strength to the UBC design strength. The resulting base shear was 0.08, with or without the FPS. Since the FPS isolators had a threshold friction force of 0.10, the FPS isolators did not slide, and the building response was the same with or without the FPS . Analysis results indicated that story drifts for the isolated and non-isolated designs would be less than the UBC code allowable drifts, and no building damage was anticipated for any of the designs at this strength event.

The earthquake loading used to represent a magnitude 6 event was the El Centro earthquake scaled to a PGA of 0.34g and run at full time scale. The response spectra plots and the tabulated analytical results are shown in Appendix A, Section 7. The results show that in the isolated design structures, the base shear was reduced from 0.54g to 0.14g, and the 1st story drift was reduced from 2.28" to 0.54". This is a 74% reduction in base shear force and story drift. The responses of the cost equivalent and full strength isolated designs were approximately the same. The FPS travel displacement was calculated to be about 1.7 inches.

The earthquake loading used to represent a magnitude 7 event was the El Centro earthquake scaled to a PGA of 0.70g and run at full time scale. The response spectra plots and the tabulated analytical results are shown in Appendix A, Section 8. The results show that in the isolated structures, the base shear was reduced from 1.11g to 0.21g and the 1st story drift was reduced from 4.64" to 0.74". This is a 81% reduction in base shear force and story drift. The FPS displacement travel was calculated to be 4.70 inches.

A summary of the analytical results for both the isolated and the non-isolated structures is shown in Figs. 2.20 to 2.22. Fig 2.20 shows the large reductions in base shear demand that were predicted for the isolated structures for the magnitude 6 and 7 earthquakes. Figs. 2.21 and 2.22 show the reductions in story shears and drifts within the building for a magnitude 7 earthquake. These predicted reductions in story shears and drifts would be expected to reduce building damage during the magnitude 7 event.

Fig. 2.23 shows damage estimates for the magnitude 6 and 7 earthquakes. Damage estimates for the non-isolated building were made using the ATC-13 "Earthquake Damage Evaluation Data For California", as estimated for low rise steel moment frame buildings. Damage estimates for the isolated designs were calculated by using the damage estimates for the non-isolated design, but for reduced earthquake strengths which would result in equivalent structural drifts as those of the isolated designs. The cost of construction of the Operations Building was approximately $6.5 million. Based on the comparative drifts for the reduced strength isolated design and the full strength non-isolated design, it was estimated that the FPS would reduce building damage for the magnitude 7 event from $1,300,000 to $138,450, a reduction of approximately 89%. Additional details and calculations of the building damage estimates are provided in Appendix A, Section 9.

The predicted reductions in story shears and accelerations (Figs. 2.21 and 2.22) would be expected to also reduce damage to the equipment and other building contents. However, within the scope of this study it was considered that there were no reliable ways of making preliminary damage estimates for the building contents.

2.6 Conclusions

The versatility of installation details offered by the FPS isolators could help achieve isolated buildings which are cost equivalent to non-isolated buildings, and yet have significantly improved earthquake performance.

The analysis results for the example building indicated that the cost equivalent isolated design would provide better seismic performance than the full strength non-isolated design. Building damage was reduced by an estimated 89%.

In summary, it was feasible and practical to incorporate the FPS into the design of a new building. A cost equivalent design could be achieved, and the seismic performance was substantially improved as compared to the non-isolated design. However, further evaluations are required to evaluate the application of the technique to different types of structures, and in buildings designed for normal occupancy as opposed to essential facilities.

2.7 References -- Chapter 2

2.1 Joyner, W. B., and Fumal, T. E., "Predictive Mapping of Earthquake Ground Motion," U.S. Geological Survey Professional Paper 1360, U.S. Geological Survey, Menlo Park, California 94025, 1985.

2.2 "Tentative Seismic Isolation Design Requirements," Base Isolation Subcommittee of the Seismology Committee, Structural Engineers Association of Northern California, September 1986.

2.3 Khatib, I. and Mahin, S., "DYNIN -- Interactive computer Program for the Nonlinear Dynamic Analysis of Buildings," SEMM Computer Program, University of California, Berkeley, 1987.

Table 2.1 Summary of Savings and Costs

Structural Savings	
1. Reductions in structural frame due to reduced lateral loads.	$82,000
2. Reductions in foundation costs.	$34,000
	$116,000
Added Structural Costs	
1. 32 FPS Seismic Isolators	$64,000
2. Bracing for exterior panel at 1st. level.	$15,000
	$79,000
Net Structural Savings	$37,000
Added Architectural Costs	$17,000
Contingencies & Miscellaneous	$20,000
Net Savings and Costs	$0

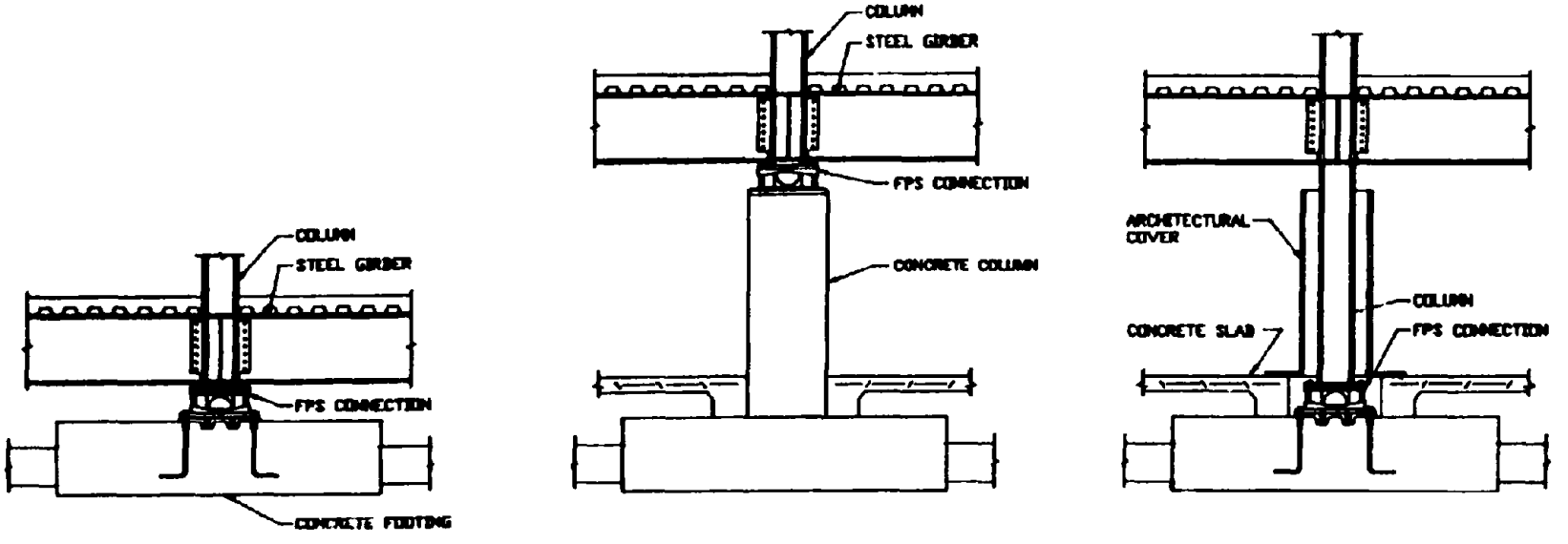

BETWEEN FOUNDATION AND FIRST FLOOR

AT TOP OF COLUMN

AT BOTTOM OF COLUMN

Fig. 2.1 FPS Installation Details

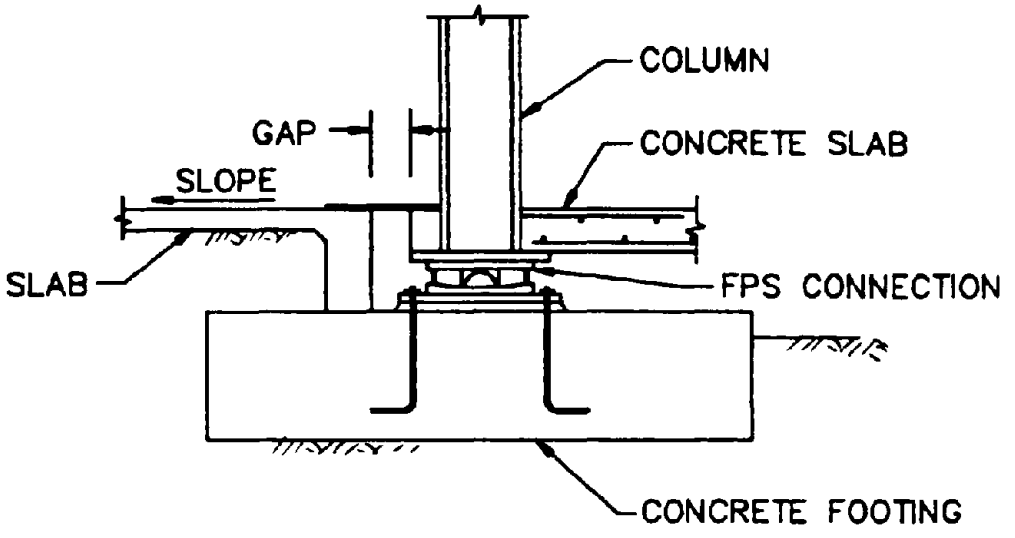

Fig. 2.2 Installation With Flat Slab Floor

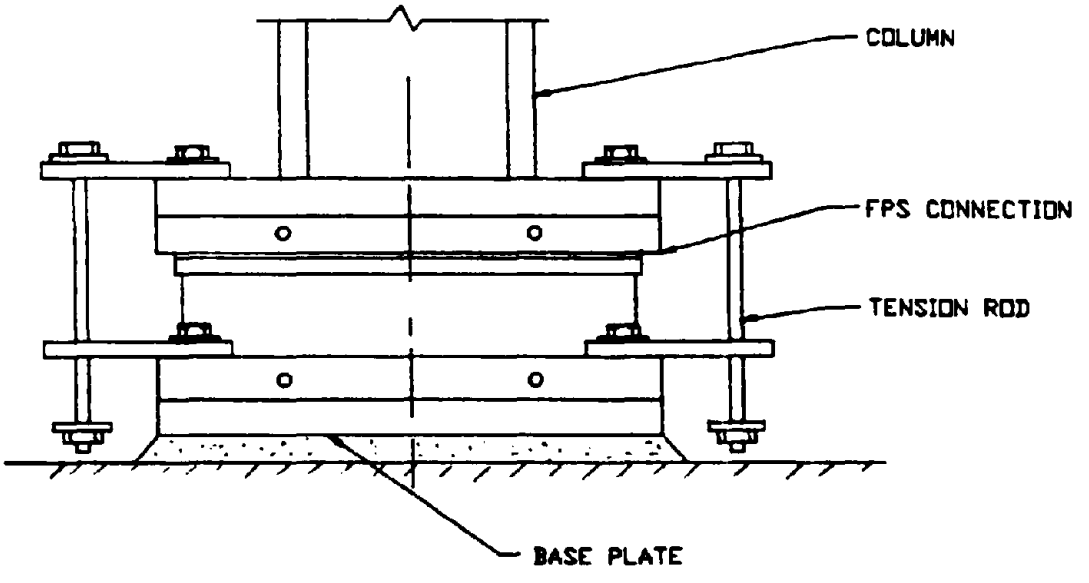

Fig. 2.3 FPS Connection With uplift Rest aint

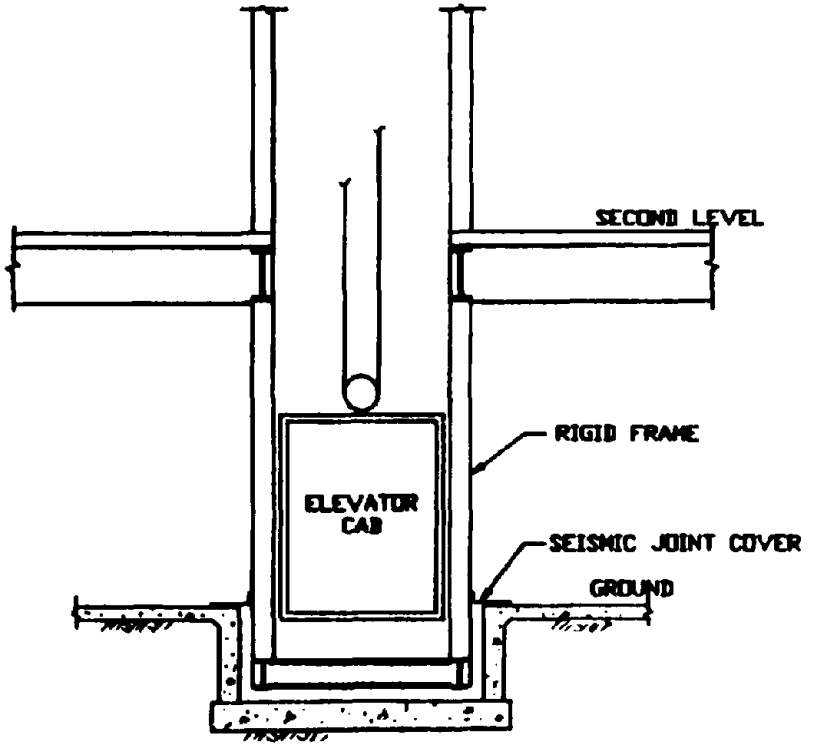

ELEVATOR DETAIL

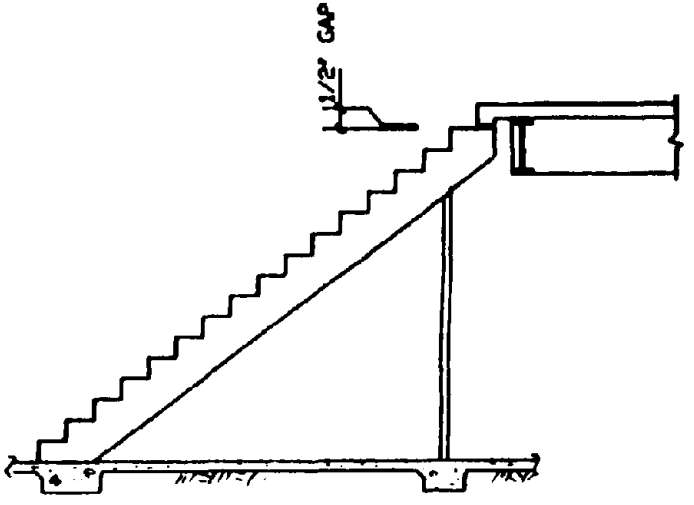

STAIR DETAIL

Fig. 2.4 Elevator and Stair Details

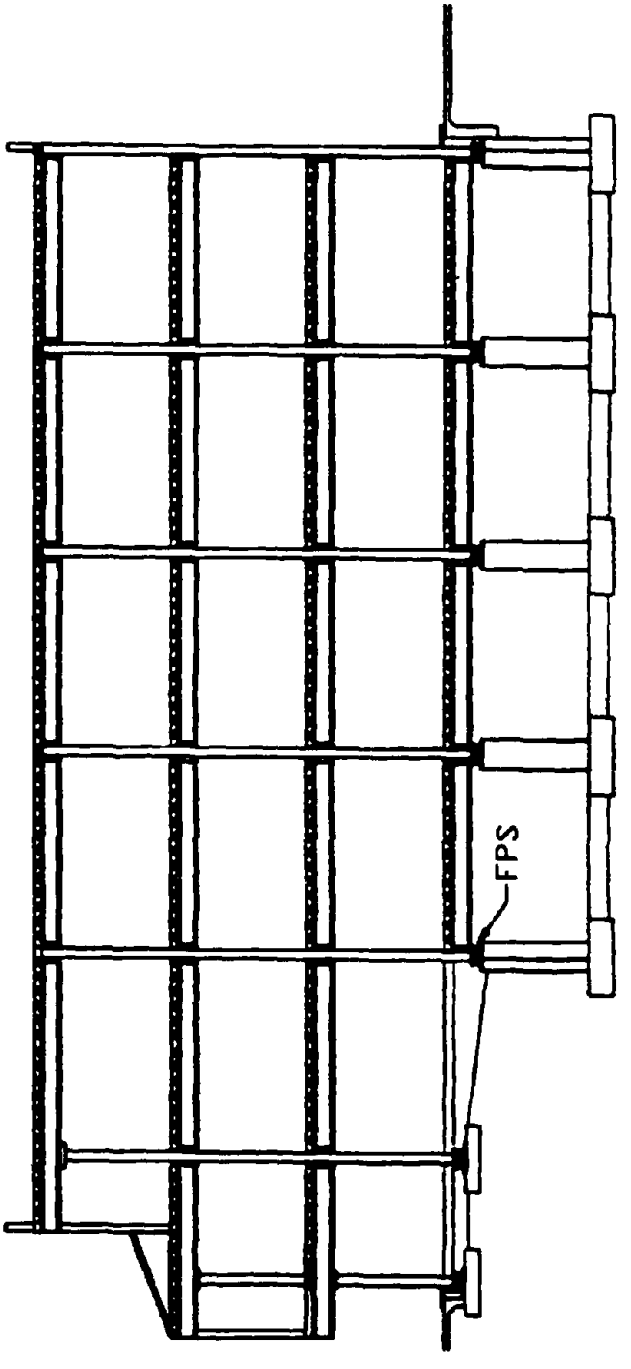

Fig. 2.5 Application for Low Rise Building

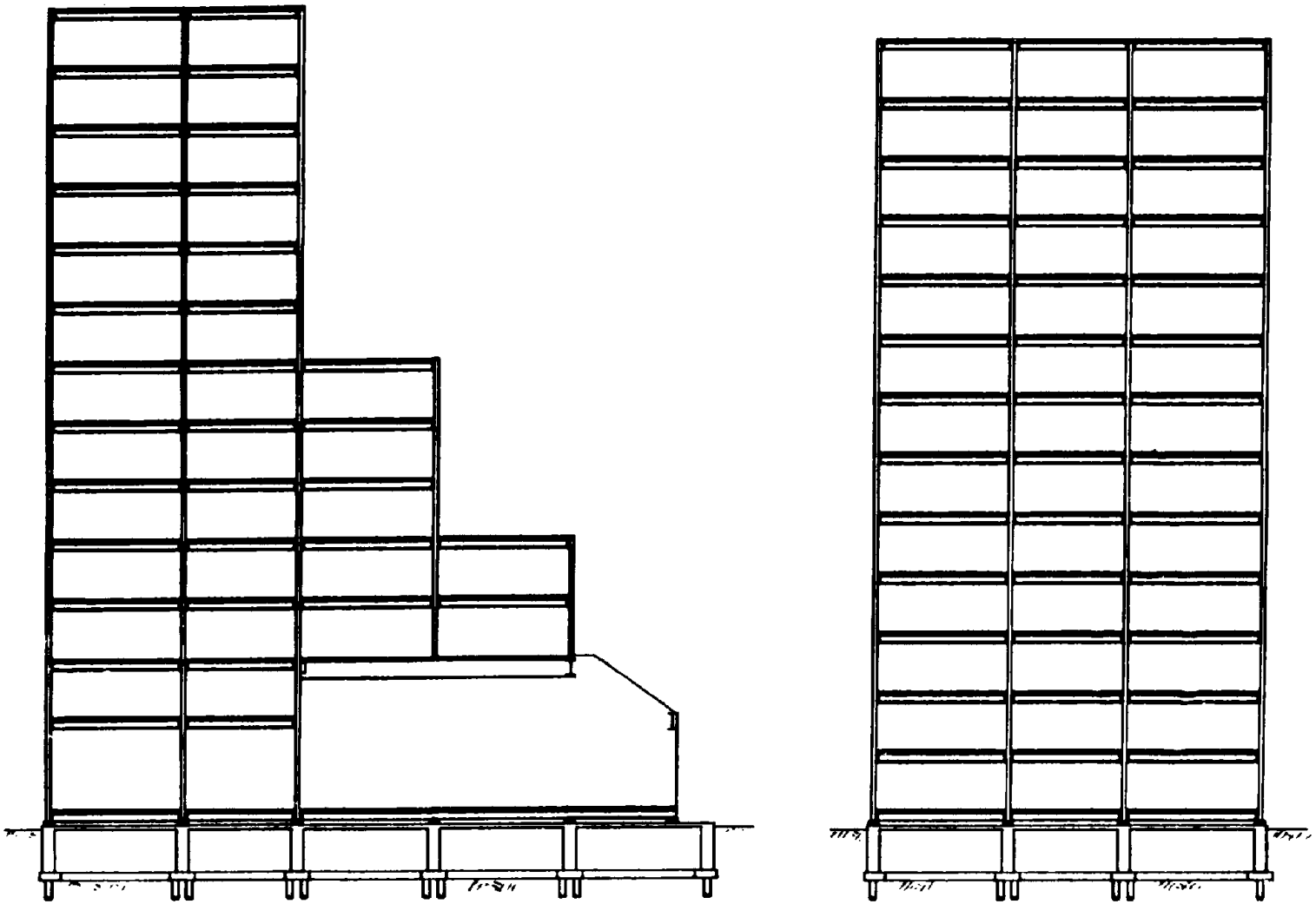

Fig. 2.6 Application for Symmetrical and Asymmetrical Building

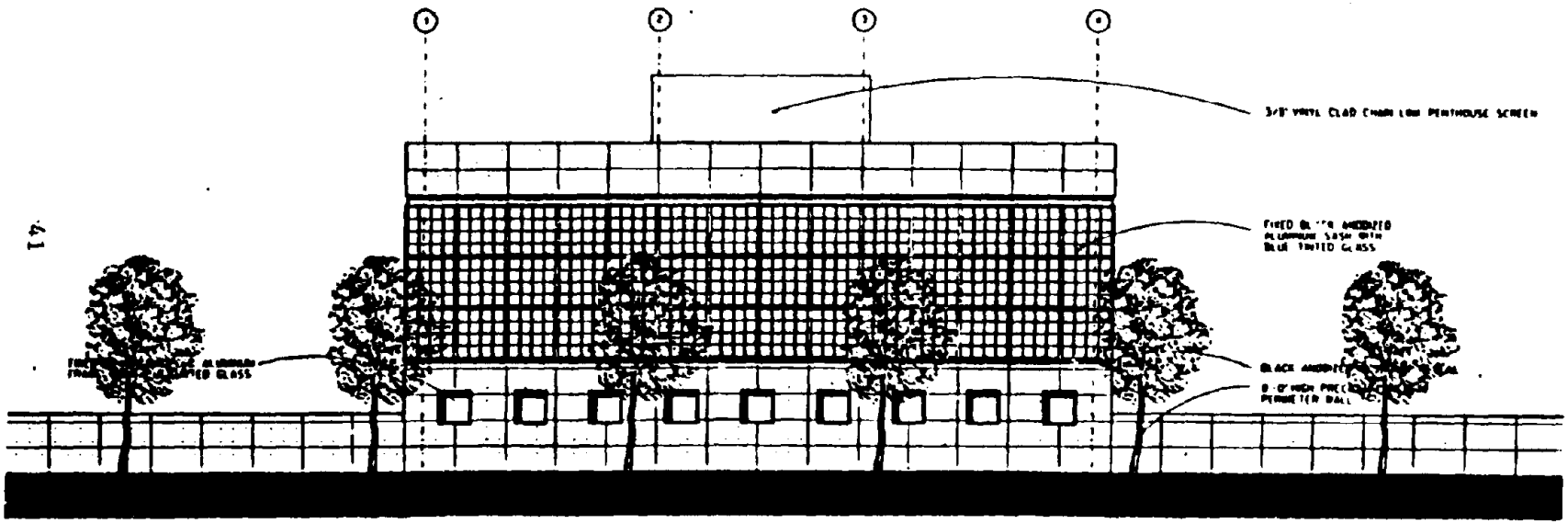

Fig. 2.7 Elevation of Operations Building

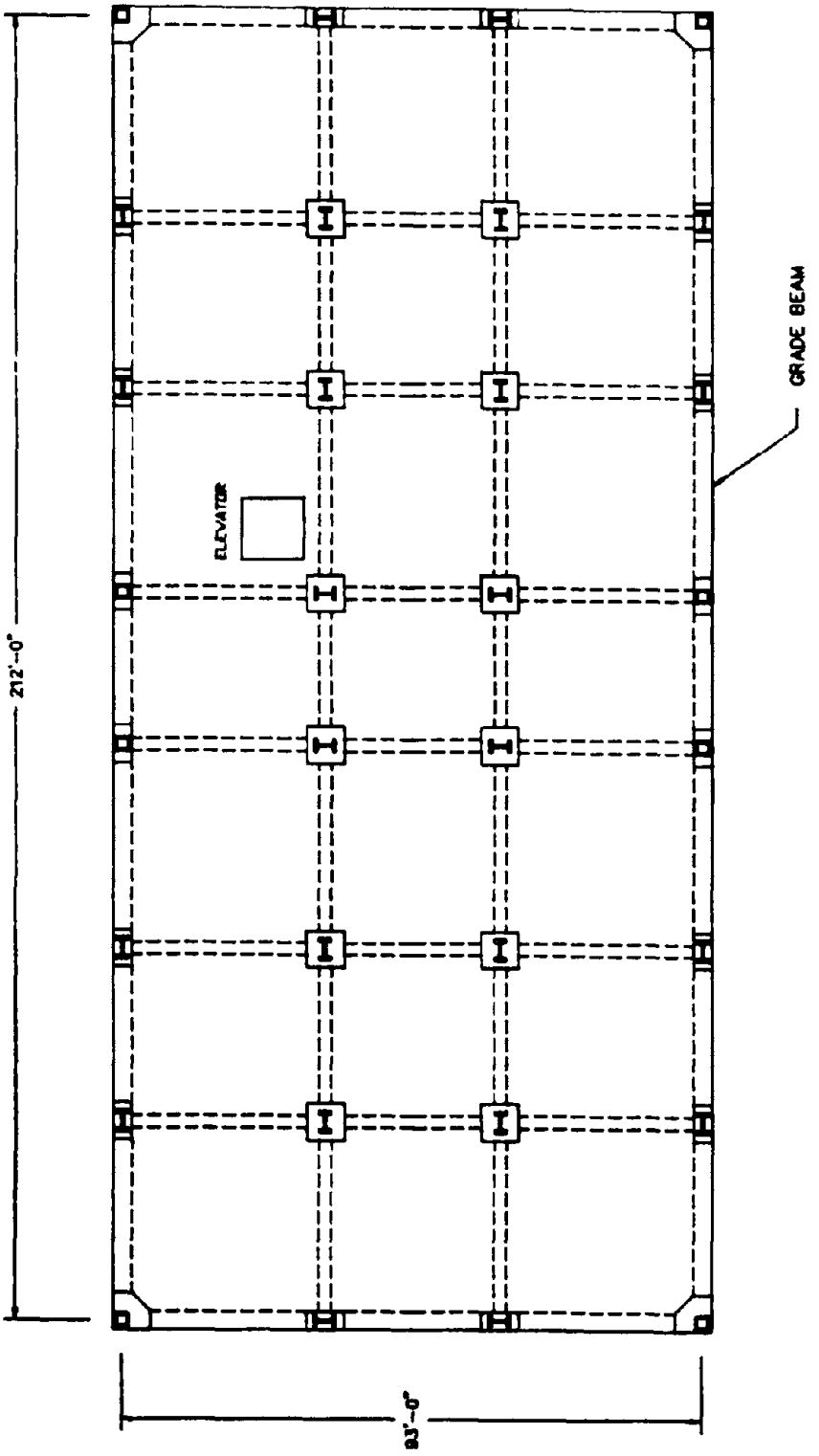

Fig. 2.8 Non-Isolated Foundation Plan

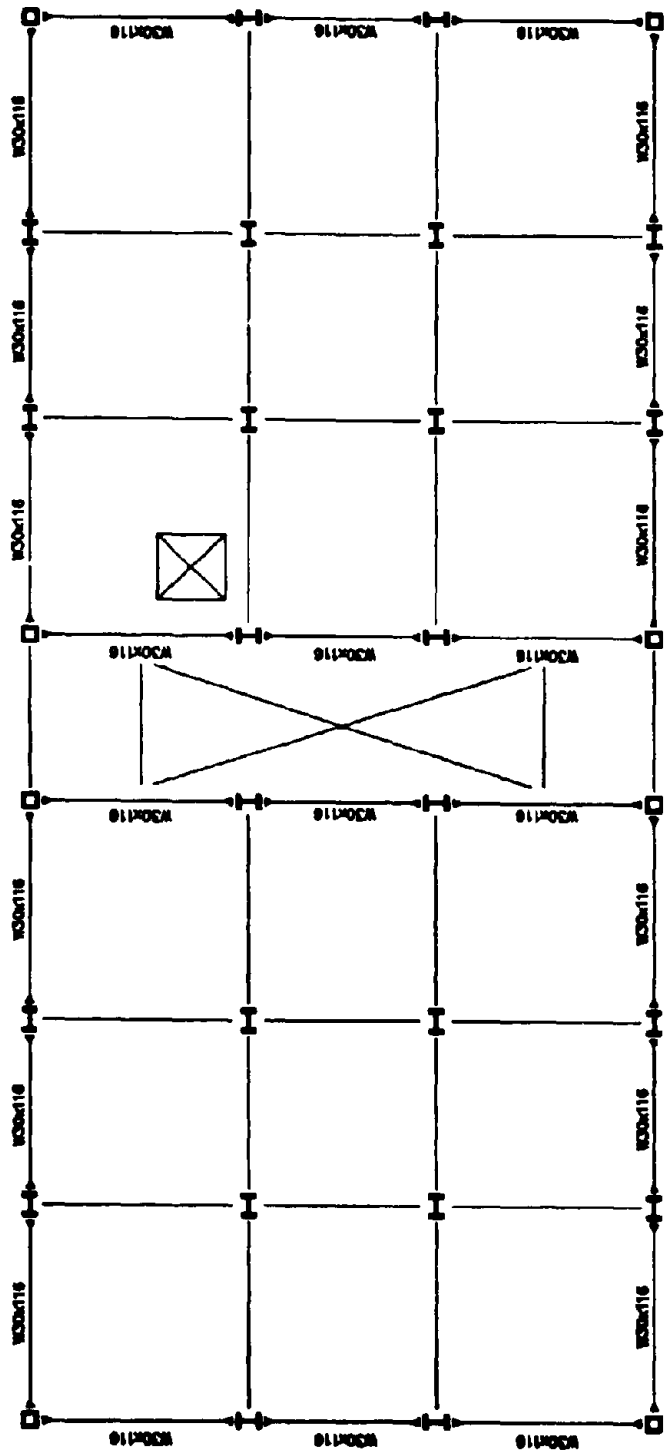

Fig. 2.9 Non-Isolated Framing Plan

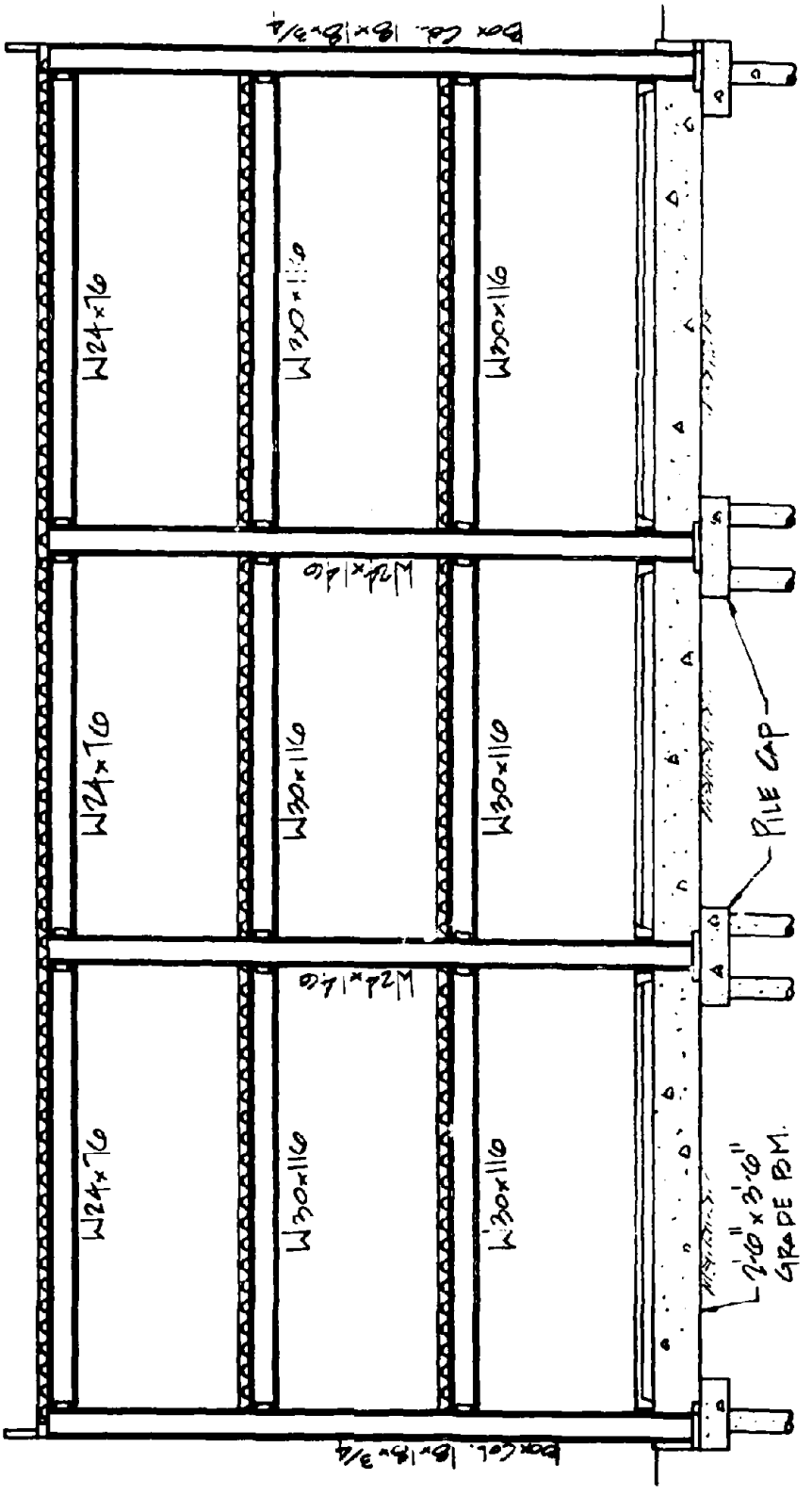

Fig. 2.10 Non-Isolated Building Section

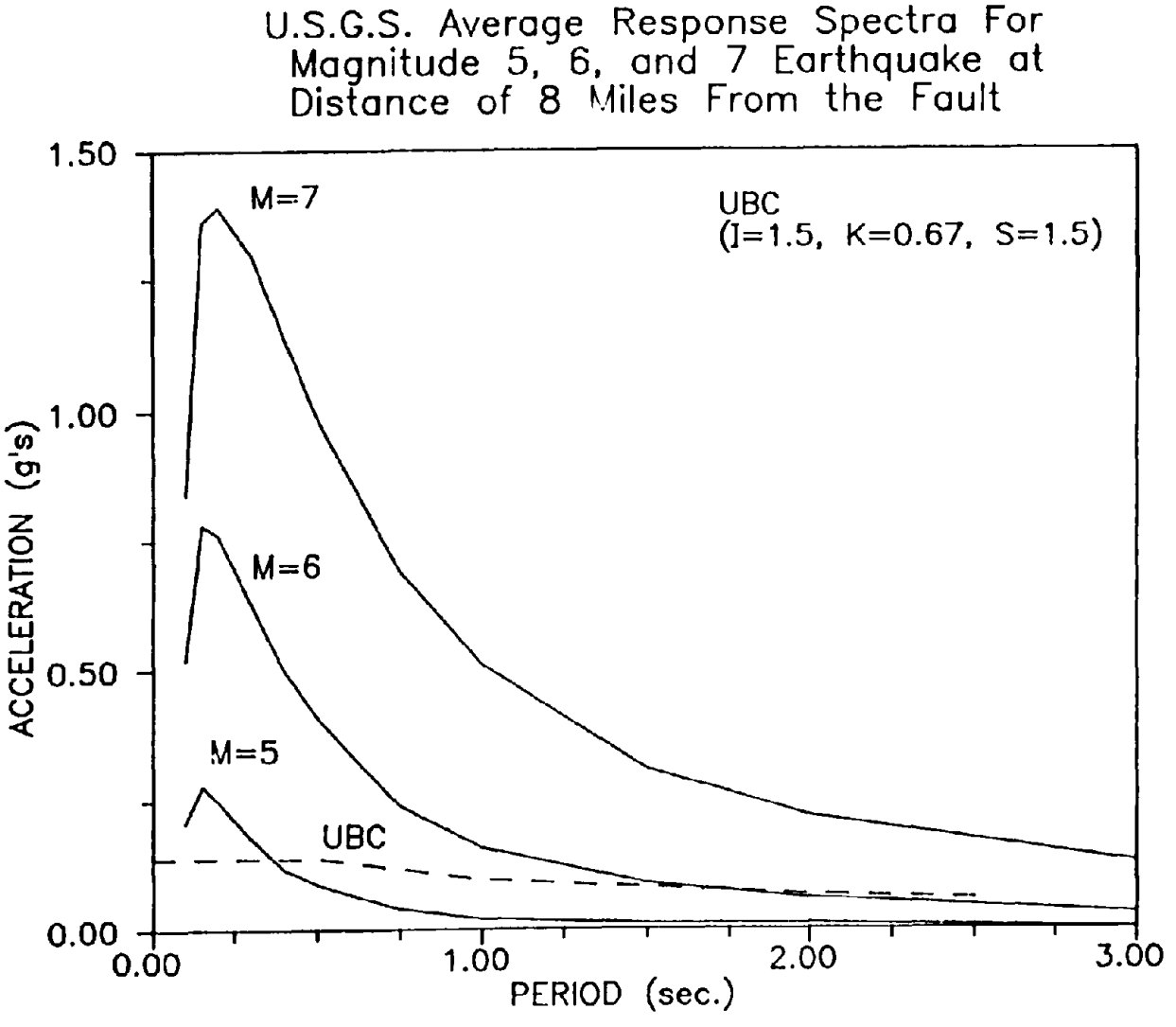

Fig. 2.11 Site Spectra

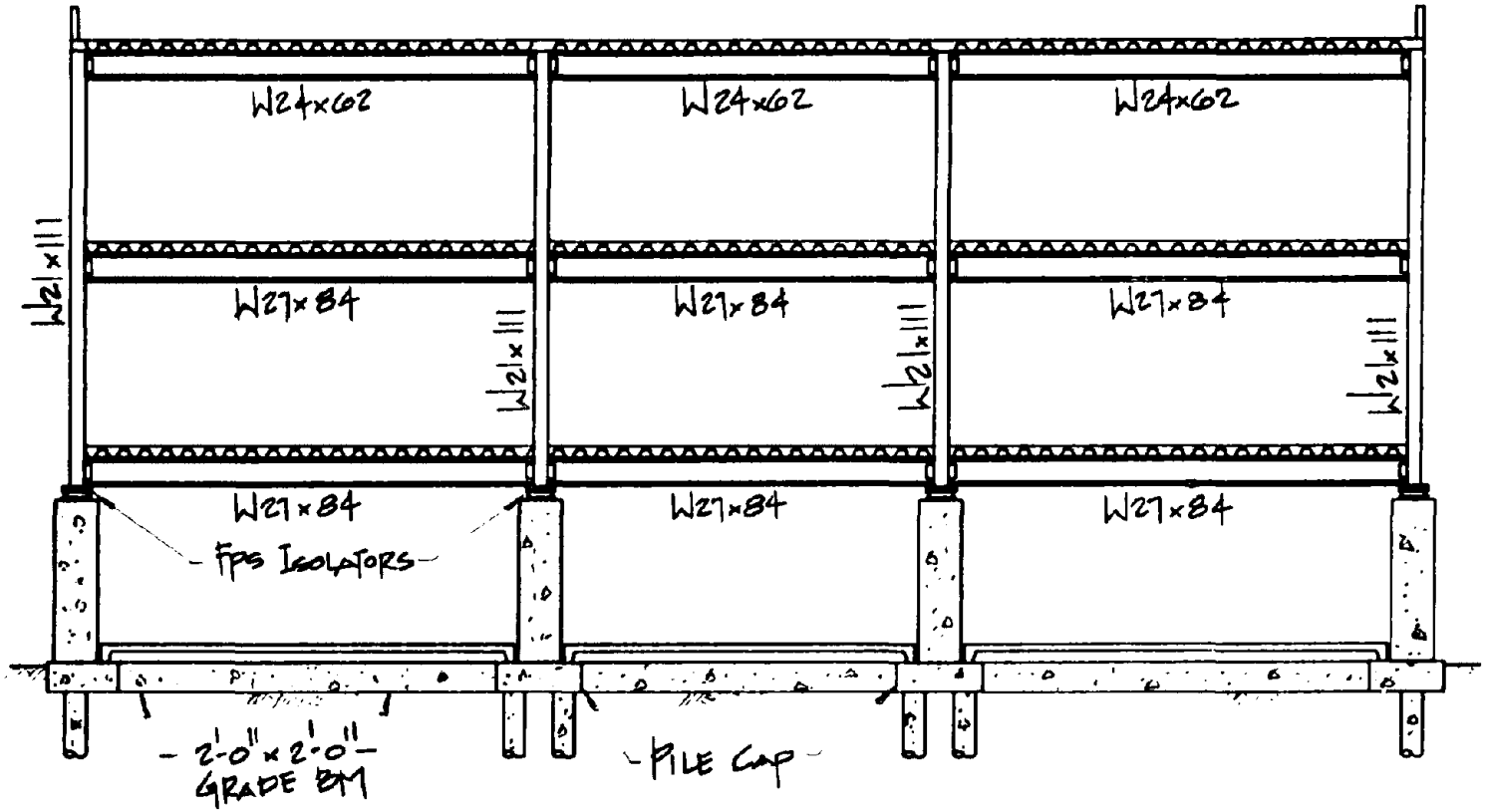

Fig. 2.12 FPS Isolated Building Section

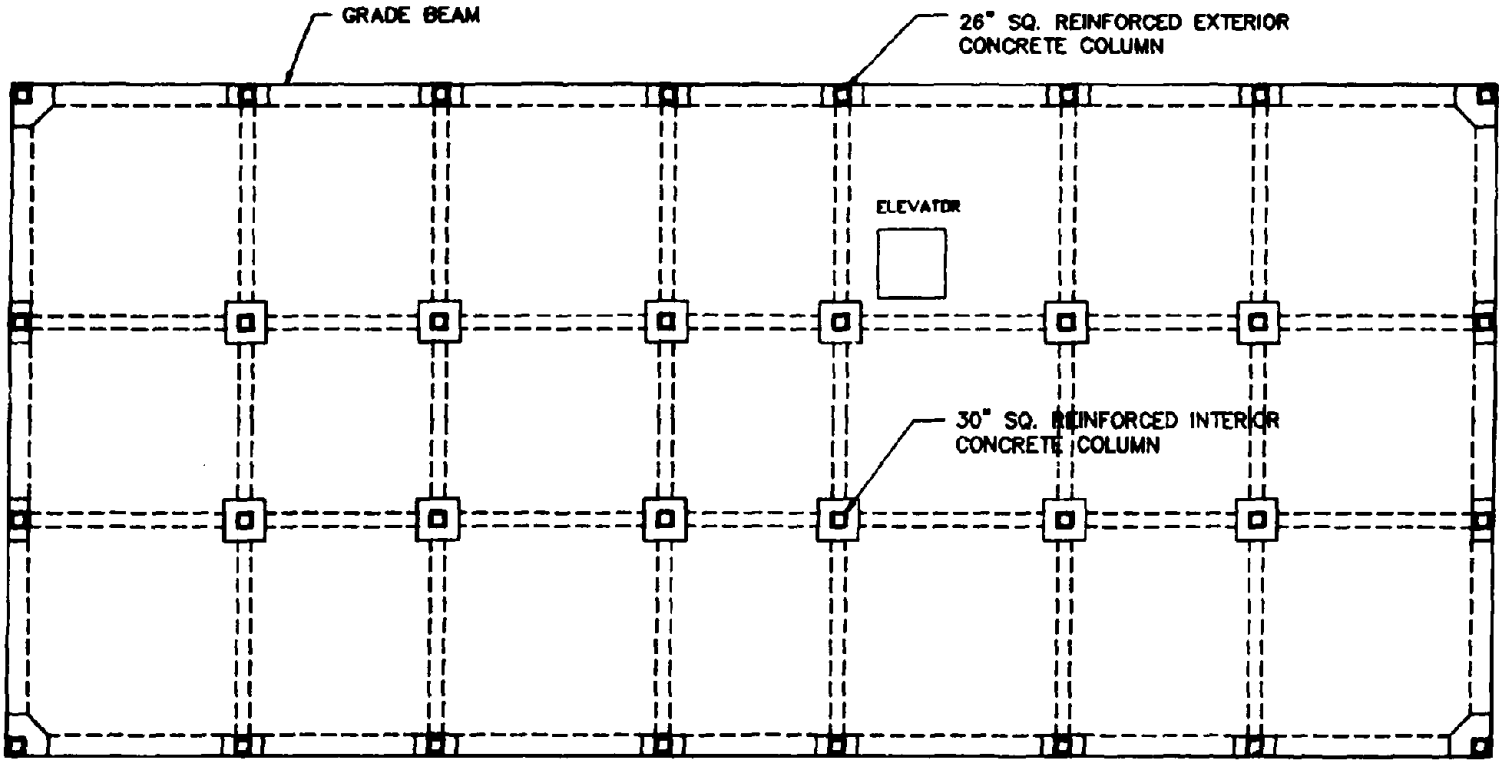

Fig. 2.13 FPS Isolated Foundation Plan

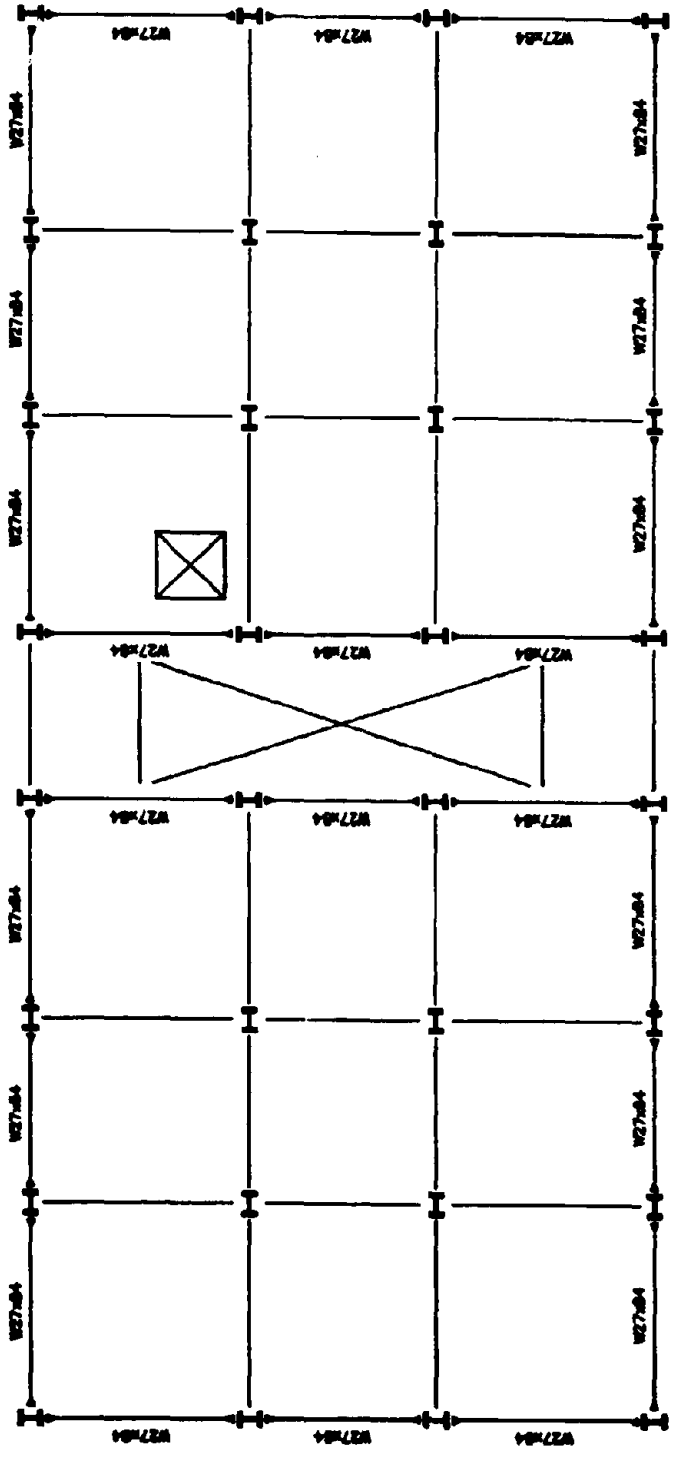

Fig. 2.14 FPS Isolated Framing Plan

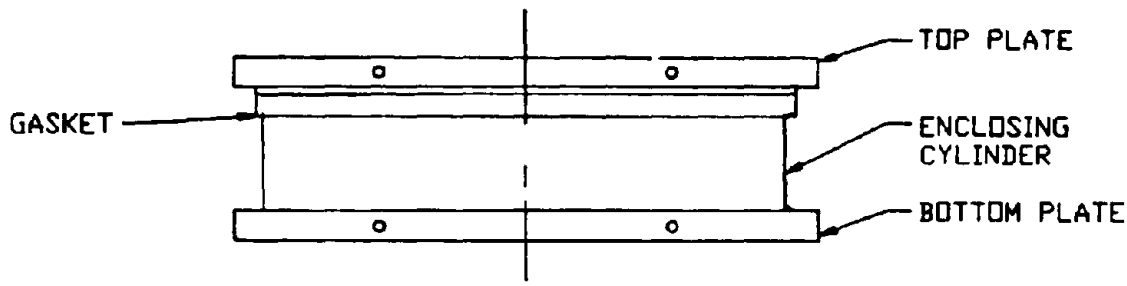

FPS ISOLATOR ELEVATION

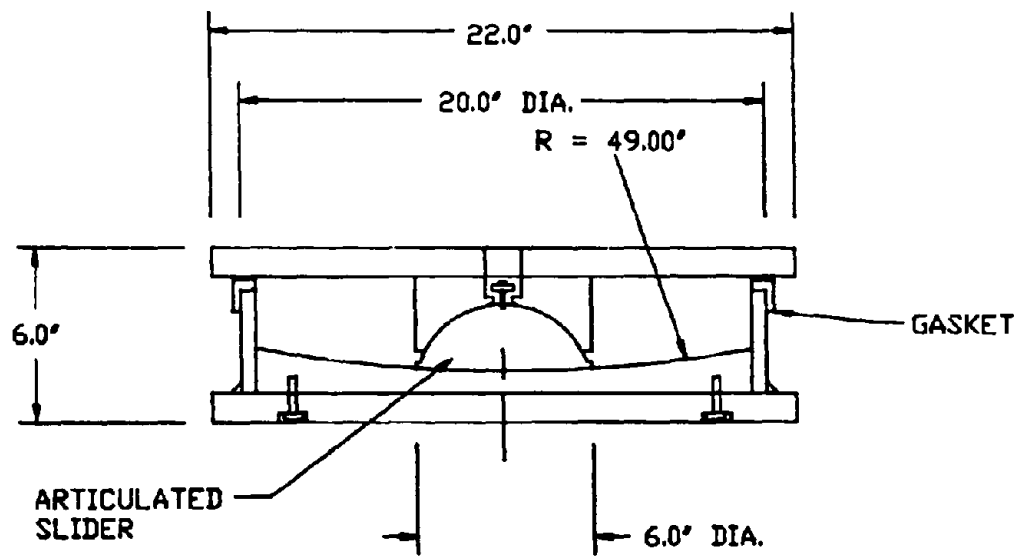

FPS ISOLATOR SECTION

Fig. 2.15 FPS Isolator Details

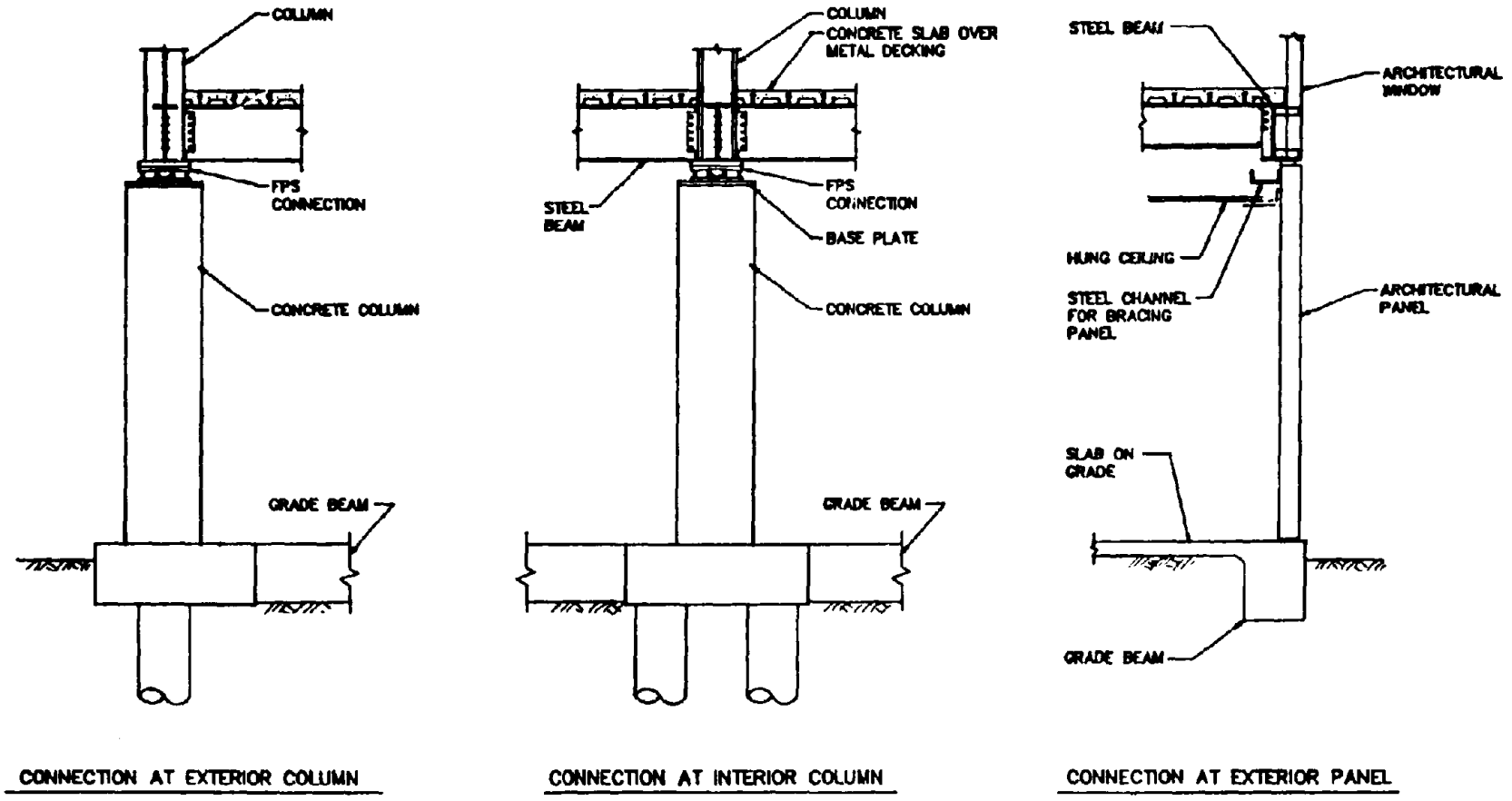

Fig. 2.16 FPS Connection Details

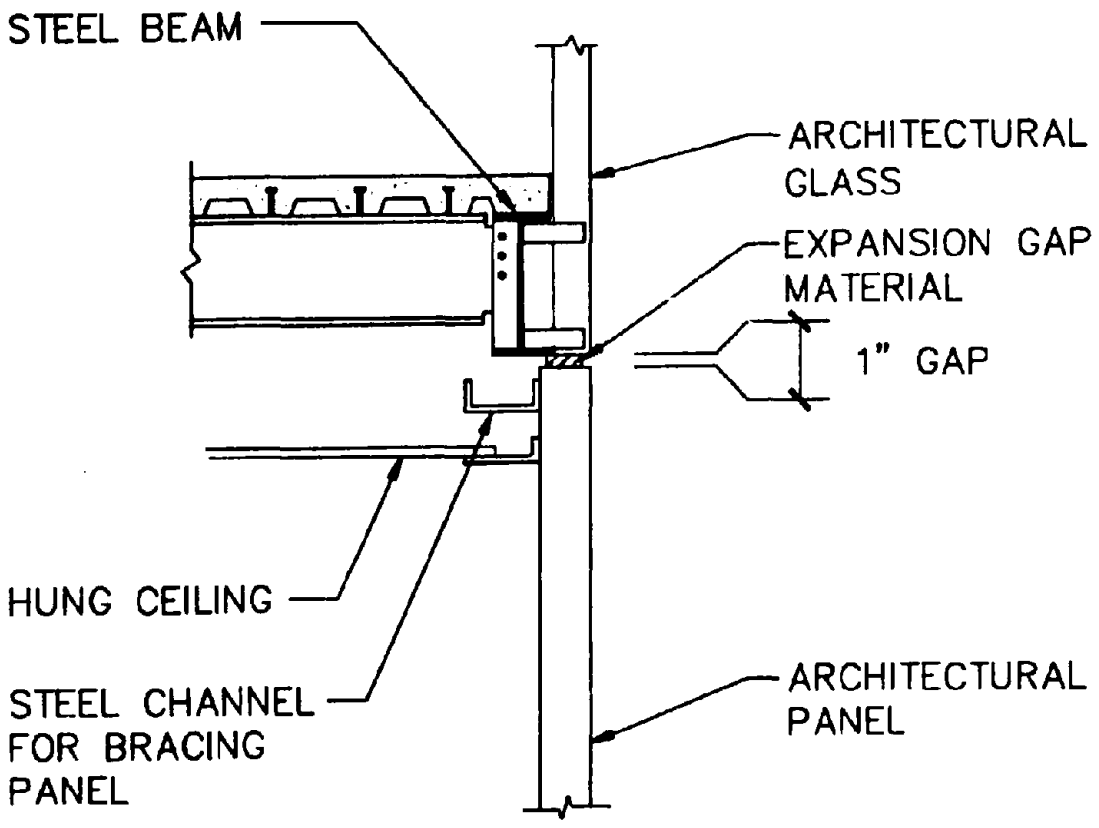

Fig. 2.17 Architectural Facial Connection

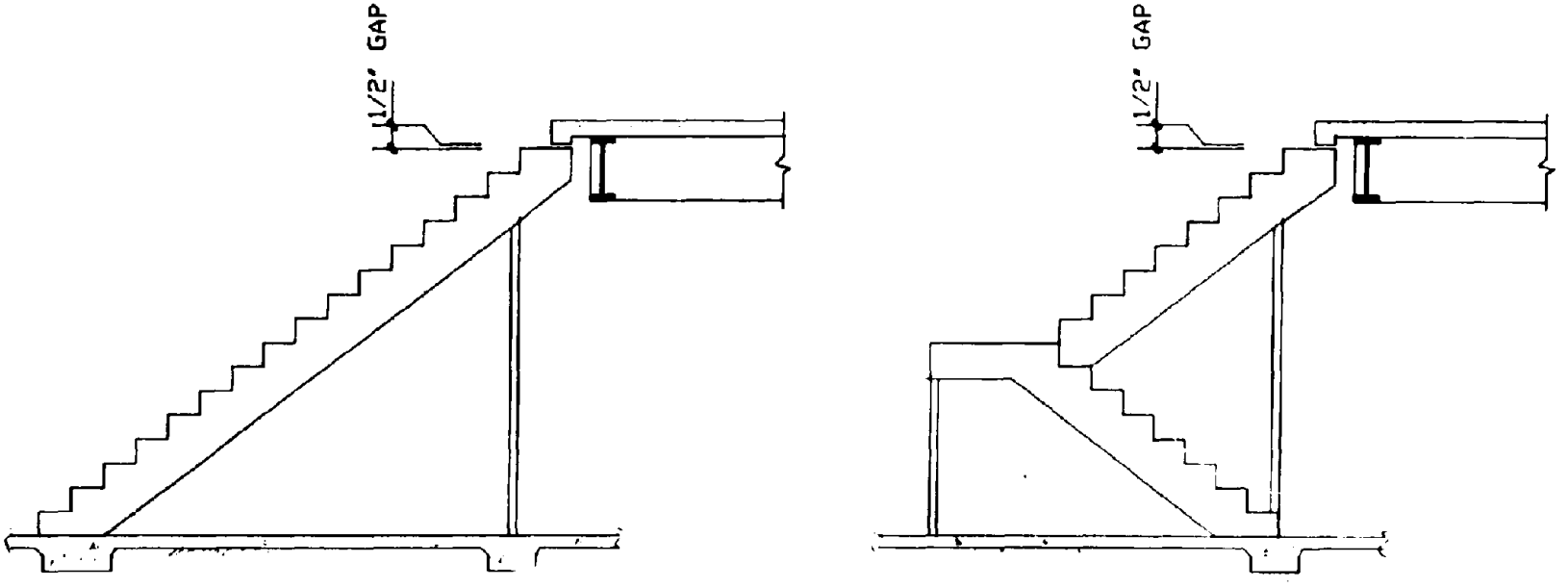

Fig. 2.18 Stair Detail

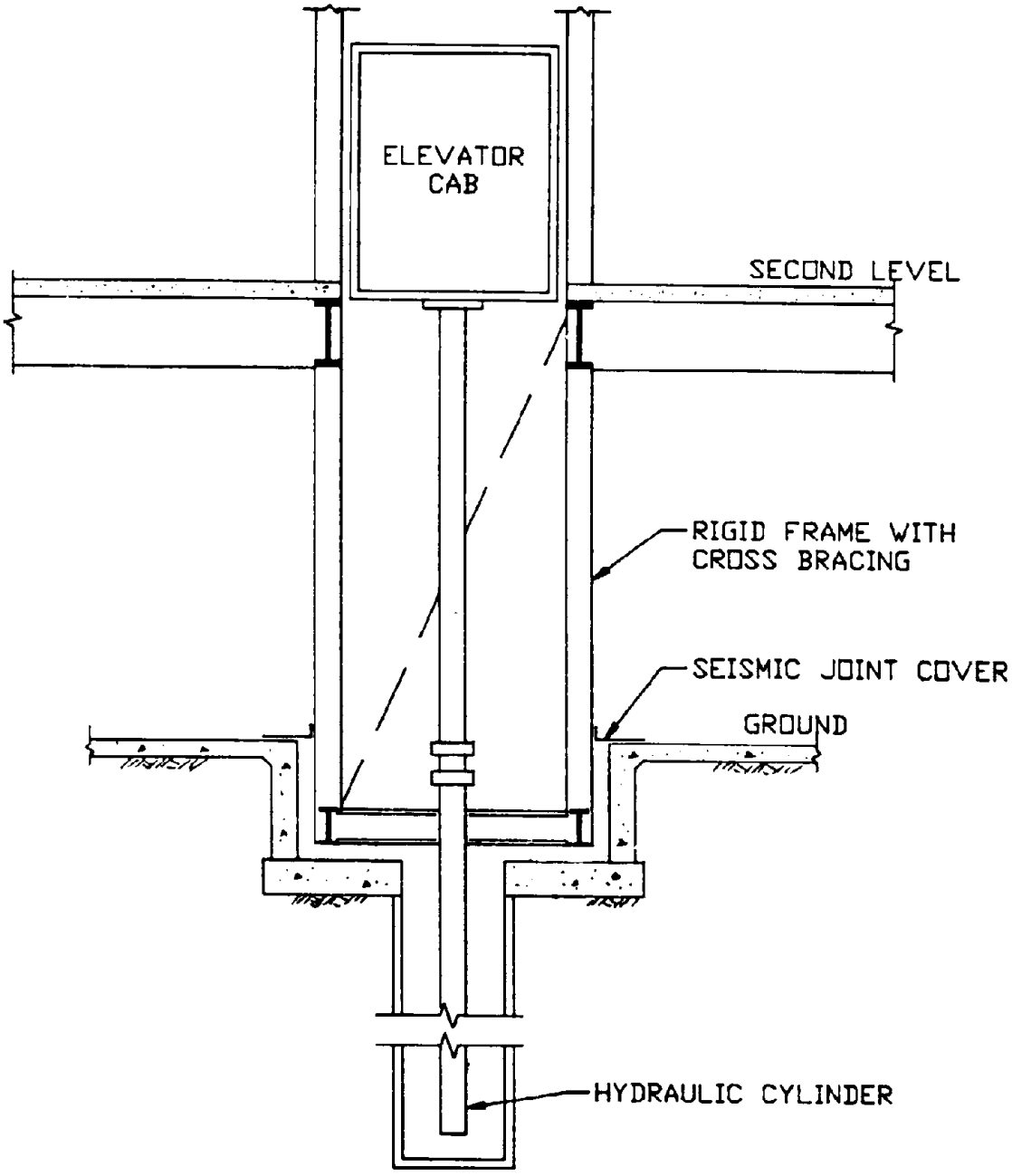

Fig. 2.19 Elevator Detail

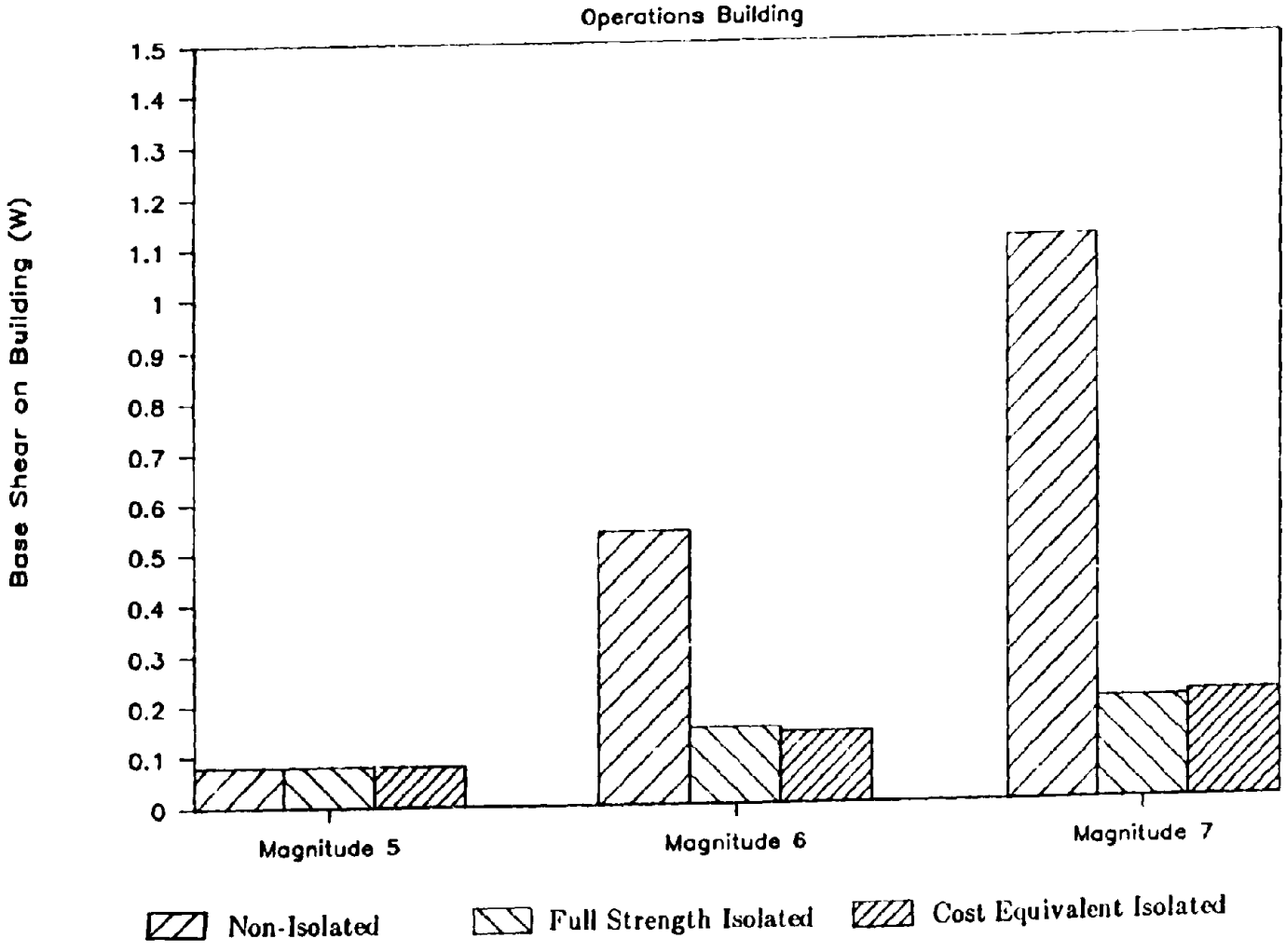

Fig. 2.20 Comparisons of Base Shears

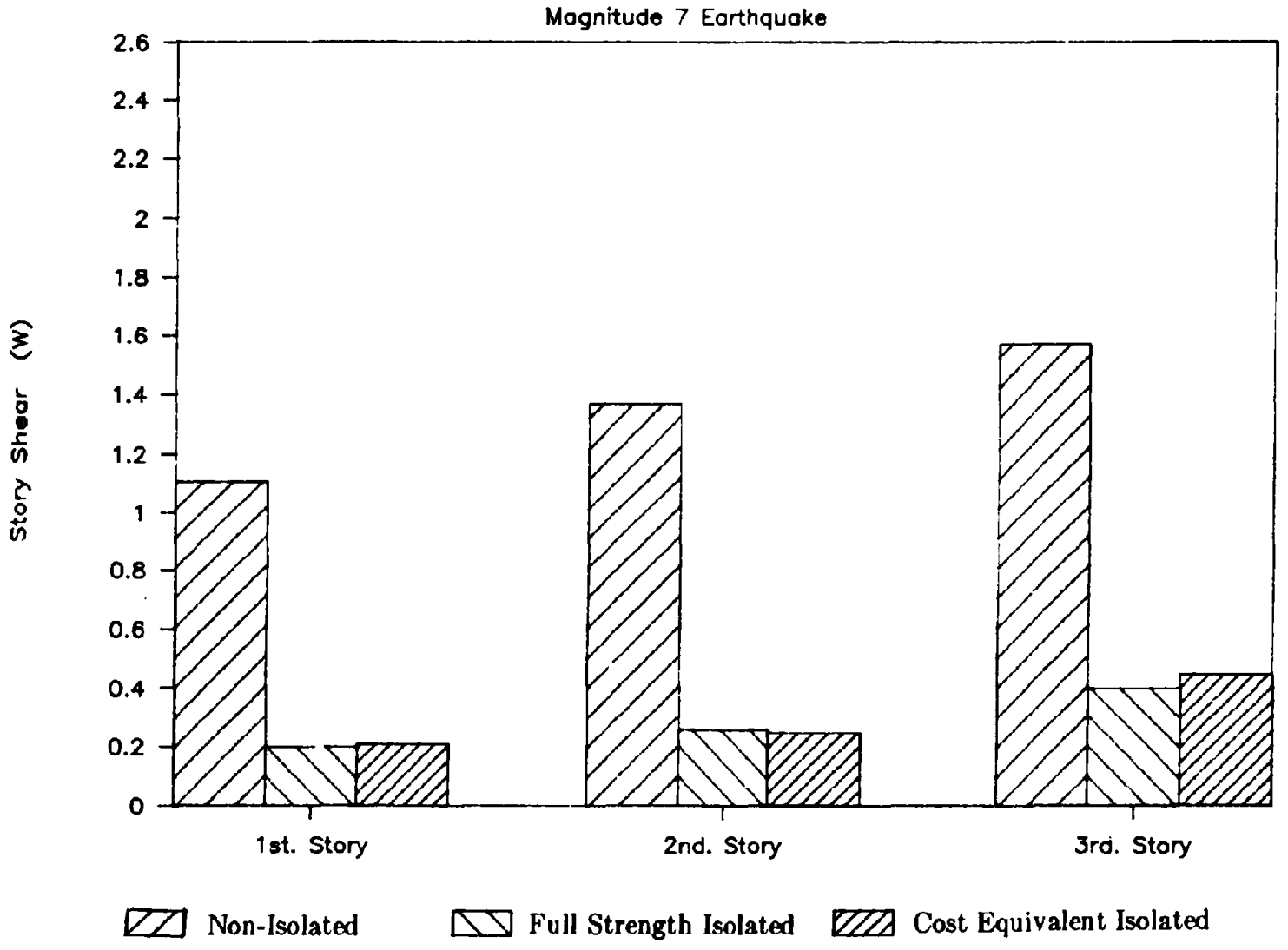

Fig. 2.21 Comparisons of Story Shears

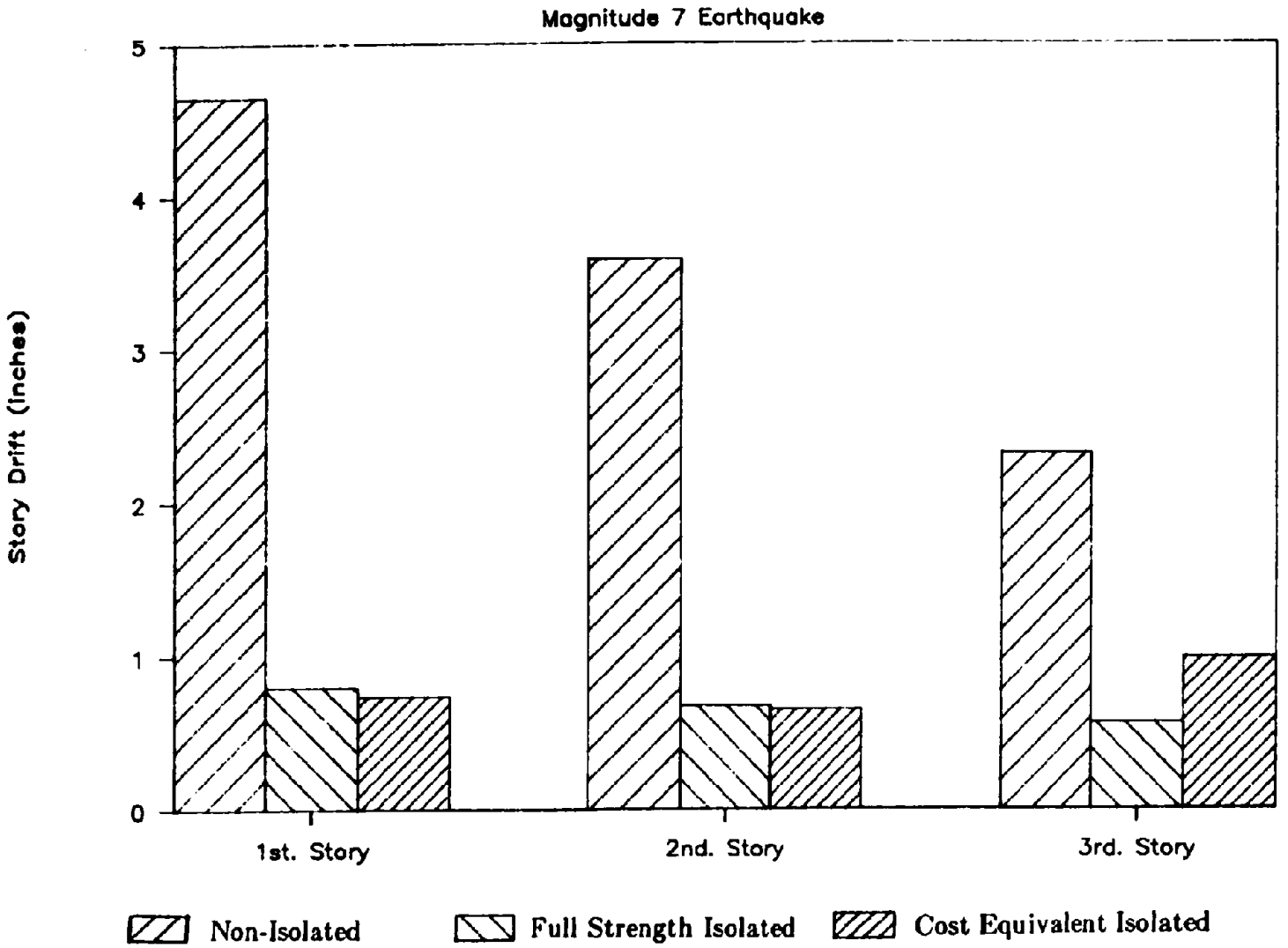

Fig. 2.22 Comparisons of Structural Frame Drifts

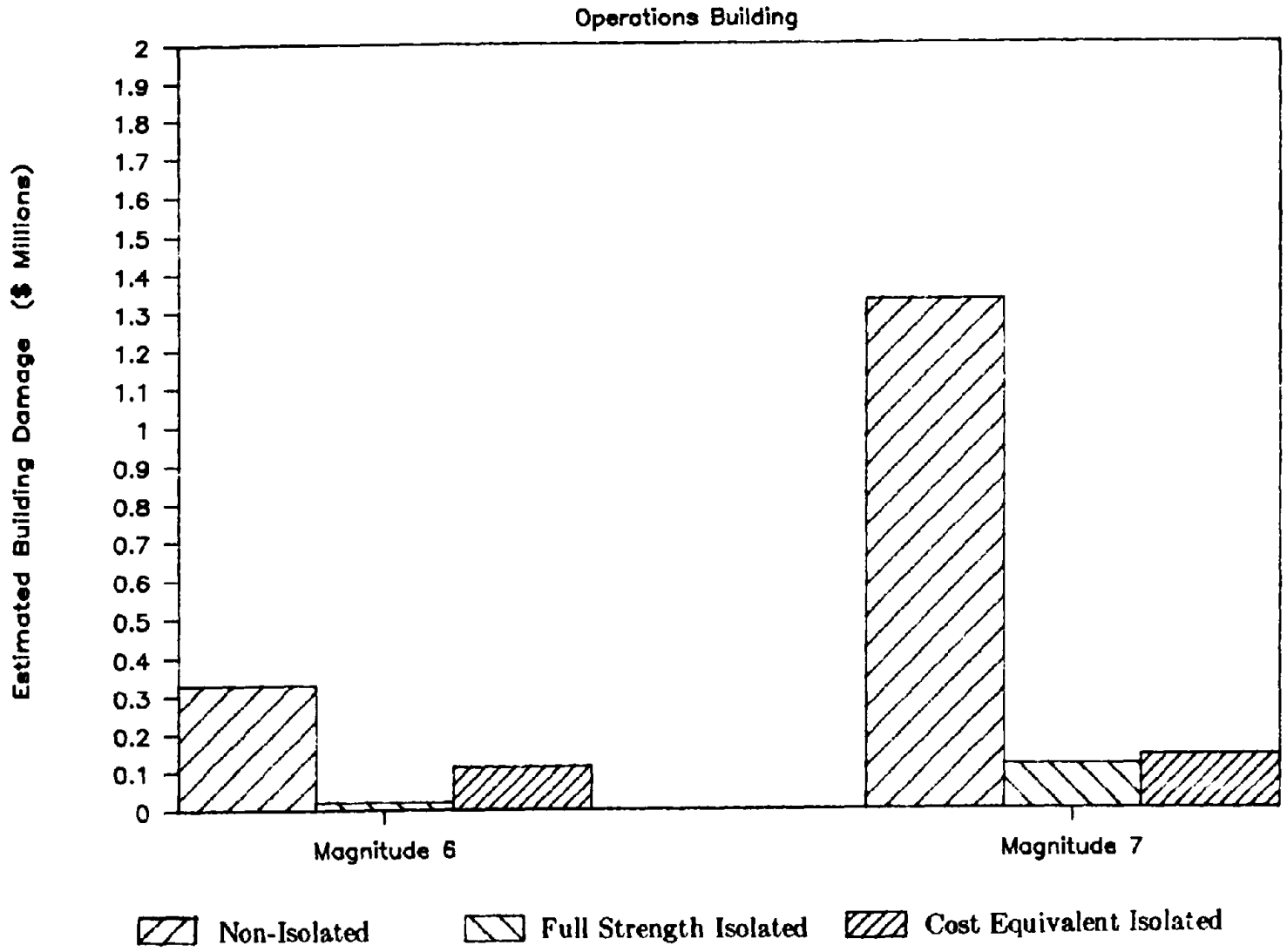

Fig. 2.23 Comparisons of Building Damage

CHAPTER 3

FEASIBILITY OF THE FPS FOR SEISMIC UPGRADING OF EXISTING BUILDINGS

by

Stephen Mahin

and

Victor Zayas

SECTIONS

3.1 Introduction

One of the most serious and challenging problems to be faced by earthquake engineers in the coming decades is that posed by existing seismically hazardous buildings. Based on research and lessons learned from recent damaging earthquakes, building code provisions applicable to new construction have been substantially improved over the past thirty years. The designer of new buildings also has at his/her disposal vastly improved analytical tools, more reliable construction practices and materials, and new seismic isolation techniques, such as the FPS connection, to help mitigate seismic hazards. As a result, it would be expected that, while the design of new structures still involves complex technical issues and professional challenges, in general these structures will perform significantly better during severe seismic excitations than those constructed in earlier eras.

However, many existing buildings will also perform well, as demonstrated by past earthquakes, due to the skill or conservatism of the designer, selection of structural systems with proven seismic resistance, and the use of inherently ductile details and materials. Thus, identification of seismically deficient structures must go beyond mere evaluation of compliance with basic code requirements, and consider their likely seismic performance. A variety of professional reports detailing methods for screening existing buildings and for evaluating their seismic vulnerability have been published (e.g., see Refs. 3.1 and 3.2). Issues such as inadequate strength, limited ductility, excessive drifts, improper tying together of structural as well as nonstructural components, excessive seismic demands due to irregular structural features and resonance with local soil conditions have been identified as some of the possible deficiencies of existing buildings.

Once a building has been identified as being seismically deficient, additional considerations to those used for the construction of new buildings must be taken into account to achieve economical and effective upgrading procedures. In particular, issues related to cost, retention of functional capabilities (or avoidance of disruption of services), preservation of special architectural or historic features, and so on have had an increasingly important role in determining the type of upgrade strategy to implemented. Augmenting the seismic resistance of old structures also raises new and special design problems.

The feasibility of using FPS connections in upgrading the seismic performance of existing buildings was studied. Technical considerations were explored along with some practical issues related to installation of FPS isolators in various types of existing buildings. Finally, a simple example structure was analyzed to assess the effectiveness of FPS isolators in improving seismic resistance. Additional information related to this topic is presented in Chapters 7 and 8.

3.2 Some Basic Considerations for Seismic Upgrading

As indicated in Ref. 3.3, the designer may choose between two basic approaches when considering options for upgrading the seismic performance of existing structures. The first, and more common approach, is to increase the resistance of the structure to the demands imposed by the seismic excitation. Reference 3.3 contains a detailed description of these strategies. They consist of general items such as increasing the strength or ductility of the existing structure by the addition of new elements or structural systems, or by modification of existing elements. The uncertainty with which the intensity of future earthquakes can be predicted raises questions about methods that rely solely on strengthening as a means of improving seismic performance.

The second basic approach is to reduce the seismic demands on the structure. Techniques for accomplishing this include reducing the mass of the structure (by removal of heavy cladding or equipment, and by reducing the overall height of the structure), and by seismic isolation of the structure. In general, both strength increases and load demand reductions can be used in combination. For example, a seismically isolated structure may also be strengthened.

The selection of an appropriate upgrade strategy depends on the type of structural system and materials used, the nature of the seismic deficiencies detected, the dynamic characteristics of the structure, the expected ground motion (including the effects of local soil conditions), the availability of local materials and qualified labor, in addition to economic, architectural and functional constraints. Many of the requirements for upgrading existing buildings differ in fundamental ways from those considered for new construction.

While economic considerations are always important in design, existing older buildings are often only marginally profitable so that the economic ramifications of the seismic upgrading approach to be selected must be carefully considered. If the required modifications are too expensive, the owner may defer the corrections entirely, elect less effective or partial solutions, or demolish or abandon the structure. Thus, cost effective methods for improving seismic safety must be identified.

Most existing buildings are already occupied and the upgrading strategy selected must consider the disruption to the tenants during construction. Furthermore, major modifications of the internal structural system could substantially interfere with the movement of people already working within the structure. For example, addition of numerous shear walls may be a technically and economically feasible solution in some cases, but it would violate the existing functional utility of most structures. Similarly, most owners would prefer to keep the building occupied during the construction process. Because of this, it is desirable to select an upgrading strategy that can be implemented successively in small

localized zones in the structure with minimum disruption of services to the existing occupants.

Also, many existing buildings are considered historic and major changes cannot be made to their exterior or interior appearance without destroying important aspects of a community's heritage. Thus, the retrofitting technique selected for these structures should be as unobtrusive as possible.

3.3 Application of FPS Seismic Isolation Techniques to Existing Structures

Seismic isolation, especially with FPS isolators, appears to be a particularly appealing means of improving the seismic safety and performance of existing structures for a variety of technical and functional reasons. Some of these are discussed below.

1. The strength of existing buildings is often substantially less than that of new buildings. The ability of FPS connections to act as structural fuses which limit the force that can be transferred from the foundation to the supported structure makes them suited for these weaker structures. In addition, the energy dissipation and period shifting characteristics of the FPS connections also help reduce the seismic demands on a structure.

2. Existing structures often possess little or no ductility. However, code design procedures rely on a significant amount of the energy input by a major earthquake to be dissipated through ductile yielding of members and connections. To add this required ductility at the local level in all the existing structural members requires massive structural intervention which is functionally disruptive and economically prohibitive. As a result, it is generally more common to strengthen these types of non-ductile structures by the addition of new shear walls, augmentation of existing structural walls, addition of new steel braces, and so on. Because of economic considerations, many retrofit strategies (e.g. Ref. 3.1) suggest design forces and ductility requirements for existing buildings which are lower than those considered for new buildings. As a result, one would generally expect the level of damage in structures retrofitted in this manner to be higher than that found in comparable new structures.

Moreover, future earthquake ground motions can not be predicted with great certainty. Consequently, the design loads considered in a retrofitting strategy may be substantially smaller than those that could develop in a future seismic event, thereby resulting in even higher strength and ductility demands than stipulated by design recommendations. Methods to make the performance of strengthened structures relatively insensitive to the likely changes in code strength requirements have not been adequately investigated.

FPS isolators can provide the structure with not only a means for limiting and controlling earthquake loading demands, but can also provide an effective and dependable means for inelastic energy dissipation. As demonstrated in the experiments (Ref. 3.4 and Chapter 4) as well as in recent analyses (e.g. Chapters 6, 7 and 8), it is possible to design FPS supported structures so that most or all of the energy dissipation occurs in the connections. In such cases, the structure remains elastic or nearly so. This ability to achieve overall ductile structural behavior while controlling the degree of inelastic damage in the structure is a important attribute of the FPS. This ability is examined in more detail below and in subsequent chapters.

3. Past earthquakes have demonstrated that a major problem causing damage to structures is irregularities in plan. The resulting torsion has caused serious damage in nearly all major earthquakes. Reducing stiffness and mass eccentricities by conventional construction procedures usually requires major structural modifications. An important aspect of the response of the FPS is its unique ability to reduce torsional responses in asymmetric structures (see Chapter 5). Since the lateral load resistance of an individual FPS isolator is proportional to the axial load (or mass) supported, the center of lateral load resistance of the isolator group as a whole will be at the center of mass of the supported structure. While eccentricities between the centers of stiffness and mass will continue to exist before the connections are activated, once sliding commences, eccentricities between the centers of mass and lateral load resistance disappear. Thus, an FPS supported structure would initially exhibit the torsional response characteristics of the original building, but the torsional response will be substantially reduced once sliding is initiated. This desirable response phenomenon was conclusively demonstrated in the previous experimental studies (Ref. 3.4) and in the analytical investigations reported in Chapter 5.

4. Many of the correction techniques used in upgrading conventional buildings are performed in the field, and require specialized equipment and skilled workers. Thus, to be assured that the designers intentions are fully realized, stringent quality assurance programs become a vital aspect of the retrofitting process. The need for high quality is, of course, not reduced by use of the FPS. However, overall quality of the project is much easier to achieve, since the FPS isolators and much of their hardware are: (a) manufactured under stringent quality control standards possible only in modern industrial manufacturing plants, (b) subjected to substantial research and development programs, and (c) subjected to pre-installation testing programs. Thus, FPS isolated structures would be expected to perform reliably and dependably in practice once issues related to the design, performance, and integration into existing buildings are resolved.

5. As discussed in Chapter 2, FPS isolators can be installed in a structure in a variety of ways. The specific location will depend on a range of factors including the type of structural system to be supported, the strength and ductility of the existing structure,

restrictions on location imposed by architectural and functional requirements, the proximity of other adjacent structures, availability of an existing basement, and so on. These considerations will be discussed in more detail later.

It is clear that FPS isolators can be installed in a basement level as with most other isolation systems. However, a special characteristic of FPS isolators is that they freely permit rotation. They thereby lend themselves to installation in columns without the need for supplemental beams to restrain rotations of the isolators. Installation in columns avoids the need for costly modifications to the existing foundations or the addition of new beams attached to the isolator. Moreover, by placing the FPS isolators at the top of the first story columns (as done in the previous experimental program (Ref. 3.4)) or in the columns of upper levels, problems associated with egress conditions or with proximity to adjacent structures can be substantially mitigated. Versatility is further enhanced by the ability to locate the FPS connections along the midspan of a column. This flexibility of the installation and the ability of the FPS connections to rotate freely are expected to be important attributes to be considered in selecting seismic upgrading strategies for existing buildings.

6. Typically, FPS isolators are added to a single level of a structure. Localization of the seismic upgrading work to a single level will help minimize the disruption of occupants that has proven to be such a problem with more intrusive and global rehabilitation methods. Furthermore, where FPS isolators are to be added to columns, construction work can be logically sequenced between successive zones of a building, further reducing disruption. Of course, it may be necessary to make changes to other portions of the structure. But the magnitude of these changes should be reduced in comparison to those required by other techniques.

7. Another feature of FPS isolators is that they are physically small. While the width of the isolator is governed by the amount of displacement to be accommodated, the height is generally quite small. Unlike other types of isolators, the height is nearly independent of the amount of lateral displacement expected. This makes the isolator very stable against overturning modes of failure that might be associated with large lateral displacements. The compact size also makes FPS isolators easier to install and architecturally more attractive in an existing building.

8. Because of the above features and the inherent simplicity of the FPS, it could provide a particularly cost effective method for upgrading the seismic safety and performance of existing structures.

The ability of the FPS isolators to limit seismically induced forces in a structure, to dissipate substantial amounts of energy and to mitigate the adverse effects of torsional response provide the primary technical motivation for their application to existing

buildings. Their dependable operation, versatility and the manner with which they could be installed provide the practicality and economy necessary for serious consideration as a means for retrofitting seismically deficient structures.

To use FPS isolators, the building should be situated on a site that would accommodate the sliding displacements. Detailed studies of frame structures responding in the elastic and inelastic ranges are included in Chapter 7. Analytical studies on the design of FPS isolators to support structures that should remain essentially elastic are also presented in Chapter 7.

3.4 Installation Details

An important consideration in selecting a particular seismic rehabilitation strategy is the feasibility and economy of the construction details. Even simple conventional retrofitting techniques, such as the addition of shear walls or braces, can become extremely complex to implement, depending on the details needed to add collectors, secure new elements to the existing structure, provide adequate foundation support and accommodate pre-existing conditions. Thus, when considering the basic suitability of FPS isolators for the rehabilitation of existing buildings, it is desirable to identify potential problems and solutions related to their installation. Due to the preliminary nature of this investigation only basic issues will be addressed for a number of standard types of structures.

The versatility of installation of FPS isolators has been highlighted in Chapter 2 as it relates to new construction. This versatility is an especially important attribute when considering existing buildings. Each building will have a different geometry; structural system; strength, stiffness and ductility characteristics; proximity to adjacent buildings; performance expectations; seismic exposure; and so on. Because of the many factors to consider, the designer will not have as much freedom to modify the structure as would be the case in new construction. As a result, ingenuity and engineering judgment are especially needed to find simple, yet effective retrofitting strategies that are practical and economical.

A number of different categories of potentially hazardous buildings have been identified by various authors (e.g., Ref. 3.1). In this study, two basic groups of buildings are addressed: bearing wall systems and frame systems. Information on application of the FPS to these systems constructed of different materials is presented, as is additional information on special problems associated with retrofitting which are not associated with building type.

Bearing Wall Systems. -- The first type of structure considered was the bearing wall or box system. These systems have been long recognized as having inherently less desirable seismic characteristics in comparison to other types of buildings.

Accordingly, new buildings which employ bearing walls for lateral resistance are designed for higher seismic force levels than considered for other building types.

Within this category of building systems, greatest concern has been expressed regarding unreinforced masonry structures. Such structures are usually quite stiff, but exhibit brittle responses when loaded beyond the elastic range. They have repeatedly demonstrated poor performance during past earthquakes throughout the world. Some research has been performed (e.g. Ref. 3.2) on methods for evaluating and retrofitting these types of structures, and design recommendations related to conventional construction techniques have been published (Ref. 3.5).

Some masonry and other bearing wall structures can be quite strong in the direction of the walls due to the large size, close spacing and large number of walls used. Nonetheless, serious deficiencies may exist which are related to out-of-plane wall capacities, wall attachment to diaphragms, and diaphragm integrity and flexibility. These types of problems would also have to be addressed and solved prior to using FPS isolators. The introduction of the FPS may change the nature of the internal forces and deformations that must be considered in the evaluation of these details.

Of course, many unreinforced masonry buildings will have inadequate lateral load capacity due to the inherent weakness of the system, deterioration of materials over time, and the intensity of the expected seismic excitations. Because of the brittle behavior of unreinforced masonry, it may be necessary that isolated unreinforced masonry buildings also be strengthened to avoid significant inelastic action. Conventional strengthening consists of overlaying masonry walls with cast-in-place concrete or shotcrete, adding supplemental steel braces, and so on.

FPS isolators could be added to many bearing wall systems and would be expected to reduce the need for strengthening and improve performance by reducing drifts and accelerations in the supported structure, and providing a dependable means of dissipating substantial amounts of seismic input energy. Such uses of FPS isolators could help the designer preserve the architectural features of the building, an important consideration for historic structures.

A simple installation method that would be applicable in many cases is shown in Fig. 3.1. In this example, short segments of an existing wall are shored and a small segment at the bottom of the existing wall is removed. Collectors and wall support beams are then cast to the sides of the wall. Shear keys and lateral prestressing may be effectively used to transfer seismic and gravity loads from the existing walls to the new support beams. FPS connections are installed at regular intervals beneath the new support beams. Where possible, existing foundations may be used.

A diaphragm should be provided at or near the base of the wall to tie the base of the structure together and to provide a new floor for the occupants. This diaphragm would permit the use of the FPS technique in buildings having interior columns as well as walls. FPS isolators would be placed beneath the columns, and the diaphragm would constrain the base of the columns to move with the reminder of the building. The floor provided by the new diaphragm would make the seismic retrofit undetectable to occupants of the building. In some cases, it may be possible to relax the need for a diaphragm immediately adjacent to the FPS isolators. However, this would require investigation of the integrity of the walls and of the overall system on a case by case basis.

Other deficiencies may also exist in the building that need to be addressed in the retrofit process. Notably, many bearing wall structures are asymmetric, raising the potential for damage associated with torsion. The use of FPS isolators may reduce the need for major structural alterations to restore symmetry to bearing wall and other types of buildings.

Frame Systems. -- The second group of structures that was considered relates to those employing moment resisting frames. Frames built of non-ductile reinforced concrete have been identified as being particularly susceptible to earthquake damage (e.g. Refs. 3.1 and 3.3). Prior to the 1972 Uniform Building Code it was possible to construct reinforced concrete frames using details intended primarily for resistance of gravity load. For example, the 1961 UBC did not require ductile detailing for reinforced concrete buildings under 13 stories in height. Later editions of the UBC still permitted the use these conventional "non-ductile" frames provided the seismic performance factor K was increased from 0.67 to 1.0. Following the 1971 San Fernando earthquake, UBC provisions for reinforced concrete buildings were changed to require special ductile detailing in all frames considered to be part of the lateral load resisting system and, in most cases, all frames along the perimeter of a building. As will be seen in more detail later, the required lateral design forces for concrete frames have more than doubled since 1961. In many instances even these early force requirements were more than double those used in the design of frames in the 1950's and earlier. Thus, the damage expected in such early reinforced concrete frames, especially those constructed without special "ductile" details, might be substantially greater than that anticipated in buildings designed using current design procedures. In many recent earthquakes in the U.S. and abroad this damage has lead to catastrophic results.

While steel frames have generally performed well during earthquakes, concern has been expressed about earlier designs incorporating masonry infills. These infills significantly influence the structural and dynamic characteristics of the structure, and the seismic response may be substantially different than that anticipated by the design engineer. In other instances, steel frames may contain members having non-compact sections, carrying heavy axial loads, or connected using bolt or rivet

details insufficient to yield adjacent critical members. These and other factors could impair the ductility capacity of these frames. Damage rates for steel frames buildings in Mexico City as a result of the 1985 Michoacan earthquake were comparable to those for reinforced concrete frames (when flat slab construction is disregarded (see Ref. 3.6). Damage to steel frame structures constructed prior to 1950 was reported as being particularly severe. Thus, instances where steel frames would be require retrofitting should be anticipated.

One of the most common conventional methods for strengthening existing frame structures, in steel or reinforced concrete, is the addition of shear walls or braced frames. While these can easily add the desired strength and in some instances ductility, there are a number of potential problems. The first of these is the difficulty of providing new foundations under the new lateral load resisting elements. Typically, these types of elements resist substantial overturning forces. Extension of existing footings or addition of new pile foundations within the confines of an existing building is a difficult and expensive undertaking. To mitigate these problems, multiple wall or bracing systems should be used. This, however, means that the retrofitting will involve large portions of all floors of the building.

Alternatively, FPS isolators may be used in most frame systems. They would help limit the forces that can be introduced into the system, reduce drifts and accelerations in the supported structure, and substantially augment the energy dissipating capacity of the existing structure.

A simple installation detail that would be applicable in many cases for reinforced concrete frames is shown in Fig. 3.2. A corresponding detail for steel frames is shown in Figure 3.3. In both cases the columns are shored and an FPS connection is installed somewhere along the length of each column. In some instances it will be necessary to strengthen the columns supporting an FPS connection. This will depend on the nature of the expected seismic response and the detailing of the existing column. Additional information regarding this topic may be found in Chapter 7. FPS connections would be installed at only one floor level and implemented sequentially a few columns at a time. Thus, disruption to the occupants would be minimized.

The location of the FPS isolator is determined by architectural considerations, relative difficulties in installing new ceilings or floors (where necessary), foundation conditions, moment and shear capacities of columns, story drift limits, and the desired base shear capacity of the structure. In general, determination of the optimal location of the FPS isolator will require a detailed evaluation. For example, placing the isolators at midheight of the columns will reduce the column moment requirements and story drift demands for the same lateral load capacity. Placing the FPS isolator at the bottom of the column will minimize the moments that need to be transferred to the existing foundation. Placing the FPS isolator at the top of the

column will minimize the need for alterations to the building for egress. The optimal location will depend on the particular set of circumstances associated with a specific building. Once functional and response criteria are established, implementation details are addressed using engineering analysis and design methods.

Buildings with irregularities in elevation may lend themselves to special treatment using FPS isolators. If analysis indicates that a building has particularly heavy seismic demands at a certain level, due for instance to setback conditions, it may be possible to install FPS isolators in this region of the superstructure. An example of this is shown in Fig. 3.4. Of course, much more study will be required to assess the feasibility of such solutions.

In the case of structures possessing very little lateral load resistance or having little or no ductility, it may be necessary to strengthen the superstructure and to provide ductile details. Generally, these may not have to be provided for the full height of the structure or for all members at all levels. An example of this is shown schematically in Fig. 3.5. In general, the required details will be substantially more severe if FPS isolators were not used. Moreover, FPS isolators control the forces that can be transferred into the structure during unanticipated earthquakes larger than those considered as part of the rehabilitation process.

Other Structural Systems. -- Other types of existing systems may be susceptible to damage during earthquakes. Notable among these are shear wall and brace frame structures. Provided these structures would tend to slide rather than rock during a major seismic disturbance, FPS isolators would be applicable in a manner similar to that described previously. Previous experimental and analytical studies have shown that limited vertical uplift of the FPS isolators, as might occur during rocking of slender walls or brace bents, does not pose a problem. However, if rocking becomes the dominant mode of behavior, other modes of rehabilitation may be more effective. Careful study of the response and design of these systems are required on a case by case basis.

Other Retrofitting Problems. -- Several types of problems are frequently encountered in retrofitting existing buildings that are not associated with a particular type of structural system. One problem encountered in the case of seismic upgrades using seismic isolation techniques is close proximity to other buildings. In some cases only a small separation exists between buildings. One of the attributes of the FPS is that the amount of sliding displacement developed can be effectively controlled by the period and friction coefficient of the connection. Several case studies are presented in Chapter 7 and the interrelationship is described in detail in Chapter 7. By choosing a FPS isolator with a lower sliding period or higher friction coefficient, the amount of sliding displacement will be reduced. Of course, this reduction in sliding displacement must be traded off against higher base shear demands on the structure. In this case, additional modifications to the building may be required. Still, these

modifications are likely to be substantially less extensive than those required if the building were not supported on FPS isolators.

In some instances the building may have a major setback near the ground level. Many building of this type are used for commercial and residential occupancies. In these cases it may be convenient to upgrade the lowrise portion of the structure using conventional strengthening techniques, such as by adding shear walls. However, these techniques may not be suitable for the tower portion due to functional or economic reasons. Conventional seismic isolation strategies will be difficult to implement due to the large overall size of the entire building and the difficulties in separating the tower portion away from the extended base portions. Using FPS connections, it may be possible to isolate the tower at a level above the extended low rise structure. A simple schematic example of this concept is shown in Fig. 3.6. Again, further studies will be required to assess the feasibility of such solutions.

In many cases, foundations in an existing building are too weak to take additional loads that may be developed if the structure is significantly strengthened. This is especially true if new elements such as shear walls and braced frames are to be added. The cost of adding piles under existing buildings would be in most instances prohibitive. The FPS connections may provide a effective solution in these cases. The relatively lower lateral load demands and reduced moment requirements associated with FPS connections will generally mean that only limited modifications to the foundations will have to be made.

3.5 A Simple Case Study

To illustrate some of the basic concepts indicated above, it is useful to consider a simple, yet quantitative, example. For this purpose, the three story Operations Building used in Chapter 2 to develop cost equivalent FPS isolation techniques will be reconsidered. However, lateral strengths will be based on estimates of values corresponding to earlier reinforced concrete moment resisting frames.

If the Operations Building were designed according to the 1985 UBC with an importance factor of unity (I=1.0), a working stress base shear coefficient of 7% would be required (i.e., 0.11/1.5 = 0.07). If one considers the same building, but designed according to the 1961 UBC, the base shear would be evaluated according to the relation:

$$V = ZKCW$$

in which

$$C = 0.05/T^{1/3}$$

and where the other terms are as used in the current code. The resulting working stress design base shear coefficients for both codes are shown in Fig. 3.7. Evaluating the 1961 UBC expression for a structure with a period of 0.86 seconds as was done for the Operations Building example, results in a base shear coefficient of about 3.5%. This means that the required design code forces for this building have doubled in only twenty-four years. Ratios for other structural periods are also shown in Fig. 3.7. It is interesting to note that if this building were designed according to requirements in force in San Francisco in 1958, the required design base shear coefficient for the period in question would be only 2.4% (Ref. 3.7), nearly three times smaller than required in 1985. It is similarly important to recognize that reinforced concrete frames were designed for the same lateral forces as steel frames, and that no special ductile detailing requirements were imposed by these early codes for either type of structure.

This comparison of required design forces is still not necessarily a good indication of the possible differences in the strengths of new and older buildings. For example, the non-isolated Operations Building considered previously was estimated using plastic analysis procedures to have an ultimate base shear coefficient of about 45%, three times stronger than 14% which was used to design the building on a elastic basis. This overstrength is a result of the control of the seismic design by drift considerations, the inherent factors of safety, conservatism in design and selection of member sizes as a result of practical considerations. Similarly, differences in nominal design loads and plastic strength capacities for older buildings could be very large.

To devise a simple numerical example the general configuration and dynamic characteristics of the Operations Building was used. According to the 1985 UBC, this building would have a design base shear coefficient of 0.07 for a ductile steel or concrete frame, assuming a period of 0.86 seconds and normal occupancies (I= 1.0). The cost equivalent isolated building (Chapter 2) was designed for a base shear coefficient of 0.067, based on an isolated period of 2.25 secs., and an occupancy importance factor I equal to 1.5. Assuming a base shear ultimate plastic strength capacity of 0.31, equal to that of the cost equivalent isolated building, the lateral strengths of this non-isolated building would be like those shown in Fig. 3.8.

This structure was analyzed considering the north-south component of the 1940 El Centro earthquake record scaled to 70%g (corresponding to the hypothetical nearby magnitude 7 event) and 5% viscous damping in all elastic modes. A summary of the building response is given in Table 3.1. The values reported are the total displacements relative to the ground, structural ductility demands, structural interstory drift displacements and hysteretic energy dissipation by structural elements. These plots show that the building develops a displacement ductility of 4.1 in the first story and less than 1.7 in the upper floors. Significantly, this building develops 4.8 inches of lateral displacement in the first

story. In view of the large interstory drifts developed for this structure, the performance of existing weaker structures might be questioned.

To assess this in a simple manner, the same structure was re-analysed with the strengths of all stories reduced by a factor of 4. This strength reduction is severe, but not unrepresentative considering the changes in building code lateral force requirements over the past 25 years. If we subject this hypothetical existing structure to the same earthquake, the results are shown in Fig. 3.9 and Table 3.1. In this case, the ductility requirements increase to more than 20 in the first story (and 2.1 and 3.4 in the second and third stories, respectively) and the first story lateral displacement increases to more than 6 inches.

The original non-isolated Operations Building would have an ultimate base shear coefficient of about 31% based on plastic analysis, if the importance factor is taken as unity. The hypothetical existing building is one-quarter as strong so it would have an ultimate base shear capacity of 7.75% of the weight of the structures. This is sufficient to permit use of FPS connections, if the friction coefficient selected is 0.05 and the period of the isolators is taken to be 3.0 sec. FPS connections are assumed to be inserted in the structure as done in the cost equivalent FPS structure, utilizing attachment methods shown in Fig. 3.2. Other combinations of parameters are considered in Chapter 7. When this weak existing building model is supported on FPS connections and subjected to the hypothetical magnitude 7 event, the response plotted in Fig. 3.10 results (also see Table 3.1). Ductility demands in the first story columns are reduced by nearly 60% to 8.4 and column displacements in the first story are reduced to 2.3 inches, as compared to the non-isolated building. Displacement ductilities in the second and third stories are reduced to 1.5 and 3.0, respectively. The total displacement of the story and of the roof are also reduced, but by smaller amounts. The difference is accounted for by the sliding of the FPS isolator.

In this example, the columns at the base of the structure were assumed so far to remain the same size as found in the original existing building. The relatively low drifts and ductilities found in the upper stories may be acceptable depending on the detailing of the structure. However, the demands on the columns of the ground story are still excessive, especially if the structure is constructed of reinforced concrete. As will be described in more detail in Chapters 7 and 8, it is possible to adjust design parameters to improve performance.

For the structure considered here, several alternatives are possible. For example, the friction coefficient of the FPS isolator could be reduced, the period of the isolator could be increased, and the strength of the column could be increased. It is unlikely, at least for the time being, that the friction coefficient could be reduced significantly below the level already used in the example. The period of the isolator governs the increase in strength of the isolator as it slides. If this rate of

increase in capacity is reduced by increasing the period of the isolator, less demands will be put on the columns. Similarly, the existing columns might be logically strengthened. For example, if the columns were constructed from reinforced concrete, the columns would be likely to need additional transverse reinforcement to provide confinement for ductility and to improve shear resistance. In this case, it would not be difficult to increase the strength as well.

For the structure considered here, additional analyses have been performed for these alternatives. In the first case, the lower level structural elements were assumed to remain elastic. The forces developed in these columns were 41% larger than those incorporated in the original structure. Thus, the columns of the lower story would have to be strengthened by 41% to make them respond elastically. While this is a significant increase, the strengthened columns are still only 35% as strong as would be required to have the columns satisfy the 1985 UBC strength provisions for a non-isolated structure. Moreover, the reserve capacity of the existing foundations may be sufficient with this level of increase to minimize any modifications to the foundations. It should be pointed out, of course, that it is not necessary for these first story columns to remain elastic. Smaller levels of strengthening can be used provided that details are used to supply the required ductility.

Similarly, a longer period FPS isolator can be used. If a period of 4 seconds is assumed in the analyses, the displacement ductility demands on the first floor columns are reduced from 8.4 to 2.8 (see Fig. 3.10 and Table 3.1). Whether this value is acceptable or not depends on the detailing of the critical regions of the columns. However, the example does clearly indicate the ease with which the designer can modify seismic performance by selection of isolator and structural parameters.

Another alternative for reducing the drift and ductility demands on the first story columns is locating the FPS isolator at the midspan of the column. The column will then act as if it had a point of inflection at its midheight, rather than one at the top. As a result, the column will develop only half the moment at its ends for the same force in the FPS connection, and the lateral stiffness of the first story will increase by a factor of 4 assuming the ends of the columns are fixed. This placement has many advantages, but the architectural and functional impacts must be carefully investigated. Since this change would modify the dynamic properties of the building as well as the moment to shear ratio in the columns, detailed analyses were not performed here.

It should be recognized, however, that in an actual design situation a more thorough investigation of the impacts of design and load variables would have to be considered. In particular, several ground motions representative of those expected at the site would have to be considered. Potential variability in structural characteristics due to material variability and workmanship would also have to be considered. Adequate factors of

safety would have to be imposed against any undesirable performance criterion established for the structure. The FPS isolators can provide the designer with a dependable device with well understood and controllable engineering properties. As seen in the simple analytical examples presented herein, FPS isolators are not only able to reduce undesirable aspects of the seismic response of existing buildings, but the response can often b/ adjusted to suit performance requirements by simple design modifications.

3.6 Summary and Conclusions

It has been shown that seismic upgrading of existing buildings introduces numerous design considerations many of which are not usually relevant or emphasized in the design of new buildings. Based on a review of these considerations, the FPS isolation technique provides a particularly effective and flexible means of seismically rehabilitating existing structures. The versatility of installing the isolators in a structure along with their well understood governing principles makes design using FPS isolators particularly attractive. It has been shown that the FPS isolators can significantly reduce the design force levels that need to be considered in the design of seismic retrofits, while providing an efficient means of augmenting the overall energy dissipation capacity of a structure. Buildings with problems associated with torsion, irregular configurations, and excessively weak or brittle structures may be well suited for upgrading with FPS isolators.

Generally, FPS isolators could be installed in many types of structures, like unreinforced masonry bearing wall buildings or reinforced concrete frames, with a minimum of disruption of services to occupants. Available numerical methods makes the preliminary design of FPS supported structures relatively simple. The examples presented herein demonstrate that design alternatives can be easily analyzed and evaluated, and improved design alternatives quickly identified based on well known properties of FPS isolators.

The studies presented here have used simplified structural models to examine overall structural performance, for purposes of examining the feasibility of using the FPS as a retrofit tool. Additional detailed studies are required to investigate the local effects on individual structural members that would result from the changes in the dynamic response and force distributions. In addition, experimental verification of the global and local effects are needed. Such studies would need to differentiate between the various kinds of existing hazardous buildings. Moreover, acceptance and use of these retrofit techniques by the building industry would require the development of reliable, yet simplified design procedures.

3.7 References - Chapter 3

3.1 Applied Technology Council, "Evaluating the Seismic Resistance of Existing Buildings," ATC-14, Redwood City, CA, 1987.

3.2 ABK, a Joint Venture, "Methodology for Mitigation of Seismic Hazards in Existing Unreinforced Masonry Buildings," ABK-TR-01, Agbabian Associates, El Sugundo, CA, 1981.

3.3 URS/Blume and Associates, "Techniques for Seismically Rehabilitating Existing Buildings (Preliminary)," San Francisco, CA, March 1989.

3.4 Zayas, V., Low, S., and Mahin, S., "The FPS Earthquake Resisting System: Experimental Report," Report No. UCB/EERC-87/01, Earthquake Engineering Research Center, University of California, Berkeley, CA, June 1987.

3.5 "Division 68, Earthquake Hazard Reduction in Existing Buildings," Building Safety Ordinances, City of Los Angeles, CA, 1981.

3.6 Martinez-Romero, E., "Damage Assessment and Seismic Behavior of Steel Buildings in Mexico City," Proceedings, International Conference on the Mexico Earthquakes - 1985, Mexico City, Sept. 1986, published by ASCE.

3.7 Berg, G., "Seismic Design Codes and Procedures," Monograph, EERI, El Cerrito, CA, 1982.

TABLE 3.1 Response Data for Existing Buildings -- 1940 El Centro (NS) Record scaled to 0.7g

Item	Displacement (inches)			Struct. Drift (inches)			Ductility		
Story	1	2	3	1	2	3	1	2	3
Non-Isolated Building Designed using 1885 UBC	4.8	5.1	6.3	4.8	2.1	2.4	4.1	1.5	1.7
Non-isolated Building with Strength Equal to 1/4th of 1985 Building --"The Existing Building"	6.2	6.5	7.4	6.2	0.8	1.2	20.4	2.1	3.4
Isolated Existing Building; Tc=3 sec.	5.2	5.3	5.8	2.3	0.5	1.1	8.4	1.5	3.0
Isolated Existing Building with Tc = 4 seconds.	4.6	4.7	5.4	0.8	0.6	1.1	2.8	1.6	2.7
Isolated Existing Building with Elastic First Story; Tc = 3 sec.	5.8	6.0	6.4	0.4	0.5	1.0	1.0	1.4	2.8

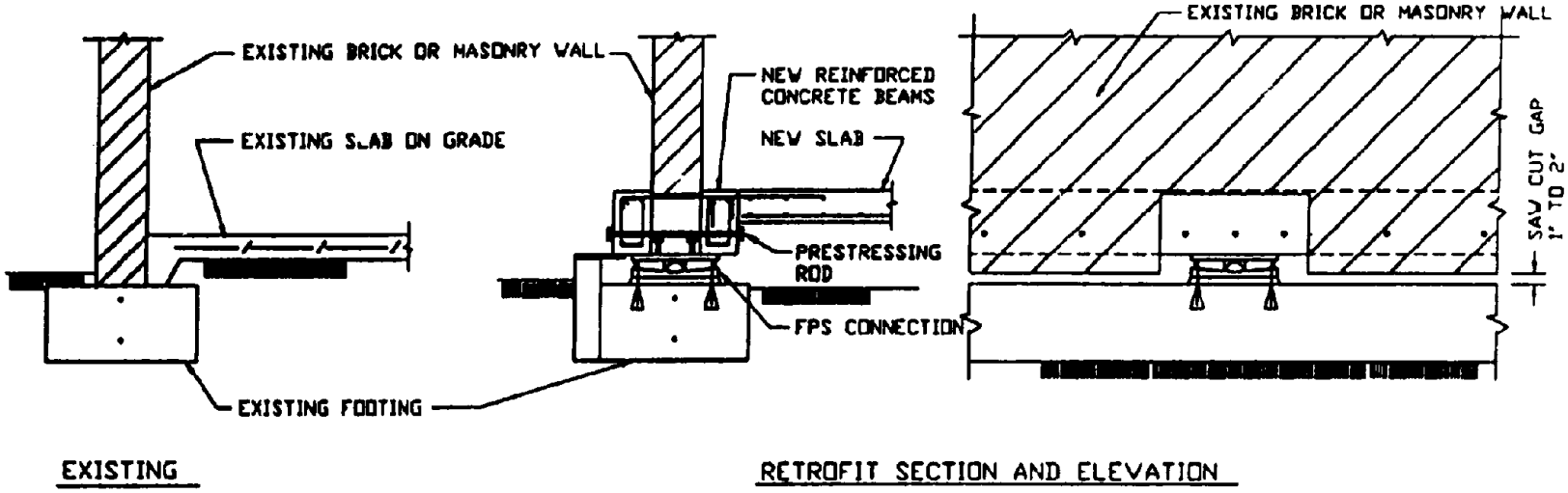

Fig. 3.1 Using FPS to retrofit an existing Shear Wall Building

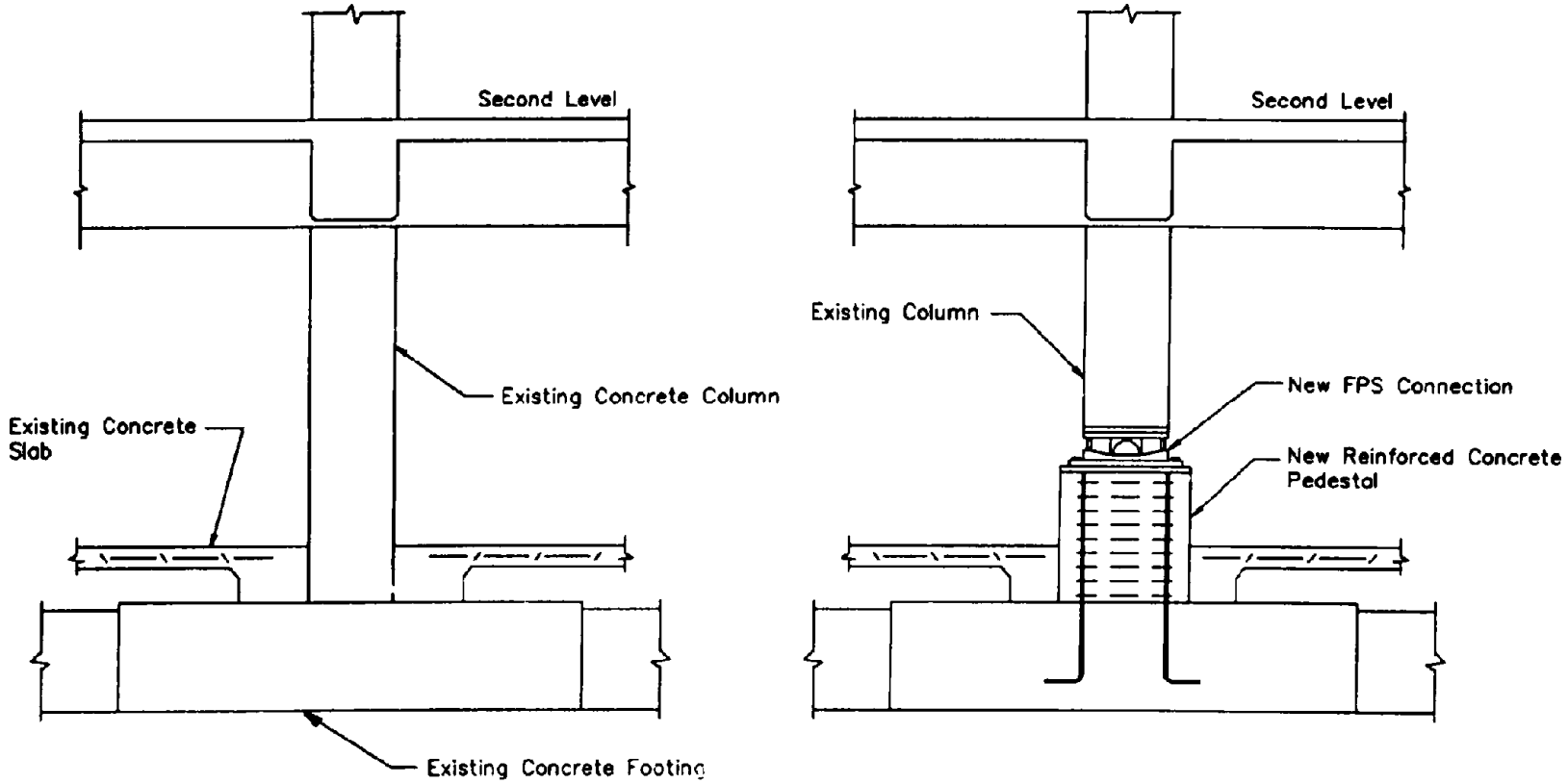

Fig. 3.2 Using FPS to retrofit an existing concrete moment frame building

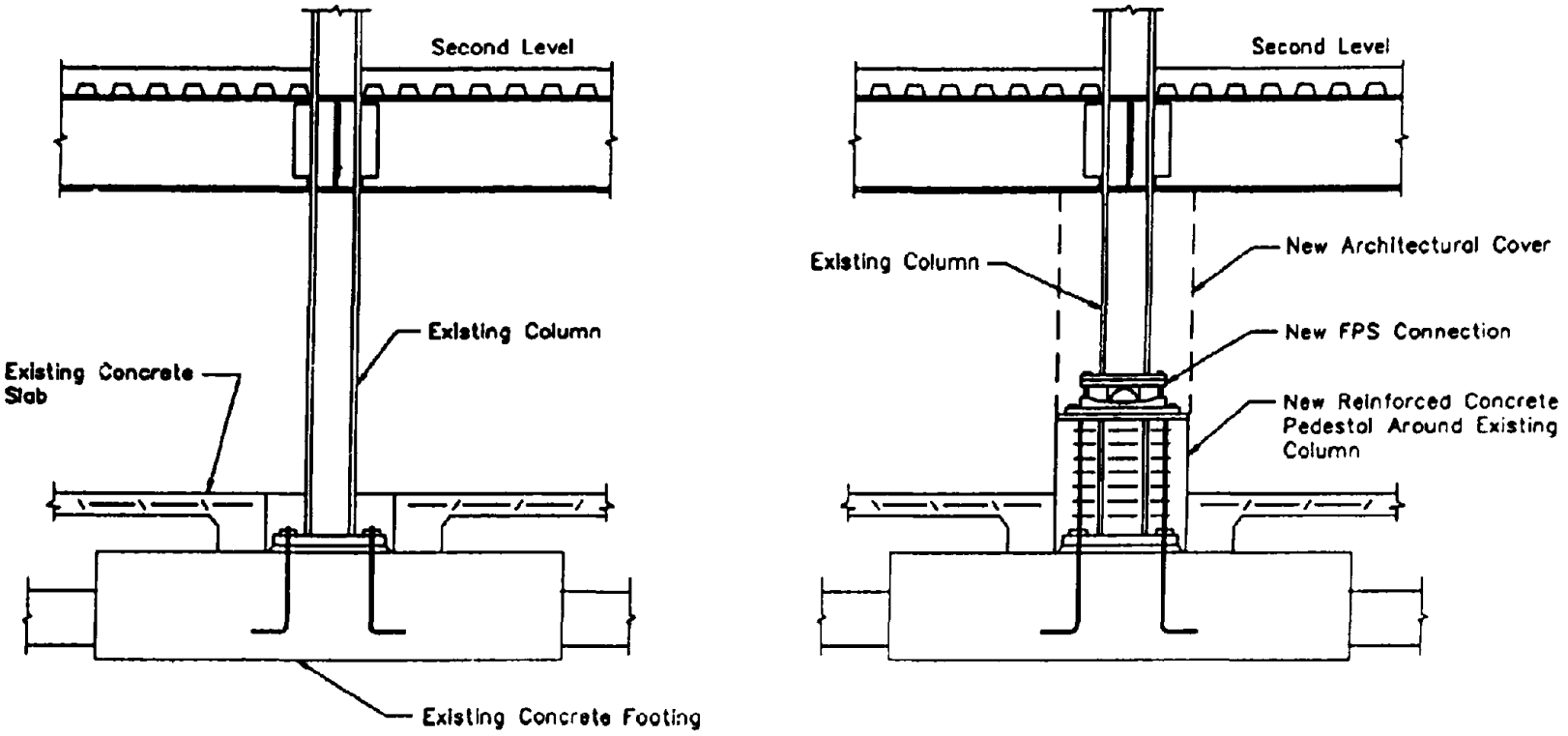

Fig. 3.3 Using FPS to retrofit an existing steel moment frame building

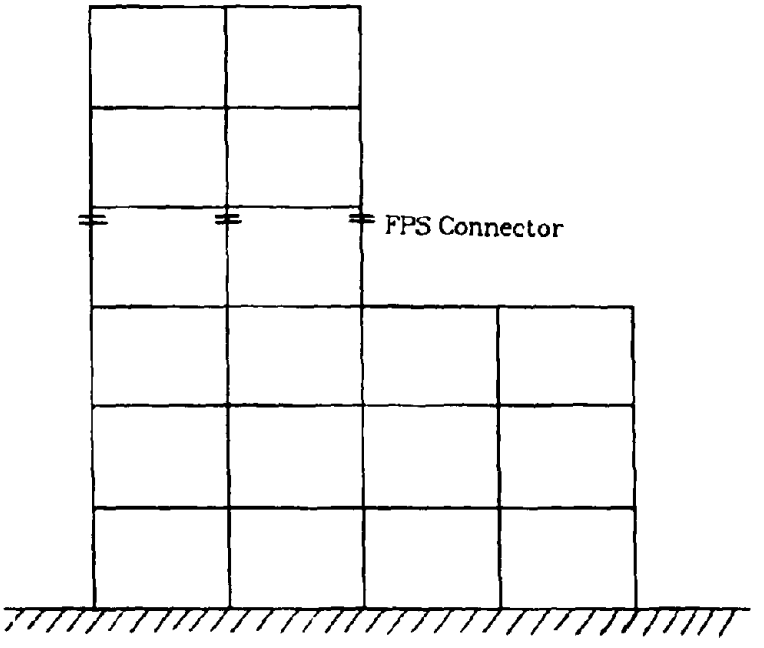

Fig. 3.4 Potential use of FPS isolators to reduce ' Stress Concentrations ' due to vertical irregularities

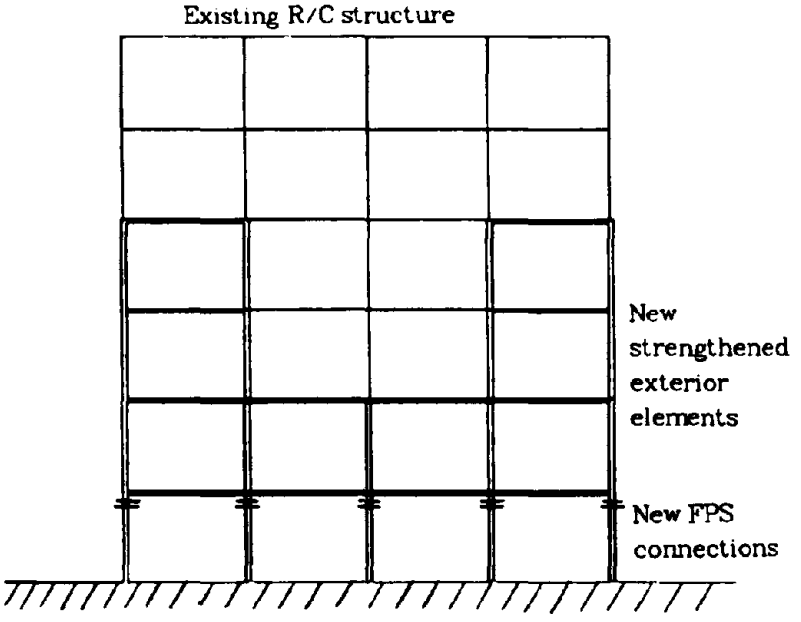

Fig. 3.5 Schematic illustration of strengthening of existing R/C elements used along with FPS connectors

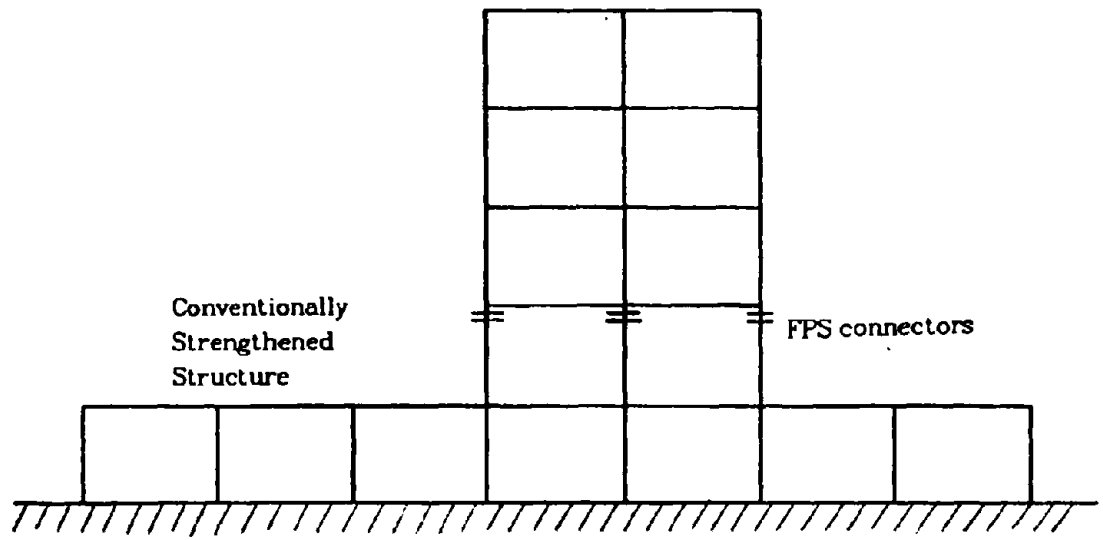

Fig. 3.6 Existing tower structure retrofitted at upper level with FPS connector

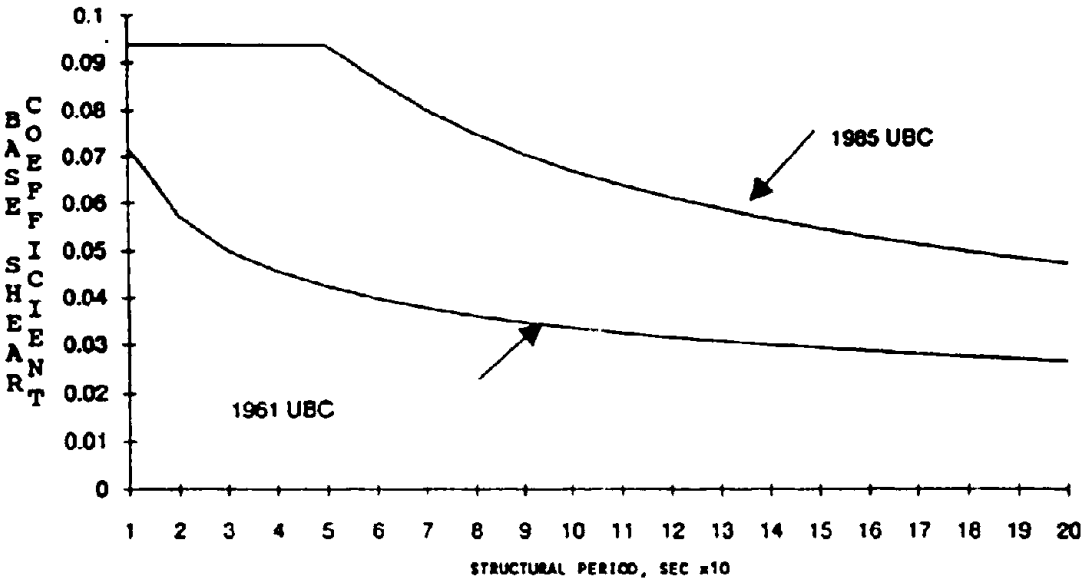

(a) 1985 and 1961 UBC base shear coefficients

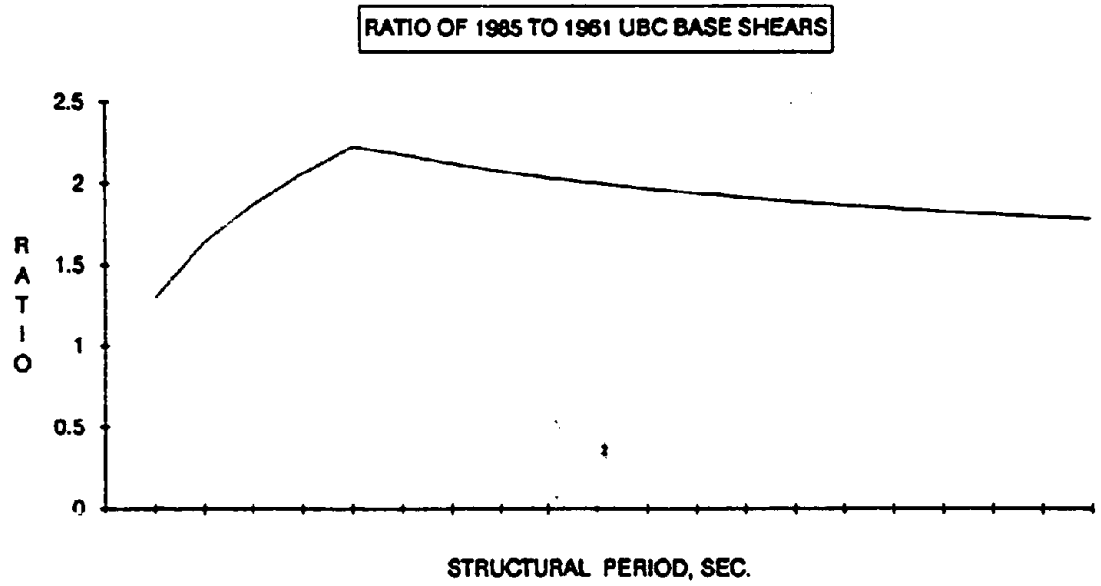

(b) Ratio of 1985 to 1961 UBC code requirements

Fig. 3.7 Comparison of code requirements for K = 0.67

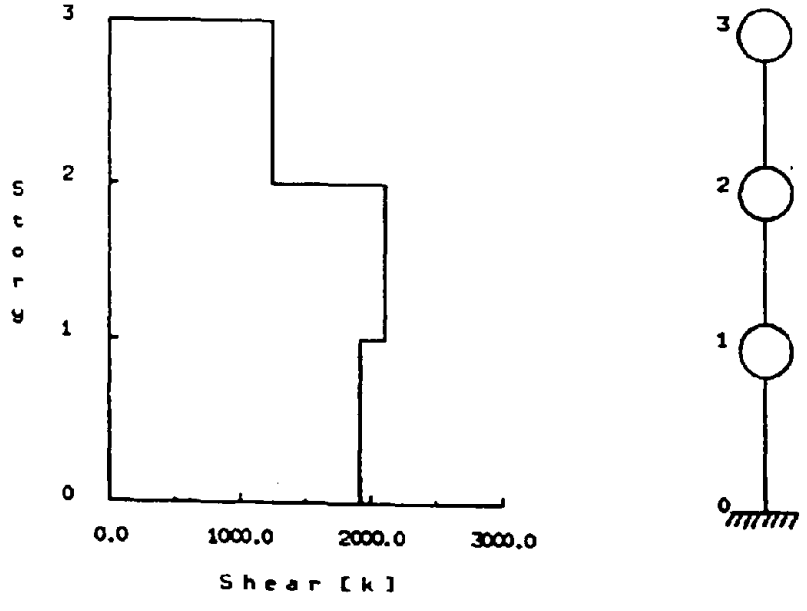

Fig. 3.8 Model and lateral shear capacities for 1985 designed non-isolated building

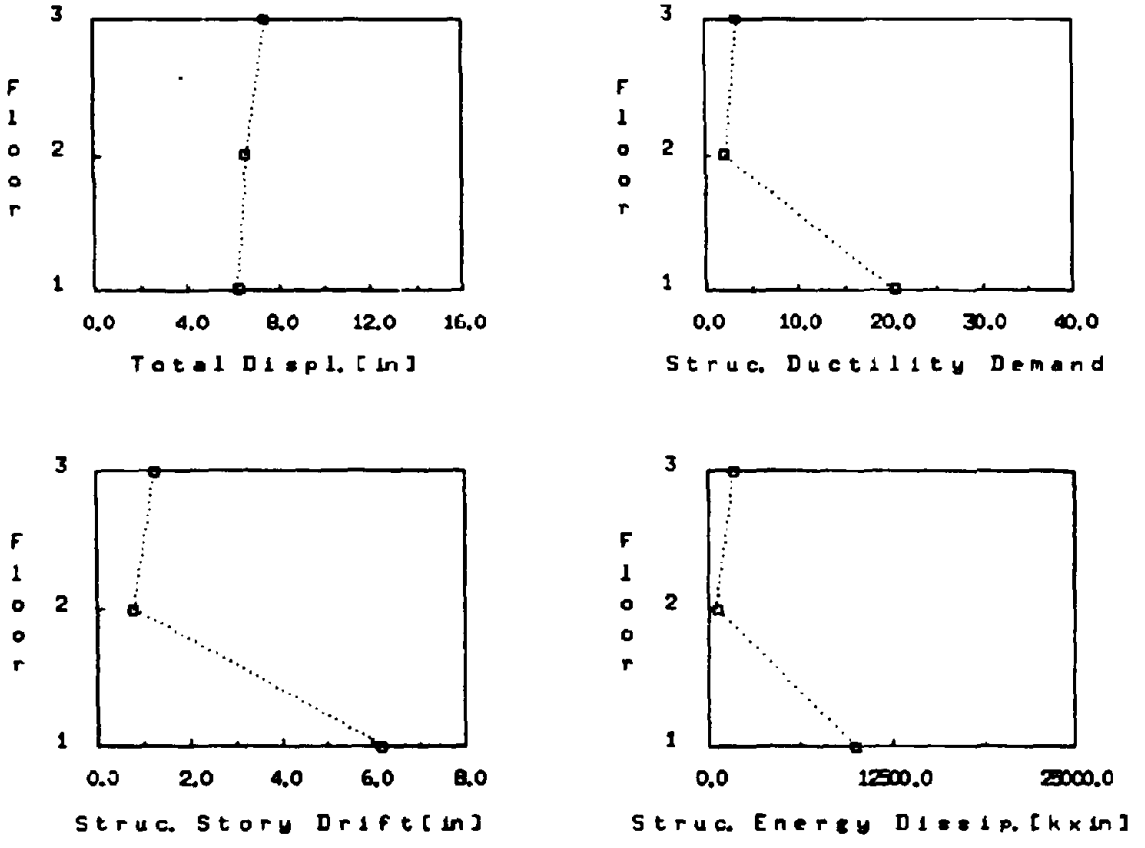

Fig. 3.9 Response envelopes for non-isolated weak building El Centro @ 0.7g

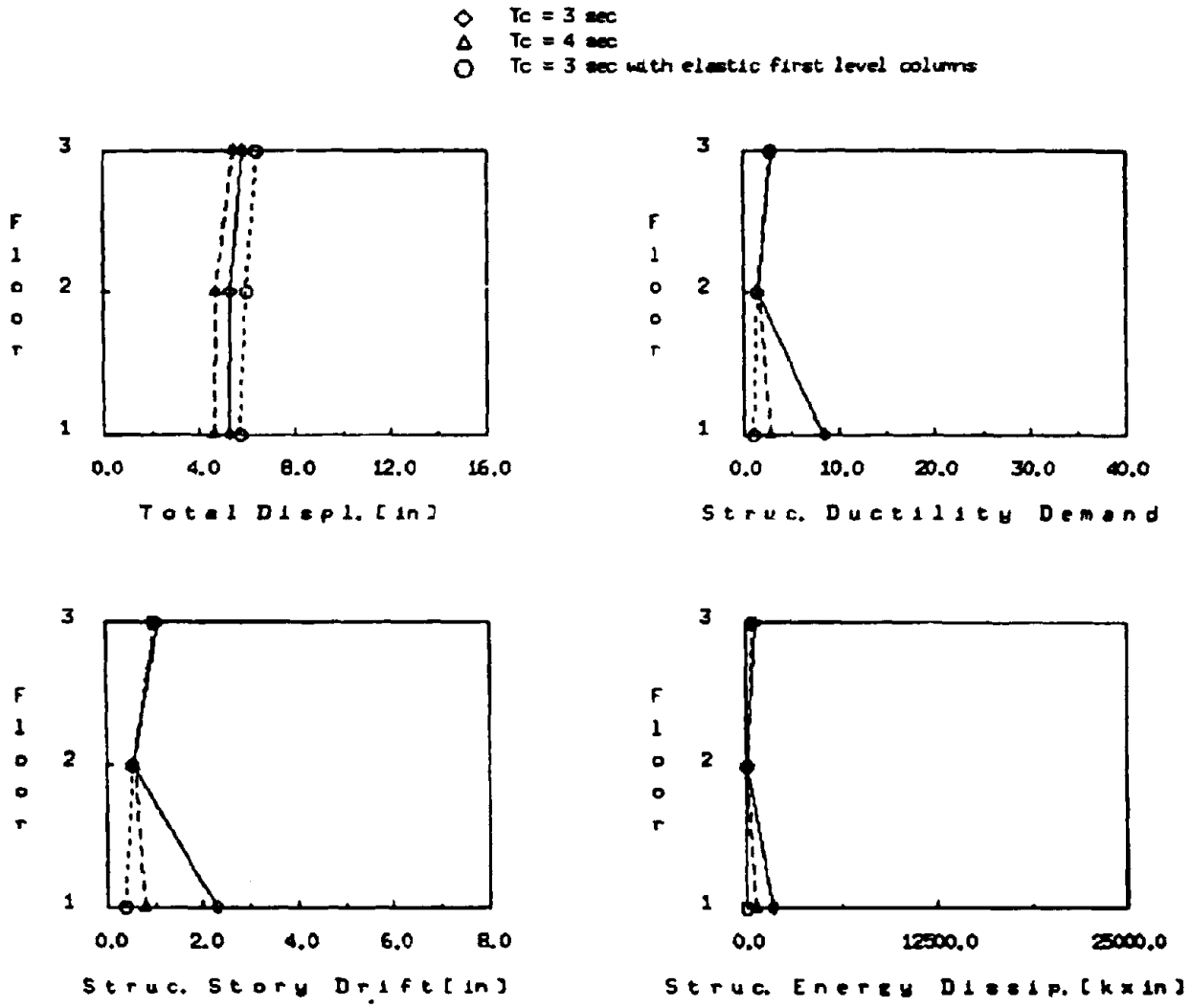

Fig. 3.10 Response envelopes for isolated weak building
El Centro @ 0.7g, friction coefficient = 0.05

CHAPTER 4

COMPONENT TESTS OF LOW FRICTION FPS ISOLATORS

by

Victor Zayas

and

Stanley Low

SECTIONS

4.1 Introduction

Application of the FPS concept requires the ability to choose and reliably achieve friction coefficients suitable to the particular building and the earthquake conditions. During prior shake table tests of simple building models on FPS connections (Ref. 4.1), the dynamic friction coefficients of the FPS components were measured to be approximately 10%. On the basis of analyses reported in Chapters 2, 6, 7, and 8, a 10% dynamic friction coefficient appeared well suited to the isolation of new buildings designed to resist very strong earthquake ground motions, such as the example Operations Building presented in Chapter 2. The 10% friction coefficient provides a large energy absorption capacity, and minimizes sliding displacements, permitting the use of relatively compact isolators. A 10% friction coefficient also facilitates the absorption of long period earthquake motions, such as occurred in the 1985 Mexico City earthquake; and the absorption of earthquake motions with strong near field pulses, such as the Pacoima Dam earthquake record.

Most existing older buildings, however, would not have the lateral load strength necessary for effective use of FPS isolators with a 10% coefficient of friction. The weak lateral strength of these buildings requires isolators with a lower friction coefficient. A lower friction coefficient isolator would also be required for the design of new cost-equivalent moment frame buildings which have a normal occupancy factor of I = 1.0. On the basis of the analyses presented in Chapters 3, 7, and 8, it appeared that a dynamic friction coefficient of 5% would be suitable for many such applications. With a 5% friction coefficient, the resulting base shears would be low enough to achieve a predominantly linear response in the upper structures. If coefficients of friction substantially lower than 5% were used, additional considerations for movements under wind loads would be required. To investigate the ability to achieve friction coefficients in the 5% range, tests of FPS components were performed and the results are reported in this chapter.

4.2 Background

It was observed during the prior tests of the 10% friction coefficient FPS assemblies (Ref. 4.1), that the dynamic friction coefficient varied with velocity. Quasi-static tests performed at very slow sliding velocities of less than 0.05 inches/sec. were observed to have friction coefficients of 4%. This was less than half the dynamic friction values of 8 to 10% observed during the shake table tests. It was considered important, therefore, to perform component tests with controlled relative velocities to better understand the relationship between dynamic friction and velocity.

Another consideration is the static break-away friction; ie, the friction value for the first sliding movement after a period of

time has elapsed during which no movement has occurred. In general, the static break-away friction is expected to vary depending on the amount of time which has elapsed without movement. During the prior tests there was no observable effect of static break-away friction. This indicated that it was always less than the dynamic friction. However, the amount of time between tests varied from a few minutes to a few hours.

During the component tests presented below the velocities could be controlled and the velocity dependency effects evaluated, However, the amount of time at full load without sliding movement was only a few minutes. This amount of time without movement was not sufficient to adequately investigate the static break-away phenomenon. A more comprehensive investigation of the break-away phenomenon, and other considerations relative to the long-term reliability of the dynamic friction coefficient is planned for the Phase II research program.

4.3 Component Test Program

In order to understand the relationship between the dynamic friction and velocity, and to confirm the ability to achieve dynamic coefficients of friction of 5%, individual FPS components were tested at the University of California, Berkeley, Earthquake Engineering Research Center. The test machine has the ability to achieve high relative velocities of up to 20 inches/second, considered representative of high earthquake velocities. This chapter documents the experiments, and presents the results.

Photographs of the FPS connections and test set-up are shown in Figs. 4.1 and 4.2. Schematic illustration of the high velocity test rig is shown in Fig. 4.3. The test rig consisted of one horizontal actuator which could achieve high speed lateral velocities, and two vertical actuators to control the vertical load and bearing pressures on the FPS components. The lateral load and vertical load on the FPS were measured by a load cell located under the FPS connection, and also by load cells located within each of the actuators. Lateral displacement was measured by the linear pot mounted on the test frame, and also by an LVDT located within the horizontal actuator. In order to accurately record the responses which occurred during the high speed and high frequency cycles, data from the instrumentation was collected at a rate of 250 data points per second.

The FPS components had self-lubricating bearings materials and mating surfaces which were designed to achieve dynamic coefficients of approximately 5%. The specific materials and manufacturing specifications of the FPS components are not disclosed for reasons of commercial competitiveness.

4.4 Test Results

Hysteretic responses of the FPS connections, tested at a constant lateral loading velocity of 0.1 inch/sec., are shown in Figs. 4.4 and 4.5. The hysteretic responses are plotted as the ratio of lateral load to axial load (coefficient of friction) versus the FPS travel displacement. The vertical load in these tests was 30 kips, resulting in a contact pressure on the bearing assembly of 17 ksi. At this pressure and very slow velocity, the coefficient of friction was observed to be 3%. The hysteretic loops were observed to have an ideal bi-linear response. The tests confirmed that the concave supporting surface results in a linear lateral stiffness throughout the displacement range. Tests performed at different vertical loads ranging from 8 to 44 kips (5 to 25 ksi), confirmed that the lateral stiffness is directly proportional to the vertical load.

Fig. 4.6 shows four hysteretic responses of the FPS connections for sinusoidal loading cycles. The lateral velocity varies sinusoidally, starting at zero at the maximum displacements, and reaching the peak velocity at zero FPS displacement travel. The peak velocities ranged from 0.2, 0.5, 1.5, and 2.5 inch/sec., and resulted in peak coefficients of friction of 4.2%, 4.6%, 4.8% and 4.9%, respectively, at a bearing pressure of 17 ksi. The coefficient of friction was observed to increase with increasing velocity, but quickly leveled off. At a relative velocity of 0.2 inches/second, the friction coefficient had achieved 85% of its peak value. Since relative velocities for earthquake motions of interest would typically vary within the range of 1 to 20 inches/second, friction coefficients for these velocities dominate the response. Lower frictions occurring at velocities less than 0.2 inch/sec. have little effect on the overall response. This effect was observed during the prior shake table tests of 10% friction FPS components, and explains why the lower friction values which were observed at very slow velocities during the component tests were essentially not noticeable during the shake table tests.

To further investigate the effects of different velocities and pressures, a standard loading set was used which included multiple sinusoidal cycles with varied peak velocities. The time history loadings for the lateral displacement and velocity plots are shown in Figs. 4.7 and 4.8, respectively. The peak velocities of the different cycles were 0.2, 1.5, 3, 6, 11, and 21 inches/sec. The frequencies of these sinusoidal cycles varied from 0.16 to 7.1 cycles/sec. The loading set was run at different bearing pressures ranging from 5 ksi. to 25 ksi. The test machine was able to maintain a relatively constant vertical load for cycles with peak velocities up to 3 inches/sec. For the higher frequency cycles, the vertical load actuators were not able to track the surface curvature quickly enough to maintain a constant vertical load. The variations in vertical load which occurred for a target load of 27 kips (15 ksi) are plotted in Fig. 4.9. The vertical loads during the high frequency cycles varied by up to 25% from the target load value.

The hysteretic responses to the sinusoidal loading set for a bearing pressure of 15 ksi are shown in Fig. 4.10. The dynamic friction for each cycle was measured from the thickness of the hysteretic loop occurring at zero displacement. The friction coefficient which occurs in first cycle, with a peak velocity of 0.2 inches/second, is observed to be lower than the friction coefficient in all other cycles. The dynamic friction in later cycles, with peak velocities ranging from 1.5 to 21 inches/second, were approximately equal. A break-away coefficient of friction of approximately 3% can be observed in this first cycle. Since the sliding friction for the first cycle was low, the effect of break-away friction could be observed. However, had the velocity of the first cycle been higher, the break-away effect would have been masked by the higher dynamic friction. Thus, for the higher sliding velocities a break-away effect is generally not noticeable. However, further investigation of the break-away effect after varied amounts of time without movement is required.

The hysteretic responses to the sinusoidal loading set for bearing pressures of 17, 20, and 25 ksi, are plotted in Figs. 4.11 to 4.13, respectively. The dynamic friction coefficient was below 5% for all cycles of loading in all load sets. A break-away friction effect was not observable in these sinusoidal load sets. The peak dynamic friction values occurred in the cycles with a 1.5 inches/second peak velocity.

The peak dynamic friction coefficients occurring in each cycle of the sinusoidal load sets are plotted in Fig 4.14. For the bearing pressures between 17 and 25 ksi, as the peak velocities increased from 1.5 to 21 inches/second, the dynamic friction coefficients decreased. It was not clear if the decrease in the friction coefficient was an an effect of the increasing velocity, or of the variations in vertical load which occurred at these higher velocity cycles. This effect will be further investigated in Phase II using shake table tests of the 5% friction coefficient assemblies.

The relationship between bearing pressure and peak dynamic friction, as measured during the sinusoidal load sets, is plotted in Fig. 4.15. As the bearing pressure was increased from 5 to 15 ksi, the peak dynamic friction was observed to decrease from 9 to 4 %. For pressures between 15 and 25 ksi the peak dynamic pressures remained fairly constant, within the target range of 4 to 5 ksi.

4.5 Conclusions

The FPS assemblies designed for low friction applications were able to consistently achieve dynamic coefficients of friction of less than 5%. These dynamic frictions of less than 5% were achieved in sinusoidal cycles with peak velocities ranging from 0.2 to 21 inches/second. The hysteretic loops were observed to have an ideal bi-linear response. The tests confirmed that the concave supporting surface results in a linear lateral stiffness throughout the displacement range. The dynamic friction values were fairly

constant for bearing pressures between 15 and 25 ksi. At pressures less than 15 ksi the dynamic friction values exceeded 5%.

In general, the peak dynamic friction coefficients were between 4 to 5%, and occurred at sliding velocities of about 1 .5 inches/second. The static break-away coefficient of friction was always less than the peak dynamic friction. At very slow velocities in the range of 0.1 to 0.2 inches/second, a reduced dynamic friction of between 2 and 3% was observed. The velocity range in which the 2 to 3% friction values occurred was very narrow, and substantially below the sliding velocities which occur during earthquake motions. This velocity dependent effect can be beneficial by reducing stick-slip motions and high frequency vibrations which might otherwise occur during earthquake motions. However, because this velocity range is small, these effects do not change the overall seismic response of FPS supported structures.

Shake table tests are required to confirm the performance of the low friction FPS assemblies under simulated earthquake conditions. Once verified, these low friction assemblies could have applications for retrofit of existing hazardous buildings, and for cost equivalent construction of new buildings.

4.6 References - Chapter 4

4.1 Zayas V.A.; Low S.S., and Mahin S.A., "The FPS Earthquake Resisting System: Experimental Report," UCB/EERC-87/01, Earthquake Engineering Research Center, University of California, Berkeley, June 1987.

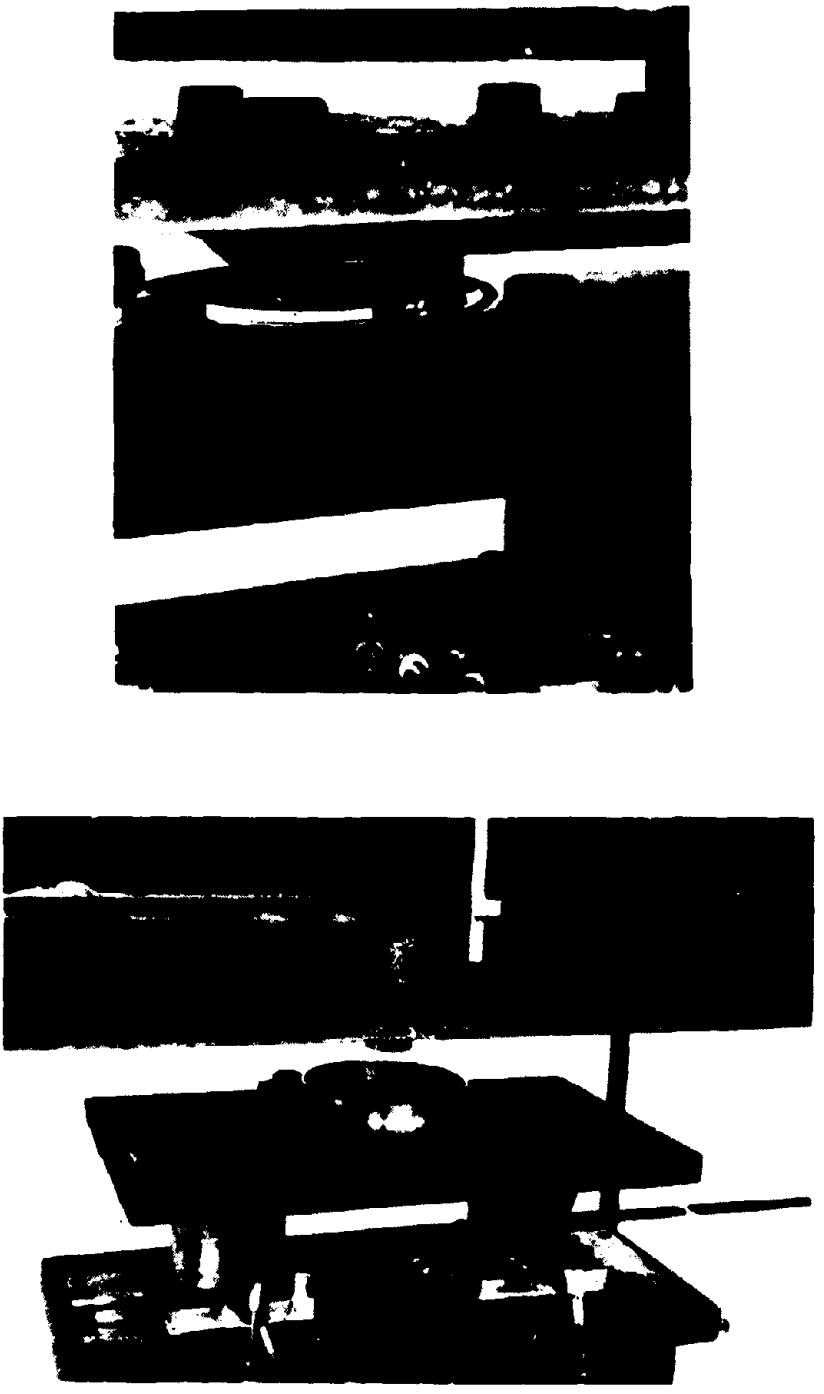

Fig. 4.1 Photographs of Test Specimen and Testing Apparatus

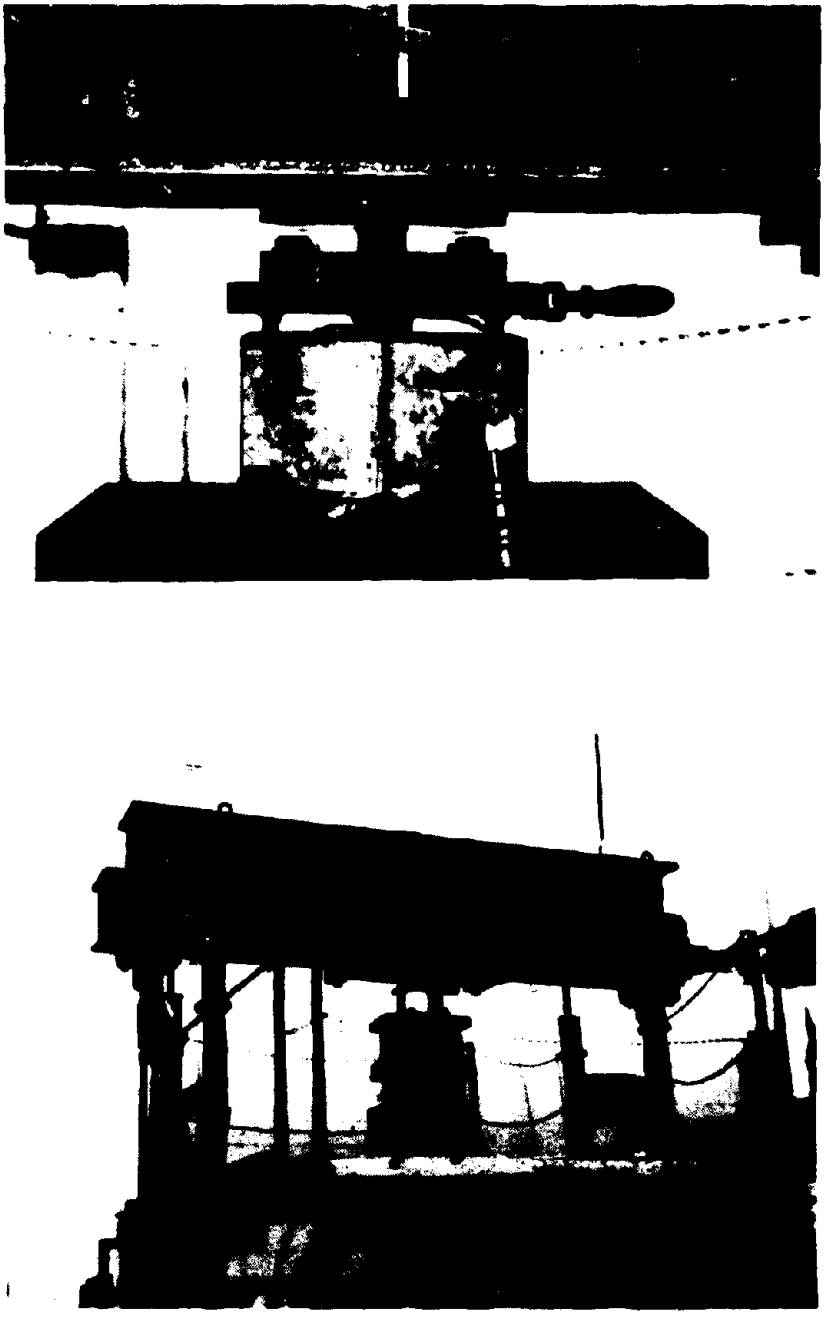

Fig. 4.2 Photographs of Test Specimen and Testing Apparatus

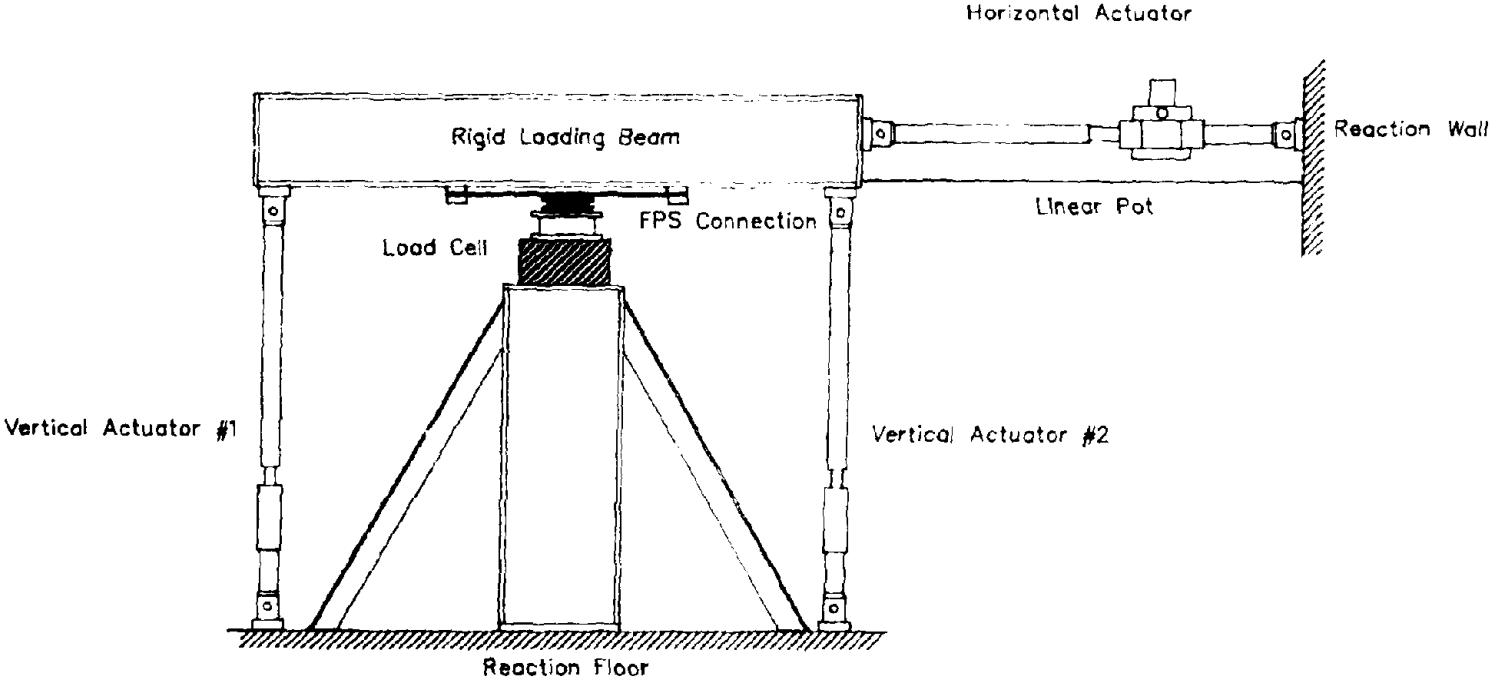

Fig. 4.3 Test Frame Set-up

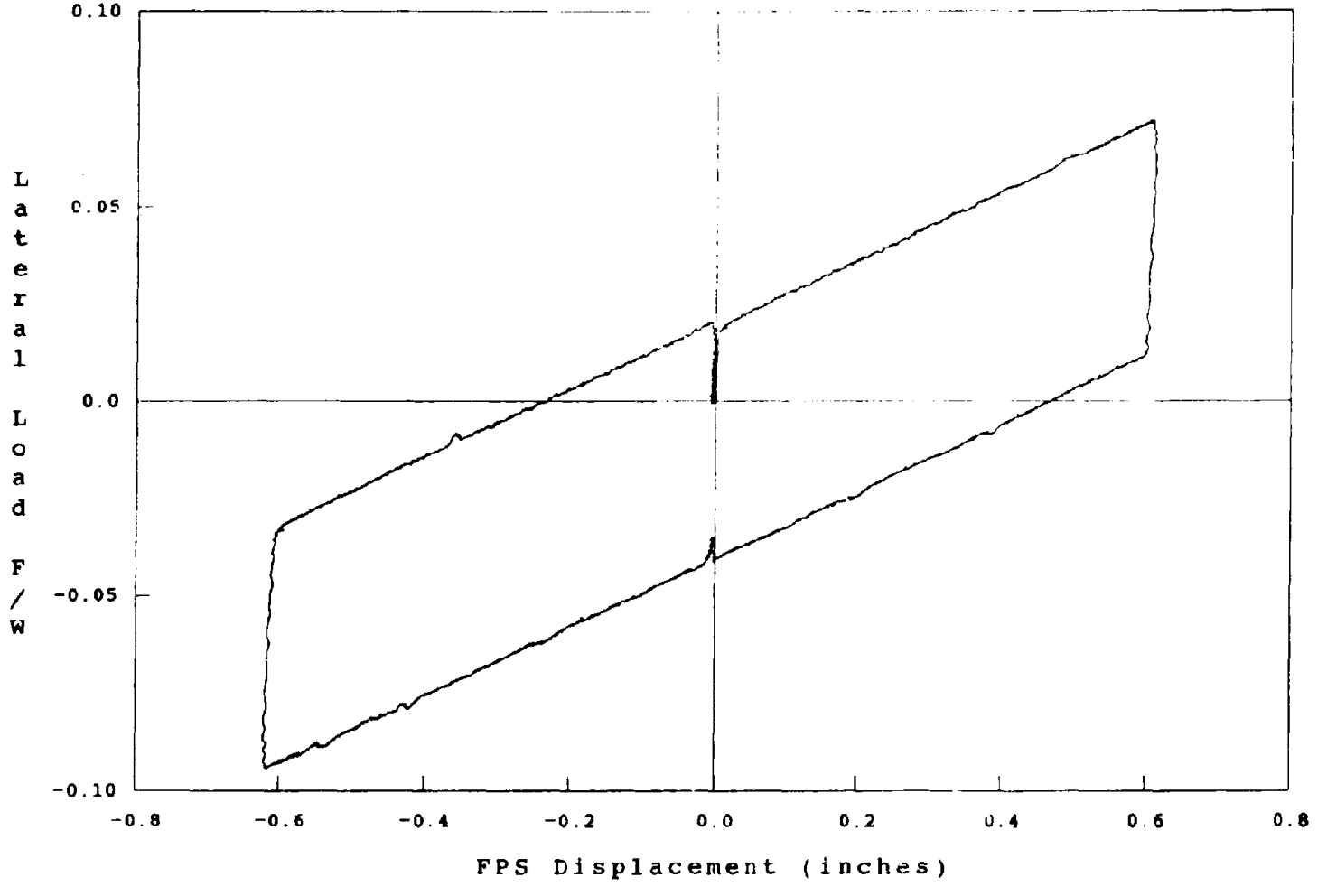

Fig. 4.4 Hysteretic Response - Constant Velocity Loading

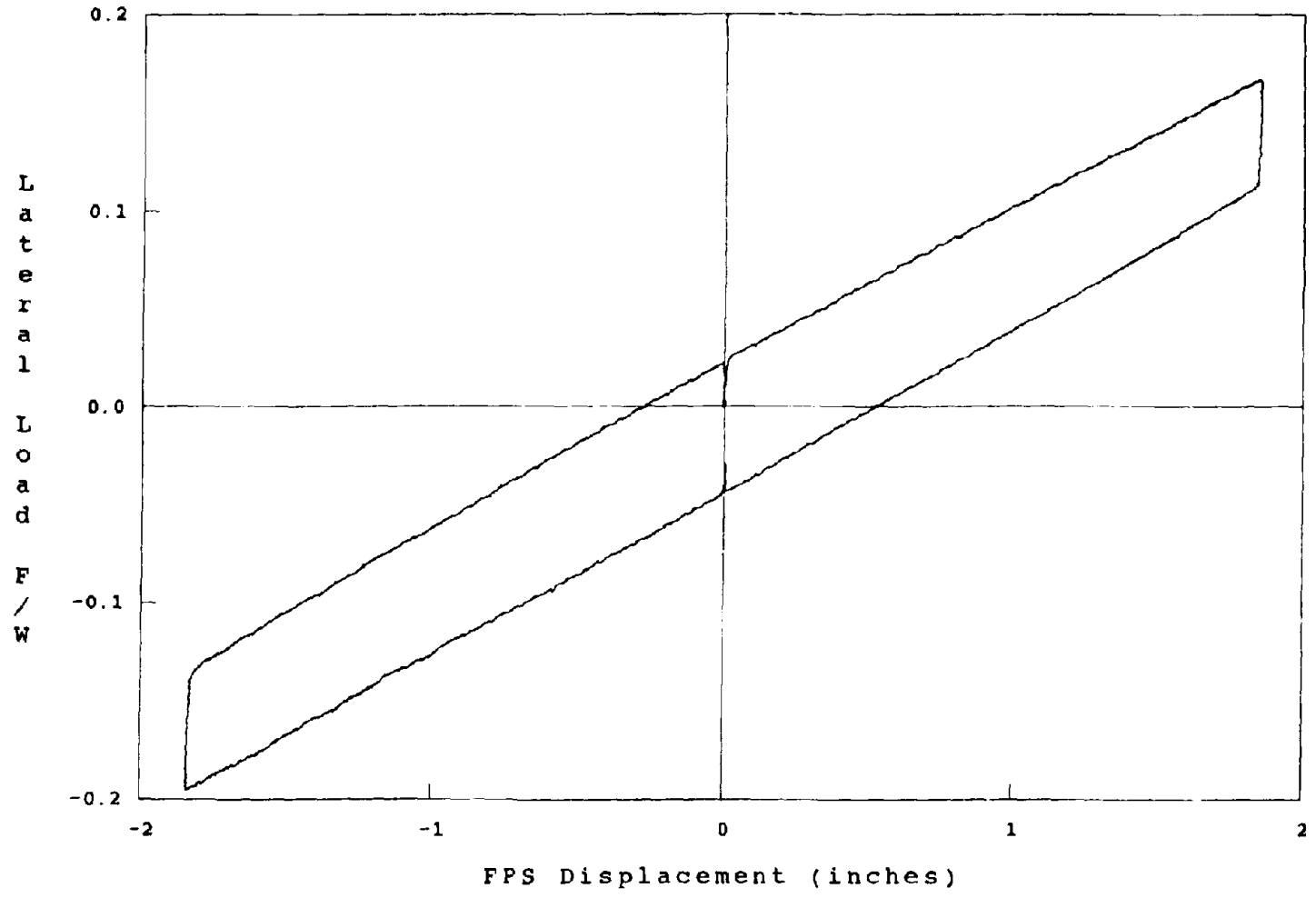

Fig. 4.5 Hysteretic Response - Constant Velocity Loading

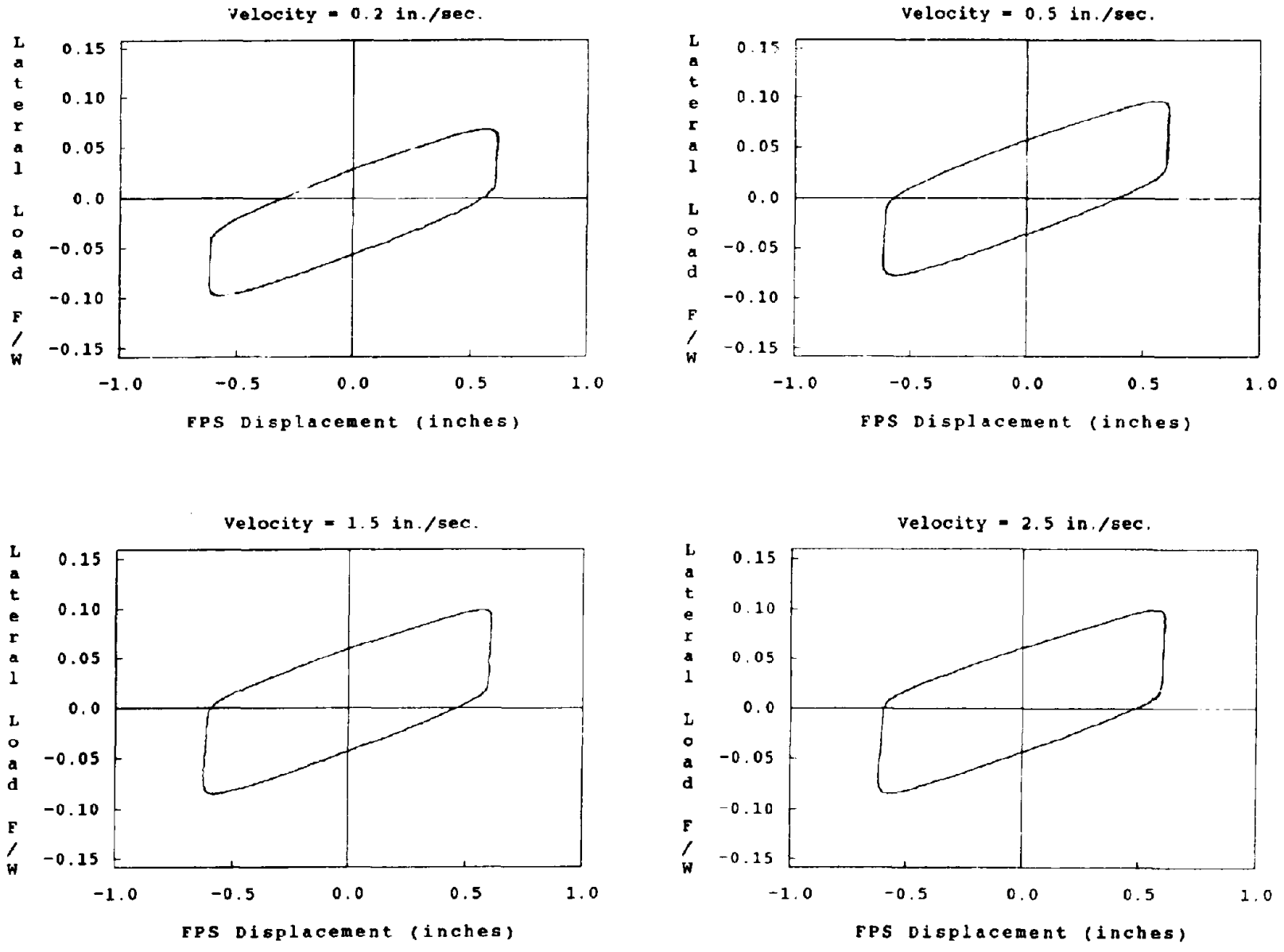

Fig. 4.6 Hysteretic Response - Single Cycle Sine Loading

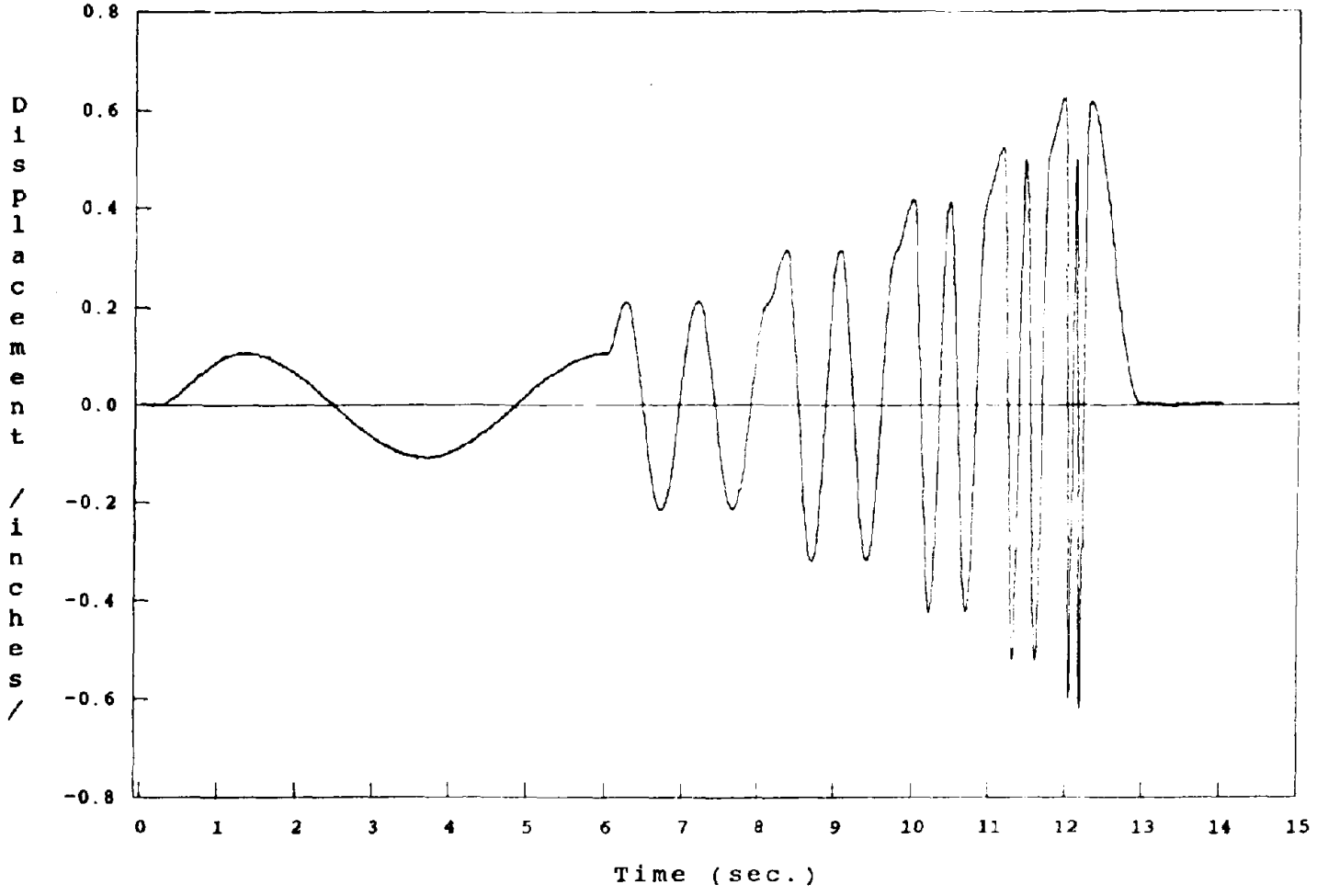

Fig. 4.7 Displacement Time History - Standard Load Set

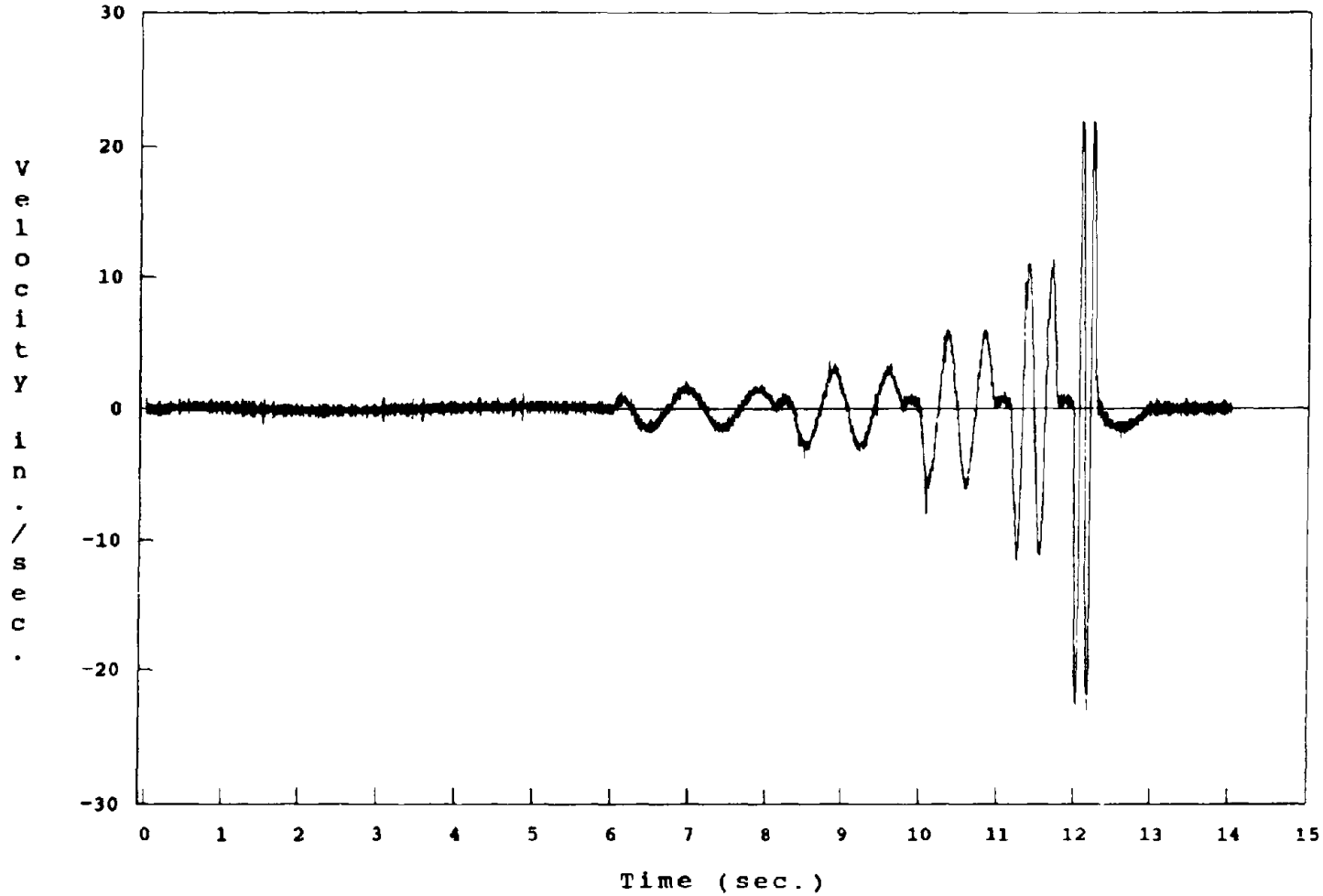

Fig. 4.8 Velocity Time History - Standard Load Set

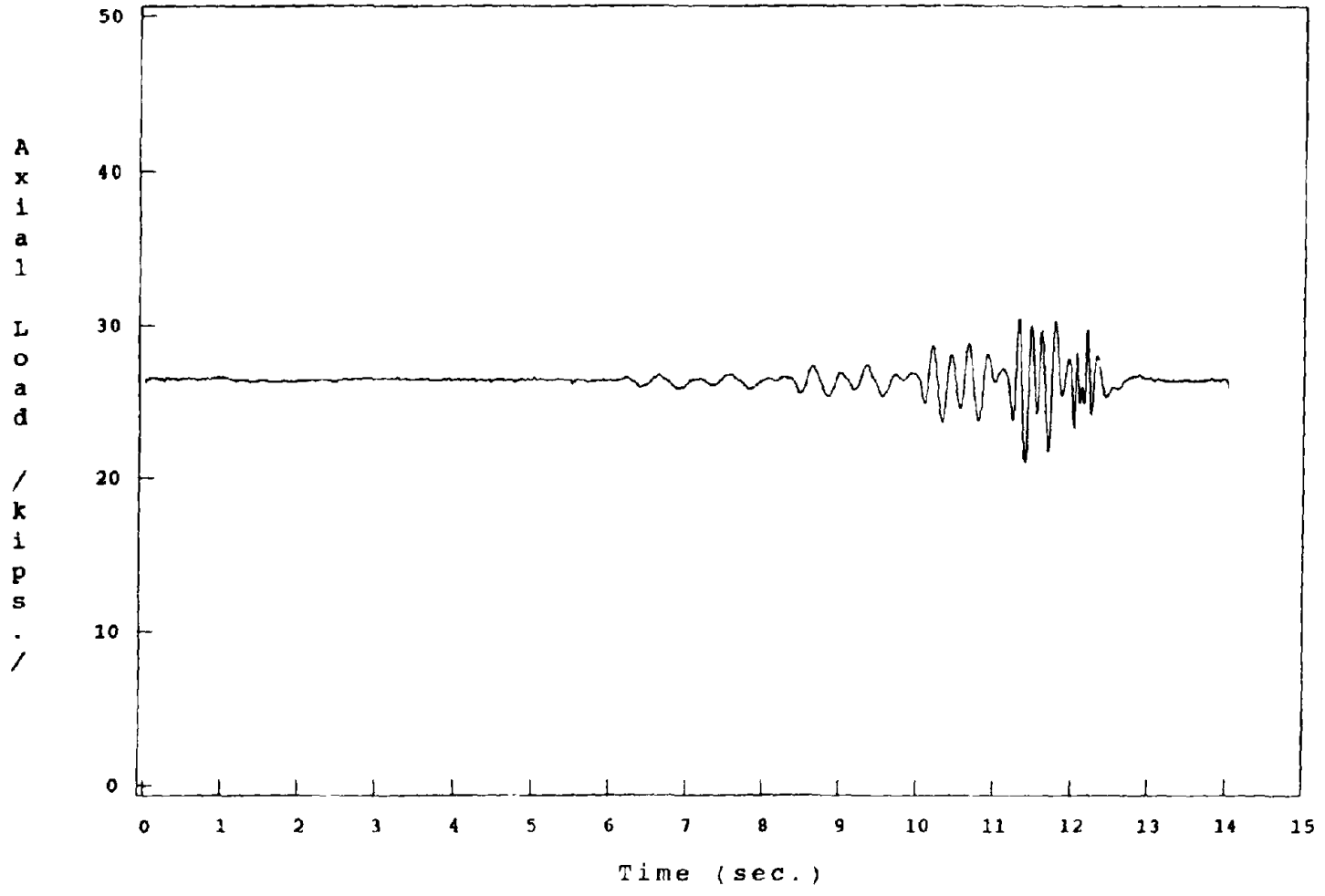

Fig. 4.9 Axial Load Time History Record - Standard Load Set

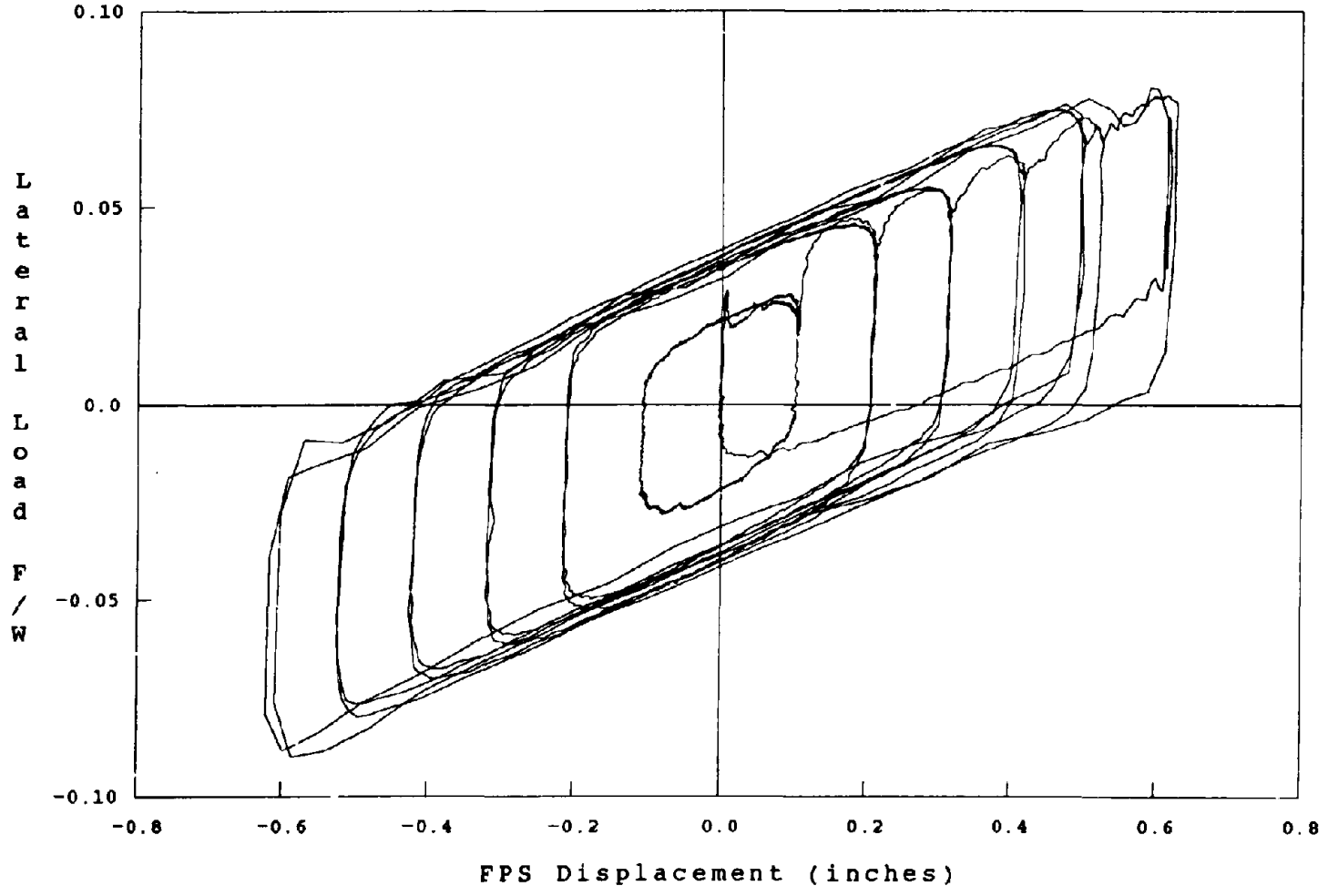

Fig. 4.10 Hysteretic Response For Bearing Pressure 15 ksi.

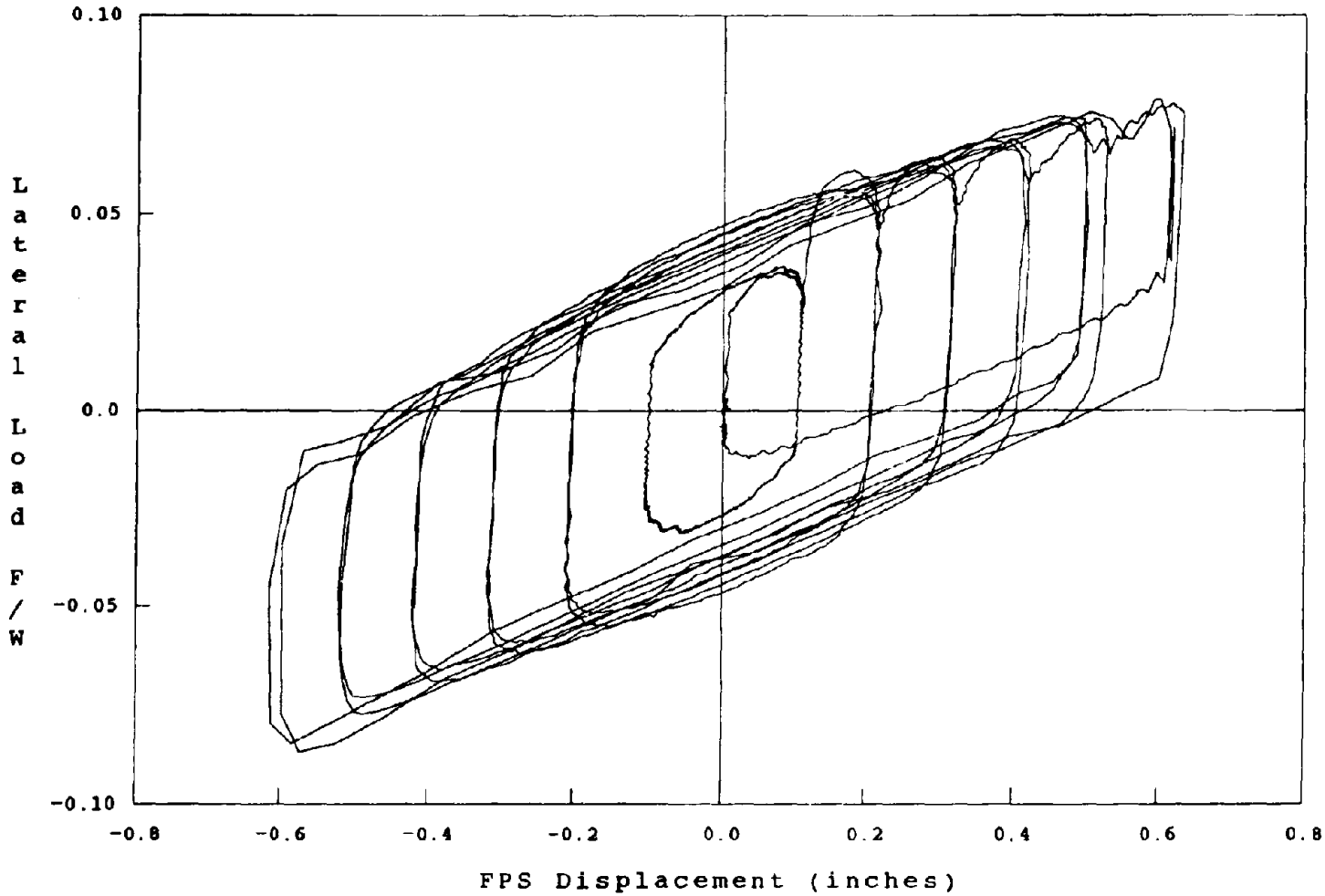

Fig. 4.11 Hysteretic Response For Bearing Pressure 17 ksi.

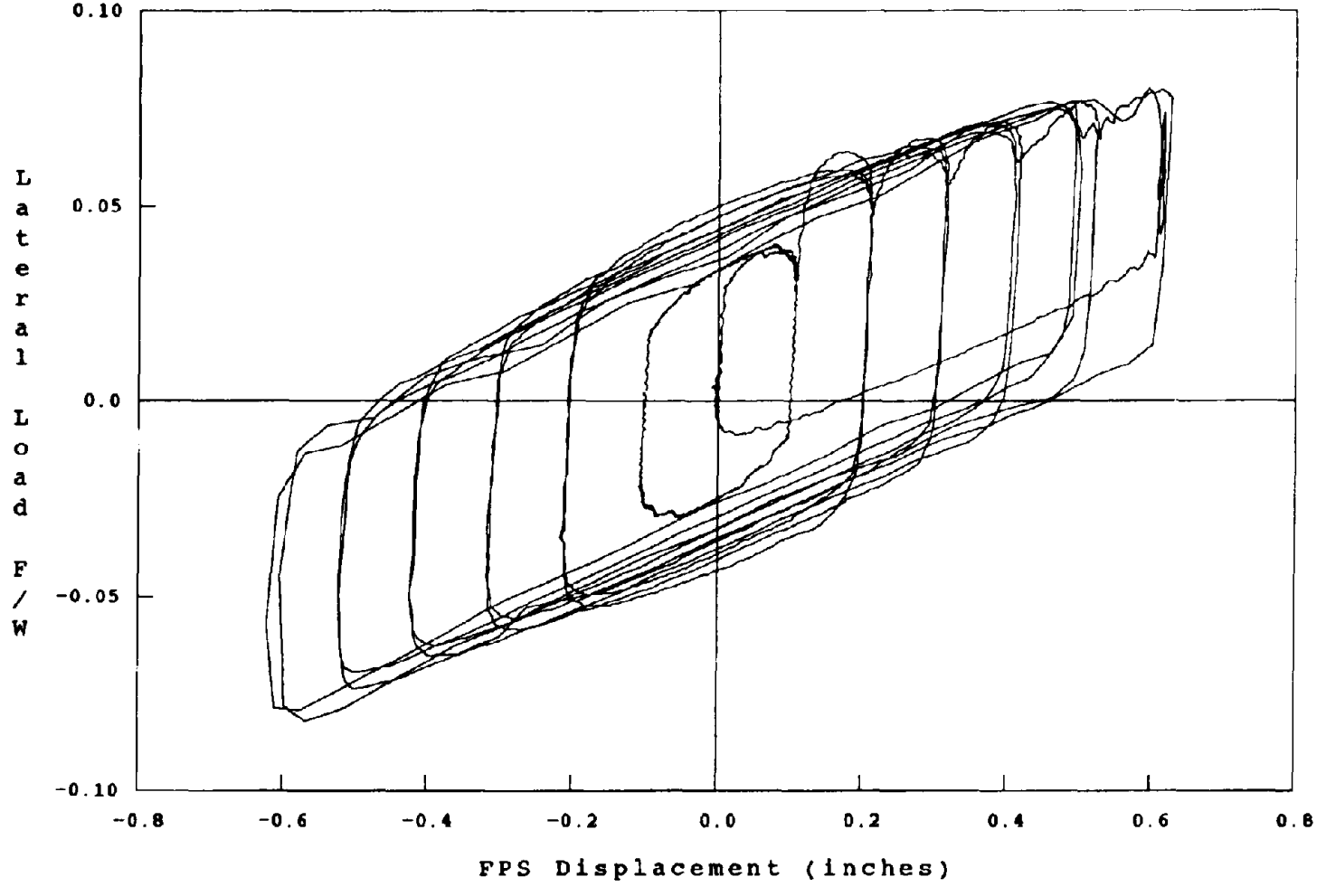

Fig. 4.12 Hysteretic Response For Bearing Pressure 20 ksi.

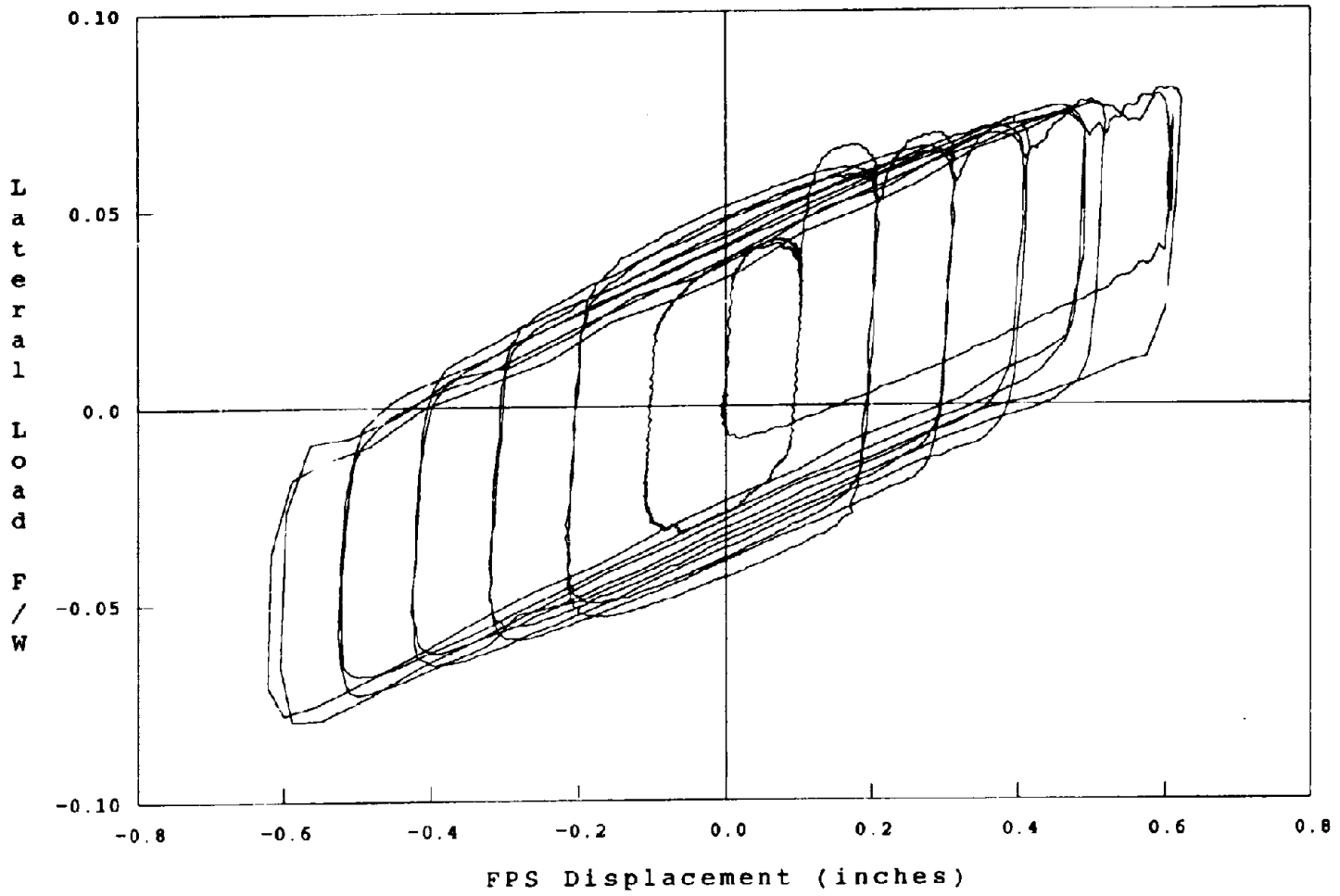

Fig. 4.13 Hysteretic Response For Bearing Pressure 25 ksi.

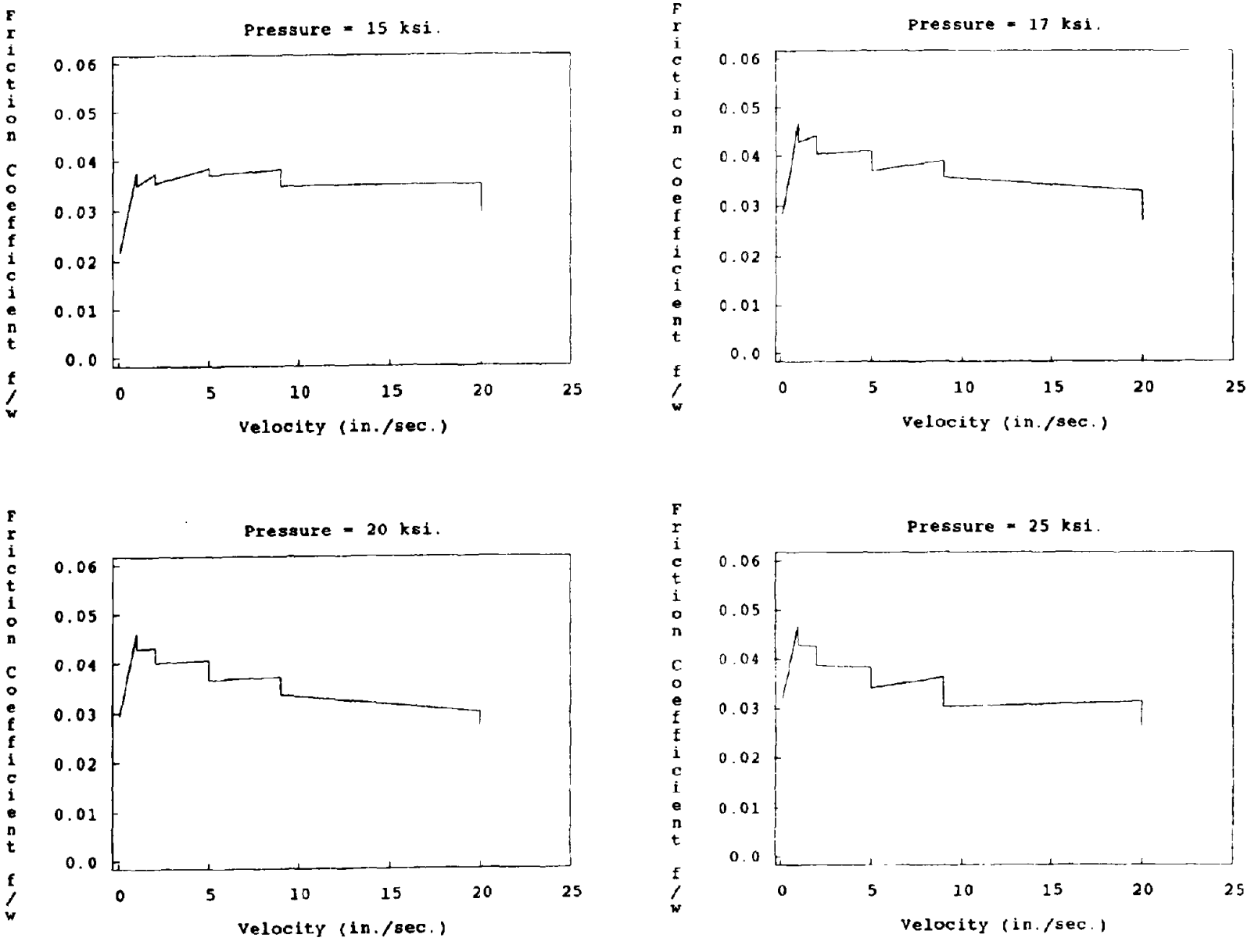

Fig. 4.14 Coefficient of Friction Versus Peak Velocity

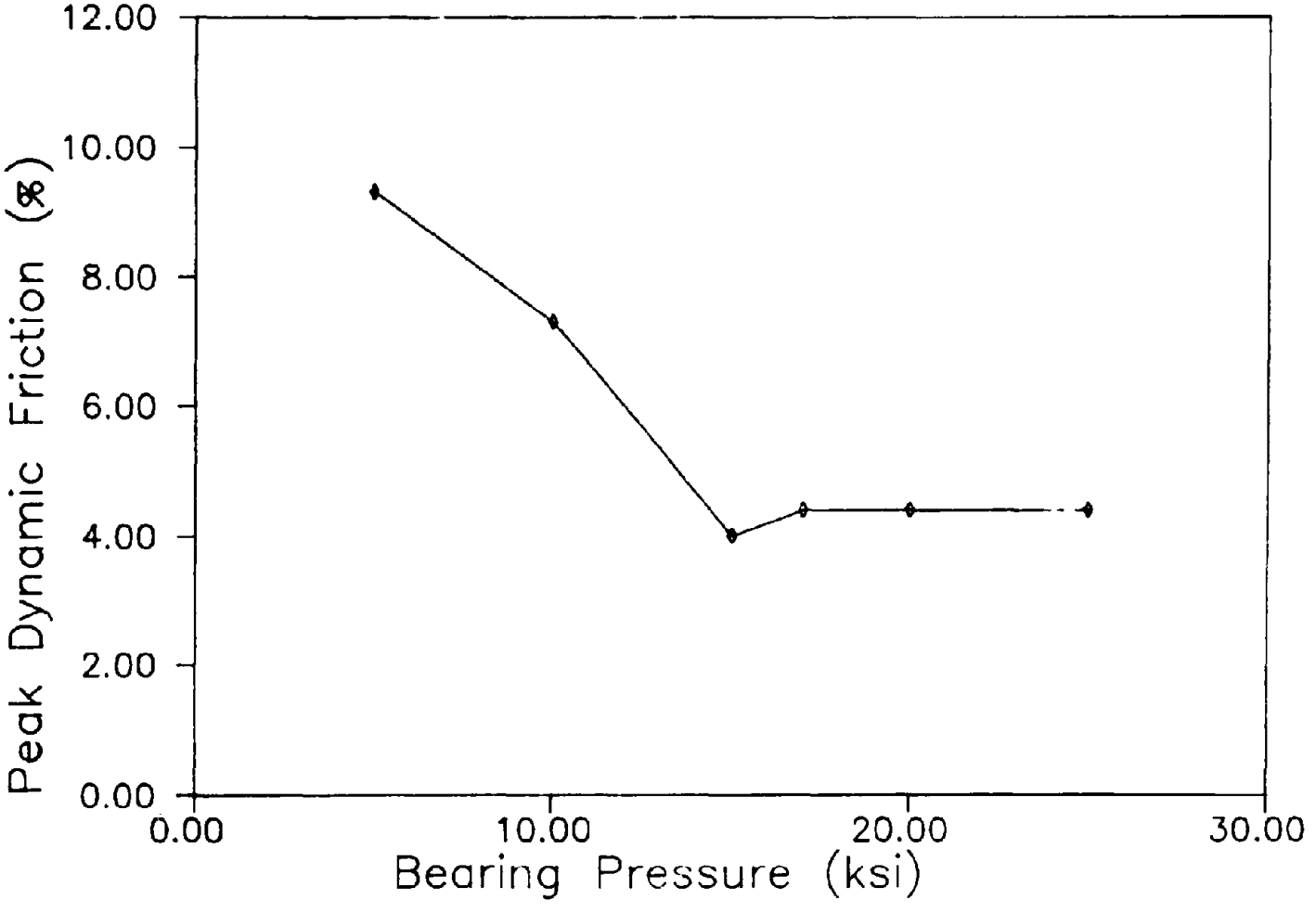

Fig. 4.15 Peak Friction Versus Bearing Pressure Relationship

CHAPTER 5

TORSION RESPONSE OF FPS ISOLATED STRUCTURES

by

Victor Zayas

and

Stanley Low

SECTIONS

5.1 Introduction

Two unique properties of pendulum motion are that: the natural vibration period is independent of the mass and; the lateral stiffness is directly proportional to the supported weight. These properties of the FPS lead to reductions in torsional motions. The reductions in torsion motions reduce torsional loads on supported buildings and give engineers and architects a method for improving the torsional response of asymmetrical and irregular buildings.

In this Chapter the torsion properties of the FPS are reviewed; experimental results obtained from tests of asymmetrical building models are evaluated; analytical models which can represent the torsional properties of the FPS are developed; the results obtained from three dimensional dynamic analyses are compared to experimental results; parameter studies are used to expand the experimental and analytical results for cases representative of building applications; and a simple equation is suggested which can conservatively estimate torsion displacements which occur in FPS supported structures.

5.2 Torsion Properties of The FPS

The lateral restoring stiffness of an FPS isolator is directly proportional to the supported weight. The friction force is also proportional to the supported weight. As a result, the center of lateral stiffness and center of friction resistance of the FPS isolator group coincides with the center of mass of the structure. When the isolator group is sliding the calculated torsion eccentricity of the FPS group is zero. The center of mass and center of rigidity remain coincident, even if the masses are moved or changed after the building is built. The properties of a coincident center of mass and rigidity can substantially reduce the torsion motions which occur in FPS isolated structures.

In an FPS supported structure, torsion motions occur prior to sliding due to the eccentricities within the building above. Torsion eccentricities which exist in the building above and small differences in friction coefficients between isolators, cause small torsion motions of the building during sliding. However, since the restoring force provided by the concave surfaces dominates the lateral stiffness and earthquake response, these torsional motions are much smaller than they would be in the same building without the FPS. Comparisons of such torsion motions are presented below.

5.3 Experimental Torsion Response of Asymmetrical Structures

Asymmetrical structural models were tested on the shake table at the Earthquake Engineering Research Center, U.C. Berkeley, to investigate the torsion response of buildings with FPS isolators (Ref. 1). Photographs and schematic illustrations of the structural models are shown in Figs. 5.1 and 5.2. The location of the mass and the structural stiffness of the structural models were modified to

achieve different torsion eccentricities. The torsion eccentricity is measured as the horizontal distance between the center of mass and the center of rigidity for the building model above the isolators, divided by the length of the building model. The center of mass of the building model is computed as the centroid of the two concrete masses above the isolator level as shown in Fig. 5.2. The center of rigidity is computed as the center of stiffness of the structural frame above the level of the isolators. The total torsion eccentricity, measured as the distance between the center of mass and center of rigidity, is referred to as the geometric eccentricity.

Mass eccentricities of 6% and 10% were achieved by moving the concrete mass at the top of the model. Stiffness eccentricities of 20% were achieved by turning one column to the strong axis direction, while leaving the other three columns oriented in the weak direction. Moving the mass towards one end of the model, and increasing the structural stiffness of the opposite end, achieved a total geometric eccentricity of 30%.

The torsion motions occurring in the structural models were measured by comparing the maximum lateral displacements which occur at the corners of the horizontal diaphragms to the maximum lateral displacements which occur at the center of the diaphragm. The percentages by which the corner displacements exceed the center displacements are the torsion displacements measured in percentage, and are plotted in Figs. 5.3 and 5.4. The results are shown for the 2 x El Centro and 1 x Pacoima Dam earthquake motions.

The corner torsion displacements occurring in the upper level of the structure with 30% geometric eccentricity were 5.6% greater than the center displacements for the 2 x El Centro loading. Considering the large torsion eccentricity of the structural model, the torsion effects were remarkably small. The FPS isolators displaced laterally under the earthquake loadings, underwent only minimal torsion motions. The torsion motions that occurred in similar models which had been tested without the FPS approached 100% (ie: pivoting around the strong column axis) (Ref. 5.2). During these previous tests of non-isolated structures, the model end with the weak axis columns yielded, while the end with the strong axis column remained elastic, resulting in a plastic torsion mode of response.

5.4 Analytical Modeling of FPS Isolated Structures

Three dimensional nonlinear time history analyses were used to investigate the torsional response of FPS supported structures. The computer program ANSR (Ref. 5.3) was used to model and analyze the test structure. The experimental results were used to verify the accuracy and capabilities of the analytical model. The analytical model was then used to predict torsional motions for full size building cases which can not be tested on the shake table. Parameter studies were then performed to extend the analytical results for buildings with different configurations and periods, and to investigate the effects of different isolator friction coefficients and periods.

The analytical model is an assembly of isolator models, and axial, and beam members as shown in Fig. 5.5. The test structure is modeled as an elastic upper structure on non-linear FPS isolators. The FPS isolators were modeled using a truss element (tension rod) to capture the curvature effects, and elastic plastic struts to represent the friction force resistance, as shown in Fig. 5.6. The length of the truss element was set equal to the radius of curvature of the concave surface. Geometric stiffness and large displacement effects were included in the analyses. This model was able to appropriately represent the natural period and weight proportional stiffness properties of the FPS isolators. The friction forces were fixed at a constant value computed on the basis of the building weight distribution. The stiffness and the mass of the test structure above the FPS were matched to the experimentally measured properties. With this modeling and analytical approach, the analyses were able to accurately simulate the response of the test structures to the earthquake ground motion.

5.5 Comparison of Analytical Results with Experimental Results

Table 5.1 compares the experimental and analytical results for test structures with four different geometric eccentricities, subjected to the 2 X El Centro earthquake motion. Table 5.2 shows results for the 6% eccentric model, subjected to three different earthquake motions. Results in Tables 5.1 and 5.2 are reported for the torsion motions of the lower level frame directly above the FPS isolators.

The analytical results were in good agreement with the experimental results. This shows that the analytical model can predict the torsion response of the FPS isolated structures, and can account for effects due to eccentricities occurring in the above structure. Differences between the analytical and experimental results are due to the structure idealization and time history digitalization effects.

It is of interest to observe from Table 5.1 that the analytical and experimental results are closer for the asymmetrical test structures, than they are for the case of the symmetrical test structure. This is due to the fact that there is always some accidental eccentricity. Imposing an intended non-zero eccentricity in both the test structure and analytical model, reduces errors in the analytical model which result from unknown accidental eccentricities. For both the symmetrical and 6% eccentric structure models, the torsional motions occurring at the corners of the structure model were equal to approximately 2% of the translational displacement. This indicated that the accidental torsion motion was approximately 2%, whether the model was symmetric or moderately asymmetric.

In order to analytically predict the torsion response of the test structures without the FPS, the analytical models were rerun eliminating the FPS elements. Without the FPS elements, the analytical model becomes a linear elastic model of the test

structure. The analytical results for the structure response with and without the FPS are compared in Fig. 5.7. The results plotted are the torsion motions of the second level horizontal frame of the test structures. The results indicate that for the test structures with 6%, 10% and 30% eccentricities, the FPS isolators reduced the expected torsional displacements by 80%, 85%, and 89%, respectively, as compared to the non-isolated structure. The analytical results for the elastic model without the FPS apply to a structure strong enough to remain elastic. The test structure without the FPS would have yielded if subjected to the prescribed loadings. If the analytical model without the FPS could have permitted yielding of the weak axis members, the computed torsion motions for the non-isolated structure would have been substantially greater. Never-the-less, torsion displacements for the the 30% eccentric model with the FPS, were one third of those occurring in the 6% eccentric model of the elastic structure without the FPS. Therefore, the FPS connections were observed to significantly reduce torsional motions, as compared to those which occur in asymmetrical structures without the FPS.

5.6 Model Scaling and Structure Size Effects

The experimental structures were quarter scale models. The experimental displacements reported in Tables 5.1 and 5.2 were multiplied by four to represent the full size prototype structure response. To indicate that the data has been scaled to the equivalent full scale value, the classification NFS (Normalized Full Scale) is used alongside the scaled data. Analyses of the test structure were first performed using the plan dimensions (6' X 9') and structure properties set equal to those of the model size. The time scaled earthquake was used as the loading and the displacement results were multiplied by four to obtain results for the full size proto-type structure (24' X 36'). The analyses were then re-run with the plan dimensions and properties set equal to those of the proto-type structure (24' X 36'), and the real time earthquake used as loading. Both analyses of the model size structure and proto-type size structure gave the same results, which are the analyses results reported in Tables 5.1 and 5.2. This confirmed that model scaling effects were properly accounted for, and that the analyses could be used to predict the response of full size structures.

To investigate the possible effect of structure size, the analytical model of the prototype structure was scaled up to represent a more realistic full size structure with a base dimension of 100' x 150'. The results for the 100' x 150' structure were similar to those of the experimental structure (Table 5.3). The results indicated that structure size did not significantly affect the torsion displacements or the percentage torsion response.

5.7 Effects of Variations in Friction Coefficients

The effect of accidental differences in friction coefficients was studied by varying the friction coefficients of the FPS isolators

in the analytical model shown in Fig. 5.5. By varying the coefficient in the analytical model, the torsion effects caused by accidental variations in friction coefficients could be separated from and compared to the effects of other accidental torsion eccentricities.

The structure and FPS properties were set to equal those of the symmetric test structure. The friction coefficients were increased in both isolators at one end of the model, to cause a difference in the friction coefficiant between the two ends. The results for variation in coefficients of friction of 0%, 5%, 10%, and 20%, are reported in Table 5.7 and plotted in Fig. 5.8. The results show that a variation in friction coefficient of 5% to 10% resulted in torsion motions of 1.2% to 2.7%. These torsion motions were of similar magnitude to the torsion motions occurring in the FPS supported test structures with mass eccentricities of up to 10%. Thus, the variations in friction coefficients of up to 10% caused similar torsion motions to variations in mass eccentricities of up to 10%. These torsional displacements were less than one third of those predicted for the test structures without the FPS, with a 5% mass eccentricity.

The friction variation of 20%, representing a large accidental variation, resulted in a modest torsion motion of 5%. These torsion motions were of similar magnitude to the torsion motions occurring in the FPS supported test structures with mass eccentricities of up to 30%. The torsional displacements were less than half of those predicted for the test structures without the FPS, with a 5% mass eccentricity. The geometric restoring forces provided by the concave surfaces were able to compensate for large differences in friction coefficients. The observed increases in displacement requirements in the FPS isolators caused by torsion effects are considered to be negligible for purposes of design of the FPS isolator travel capacity. Moreover, imposed minimum mass eccentricities of 5% appear sufficient to account for accidental torsion eccentricities which occur due to variations in friction coefficients or other accidental torsion eccentricities.

5.8 Structure and FPS Period Effects

The nonlinear time history analyses including geometric stiffness and large displacement effects could be performed for the test structures because they were relatively simple models. Detailed analyses of full size structures using this approach would be a very large and difficult numerical undertaking. The analyses cases representing full size structures, which are reported below, used simplified structural models which can capture the overall structural response, but not the localized response at individual structural members or isolators.

The test structure and analytical model had four FPS isolators. In order to further study parameters which could be expected to affect the torsional responses of full size structures, a revised analytical model was developed which included eight FPS isolators and

a simple frame model of the structure above (Fig. 5.9). Again, the model is an elastic structure on nonlinear FPS supports. This model was used to investigate the effects of structural period, isolator period, and base length to width aspect ratio as reported below.

The model shown in Fig. 5.9 was analyzed for torsional motions assuming building plan dimensions of 100' X 200'. The mass eccentricity was set at 5% of the building length to represent a code required minimum accidental eccentricity. First, the FPS sliding period was fixed at 2.25 sec., and the period of the structure above was varied from 0.18 secs. to 0.94 secs. This achieved structure to isolator period ratios ranging from 0.08 to 0.42. The results are given in Table 5.4. As the structural period was increased, the torsional displacements also increased.

The model was again analyzed assuming a stiff structure with a period of 0.18 secs., but varying the FPS sliding periods from 2.0 to 3.0 seconds. This achieved changes in isolator period while maintaining a low structure to isolator period ratio. The results are given in Table 5.5. Increasing the isolator FPS period decreased the lateral loads, increased the isolator displacements, and increased the total torsional displacements. However, the total torsional displacements remained very low since the FPS was dominating the response.

From these results it was observed that increases in the structure period or the isolator period result in increased torsion displacements. However, it appears that by increasing the isolator period, and decreasing the structure to isolator period ratio, a greater portion of the torsion displacements may be absorbed by the FPS, and torsional strains and damage may be reduced. Verification of this possible effect is planned for the Phase II research program.

5.9 Horizontal Aspect Ratio

The effect of a building's plan configuration was examined by changing the length of the analytical model shown in Fig. 5.9. This achieved different base length to base width aspect ratios. An FPS sliding period of 2.25 sec. was used. The mass eccentricity was maintained at 5% of the building length to represent an accidental eccentricity. The results for horizontal aspect ratios of 1, 2, 4 and 6 are presented in Table 5.6 and Fig. 5.10. Results are given for the FPS supported structure, and for an isolated structure which is supported on elastic isolators for which the stiffness are not proportional to the weight.

The results show that the torsion motions (Dt/D) increase with increasing aspect ratio, but that torsion motions for the FPS supported structure remain relatively small. This illustrates the effects of weight proportional stiffness, as compared to non-weight proportional linear elastic stiffness, when considering accidental eccentricities for structures with different plan geometries. For relatively long buildings with horizontal aspect ratios ranging from 2 to 6, the FPS reduced the torsion from accidental eccentricities by a factor of 5 or more.

It is observed from the results that for accidental mass eccentricities of 5%, a long rectangular building will undergo greater torsional motions than a square building. This applies to non-isolated buildings, buildings isolated with linear elastic isolators, and FPS isolated buildings. However, the FPS substantially reduced the torsional motions which occurred because of the required minimum 5% mass eccentricities.

5.10 Simple Equation For Estimating Torsion Displacements

A simple equation developed by Prof. James Kelly, of University of California, Berkeley, for estimating the torsion displacements occurring in linear elastic isolation systems is shown below (Ref. 5.4):

$$Dt = 6eD \frac{1}{1 + b^2/d^2} \qquad \text{.....} \qquad \text{EQ. [1]}$$

where e is the eccentricity occurring between the center of mass and center of stiffness, D is the lateral seismic displacement, b is the minimum base dimension, and c is the maximum base dimension of the building. This equation assumes a linear uniform stiffness under the base of a rectangular building, and has been shown by Prof. Kelly to give reasonably good results for linear elastic base isolation systems. By inputting the code required minimum eccentricity of 5%, this equation can be useful for making estimates of accidental torsion motions for purposes of isolation system design.

The experimental and analytical results have shown that torsion displacements occurring with the FPS are consistently smaller than those occurring in linear elastic systems. By utilizing the parametric results presented herein, a empirically based modification to this equation will be suggested that conservatively estimates the torsion displacements observed in the FPS supported test structures.

First, Equation 1 is used to compute an "effective eccentricity" for the FPS system from the test results as follows;

$$e = \frac{Dt}{6D}\left[1 + b^2/d^2\right]$$

where Dt is input as the experimentally measured torsion motion. The "effective eccentricity" is the equivalent eccentricity for a linear elastic system which would result in the same torsion displacement Dt as measured in the FPS test structures.

The effective eccentricities, as calculated using the test results reported in Tables 5.1 and 5.2, are reported in Table 5.8. The results show that for geometric eccentricities up to 30%, the computed effective eccentricities are less than 0.85%. Thus for imposed torsion eccentricities substantially exceeding a 5% minimum eccentricity, the resulting effective eccentricity was less than 1%. This suggests that a very conservative estimate of accidental torsion motions for 5% mass eccentricities occurring in FPS supported structures can be computed from Equation 2 as shown below:

$$Dt = 1.2eD \frac{1}{1 + b^2/d^2} \qquad \text{..... EQ. [2]}$$

To examine the suggestion that Equation 2 may be used as a conservative estimate of torsion displacements for the FPS, the analytical results obtained from the parameter study of different base width to length aspect ratios are compared to the torsion displacements calculated using Equation 2. From the comparison shown in Table 5.9, it can be seen that Equation 2 overestimates the torsion displacements, as compared to those computed from three dimensional dynamic analyses for a 5% mass eccentricity.

A comparison of Equation 1, Equation 2, and the experimental FPS results is shown in Fig. 5.11. Although Equation 2 is a simply derived empirical envelope, it appears to more adequately represent the FPS torsion response than Equation 1. A theoretically derived equation for estimating may be possible, and preferable to the simple empirical correlation suggested herein. This will be considered further during then Phase II research program.

5.11 Conclusions

The properties of pendulum motion were effective in minimizing the torsional response of asymmetrical structures. The weight proportional stiffness of the FPS isolators directly compensated for imposed mass eccentricities. Torsion motions resulting from accidental or imposed eccentricities were found to be small. In general, the torsional motions of FPS supported structures were substantially smaller than those occurring in linear elastic systems with equivalent eccentricities.

The parameters which increased the torsion motion response of FPS supported structures were: differences in friction coefficients between isolators; mass eccentricities; base length to width aspect ratio; structure period; and isolator period. In the worst cases of imposed torsion eccentricities, the torsion motions were found to add 5% to the lateral displacement motions, which could be ignored for the design of the FPS isolators for most applications.

5.12 References - Chapter 5.

5.1. V.A. Zayas; S.S. Low, and S.A. Mahin, "The FPS Earthquake Resisting System: Experimental Report," Report UCB/EERC 87/01, Earthquake Engineering Research Center, University of California, Berkeley, June 1987.

5.2 Thewalt, C.R.; and Mahin, S.A., "Bidirectional Seismic Response of Simple Structures", American Society of Civil Engineers Structures Congress, New Orleans, 1986.

5.3. D.P. Mondkar, and G. H. Powell, "ANSR 1: General Purpose Program For Analysis of Nonlinear Structural Response," Report UCB/EERC 75/37, Earthquake Engineering Research Center, University of California, Berkeley, December 1975.

5.4 By personal communication with Prof. James Kelly of the University of California, Berkeley.

TABLE 5.1 COMPARISONS OF TORSIONAL RESPONSE TO DIFFERENT ECCENTRICITY

GEOMETRIC ECCENTRICITY e	EARTHQUAKE	ANALTYICAL RESULTS			NFS EXPERIMENTAL RESULTS		
		MEAN DISPL. (in.)	MAX. DISPL. (in.)	Dt/D (%)	MEAN DISPL. (in.)	MAX. DISPL. (in.)	Dt/D (%)
0%	2x EL CENTRO	5.68	5.68	0.0%	5.74	5.84	1.7%
6%	2x EL CENTRO	5.64	5.76	2.1%	5.60	5.72	2.1%
10%	2x EL CENTRO	5.62	5.76	2.5%	5.60	5.80	2.8%
30%	2x EL CENTRO	5.62	5.86	4.3%	5.68	5.88	3.5%

TABLE 5.2 COMPARISONS OF TORSIONAL RESPONSE TO DIFFERENT EARTHQUAKES

EARTHQUAKE	GEOMETRIC ECCENTRICITY e	ANALTYICAL RESULTS			NFS EXPERIMENTAL RESULTS		
		MEAN DISPL. (in.)	MAX. DISPL. (in.)	Dt/D (%)	MEAN DISPL. (in.)	MAX. DISPL. (in.)	Dt/D (%)
1x PARKFIELD	6%	3.20	3.28	2.5%	3.54	3.64	2.8%
2x EL CENTRO	6%	5.64	5.76	2.1%	5.72	5.72	2.1%
1x PACOIMA DAM	6%	7.30	7.36	0.8%	8.52	8.80	3.3%

TABLE 5.3 STRUCTURE SIZE EFFECT ON THE TORSION RESPONSE

STRUCTURE		EARTHQUAKE	RESPONSE		
			MEAN DISPL. (in.)	MAX. DISPL. (in.)	Dt/D (%)
PROTOYPE STRUCTURE 24' x 36'(NFS)	(NFS) EXPERIMENTAL RESULTS	2x EL CENTRO	5.60	5.72	2.1%
FULL SCALE STRUCTURE 100' x 150'	ANALYTICAL RESULTS	2x EL CENTRO	5.82	5.95	2.2%

TABLE 5.4 EFFECT OF STRUCTURE PERIOD

STRUCTURAL PERIOD (sec.)	STRUCTURAL TO ISOLATION PERIOD RATIO	EARTHQUAKE	ANALYTICAL RESULTS e = 5%		
			MEAN DISPL. (in.)	MAX. DISPL. (in.)	Dt/D (%)
0.18	0.08	2x EL CENTRO	5.50	5.53	0.5%
0.54	0.24	2x EL CENTRO	4.60	4.67	1.5%
0.94	0.42	2x EL CENTRO	5.05	5.34	5.7%

TABLE 5.5 EFFECT OF SLIDING PERIOD ON TORSION RESPONSE

SLIDING PERIOD (sec.)	EARTHQUAKE	STRUCTURAL TO ISOLATION PERIOD RATIO	ANALYTICAL RESULTS e = 5%		
			MEAN DISPL. (in.)	MAX. DISPL. (in.)	Dt/D (%)
2.00	2x EL CENTRO	0.09	5.31	5.30	0.2%
2.25	2x EL CENTRO	0.08	5.50	5.53	0.5%
3.00	2x EL CENTRO	0.06	6.20	6.26	0.9%

TABLE 5.6 EFFECT OF HORIZONTAL ASPECT RATIO ON TORSION RESPONSE

BUILDING DIMENSION AND ASPECT RATIO	EARTHQUAKE	FPS WEIGHT PROPORTIONAL STIFFNESS ISOLATION SYSTEM ANALYTICAL RESULTS			GENERIC NON-WEIGHT PROPORTIONAL STIFFNESS ISOLATION SYSTEM ANALYTICAL RESULTS		
		MEAN DISPL. (in.)	MAX. DISPL. (in.)	Dt/D (%)	MEAN DISPL. (in.)	MAX. DISPL. (in.)	Dt/D (%)
100' x 100' 1:1	2x EL CENTRO	5.48	5.54	1.1%	7.73	8.00	3.3%
100' x 200' 1:2	2x EL CENTRO	5.50	5.53	0.5%	7.74	8.46	9.3%
100' x 400' 1:4	2x EL CENTRO	5.50	5.64	2.5%	7.74	9.06	17.0%
100' x 600' 1:6	2x EL CENTRO	5.48	5.74	4.7%	7.74	9.28	20.0%

PROPERTIES OF FPS ISOLATED STRUCTURE

SLIDING PERIOD = 2.25 sec.
THRESHOLD FORCE = 0.10W
STRUCTURAL PERIOD = 0.18 sec.
GEOMETRIC ECCENTRICITY = 5%

PROPERTIES OF THE GENERIC ISOLATED STRUCTURE

POST YIELD PERIOD = 2.25 sec.
THRESHOLD FORCE = 0.05W
STRUCTURAL PERIOD = 0.18 sec.
GEOMETRIC ECCENTRICITY = 5%

TABLE 5.7 TORSION RESPONSE DUE TO VARIATION OF COEFFICIENT OF FRICTION

VARIATION IN COEFFICIENT OF FRICTION (%)	EARTHQUAKE	GEOMETRIC ECCENTRICITY e	ANALYTICAL RESULTS		
			MEAN DISPL. (in.)	MAX. DISPL. (in.)	Dt/D (%)
0%	2x EL CENTRO	0%	5.68	5.68	0.0%
5%	2x EL CENTRO	0%	5.66	5.73	1.2%
10%	2x EL CENTRO	0%	5.62	5.77	2.7%
20%	2x EL CENTRO	0%	5.58	5.86	5.0%

TABLE 5.8 COMPUTING THE EFFECTIVE ECCENTRICITY FROM TORSION EQUATION [1]

GEOMETRIC ECCENTRICITY e1	EARTHQUAKE	NFS EXPERIMENTAL RESULTS				EFFECTIVE ECCENTRICITY e
		D (in.)	Dt (in.)	b (ft.)	d (ft.)	
0%	2x EL CENTRO	5.74	0.14	24'	36'	0.59%
0%	1x PACOIMA DAM	8.00	0.04	24'	36'	0.12%
6%	1x PARKFIELD	3.54	0.10	24'	36'	0.68%
6%	2x EL CENTRO	5.60	0.12	24'	36'	0.52%
6%	1x PACOIMA DAM	8.52	0.28	24'	36'	0.79%
10%	2x EL CENTRO	5.64	0.16	24'	36'	0.68%
10%	1x PACOIMA DAM	8.56	0.24	24'	36'	0.67%
30%	2x EL CENTRO	5.68	0.20	24'	36'	0.85%
30%	1x PACOIMA DAM	8.56	0.28	24'	36'	0.79%

EQUATION [1]

$$Dt = 6eD \frac{1}{1 + b^2/d^2}$$

$$e = \frac{Dt}{6D}\left[1 + b^2/d^2\right]$$

TABLE 5.9 COMPARING ANALYTICAL RESULTS WITH EQUATION [2]

ASPECT RATIO	ANALYTICAL RESULTS e = 5% 2 x EL CENTRO EARTHQUAKE				Dt/D (%)	Dt/D FROM EQUATION [ ] (%)
	D (in.)	Dt (in.)	b (ft.)	d (ft.)		
1 : 1	5.48	0.06	100'	100'	1.1%	3.3%
1 : 2	5.50	0.03	100'	200'	0.5%	4.8%
1 : 4	5.50	0.14	100'	400'	2.5%	5.6%
1 : 6	5.48	0.26	100'	600'	4.7%	5.8%

EQUATION [2]

$$Dt = 1.2eD \frac{1}{1 + b^2/d^2}$$

$$\frac{Dt}{D} = 1.2e \frac{1}{1 + b^2/d^2}$$

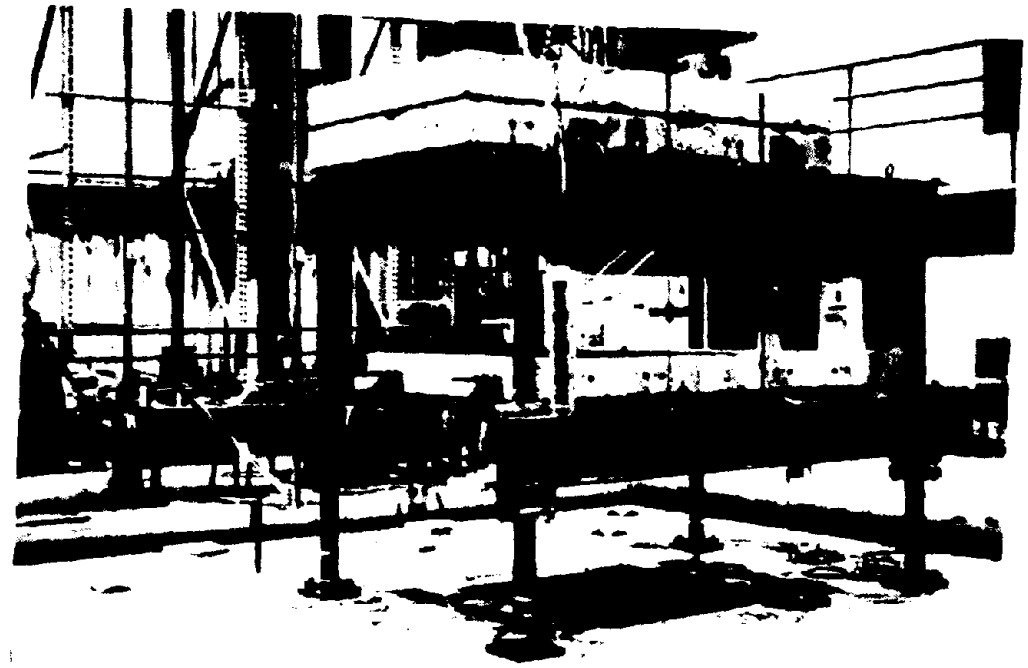

Fig. 5.1 Photograph of Asymmetrical Test Structure

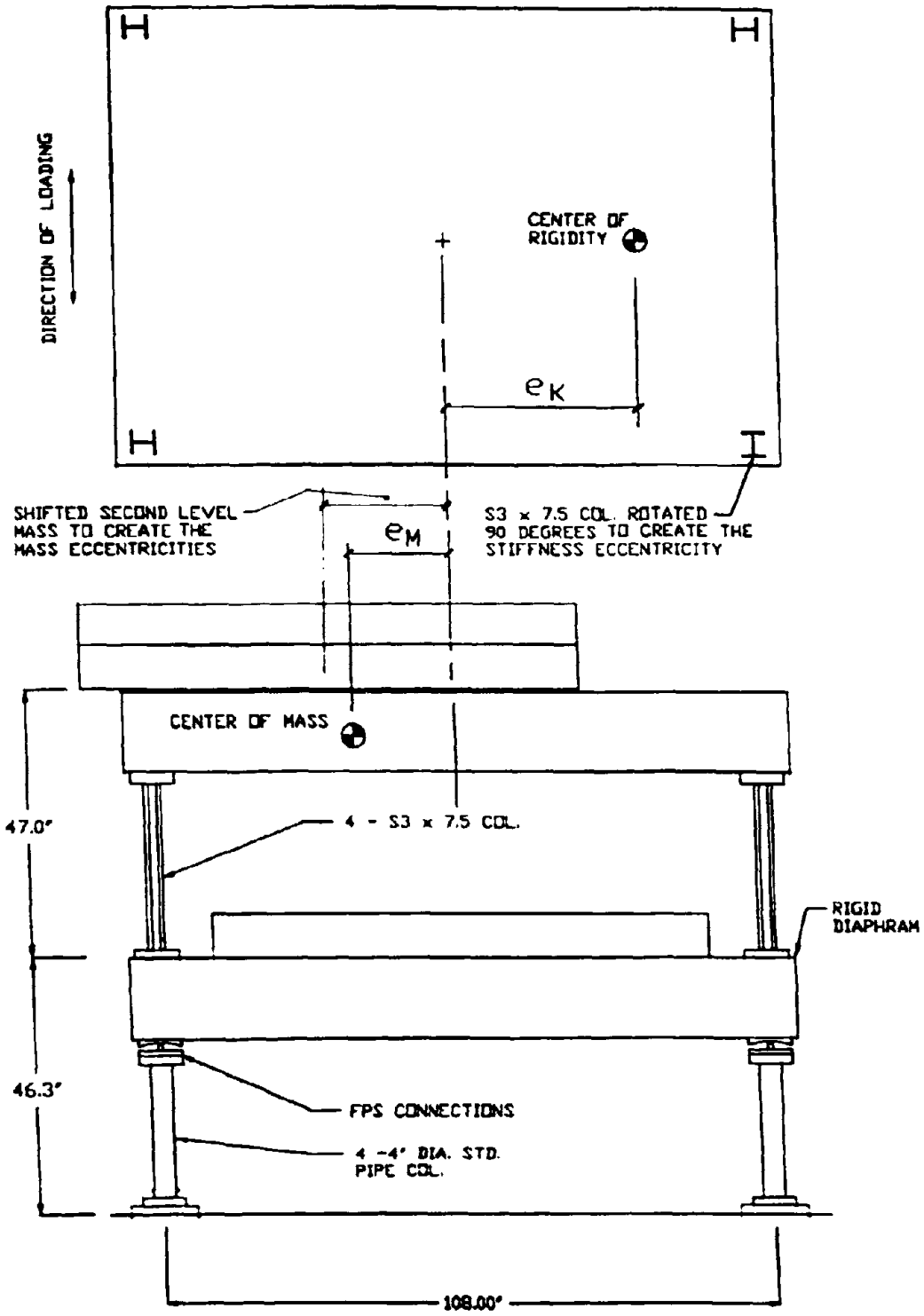

Fig. 5.2 Asymmetrical Structure Model

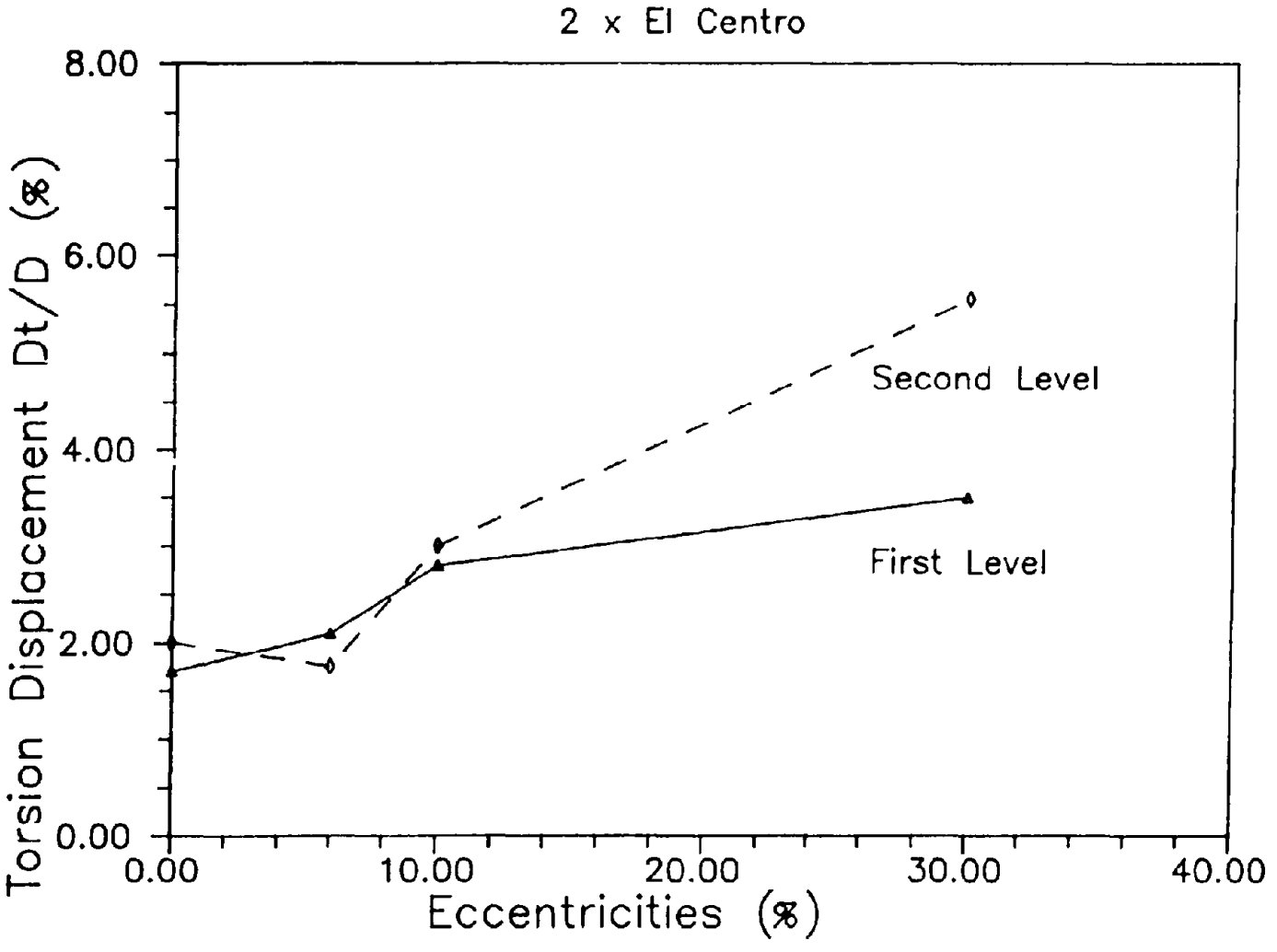

Fig. 5.3 Maximum Torsional Displacements - 2 x El Centro

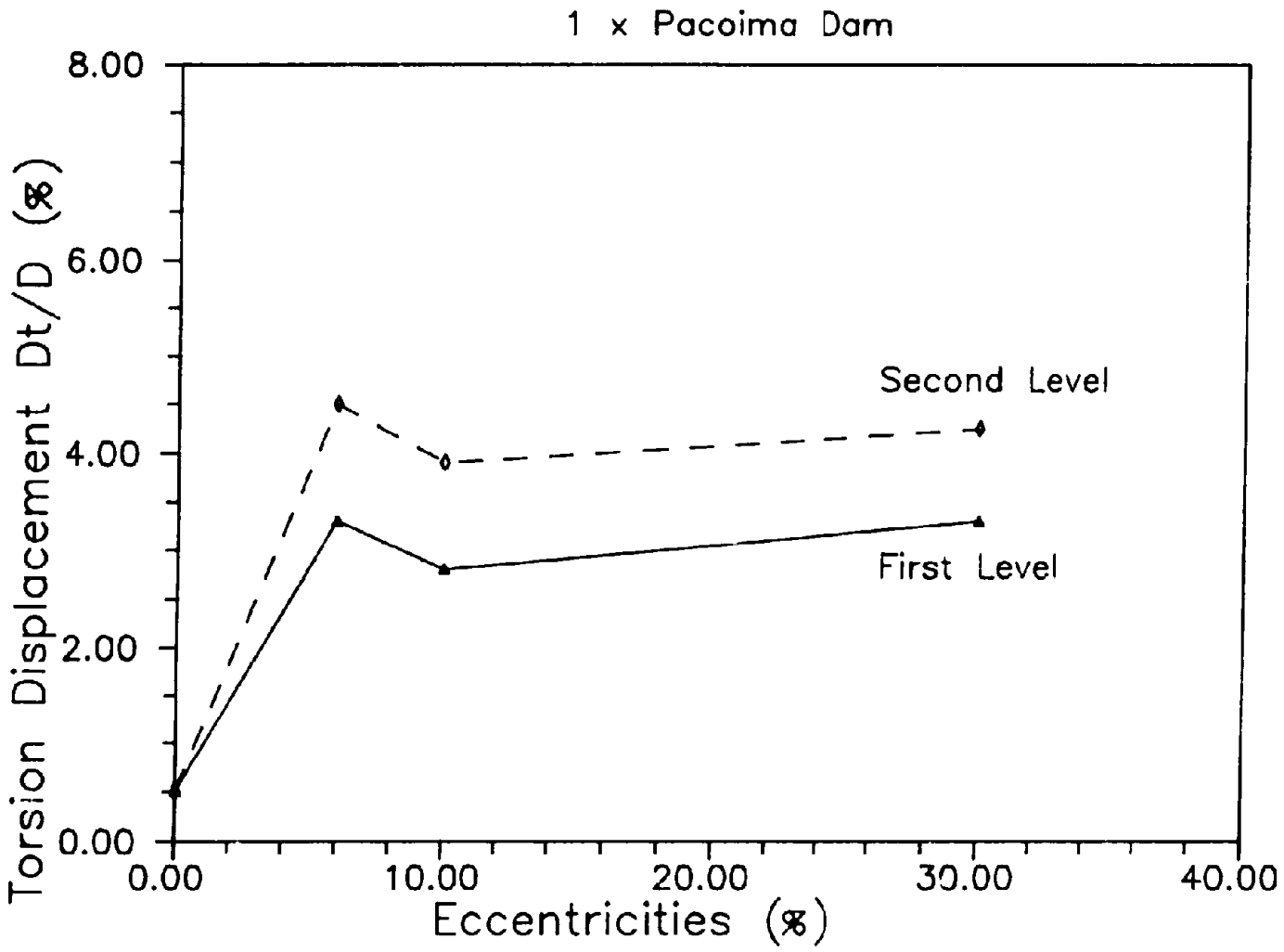

Fig. 5.4 Maximum Torsional Displacements - 1 x Pacoima Dam

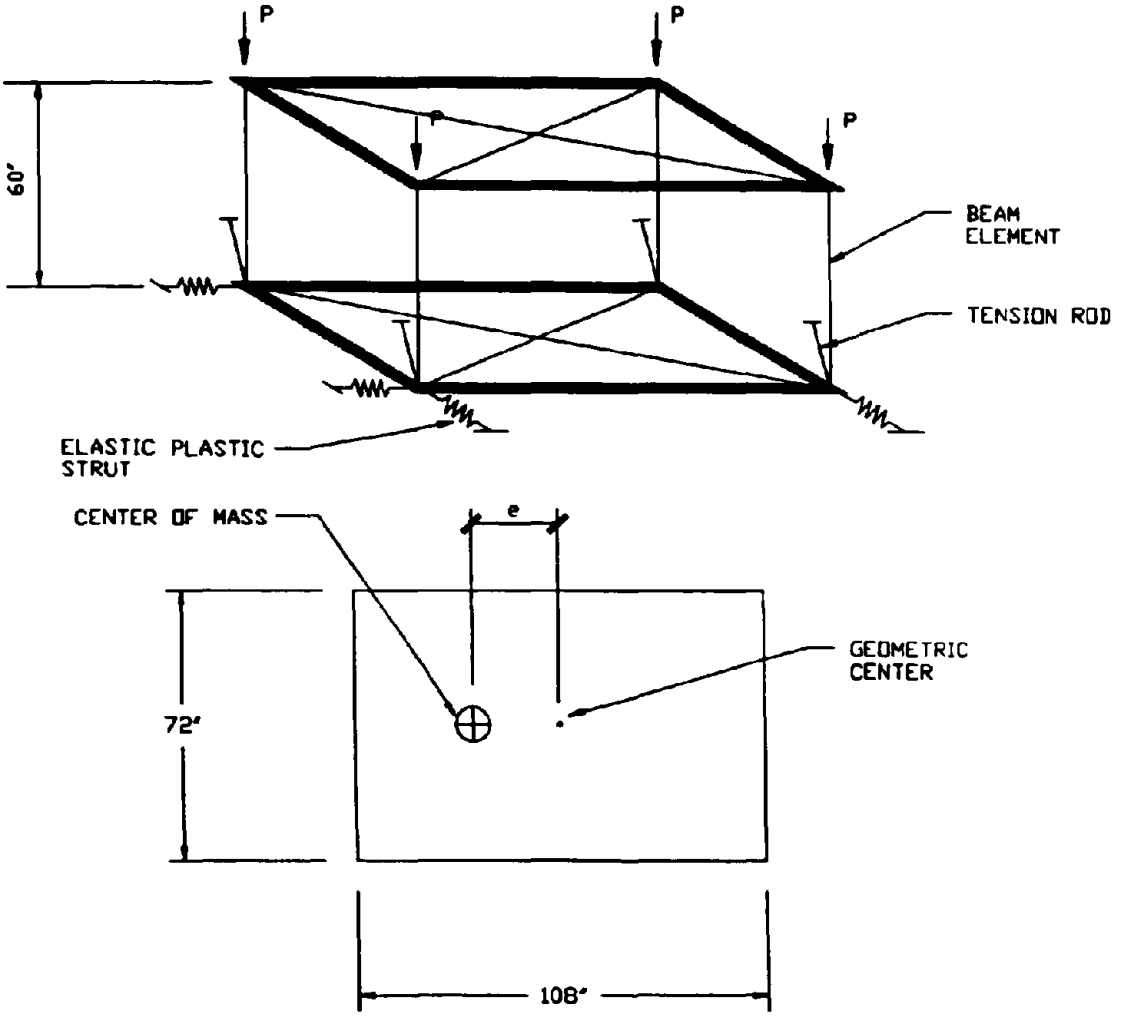

Fig. 5.5 Analytical Model of the Test Structure

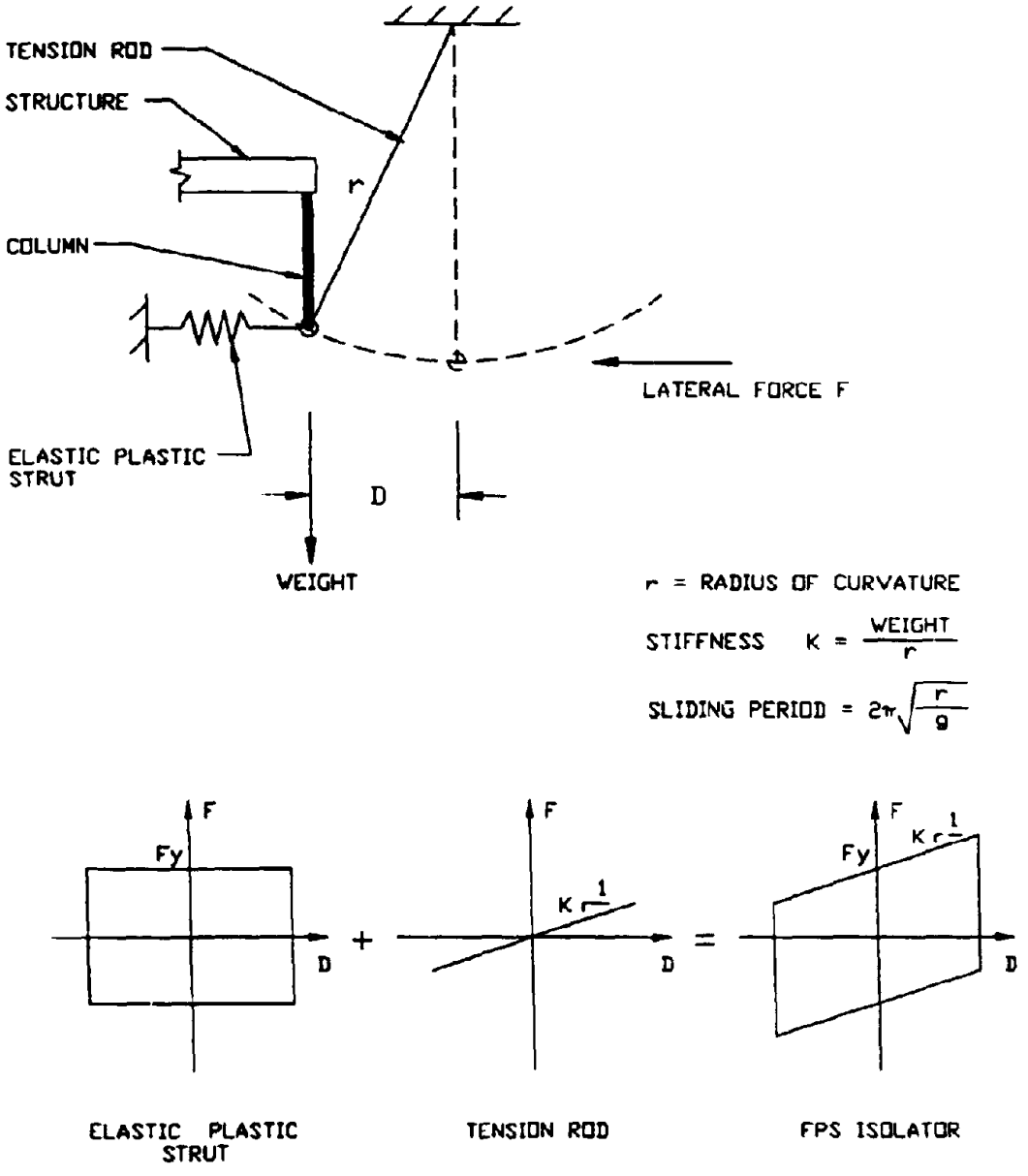

Fig. 5.6 Analytical Model of the FPS

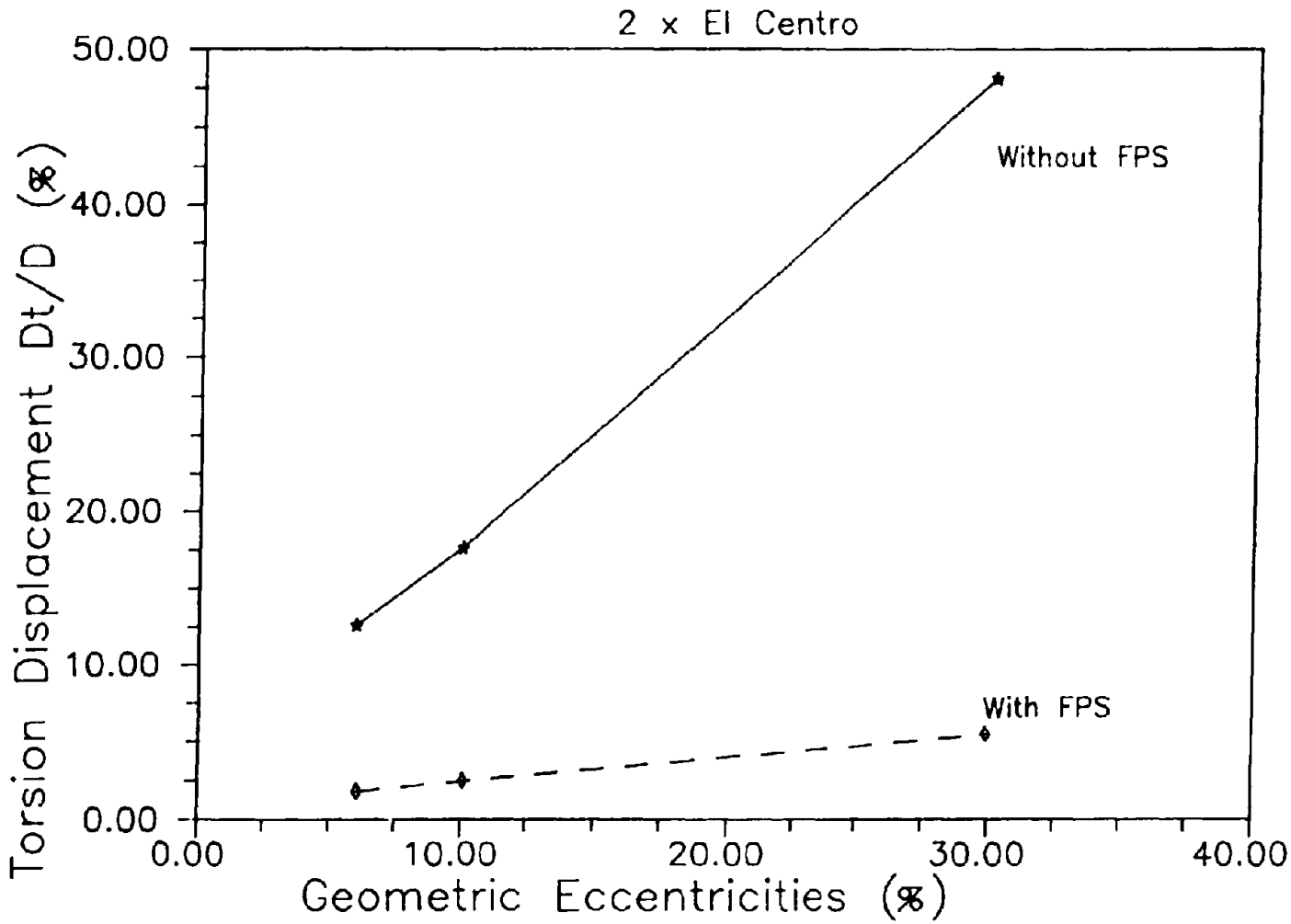

Fig. 5.7 Torsion Response to Variations in Geometric Eccentricities

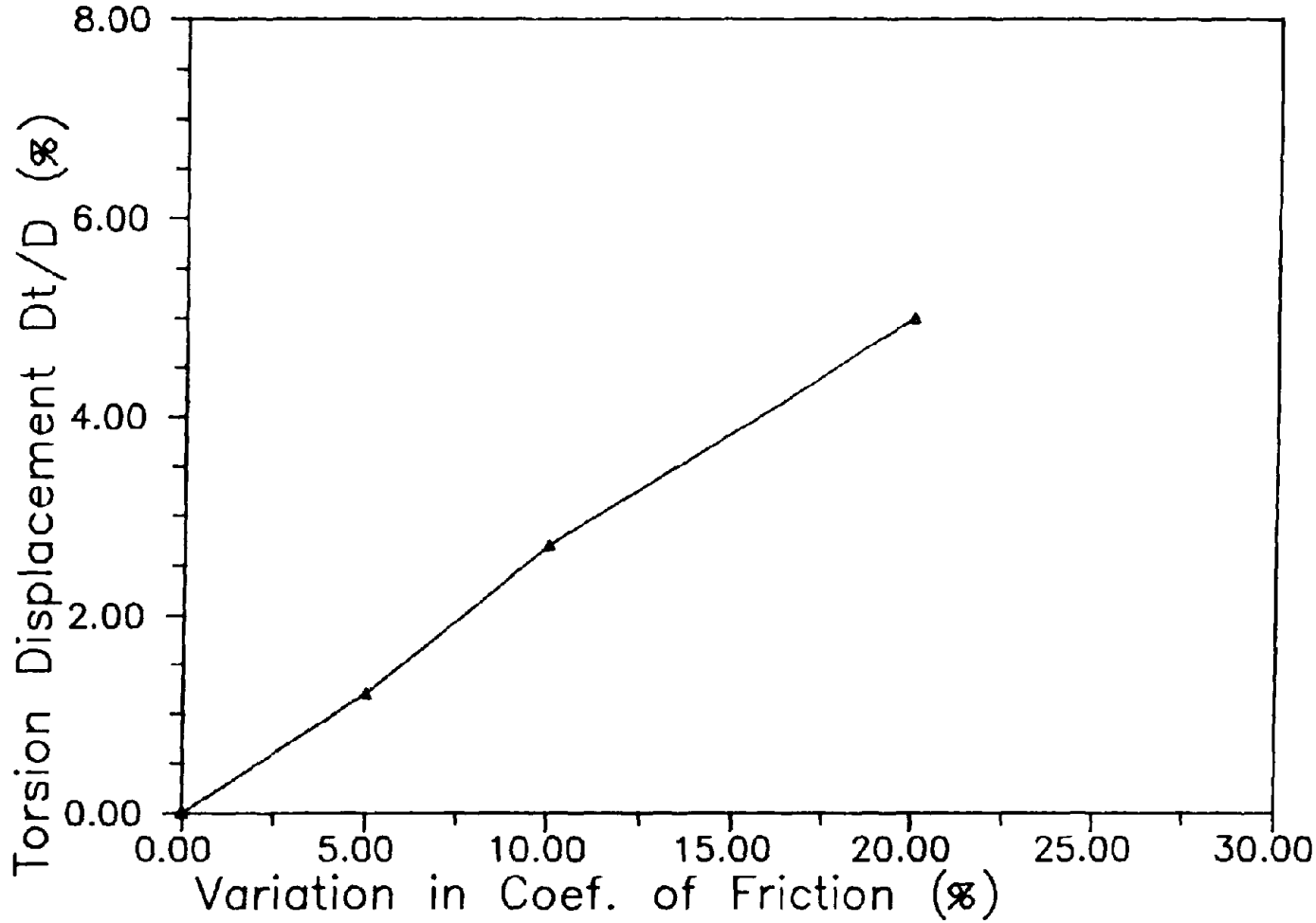

Fig. 5.8 **Torsion Responses Caused by Variation in Coefficient of Friction**

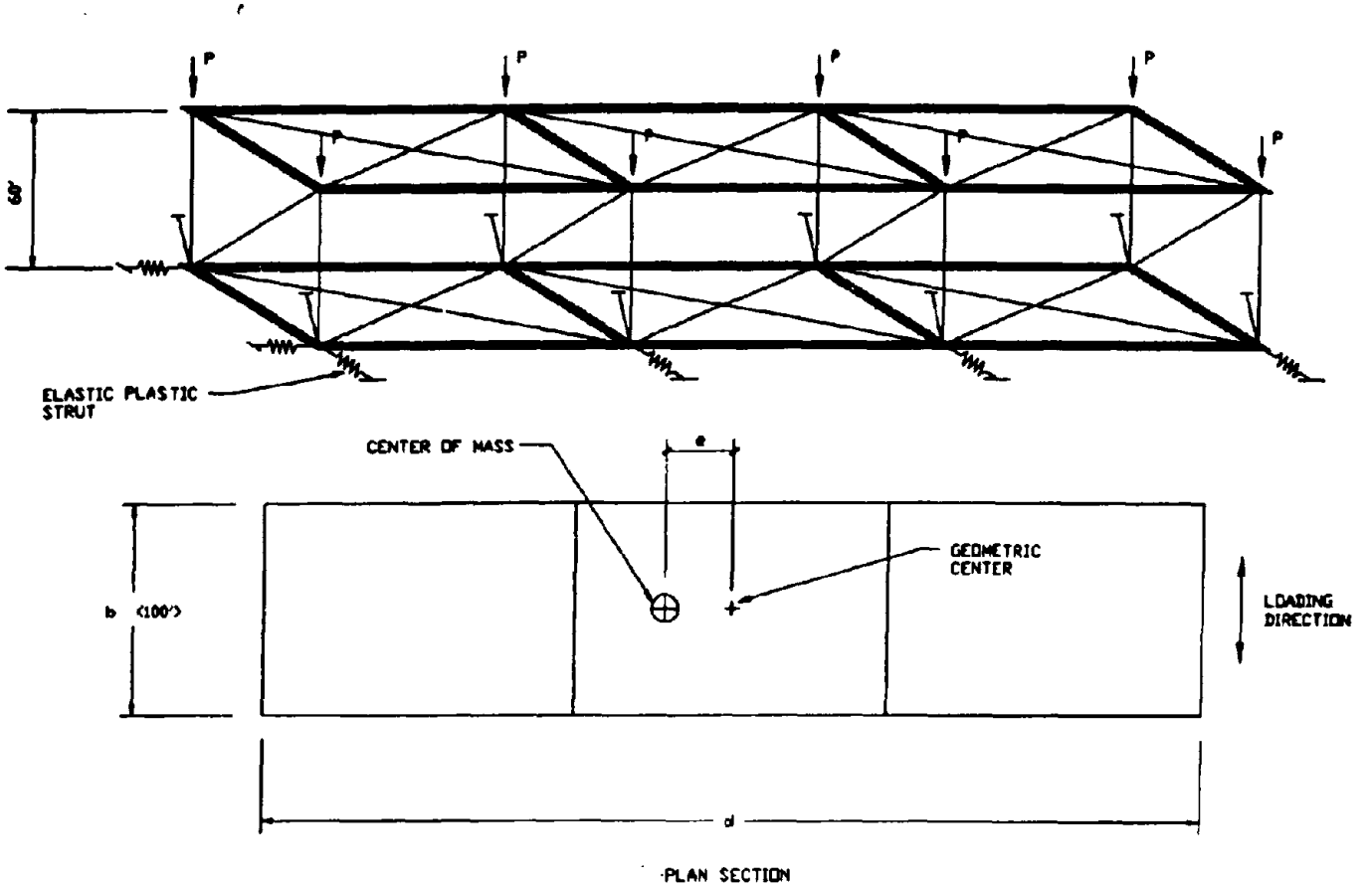

Fig. 5.0 Analytical Model of the Full Size Structure

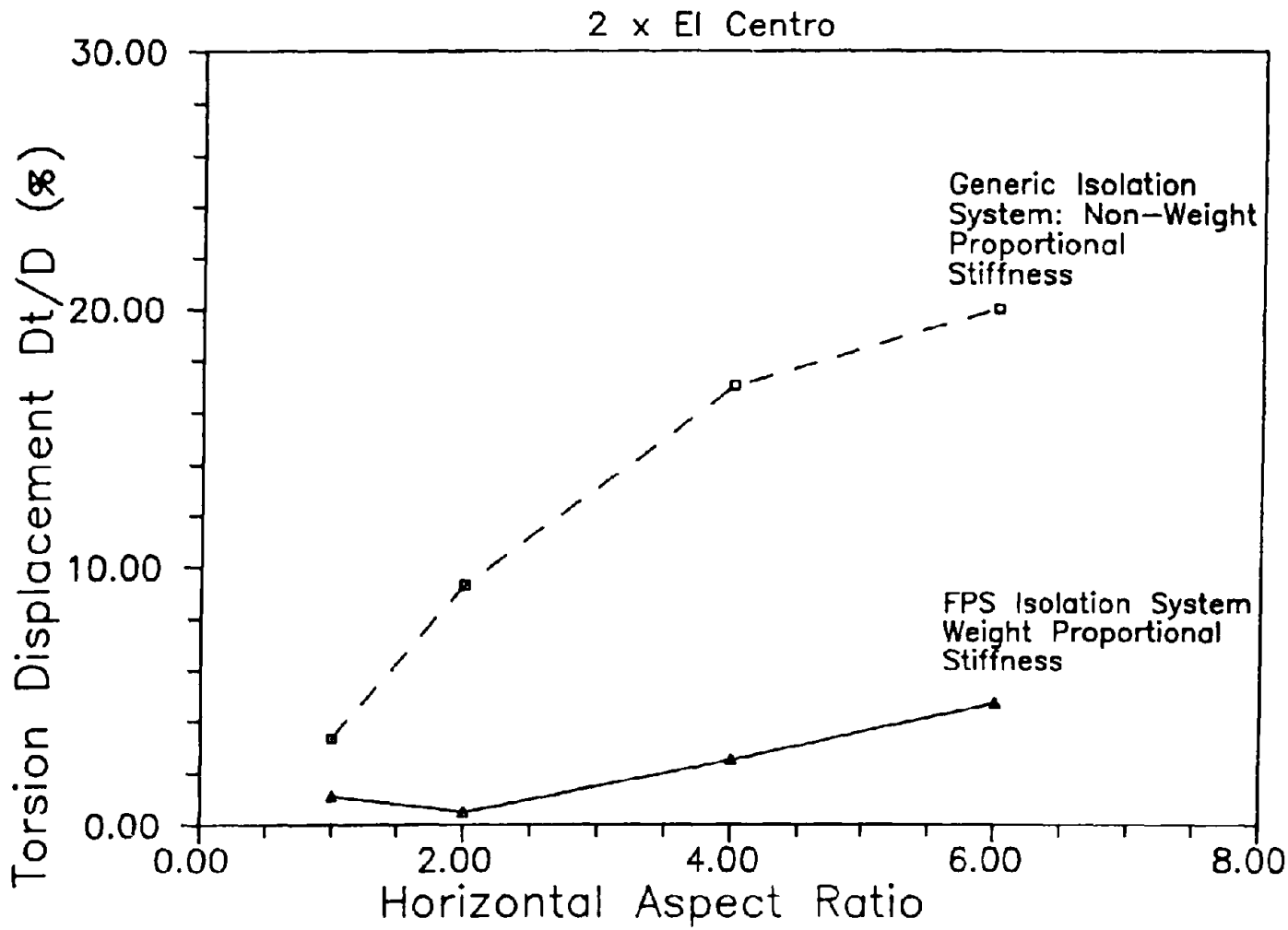

Fig. 5.10 Torsion Response of Building with Different Horizontal Aspect Ratios

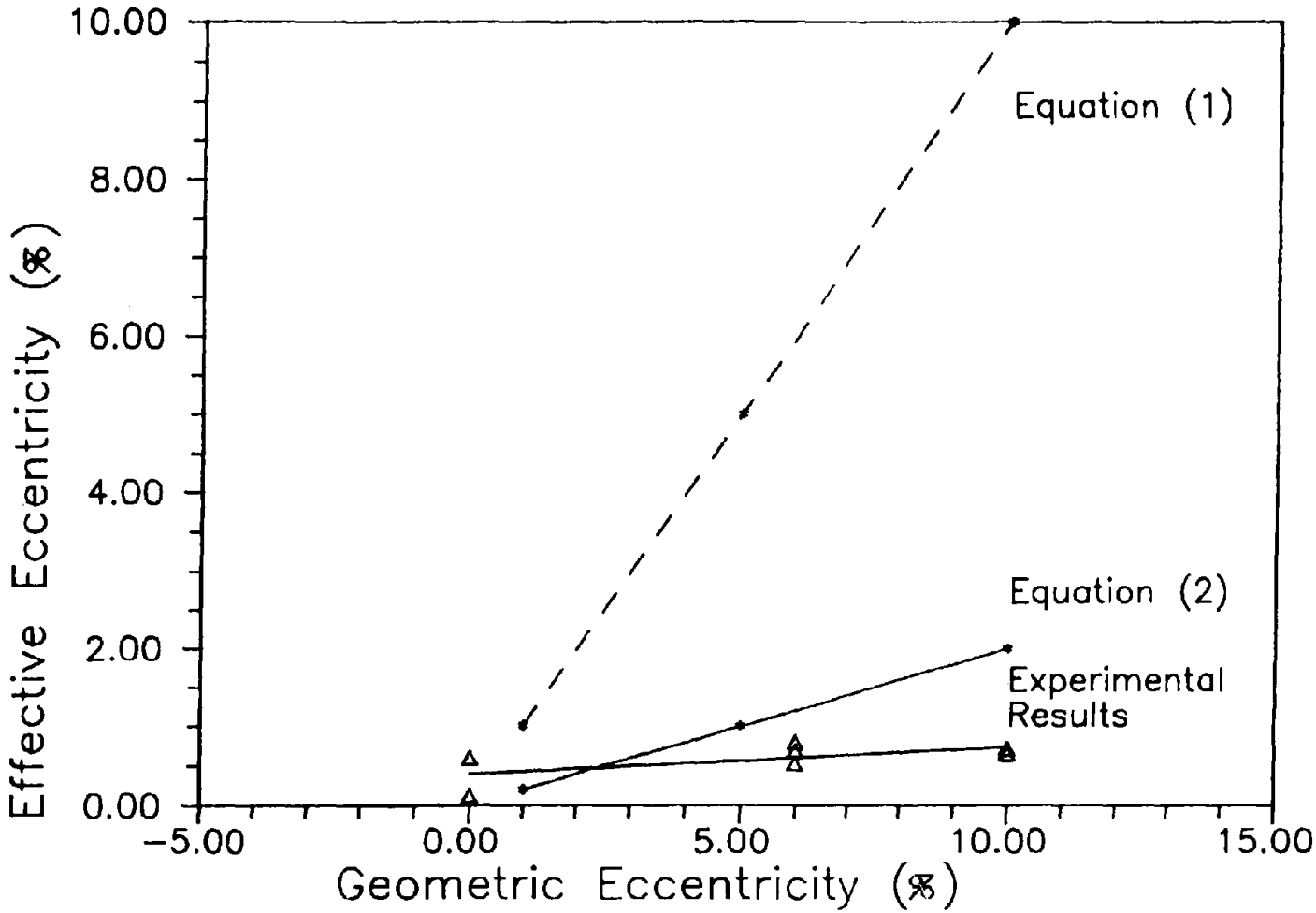

Fig. 5.11 Comparison of Equation [2] Results

CHAPTER 6

EFFECTS OF DISPLACEMENT RESTRAINTS ON BUILDING RESPONSE

by

Victor Zayas

and

Stanley Low

SECTIONS

6.1 Introduction

The design of the FPS isolators includes a steel cylinder which encloses the concave surface and slider components (Fig. 6.1). This enclosing cylinder protects the internal components from environmental contamination (dirt, corrosion, fire, etc.). It also serves as a displacement restraint which limits the maximum lateral displacement of the slider to that permitted by the cylinder. The cylinder also provides a redundant shear strength and vertical load carrying capacity.

Selecting the size of the cylinder defines the lateral displacement travel capacity of the FPS isolators. The size is selected by determining the travel required to accommodate the strongest design earthquake. In general, the displacement restraint would never be utilized, provided that the selected design earthquake is stronger than the strongest earthquake which occurs during the life of the building. However, in the event an earthquake exceeds the design earthquake, the displacement restraint would be engaged if the displacement demand exceeds the displacement capacity.

To examine possible effects of engaging the displacement restraints, analytical studies were performed as described below. Experimental data on engagement of the displacement restraints was evaluated and the data was used to guide the development of an analytical model which could model the effects of the displacement restraint. Analyses of the test structures were performed and these results were compared to experimental results in order to confirm the adequacy of the analytical model. With this analytical model confirmed, analyses which included engagement of the displacement restraints were performed for the example Operations Building which was presented in Chapter 2. The results are reported below.

6.2 Developing the Displacement Restraint Model

During the shake table tests reported in Ref. 1, some earthquake loading cases were intentionally run at strengths which exceeded the travel capacity of the FPS isolators for purposes of examining the effects of engaging the displacement restraints. Data from the resulting engagement of the displacement restraint was used to guide the development of an analytical model.

In order to include the displacement restraint effects in the FPS properties, modifications were made to the FPS element subroutines in the dynamic analysis program DYNIN. The analytical model was developed assuming that the FPS isolator are located at the top or bottom of a column. This avoided numerical problems which would otherwise occur when trying to model elements with a stiffness much higher than other structural elements in the model.

The normally bi-linear force displacement relationship of an FPS

isolator on a column was modified to a tri-linear hysteretic loop as shown in Fig. 6.2. The tri-linear hysteretic loop has an initial stiffness k0 which models the elastic stiffness of the column below the isolator. The sliding stiffness Kfps represents the combined flexibility of the isolator and the column below. When the sliding travel reaches the prescribed displacement limit, the displacement restraint will engage, resulting in an engagement stiffness. The engagement stiffness represents the combined flexibility of the displacement restraint and the column below. It is input into the analysis as a fraction of the initial stiffness @K0. From examination of the experimental results (Figs. 6.3 to 6.4) an engagement stiffness of 50% of the initial stiffness appeared to provide a reasonable representation of the hysteretic loops.

With this modeling approach, loading of the displacement restraint results in plastic deformations which represent the permanent deformations of the enclosing cylinder, as well as other energy absorbing phenomena which occur during the engagement of the displacement restraint. Unloading occurs at the initial elastic stiffness of the column below. The energy absorption of the plastic deformations is an important characteristic of the displacement restraint model. This enabled the model to dissipate energy and achieve a dynamic response consistent with the experimentally observed responses.

Nonlinear time history analyses of the test structures at different loadings were used to verify the performance of the displacement restraint model. Bi-linear elastic plastic models of the test structures were used in order to permit yielding of the upper structure. The mass, stiffness, and plastic strength of the test structure frames, as measured from the test results, were used. The earthquake loading recorded from the shake table tests was used as the input loading. In Figs. 6.3 to 6.5 are the comparisons of the experimental and analytical hysteretic responses for different test structures and different degrees of engagement of the displacement restraint. Responses to the Pacoima Dam and El Centro earthquake records are examined. The results show a good correlation between the experimental and analytical results.

If the displacement restraint of the FPS is assumed to be perfectly rigid, an engagement stiffness equal to 100% of the initial stiffness would result. This would result in a purely elastic response of the FPS model upon engagement of the displacement restraint. Analyses using an engagement stiffness of 100% of the initial stiffness were performed, and the results compared to the experimental results. These analytical results did not compare well with experimental observations. Displacement restraint forces were substantially over estimated, and energy absorption substantially under estimated. The model would rebound, resulting in engagements of the displacement restraint at the other end of the travel which was not consistent with experimentally observed results. Thus, the plastic displacement restraint model was preferable.

Having confirmed the analytical model using the test structures, the model was then used to estimate the effects that engaging the displace restraint would have for an actual building.

6.3 Displacement Restraint Effects For The Example Building

To examine effects that engaging the displacement restraint would have on a building, the cost equivalent isolated design of the Operations Building described in Chapter 2 was considered as an example. The design earthquake used for the FPS isolator design was the EL Centro loading scaled to a peak ground acceleration of 0.7 g (2 X El Centro). The dynamic analyses predicted an isolator travel displacement of 4.7 inches for this event. In the Chapter 2 design, the travel displacement of the FPS isolators was conservatively selected to be 6.5 inches to allow for a margin of safety against reaching the displacement restraint. Since the design earthquake was already a strong 0.7g record, it was considered preferable to examine cases of smaller displacement capacity rather that stronger ground motions. Analyses results are presented below for design cases in which the displacement travel capacity is less than that required to accommodate the design earthquake.

A revised analytical model of the building was used for these analyses that included modeling of the displacement restraint, and included bi-linear elastic plastic modeling of the building structure that would permit yielding. The model of the structure is shown in Fig. 6.6. The model consisted of a 3 nodal mass representing the second floor, third floor, and roof. The FPS was placed in the first level. The stiffness and strength of each level were derived from the section properties of the structure (Appendix A - Section 5). The bi-linear elastic plastic yield was set equal to the plastic strength, which was computed using ultimate strength plastic analysis techniques.

For numerical analysis purpose, the stiffness of the first level columns was distributed equally between the isolator model and the model of the first level column. This permitted yielding in the first story columns to be measured separately from the isolator response. The initial flexibility of the isolator model avoided numerical difficulties. The combined initial stiffness was set equal to that of the first story column. The FPS isolator had a sliding period of 2.25 sec. and a coefficient of friction of 10%.

The analyses were performed for the 2 X El Centro, 1940 NS loading, both with and without the FPS. For the case with the FPS, the structure was analyzed for the design displacement capacity, then for incremental reductions in the travel displacement capacity to get different levels of engagement. The ductility demand, energy demand, base shear and story drift effects on the isolated and non-isolated models were compared.

The displacement ratio, is defined herein, as the ratio of the displacement travel capacity required for there to be no engagement divided by the actual displacement capacity provided. At displacement ratios less than 1.0 there is no engagement. The displacement ratio for the initial design proposed in Chapter 2 was 0.72. At a displacement ratio greater than one, the displacement restraint will be engaged. The greater the displacement ratio, the greater the effects of engagement. However, the plastic strength of the first story columns limits the base shear loads that can be transmitted to the FPS and structure above. This upper limit on base shear is the same base shear which occurs for the non-isolated case.

In Fig. 6.7 are the base shear results for different displacement ratios. Without engagement the base shear remained constant. Once engagement occurred the base shear began to increase until it reached the base shear level of the non-isolated structure.

In Fig. 6.8 the results for maximum story ductility are plotted versus the displacement ratio. The results show that the ductility demands with the FPS are less than one third the ductility demands without the FPS, for displacement ratios up to 1.84. A displacement ratio of 1.84 is a displacement travel capacity of 2.5 inches, as compared to 6.5 inches which was allowed for in the initial design. Essentially the results show that when the displacement demand exceeded the displacement capacity by 84%, the isolators reduced ductility demand on the structure by two thirds. Thus, even when the displacement capacity provided is less than the displacement capacity required to fully accommodate the earthquake motions, the FPS is still effective in reducing ductility demand.

Another important consideration when considering damage to the structure, is the number of inelastic yield excursions which occur. For the cases with the FPS, fewer inelastic excursions occurred, and the magnitudes of the excursions were reduced. Total inelastic energy dissipated by the structural frame is a measure of damage to the structure which measures both the magnitude and number of yield excursions.

Fig. 6.9 shows the inelastic energy dissipated by the structural frame versus the displacement ratio. For the cases with the FPS, the results show that most of the energy is absorbed by the FPS connections and only a small portion of the energy is absorbed by the structure. At displacement ratios less than 1.0, the FPS absorbed 100% of the inelastic energy. At a displacement ratio of 1.84, the FPS isolators absorbed 95% of the inelastic energy. At a displacement ratio of 2.0, the FPS isolators absorbed 92% of the inelastic energy.

Thus, when the displacement demand exceeded the displacement capacity by 100%, the FPS is still absorbed more than 90% of the inelastic energy. This high effectiveness is a result of the fact that many fewer inelastic excursions occur. The response is

similar to that which would occur in the non-isolated building during a reduced strength earthquake of much shorter duration.

A measure of damage to the architectural and non-structural components of a building is the maximum story drift divided by the UBC allowable story drift. These normalized story drifts for the first, second and third stories, are plotted in Figs. 6.10 to 6.12, respectively.

Engagement of the displacement restraint was observed to increase the drift of the first story (see Fig. 6.10). This is consistent with the response of the non-isolated structure, which had the largest ductility demands and drifts occurring in the first story. When the displacement ratio was less than 1.0, the drifts in the first story were reduced by 85%. When the displacement ratio was 1.5, the drifts in the first story were reduced by 70%. When the displacement ratio was 2.0, the drifts in the first story were reduced by 60%. Thus, even when the isolator travel demand exceeded the travel capacity by 100%, drifts in the first story were reduced by 60%.

When the displacement ratio was less than 1.0, the FPS reduced the second story drift by 60%, and the third story drift by 48% (Figs. 6.11 and 6.12). Engaging the displacement restraint had little effect on the second and third story drifts. Independent of displacement restraint effects, it can be observed from Figs. 6.10 to 6.12, that the FPS was less effective at reducing drift in the second and third stories, as compared to the first story. This appears to be related to higher mode effects, which in turn are affected by the friction coefficient. A 10% friction coefficient was used for the isolators in this example. It is believed that a lower friction coefficient would reduce higher mode effects. A study of higher mode effects for FPS supported structures is required, and should include investigations of how the friction coefficient affects these responses. These studies are planned for the Phase II research program.

6.4 Conclusions

The engagement of the displacement restraints caused localized short duration increases in the first story shears and drifts. However, the isolation system retained its overall effectiveness in improving earthquake performance. When displacement loading demand exceeded displacement capacity by 50%, the isolation system retained 85% of its effectiveness as an isolation system in reducing inelastic ductility demand, 95% of its effectiveness in reducing structural inelastic energy dissipation, and 80% of its effectiveness in reducing first story drift. Thus, an earthquake event which exceeds the FPS displacement capacity reduces the effectiveness of the FPS, but the response is still significantly better than the response of the same structure without the FPS.

The displacement restraints appear to break up the modes of vibration, preventing resonant dynamic responses from building up in any one set of modes. Initially the building responds at the non-isolated modes of vibration, then the modes change to the sliding modes for most of the earthquake duration, but with brief interjections of the displacement restraint modes. The displacement restraint modes are unique in that they occur for loading in only one direction, and upon reversal the building reverts to the sliding modes. Therefore, the displacement restraint modes are effective for only one-half a cycle which gives no opportunity for resonance buildup in these modes. Furthermore, brief interjection of the displacement restraint modes appears to break up the sliding modes and prevent a build up of displacements in these modes. It appears that a system that avoids the build up of resonant vibrations in any one set of modes could be an advantage in circumstances of uncertain or varied ground motion characteristics. Further investigations of this behavior appears warranted. Further studies are planned for the Phase II research program.

The performance of the isolation system was best when the full displacement demand was accommodated, and no engagements occurred. However, because the FPS isolators retained overall effectiveness when engagements of the displacement restraint did occur, large factors of safety in displacement travel capacity may not be required.

These observations and conclusions are based on evaluations of the moment frame responses of the example building and test structures. A very limited number of earthquake loading cases were examined. The responses for other structural systems such as braced frames, shear walls, or bearing walls, or other earthquake loadings could be different. However, the observed responses are encouraging. Further examination of the displacement restraint effects for other structural systems and earthquake loadings is needed. These are planned for the Phase II research program.

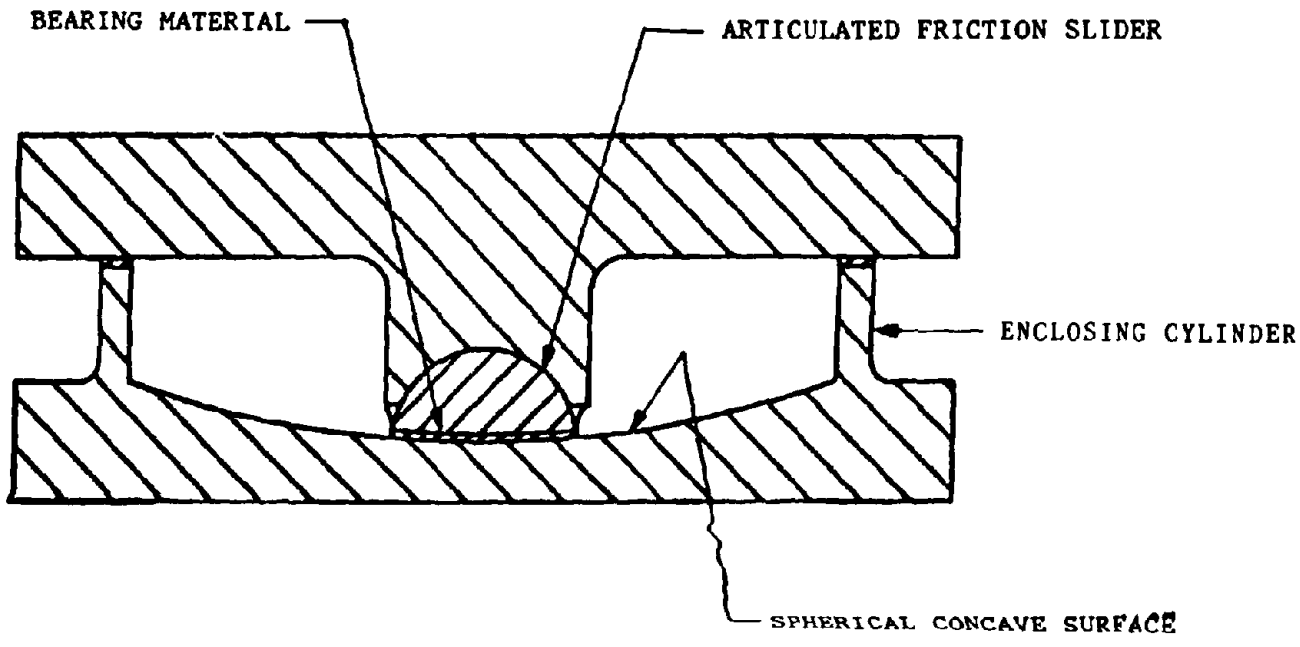

Fig. 6.1 Section view of FPS Isolator

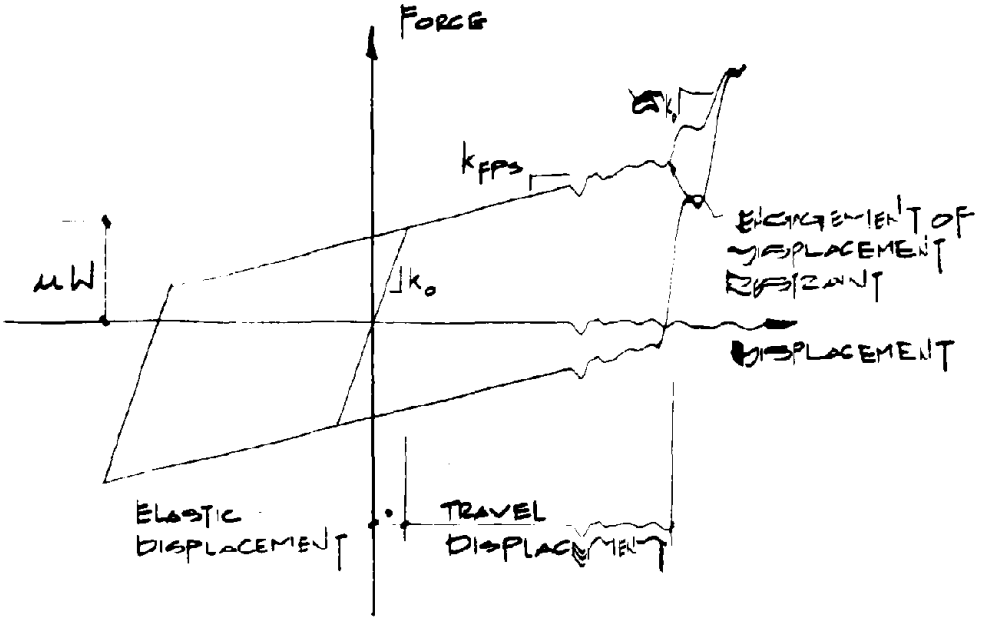

DISPLACEMENT RESTRAINT MODEL

DEFINITION:

k_o ⇒ INITIAL STIFFNESS

k_{FPS} ⇒ STIFFNESS OF THE FPS = $\frac{W}{r}$

δ ⇒ RATIO OF DISPLACEMENT RESTRAINT TO INITIAL STIFFNESS (APPROXIMATELY = 5%)

μ ⇒ COEFFICIENT OF FRICTION

W ⇒ WEIGHT

Fig. 6.2 Analytical Model of Displacement Restraint

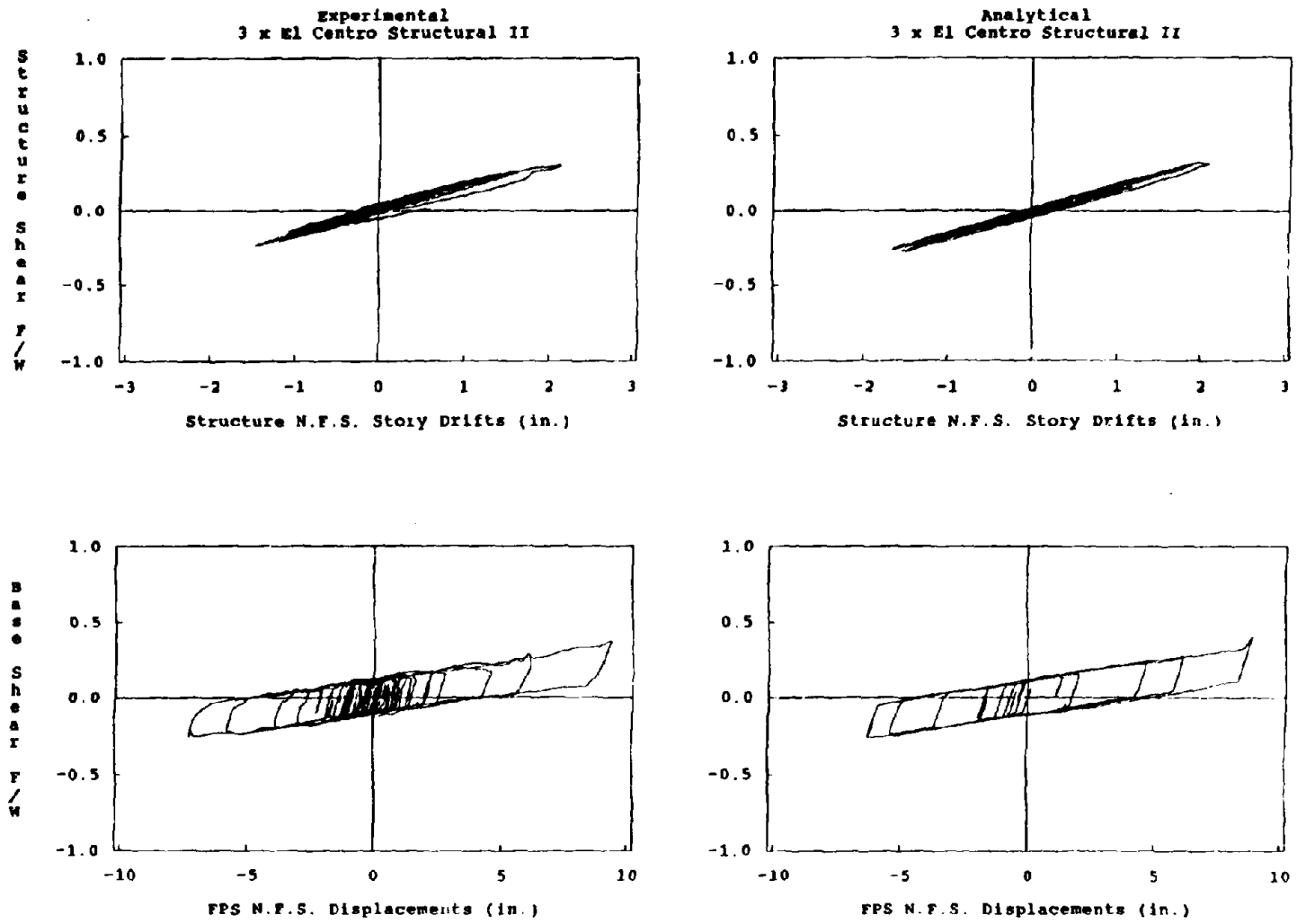

Fig. 6.3 Hysteretic Response for 3 x El Centro - Structure II

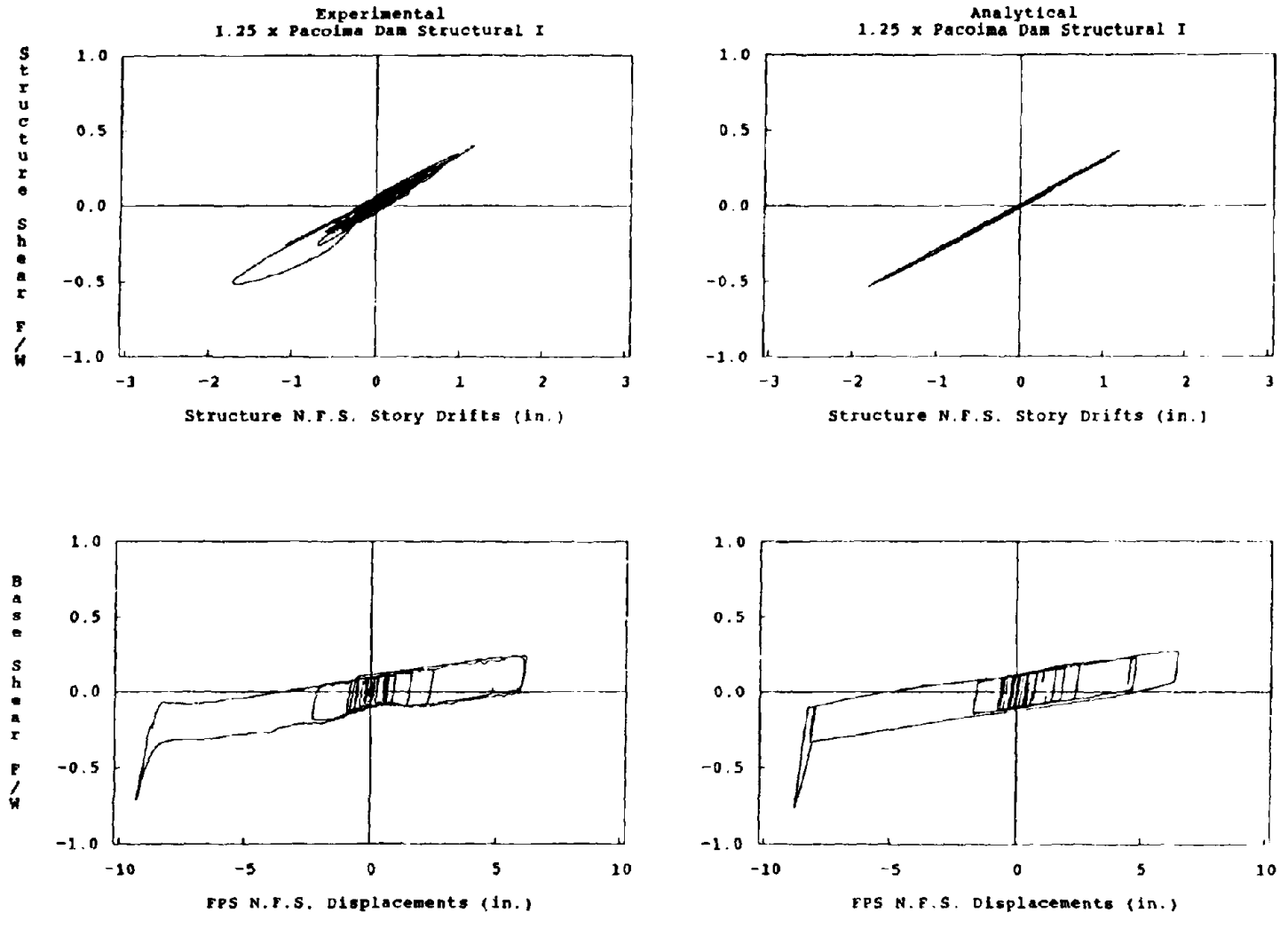

Fig. 6.4 Hysteretic Response for 1.25 Pacoima Dam - Structure I

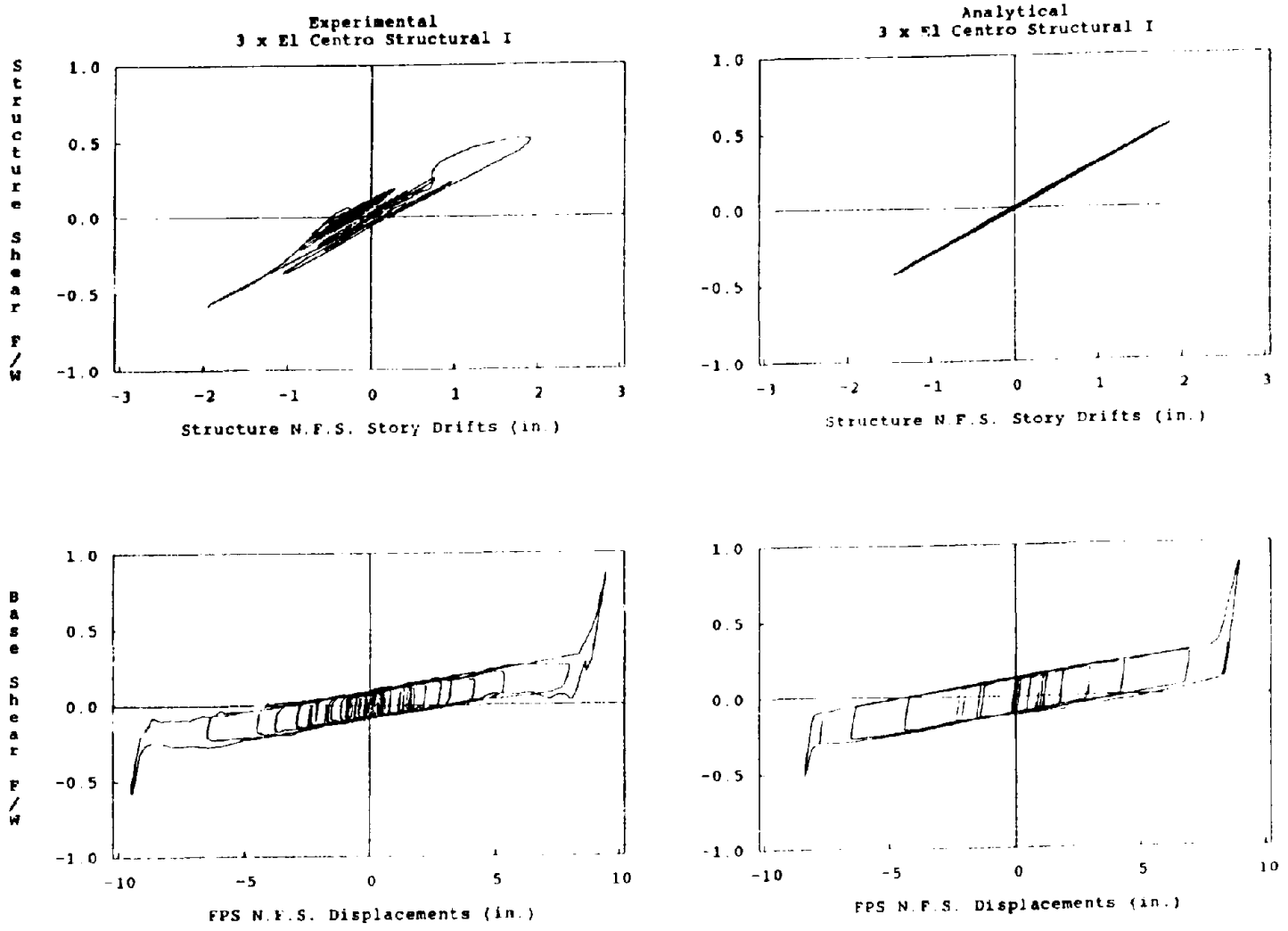

Fig. 6.5 Hysteretic Response for 3 x El Centro - Structure I

DISPLACEMENT RESTRAINT MODEL FOR DYNIN

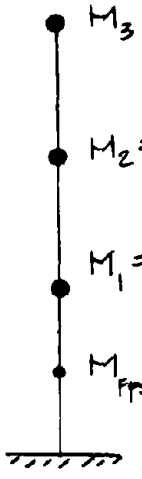

STIFFNESS

$k_3 = 877^{k/IN}$

$k_2 = 1677^{k/IN}$

$k_1 = 3459^{k/IN}$

$k_0 = 3100^{k/IN}$

SHEAR CAPACITY

$V_3 = 1252^k$

$V_2 = 2116^k$

$V_1 = 1920^k$

PROPERTY OF ISOLATOR

$T = 2.25 SEC. \quad \mu = 10\%$

DESIGN TRAVEL = 6.5"

$k = \frac{W}{r} = \frac{6126}{49.5} = 124^{k/IN}$

FPS ISOLATOR MODEL

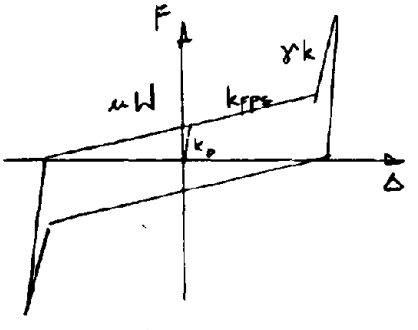

TRI-LINEAR HYSTERETIC MODEL

STRUCTURE MODEL

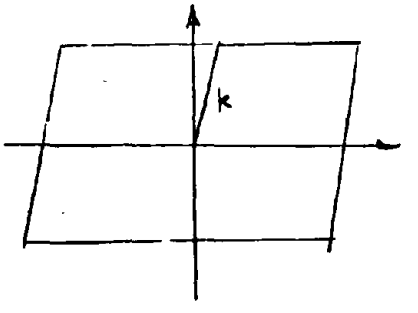

ELASTIC PLASTIC MODEL

EARTHQUAKE LOADING

2 x EL CENTRO N.S. 1940

Fig. 6.6 Dynin Displacement Restraint Model

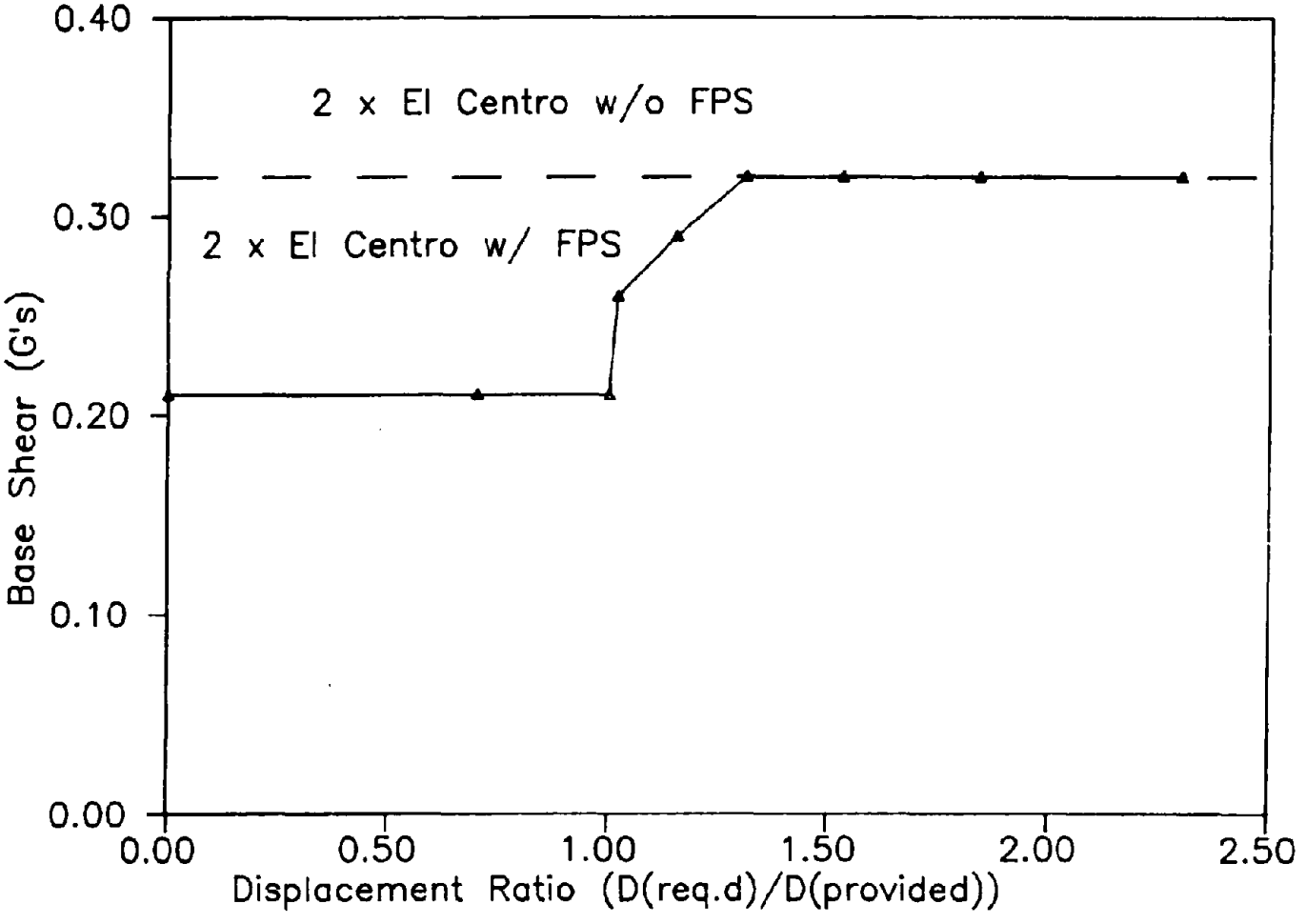

Fig. 6.7 Comparison of Base Shear Response

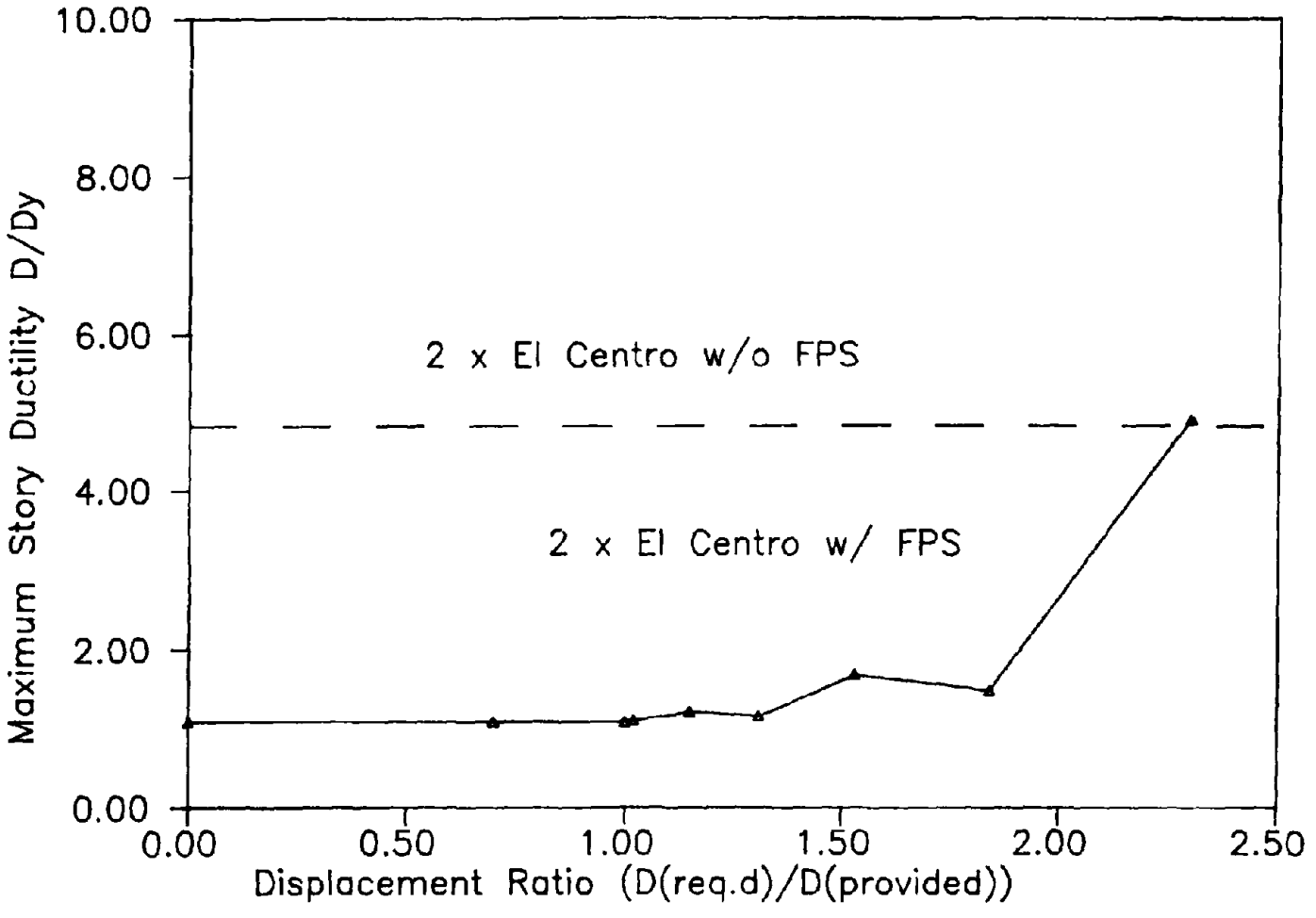

Fig. 6.8 Comparison of Ductility Demand

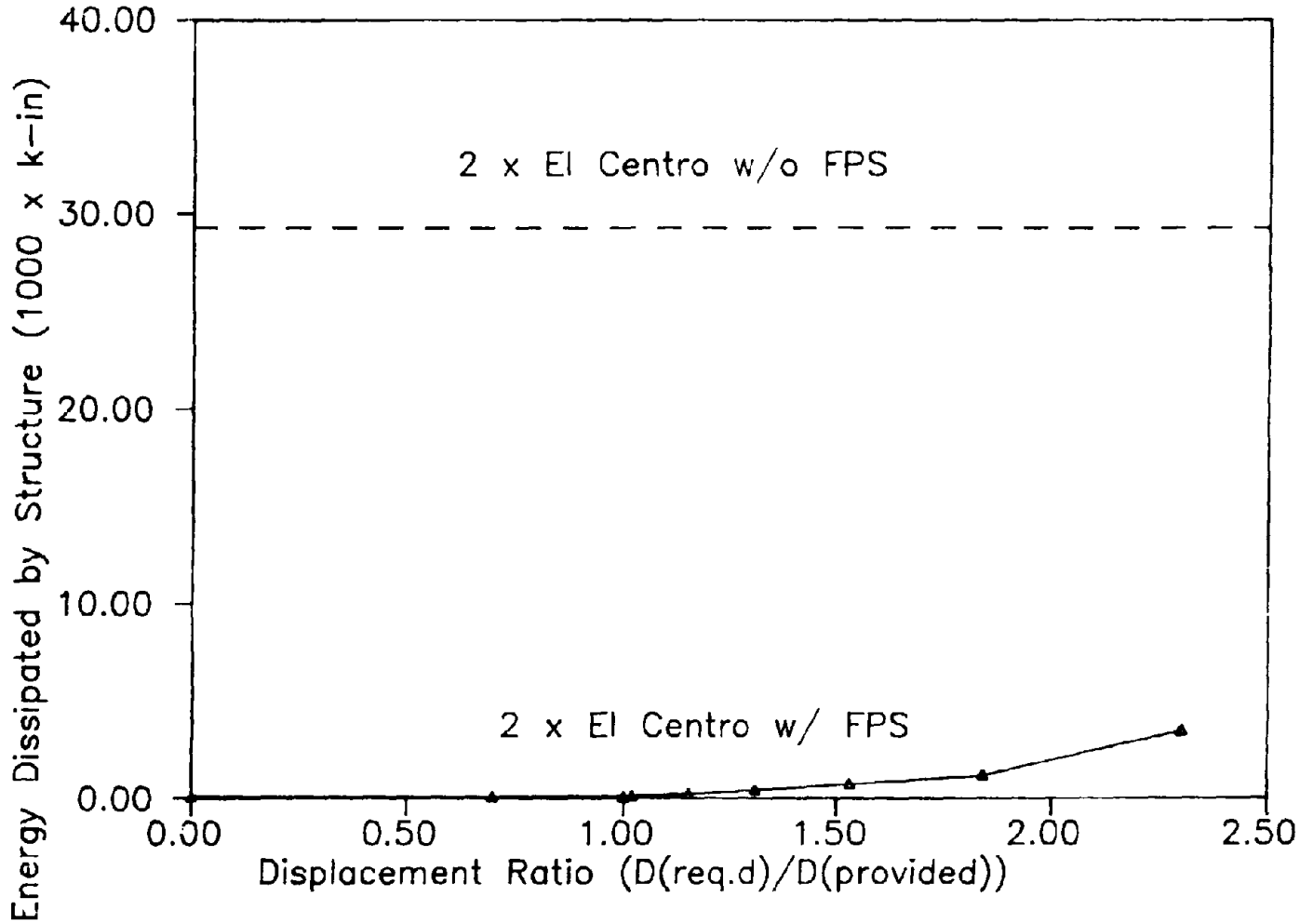

Fig. 6.9 Comparison of Energy Dissipated by Structure

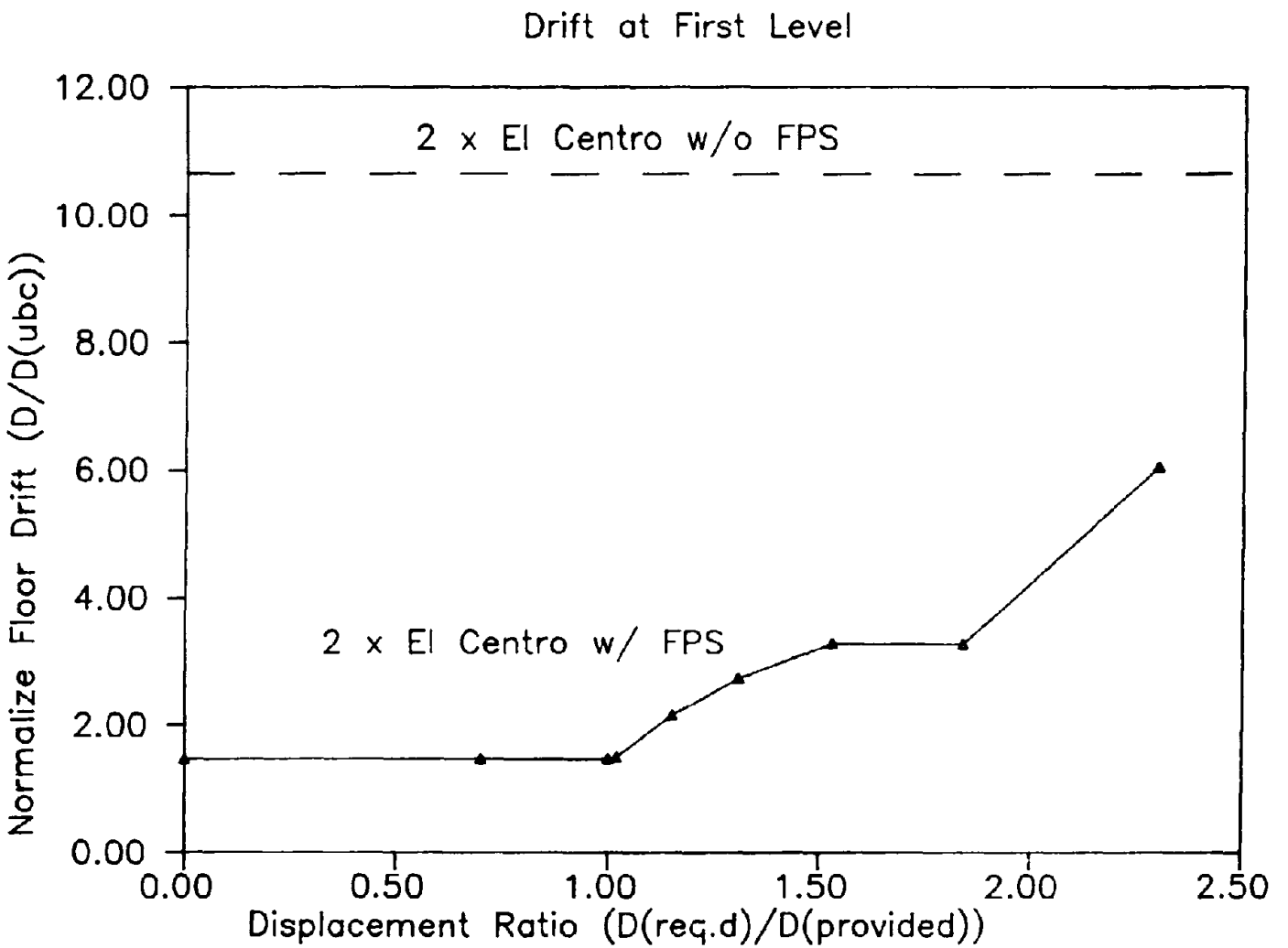

Fig. 6.10 Comparison of Drift at First Level

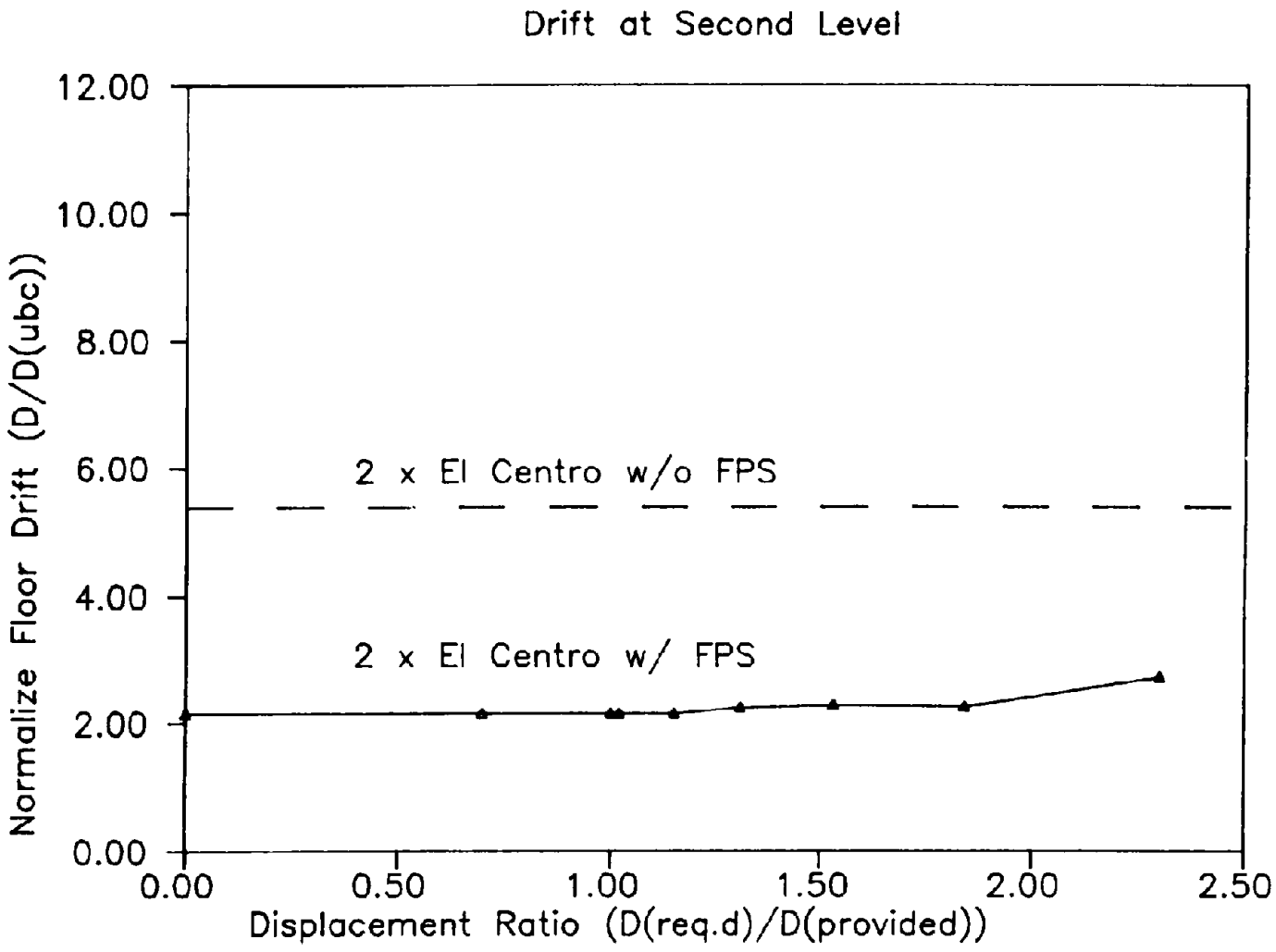

Fig. 6.11 Comparison of Drift at Second Level

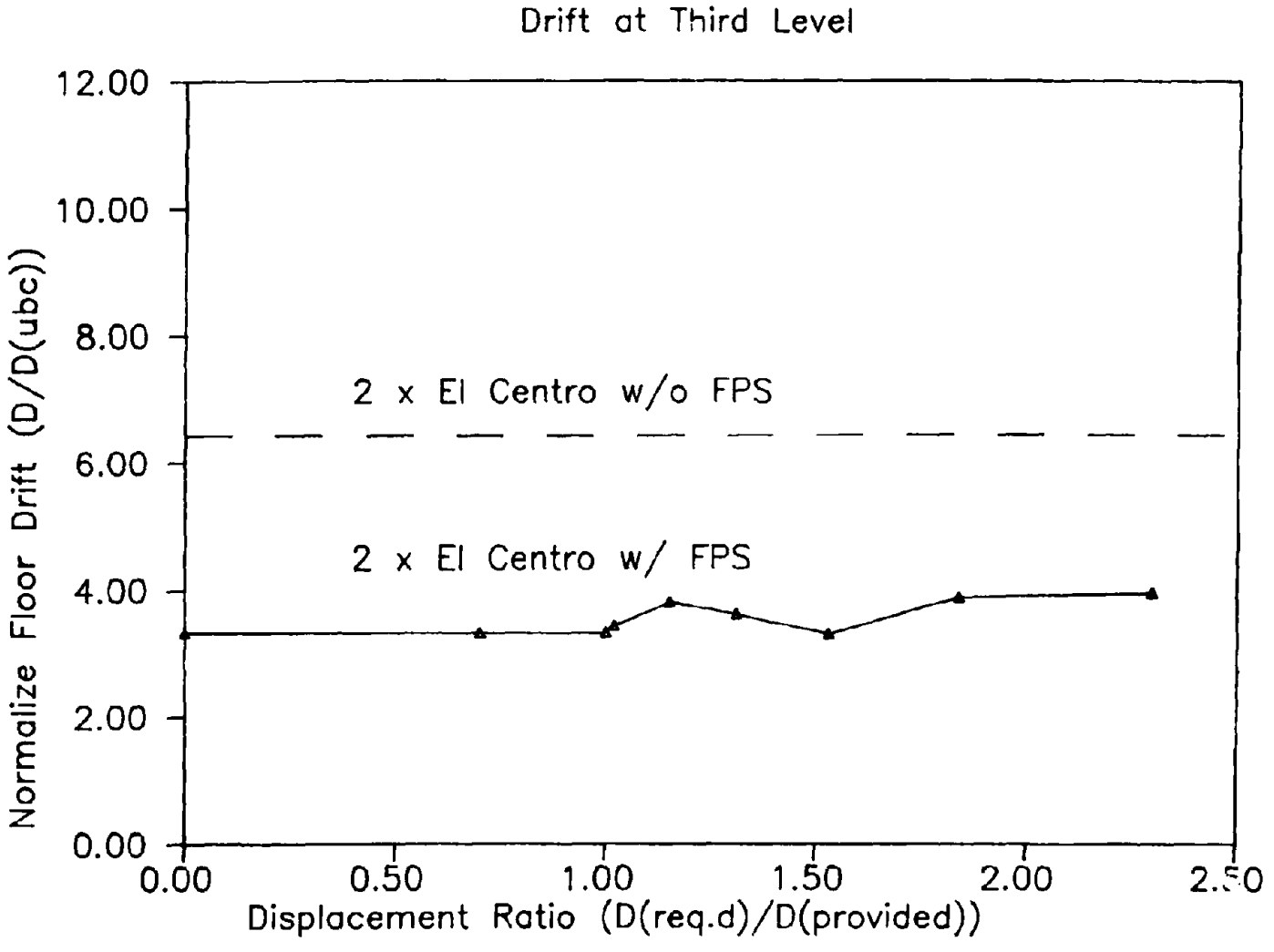

Fig. 6.12 Comparison of Drift at Third Level

CHAPTER 7

RESPONSE OF INELASTIC MULTISTORY STRUCTURES SUPPORTED ON FPS CONNECTIONS

by

Stephen Mahin

Luis Bozzo

Victor Zayas

and

Stanley Low

SECTIONS

7.1 Introduction

It was shown in Chapter 2 that FPS connections can be used to achieve structures that are cost equivalent to conventional buildings designed according to current code provisions. In addition, damage resulting in these FPS supported structures was far less than that expected in non-isolated structures. This study of the cost equivalent structure, while demonstrating the technical and economic practicability of the FPS concept did not, however, identify the interrelationships that exist between various design and response parameters, nor did it investigate appropriate design methods for FPS supported structures. The results presented in this Chapter provide some significant insight into these broader issues. A preliminary parameter study on the response of multiple degree of freedom inelastic systems was undertaken. Also, general information on the effect of structural yielding on the basic behavior of FPS supported systems is obtained.

The potential scope of this investigation is extremely large, considering the various types of structures, FPS isolators and ground motions that should be considered. Given the preliminary nature of this report, a more applied and possibly more instructive approach has been taken. The Operations Building introduced in Chapter 2 was studied in considerable detail. In this Chapter, nonlinear dynamic analyses are presented for a variety of modifications to this structure to help assess the sensitivity of response to variations in basic design parameters, such as the stiffness (period) and strength of the structure, and FPS isolator characteristics. In addition, sensitivity of response to increasing intensities of ground shaking was assessed. Special studies were also performed to evaluate the ability of the designer to predictably alter seismic performance by selective alteration of FPS isolator and structural design parameters. Results are also presented of systematic investigations related to the effect of the strength (and consequent yielding) in the supported portion of the building on overall structural and FPS isolator behavior. These studies provide insight into the factors controlling the response of multiple degree of freedom systems and the identified trends suggest means for achieving even more cost effective structural designs. By considering a large range of periods and strengths, the studies provide information on the response of a wide variety of buildings.

In all cases presented, results for FPS supported structures are compared with similar structures without FPS isolators. This permits a clear identification of the influence of the FPS isolators on seismic performance. To simplify the analyses and the interpretation of the results, a simplified lumped mass idealization was adopted for the structures, as was done in Chapters 2 & 6. This should, nonetheless, provide very realistic and reliable information regarding the comparative overall response characteristics of these structures.

After describing the basic structural models considered in this Chapter, the analysis techniques and assumptions are examined.

Results for the basic cases are then presented individually and as functions of fundamental parameters, such as structural period, ultimate strength, ground motion intensity, etc. Implications for design are then offered based on trends observed in the results.

7.2 Analytical Models

Because of the preliminary nature of these feasibility studies and the need for computational efficiency in performing nonlinear parametric studies, the structures considered in this Chapter have been idealized as having a single lateral degree of freedom per floor. Thus, equivalent interstory shear, relative displacement relationships, are used to characterize the mechanical properties of the structure. This permits the overall aspects of the nonlinear response to be identified without undue attention to analysis details or design refinements.

A specially modified version of the computer program DYNIN (Ref. 7.1), capable of analyzing FPS supported structures, was used in the parametric and case studies presented in this Chapter. Modifications consist of the addition of various input and output features to facilitate this study, and the addition of an element to represent the rate dependent and displacement restraint effects (see Chapter 6) of FPS connections. The DYNIN program idealizes a structure as having a single lateral degree of freedom for each floor level. Lateral force-displacement relationships are specified for each story. The program has a built-in library of standard story shear-drift hysteretic relations, such as bilinear, degrading stiffness, Minegatto-Pinto and other such models, that can be used to represent various types of structures. Masses are assumed in the program to be lumped at the floor levels. Viscous damping ratios may be specified independently for each of the modes of the initially elastic structure. Gravity effects and geometric nonlinearities are disregarded in the program. The base of the structure is assumed to be fixed to the ground. A single horizontal component of excitation may be considered. Options exist for computing a variety of structural performance parameters.

The DYNIN program is efficiently written in order to minimize the computational effort needed for parametric studies such as those considered herein. The dynamic equations of motion are solved using the central difference method. Time steps are automatically selected by the program to minimize computational errors.

In these studies, the structure is idealized using elasto-perfectly plastic mechanical models. For the basic case considered herein, the lateral stiffnesses employed were the same as those used for the cost equivalent isolated design of the Operations Building described in Chapter 2. That is, the lateral elastic stiffnesses were 1635 k/in, 1477 k/in and 877 k/in, for the first, second and third (roof) stories, respectively. Information on how these values were obtained can be found in Chapter 2.

The hysteretic characteristics of the story containing the FPS connections was idealized in one of two ways. First, if the columns attached to the connections remained elastic, a single equivalent lateral spring was employed. As was done in Chapter 2 for the elastic building model supported on FPS connections, this equivalent spring was bilinear hysteretic in character, representing in serial fashion the cumulative properties of the rigid-strain hardening FPS connections and the elastic columns. In the second instance, as was done in Chapter 6, where the supporting columns yield, the story was subdivided into two sub-stories, one representing the FPS connection and the other the nonlinear column. A small mass was associated with the connection between the FPS isolator and the ground story column. None of the cases studied herein developed sufficient lateral displacement in the FPS isolators to engage the displacement restraints.

The masses used to represent the structure are the same as those derived in Chapter 2 for the Operations Building. These were 5.42 k-sec2/in, 5.42 k-sec2/in and 5.2 k-sec2/in for the second, third and roof levels, respectively. Viscous damping was considered in all of the analyses to equal 5% of critical. Damping is assumed to be constant for all vibration modes of the initially elastic models.

Various response quantities are computed by the DYNIN program. In this chapter emphasis will be placed on maximum values of story displacements relative to the ground, interstory structural drifts, story structural ductilities, shears and energy dissipation. Structural ductility is defined as the maximum story drift divided by the corresponding yield displacement for that story. Structural drifts in the first story contain only contributions from the columns, so that ductility values at this level are not influenced by FPS connection deformations. Similarly, displacements in the FPS isolator can be estimated as the difference between the total relative displacement at the top of the first story and the first story structural drift. In some instances envelopes of maximum values of response qualities for all levels are plotted against various parameters.

7.3 Ground Motions Considered

It is not, in general, possible to normalize completely the equations of motion for a multiple degree of freedom nonlinear system. Thus, information on the sensitivity of the seismic performance of the the buildings was obtained by scaling ground motions to pre-selected levels. This was done as described in Chapter 2 to obtain ground motion excitations roughly consistent with the dynamic characteristics corresponding to Richter magnitude 5, 6, 7 and 8 events.

For these studies only the north-south component of the 1940 El Centro earthquake record was used. As done in Chapter 2, the record was scaled to make it representative of the various intensities of ground motion. The scaling relations used are

summarized in the following table.

Target Magnitude	Peak Acceleration	Time Scale Factor
5	0.15g	0.5
6	0.35g	1.0
7	0.70g	1.0
8	0.88g	1.0

Before any definitive design guidelines and can be validated, additional ground motions must be considered. The current study will, however, still give a clear indication of the effect of severity of excitation on system performance.

7.4 Structures Investigated

The basic structure considered is the cost equivalent FPS supported Operations Building shown in Fig. 7.1. FPS isolators with a period of 2.25 seconds, a friction coefficient of 10% and a lateral sliding displacement limit of 6.5 inches were used. The design of this building is examined in detail in Chapter 2. The building was designed in accordance with the 1985 UBC assuming the structural period equals the period of the FPS connection (2.25 seconds), the system performance factor K equals 0.67, a soil coefficient S of 1.5 was assumed, and an importance factor of 1.5 was used, reflecting the importance of the structure. This results in a working stress base shear coefficient of 0.067. Following a detailed design of structural members, elastic and plastic analyses were performed on the structure to determine the lateral inter-story stiffnesses and strengths. These values are summarized in the following table.

Level	Lateral stiffness (kip/in)	Plastic Yield Strength (kips)
Roof (3)	877	1252
2	1477	2116
1	1635	1920 (618)*

* Note that the shear in the first story, when the FPS connections initiate sliding, equals 618 kips for a friction coefficient of 0.10.

The distribution of story shear capacity is also shown in Fig. 7.2. This structure has an ultimate base shear coefficient of 0.31. The elastic period of the structure (with the FPS connections locked up) was computed to be 0.86 seconds.

To assess the effects of various design parameters on building performance, the period and strength of the above design was changed systematically. The resulting structures are shown in Table 7.1. The cost equivalent design of the Operations Building is Case V. To assess the effect of building strength on response, stronger and weaker designs were formulated. In the first instance, the strength was increased to that of the original non-isolated design of the Operations Building, with a calculated ultimate base shear capacity of 0.45. Thus, the non-isolated result for Case VI, provides the response of the original non-isolated design of the Operations Building. The isolated results for Case VI represent the response of the full strength isolated design. The strength of the basic building was also reduced. Here, the story shears were reduced uniformly to about 25% of their original values so that the ultimate base shear was lowered to 0.08. This is representative of an existing building with low lateral load capacity. In making these strength alterations to the models, lateral stiffnesses were held constant.

Similarly, different periods were considered for the structure. The period of the basic structure was elongated to 1.5 seconds by decreasing the story lateral stiffnesses proportionately. This represents a very flexible structure or a taller structure being approximated by a simpler four degree of freedom model. The period of the basic structure was also reduced to 0.25 seconds. This represents a stiffer and/or shorter structure. In making these period alterations, the lateral story load capacities were held constant.

By combining the three different periods and three different lateral ultimate strengths, nine different hypothetical buildings result with a wide range of strengths and stiffnesses (see Table 7.1). In view of the preliminary nature of these investigations, it is believed that this simplified method of formulating the hypothetical building cases is acceptable. More refined design cases, in which actual members sizes are determined, would be more realistic and would result in different distributions of strength or stiffness with height. However, these secondary design changes would make interpretation of the results more difficult. It is believed that the hypothetical designs considered herein are consistent with design practice.

The characteristics of the FPS isolators are altered for each of the hypothetical designs. Generally, the period of the FPS connection was selected based on the period of the structure, and the friction coefficient was selected based on the ultimate strength of the structure. While reasonable values were selected, no attempt was made to optimize the isolation system design. FPS connection characteristics used are presented in Table 7.1. The effect of selecting other FPS connection parameters on seismic performance will be explored in subsequent sections.

For comparison purposes, a non-isolated structure is associated with each of the nine FPS supported structures. To have a consistent basis for comparison, the stiffness and strength of the non-isolated structures are identical to those for each of the FPS supported systems. The only difference is that the FPS connection is absent for the non-isolated structure.

Several other individual designs in addition to the 9 parametric variations will also be evaluated in subsequent sections.

7.5 Basic Response Results

The nine pairs of isolated and non-isolated buildings were analyzed using the DYNIN program for each of the four levels of earthquake ground motions. A variety of response parameters were computed. Primary focus was on total displacement of each floor relative to the ground, interstory structural displacements, inelastic energy dissipation, and structural displacement ductility factors. Results are presented in the plots shown in Figs. 7.3 through 7.11. The original basic case adopted from the cost equivalent Operations Building is refered to as Case V. This case will be presented first and other eight cases will be compared to this basic case.

Response of Case V Structure. -- The response envelopes for the basic structure are shown in Fig. 7.3. To simplify the plots, information for the ground level has been disregarded. Looking at information on the total displacement of a floor relative to the ground, one can see that the displacements of the isolated and non-isolated structures are identical for the case of the El Centro record scaled to 15%g. This is because the response to this earthquake is insufficient to cause the FPS connections to slide. As the intensity of the ground motion increases, sliding takes place and the curves for the isolated and non-isolated structures separate. In general, the total lateral displacement of the FPS supported structure, relative to the ground, is somewhat less than for the non-isolated structure. However, the difference, while significant, is not large. Although the longer period of the isolated structure tends to cause larger displacements, the hysteretic damping of the FPS connections reduces the displacements. Thus, the net total displacements which occur are similar to those of the non-isolated structure. This differs from the response of buildings on elastic seismic isolators which would have larger displacements than those which occur in FPS isolated structures. Another similarity of the FPS isolated structure displacement response to that of the non-isolated structure is the upper portions of both structures tend to behave as stiff structures supported on a soft first story. For example, the displacement at the roof for both structures when the structures are subjected to the El Centro record scaled to 0.7g averages 5.8 inches, whereas the displacement at the top of the first story is 78% of this value. However, in the case of the non-isolated structure, all of this displacement occurs in the structural

members while that in the isolated structure develops largely in the FPS connections.

This difference in response can be more easily seen in the curves for structural interstory drifts, also shown in Fig. 7.3. The differences are particularly apparent in the bottom level where the structural drifts for the FPS supported structure are only 11% of those developed in the non-isolated structure when considering the 88%g peak acceleration record. Differences in drifts developed by the two structures are also significant in the upper levels, where for instance the drifts in the second and third stories of the FPS supported structure are only 38% and 52%, respectively, of the those developed in the non-isolated structure.

Similar trends can be seen in Fig. 7.3 for the maximum structural ductility factors. Here one can note that the FPS supported structure remains elastic for all of the earthquake records considered, including El Centro scaled to 88%g. The non-isolated structure requires displacement ductilities on the order of 1.5 in the upper two levels and 4.1 at the ground level for the 70%g excitation.

It is clear from the above discussions that the non-isolated building performs reasonably, and given modern construction and inspection practices would be expected to demonstrate reasonable structural performance for the earthquake ground motions considered here. The building did, however, behave as a soft story structure with concentrations of displacement and ductilities in the lower story. This would be expected to cause significant non-structural damage. The isolated structure behaved better by all measures considered. Significantly, the structure remained well within the elastic range of response during all of the excitations considered. While significant sliding of the FPS connection developed, this was at most 4.9 inches, significantly less than the 6.5 inch limit.

Other example analyses are presented later related to the Case V basic structure. However, before doing this, results for the other cases in Table 7.1 will be reviewed.

Response of Other Structures. -- The effect of period and strength of the structure can be assessed by reviewing Figs. 7.3 through 7.11 in a manner similar to that undertaken above. This will indicate the same general tendencies as observed for Case V. That is, the structure tends to act as a soft story with the drifts, ductilities and energy dissipation demands concentrated in the lower level. Again, in the case of the non-isolated structures, all of the displacements occur in the structural members while those in the isolated structures develop largely in the FPS connections.

Effect of Ultimate Strength of Structure. -- To clarify the influence of various parameters on the overall response, a new set of plots was prepared. In these plots, the maximum response quantity anywhere in the structures is plotted against the design

variable of interest. For example, the maximum ductility at any level is plotted against the strength of the structure as well as against peak ground acceleration (for the Scaled El Centro record) in Figs. 7.12 to 7.14. Similarly, maximum ductility at any level is plotted against structural period (stiffness) in Fig. 7.15. While these plots do not indicate the distribution of response quantities over height, they are more useful in determining the sensitivity of response to various parameters.

These plots indicate that ductility for isolated and non-isolated structures alike tends to decrease with increasing ultimate base shear coefficient and increase with increasing peak ground acceleration. It clear from these figures that the FPS supported structure requires considerably less ductility that the comparable non-isolated structure. For example, considering the structures with a period of 0.25 seconds, the non-isolated structure would have to be nearly 4 times stronger that the FPS supported structure to limit displacement ductilities in the structure to 5. It is also significant to note that over a wide range of strengths it is possible to achieve FPS supported structures that remain entirely elastic (with the exception of the isolator). However, as the structures become weaker, especially for Case I with a period of 0.25 seconds, large ductility demands occur in the columns in the FPS supported structure. Methods for reducing the ductility requirements for case I will be examined in Section 7.6.

An important indication of nonstructural damage is interstory drift. Again it is clear that the FPS system provides much superior protection from this form of damage in comparison to conventional non-isolated structures. Significantly reduced drifts occurred in the stiff and flexible isolated structures.

Required energy dissipation demands in structural elements are substantially less in the FPS supported structures. Total energy dissipation, including the energy dissipation by the FPS connections, is roughly the same for isolated and non-isolated buildings.

Effect of Structural Period. -- As the structures in Table 7.1 are stiffened to obtain the desired natural period, the response varies as well. This is shown in Fig. 7.15 for the structures with a ultimate base shear coefficient of 0.08 and subjected to the El Centro record scaled to 70%g. This weak structure developed greater inelastic deformations than the other structures and is, thus, interesting to plot. This figure shows that the maximum total displacement increases slowly with period. The displacements for the FPS supported systems are consistently smaller than those developed by the non-isolated structure. The same basic trend is observed for the interstory drifts except for the fact that the differences between the values increase with increasing period. This is due to the fact that the non-isolated building is acting as a soft story structure concentrating nearly deformations in the first story. The FPS supported structure is able to distribute the yielding to other levels due to its deformation hardening characteristics.

The ductility demands developed by the structures are inversely proportional to period. The stiffer structures have yield displacements that change with the square of natural period. The FPS supported structure develops ductility similar to a structure with a significantly longer period.

Effect of Ground Motion Intensity. -- The influence of peak ground motion is shown in Fig. 7.12 to 7.14. This indicates that ductilities increase monotonically with increasing peak ground acceleration. Greater acceleration is needed to induce ductility into structural elements in FPS supported structures than in non-isolated structures. The figures show that the rate of increase of ductility with peak ground acceleration for structures with periods of 0.25 and 0.88 seconds is about the same and lower, respectively, for FPS supported structures than for non-isolated structures. For the case of a structure with a period of 1.5 seconds, the rate is initially lower then it becomes higher.

Observations. -- While the details of the above responses are likely to change with variations in modeling assumptions and for different ground motions, it is believed that the basic characteristics of the response will remain the same. In all cases examined, the FPS supported structure performed better than the same structure without the FPS. Additional analyses are needed to assess the effects of different ground motions and modeling idealizations.

7.6 Influence of FPS Connection Design Parameters on Response

In several cases involving weak structures, large inelastic deformations were required in the FPS supported structures. This was most apparent for the Case I structure where first story column ductilities were nearly 80 for the El Centro record scaled to 0.7g. While this is considerably better that the value of 130 required for the non-isolated structure, it is far in excess of the value that can be dependably achieved by most conventional structural details. Case I is thus a particularly useful example to review because one might interpret the results to indicate that FPS connections were not practicable for such structures. This is not the case as will be shown below.

One of the features of the FPS connections is that they automatically impart to the structure deformation hardening as the structure slides along the spherical bearing surface. This provides beneficial effects related to centering of the structure and helps control the magnitude of the lateral siding displacements. However, it also increases the load that can be transferred across the FPS connection. In cases such as these, where the strength of the supporting column exceeds that needed to maintain sliding in the FPS isolator, column yielding is induced by this deformation hardening phenomenon. However, if the period of the connection is increased, the rate of deformation hardening decreases. Since the maximum sliding displacements increase by only small amounts with increase in the period of the FPS

connection, increasing the FPS period has a dependable tendency to reduce the maximum forces that can be transferred by the FPS connection.

To explore this possibility, three modifications were considered for the Case I structure subjected to the hypothetical magnitude 7 event (El Centro scaled to 70%g). In the first of these, the period of the isolator was left unchanged, but the base column was assumed to remain elastic. In this manner, it was possible to determine the degree of strengthening needed to obtain elastic behavior in the base column. In this case the column had to be strengthened by 92%, a large increase. In the second case, the period of the isolator was increased to 3 seconds. In this case, it would only be necessary to strengthen the column by 11% to maintain elastic behavior. This is a small amount and well within reason. If, in the third case, the period of the isolator was increased to 4 seconds, the column would remain elastic without any change in the strength of the column (in fact, the column could be reduced in strength by 9%).

The results of these cases subjected to the El Centro excitation scaled to 70% g are shown in Fig. 7.16. It is clear that the period of the FPS isolator and the elastic behavior of the supporting columns has only limited influence on the overall lateral displacement of the structure. However, the structural drifts decrease with increasing FPS isolator period, especially at the bottom level. Since the columns were strengthened, ductility demands at the base were unity. Ductility at the upper levels was kept to a minimum (a maximum displacement ductility of 5.7 was observed for the case of the FPS isolator period Tc equal to 4 seconds). It should be kept in mind that all of these values are substantially less than that obtained for a comparable non-isolated structure. It would appear that the relatively small increase in base column strength and lateral displacements is a reasonable tradeoff against the significant reduction in displacement ductility demands and interstory drifts.

Similar approaches were explored for the Case IV structure. Here, the original design resulted in a displacement ductility of about 8 in the ground level columns, a much smaller, but still excessive value. In this case, two modifications were studied. In the first, the period of the isolator was kept constant and the columns were strengthened to insure their elastic behavior. In this case the columns had to be strengthened by 41%. In the second case, the columns were not strengthened, but the period of the isolator was increased to 4 seconds (from 3 seconds).

Results for this study of modifications to the Case IV structure are plotted in Fig. 7.17. In this figure, the original structure is indicated by the curve with Tc equal to 3. Again the lateral displacements are only marginally influenced by these modifications. The increase of the isolator period tends to decrease lateral displacements, whereas strengthening of the columns tends to increase the displacements. In both cases ductility, drift and energy dissipation demands on the structure

decrease dramatically. Ductility demands for the unstrengthened column with a Tc of 4 seconds were only 2.8.

Thus, the designer has several options for improving structural response. These options include modification of the FPS connection characteristics and locally strengthening regions of excessive ductility demand. These options may be particularly useful for retrofitting existing hazardous buildings. The behavior of the structure follows trends that would be anticipated on the basis of earlier results. It should be noted that in the design of an actual structure, additional ground motions would have to be considered and appropriate factors of safety would have to be applied against the occurrence of any undesirable behavior.

7.7 Influence of Structural Strength on Response

In all of the previous examples, the distribution of strength in the upper stories has been kept the same as that obtained in the original design of the cost equivalent FPS supported structure. However, the previous results indicate a number of important observations. First, the distribution of strength with height, as shown in Fig. 7.2, is biased toward yielding in the FPS connections. Only in the cases with large amounts of deformation hardening, or substantial higher mode contributions would one expect the members of the upper levels to yield significantly. Second, the numerical results show that yielding is generally most severe for the bottom level. Lastly, the previous examples have indicated that the total lateral structural displacement is relatively insensitive to the strength of the structure or isolator for the same structural period. Thus, one might conjecture that it would be possible to significantly reduce the strength of the upper levels of the structure without detrimental effects on overall seismic performance. To assess this possibility several additional analyses were made on the basis of the Case V example structure.

In these analyses, various distributions of strength are used in the upper portions of the structure. The FPS isolators and the strength of the ground story columns are kept the same as use in the previous analyses. The new distributions of strength are shown in Fig. 7.18. The first case is based on the force on the isolator when it begins to slide. This value is 618 kips. This was taken to be a constant for the full height of the structure in case A. In an attempt to obtain a better estimate of a proper distribution of strength with height, the strength needed to sustain a Richter magnitude 6 seismic event (El Centro at 35% g) without yielding was selected as case B. As it was felt that this might result in excessive ductility demands for the largest earthquake records considered, case C was also formulated and taken to be the strength needed to keep the structure elastic under the Richter magnitude 7 recent (El Centro at 70% g). The strengths used are summarized below.

Strengths (in Kips) of Various Alternative Distributions

Level	Original Design	Case A	Case B EC @ 35%g	Case C EC @ 70%g
Roof(3)	1252	618	821	1078
2	2116	618	1043	1200
1	618*	618*	618*	618*

* Indicates strength of isolator, actual column strength is 1920 kips.

Case A reflects a 71% reduction in capacity at the second level. Case B and C represent still significant reductions of 51% and 43%, respectively, at this level. The effect of such large changes in strength on overall seismic performance was evaluated in a series of analyses. Results for these analyses are presented in Figs. 7.19 and 7.20 along with the results for the original Case V example structure.

When the various alternatives are subjected to the El Centro record scaled to 70% g, the results are shown in Fig. 7.19. By definition, the structure for case C remains elastic for this design and excitation. With the exception of case A, the various alternatives have only imperceptible effect on lateral displacements and drifts. The values for case A increase associated with significant yielding that occurs in the second story. In spite of the large reductions in strength, ductility demands increase only moderately, to a maximum of about 1.7 at the roof for case B and to about 6.7 for case A.

When the El Centro record is scaled to 88% g, response values increase proportionately, but relative relations between design alternatives remain constant. Maximum ductilities for the case B structure are still less than 1.8, in spite of the substantial reductions in strength. This can be seen in Fig. 7.20.

Based on these analyses it appears that significant savings can be obtained by permitting controlled yielding in the structure. To an extent, yielding of the structure can be viewed as a means of limiting the deformation hardening of the FPS isolator. Once the structure reaches its ultimate capacity, it cannot take any additional load. This will tend to limit sliding on the isolators which must harden to continue sliding. Thus, the structure will be initially isolated by the FPS connection while it is sliding and as the structure begins to yield, the slider is no longer needed and stops sliding. Methods for obtaining a desirable balance between

sliding in the FPS isolator and yielding in the structure remain to be determined. However, it is clear that yielding is not necessarily detrimental to the response of FPS supported structures, and may have beneficial influences on cost.

7.8 Summary and Conclusions

The response of inelastic multiple degree of freedom systems supported on FPS connections was found to follow many of the same trends which are presented in Chapter 8 for single elastic degree of freedom systems. Total displacement relative to the ground was similar for isolated and non-isolated buildings. It is possible for a wide range of structures designed in conformance with current design practices to obtain elastic or near elastic response in all structural elements except for the FPS connection. Thus the isolators can be used as the primary elements which provide ductility and energy absorption. When yielding of isolated structures was permitted, the response of the structure was found to be consistent with good seismic performance. Design methods permitting selective yielding in the structure are able to reduce structural strength requirements.

The designer has the ability to control response by modification of FPS isolator characteristics. This can be used to achieve improved seismic performance and safety while reducing overall costs.

While the results presented herein are believed to indicate general trends, additional analyses are needed to assess the detailed influences of other ground motion characteristics, different types of structural hysteretic models, damping assumptions, distributions of stiffness and strength. Of course, more detailed analyses and design studies are warranted to assess local behavior and the interaction between various design constraints (live loads, drift limitations, etc.).

7.9 REFERENCES -- CHAPTER 7

7.1 Khatib, I. and Mahin, S., "DYNIN -- Interactive Computer Program for the Nonlinear Dynamic Analysis of Buildings," SEMM Computer Program, University of California, Berkeley, 1987.

TABLE 7.1 DESCRIPTION OF MULTISTORY BUILDINGS CONSIDERED

STRUCTURAL PERIOD (SEC.)	FPS CONNECTORS *	ULTIMATE BASE SHEAR COEFFICIENT ** 0.08	0.31	0.45
0.25		Case I	Case II	Case III
	Period (sec.)	2.0	2.0	2.0
	Fric. Coeff.	0.05	0.10	0.10
0.86		Case IV	Case V ***	Case VI
	Period (sec.)	3.0	2.25	2.25
	Fric. Coeff.	0.05	0.10	0.10
1.50		Case VII	Case VIII	Case IX
	Period (sec.)	3.0	3.0	3.0
	Fric. Coeff.	0.05	0.05	0.1

NOTES:

* The sliding displacement travel permitted is assumed to be 6.5 inches in all cases.

** The FPS connectors begin to slide at a story shear of 309 kips for an effective friction coefficient of 0.05 and at 618 kips for an effective friction coefficient of 0.10.

*** Case V is the basic case considered in the study.

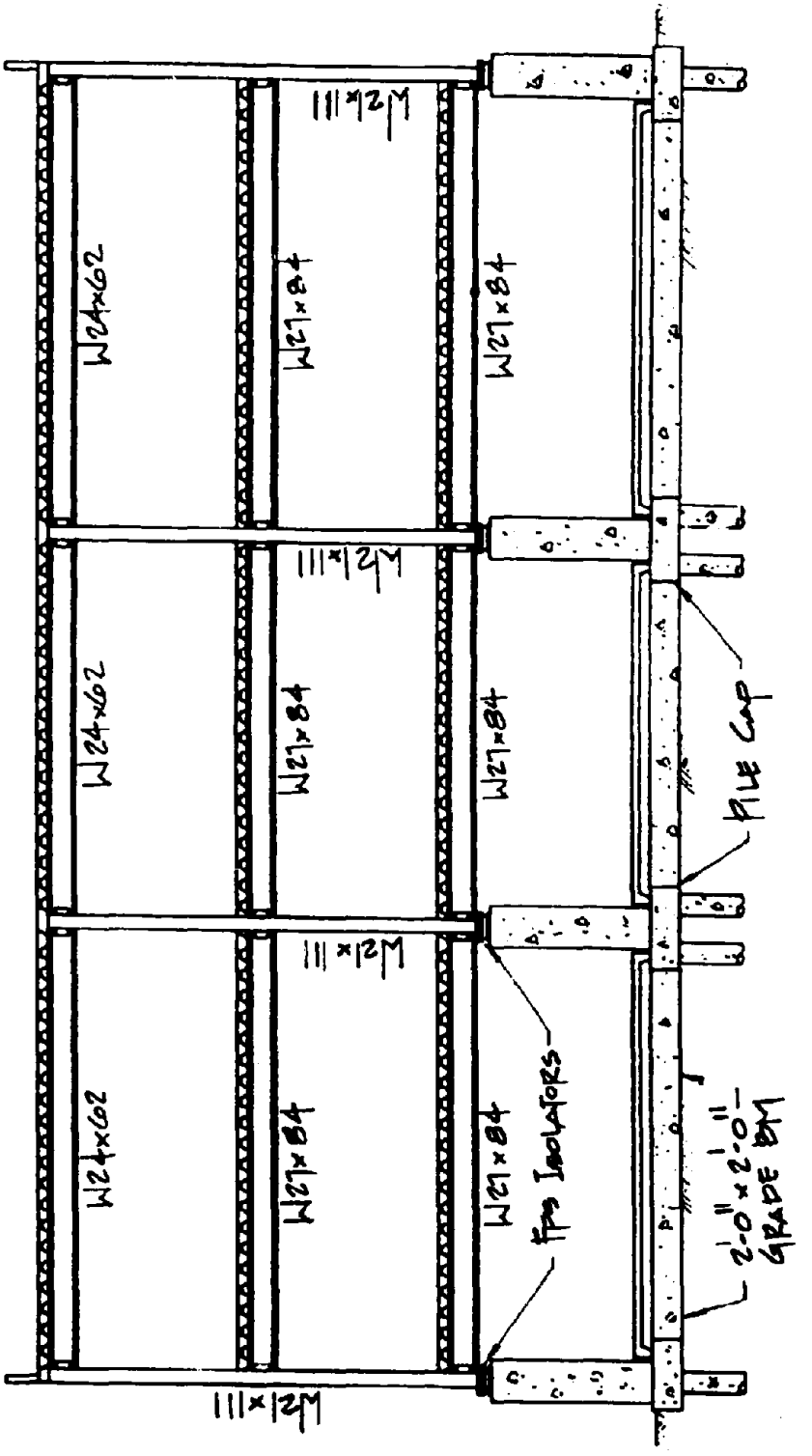

Fig. 7.1 Isolated Building for Case V

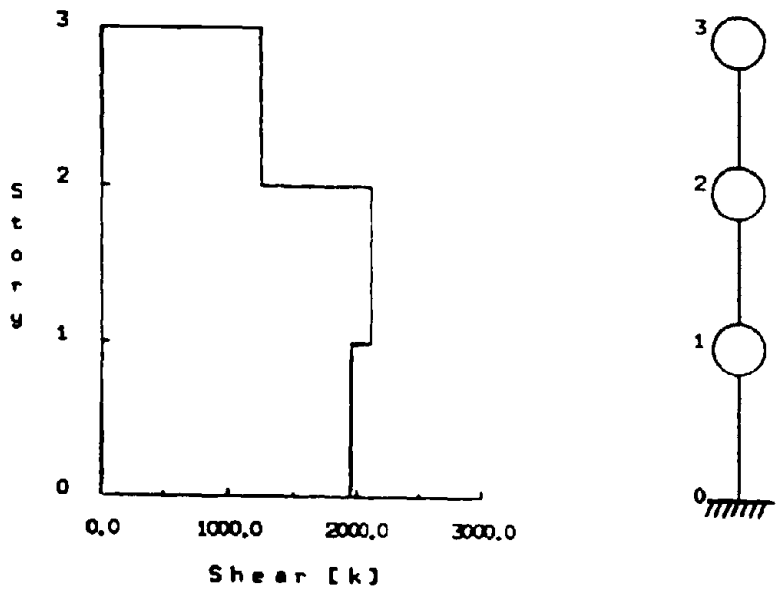

Fig. 7.2 Story Shear Capacities and Structural Model for Case V

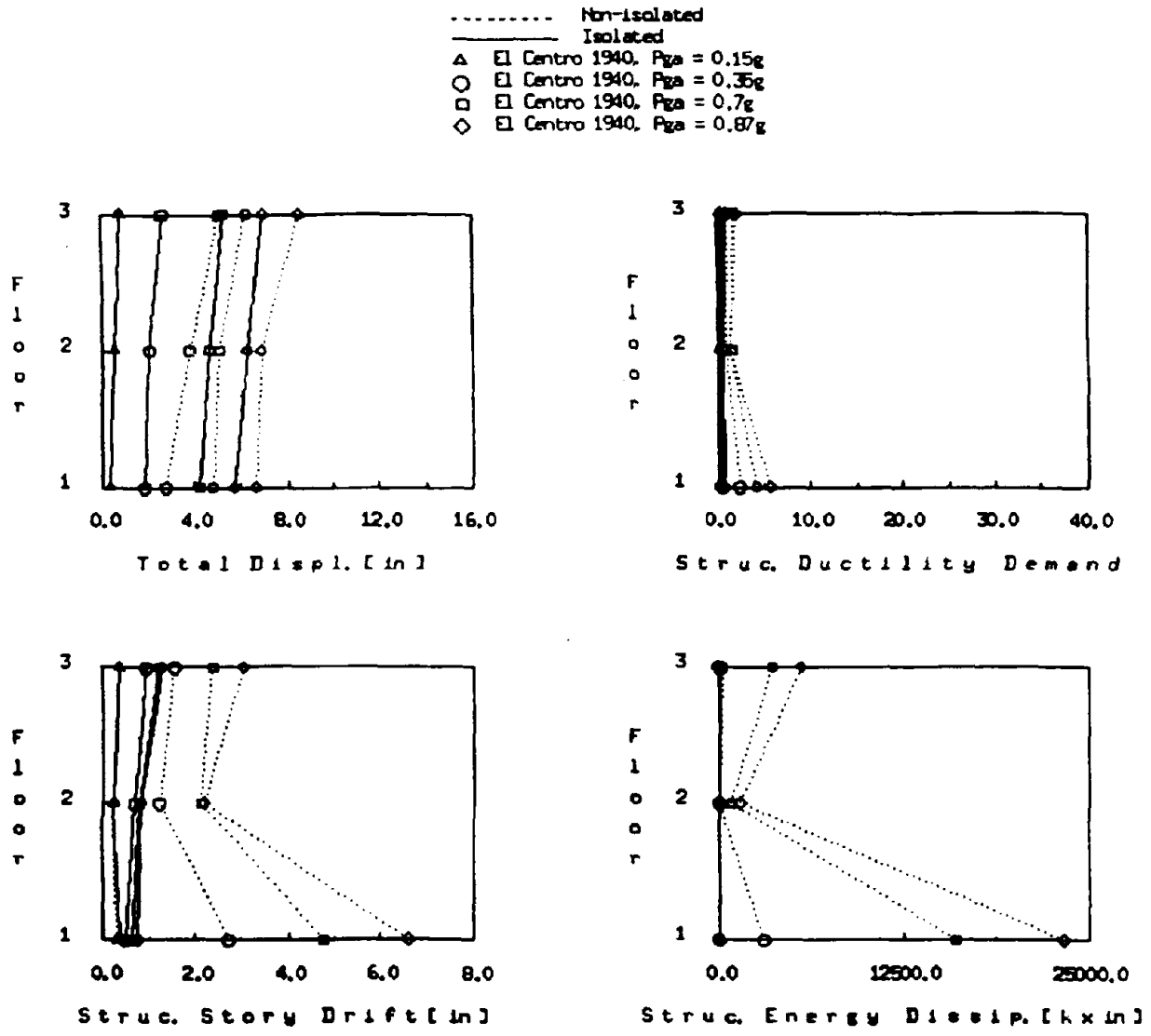

Fig. 7.3 Response Envelopes for Case V Structure

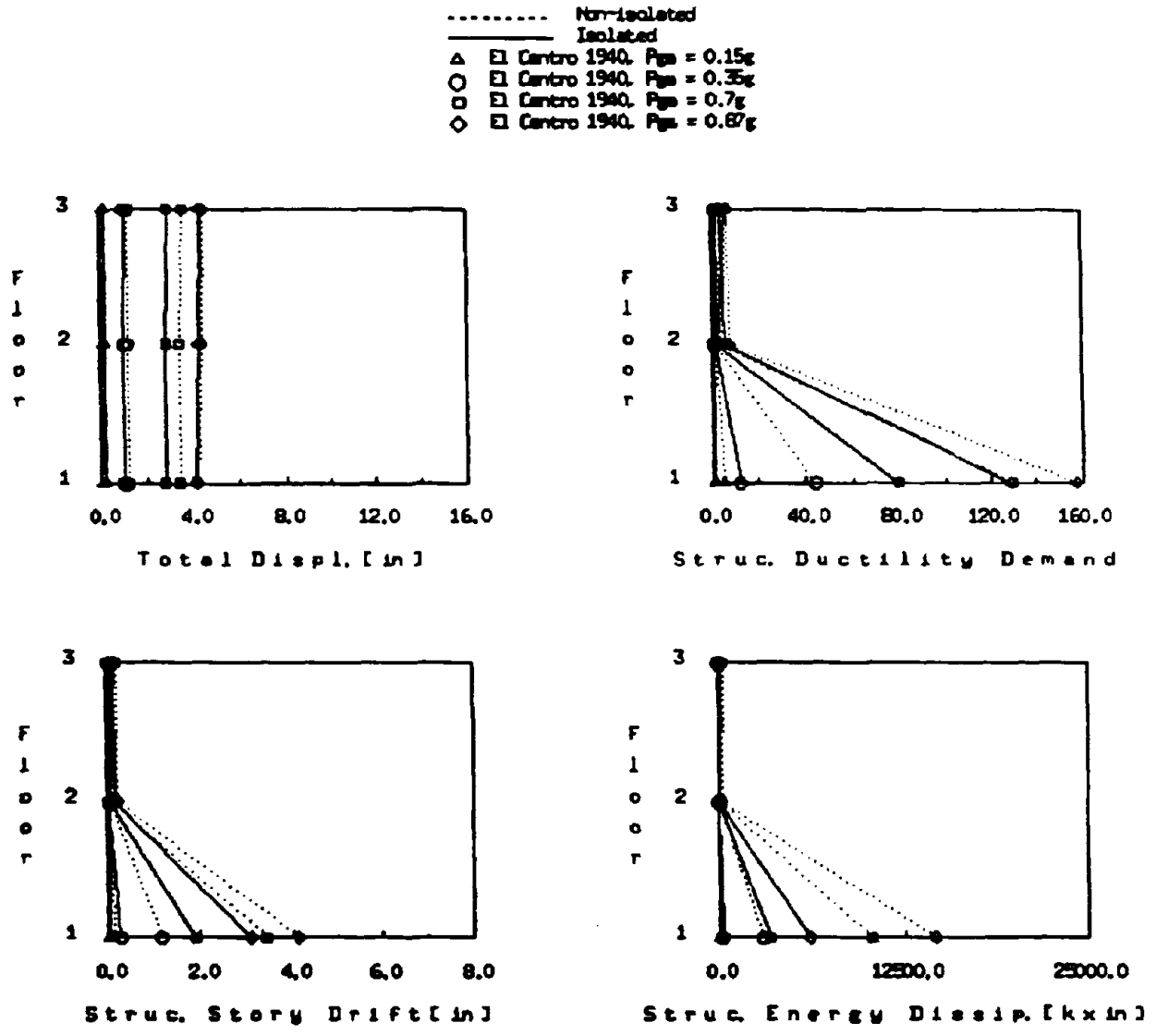

Fig. 7.4 Response Envelopes for Case I Structure

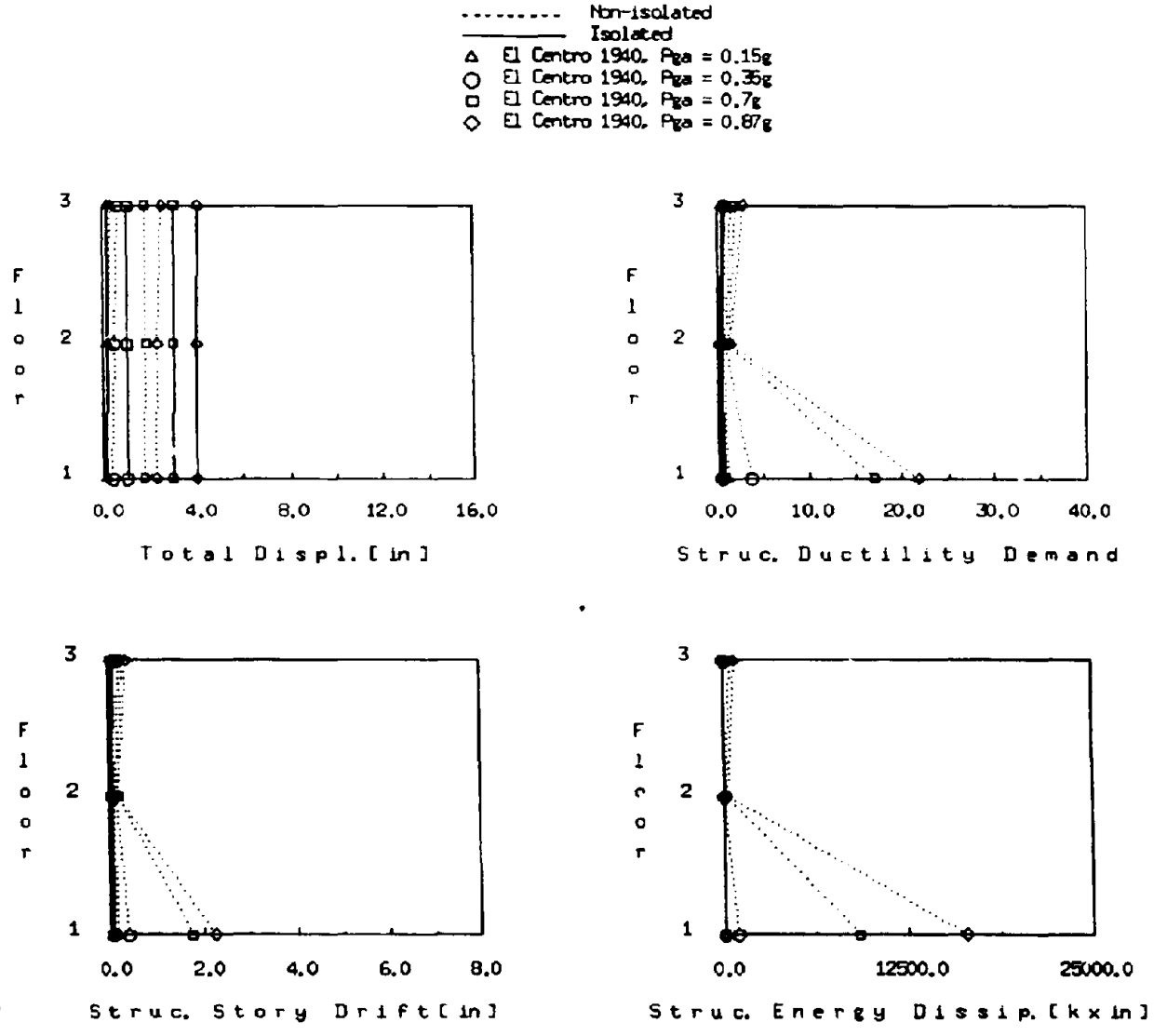

Fig. 7.5 Response Envelopes for Case II Structure

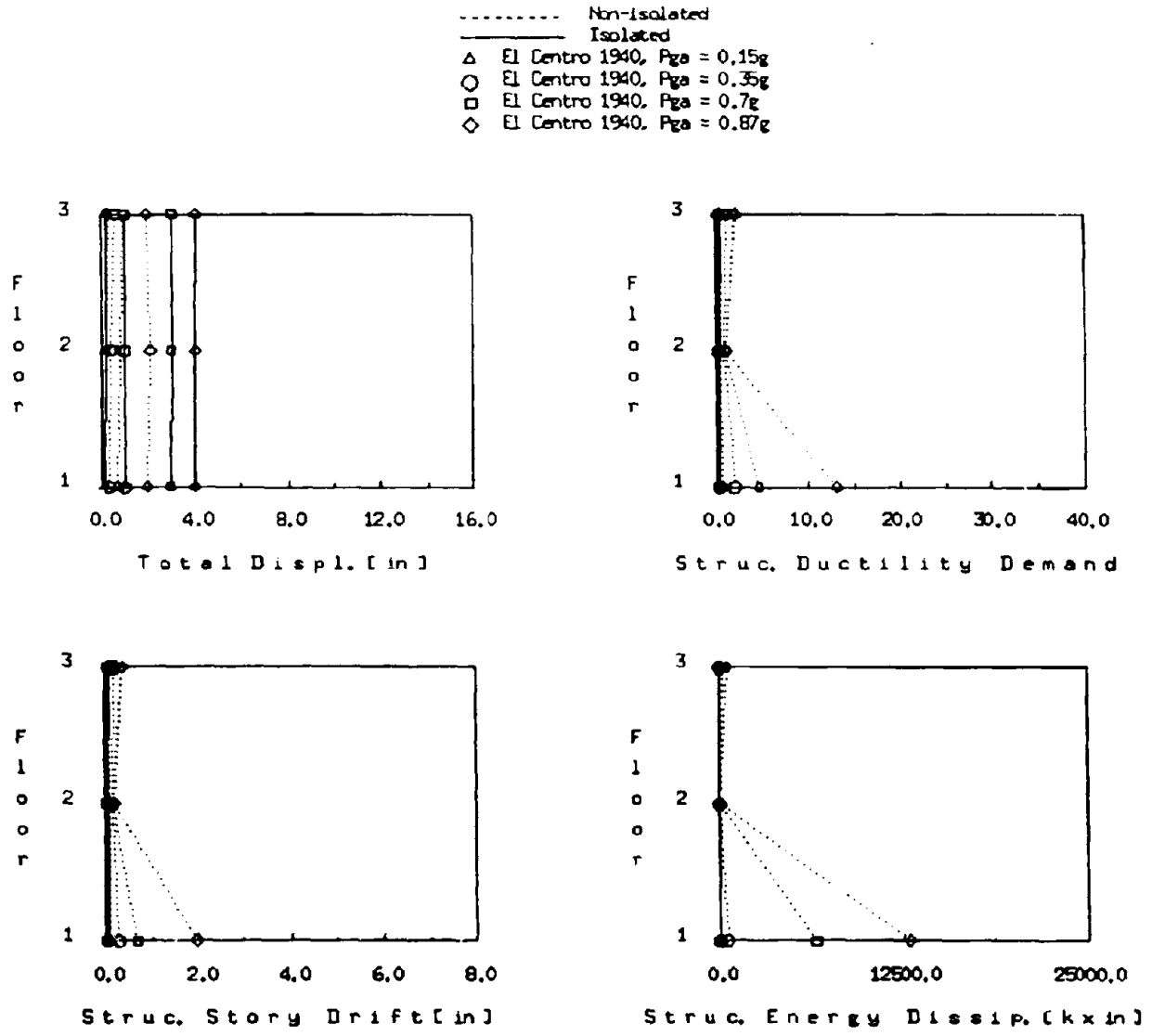

Fig. 7.6 Response Envelopes for Case III Structure

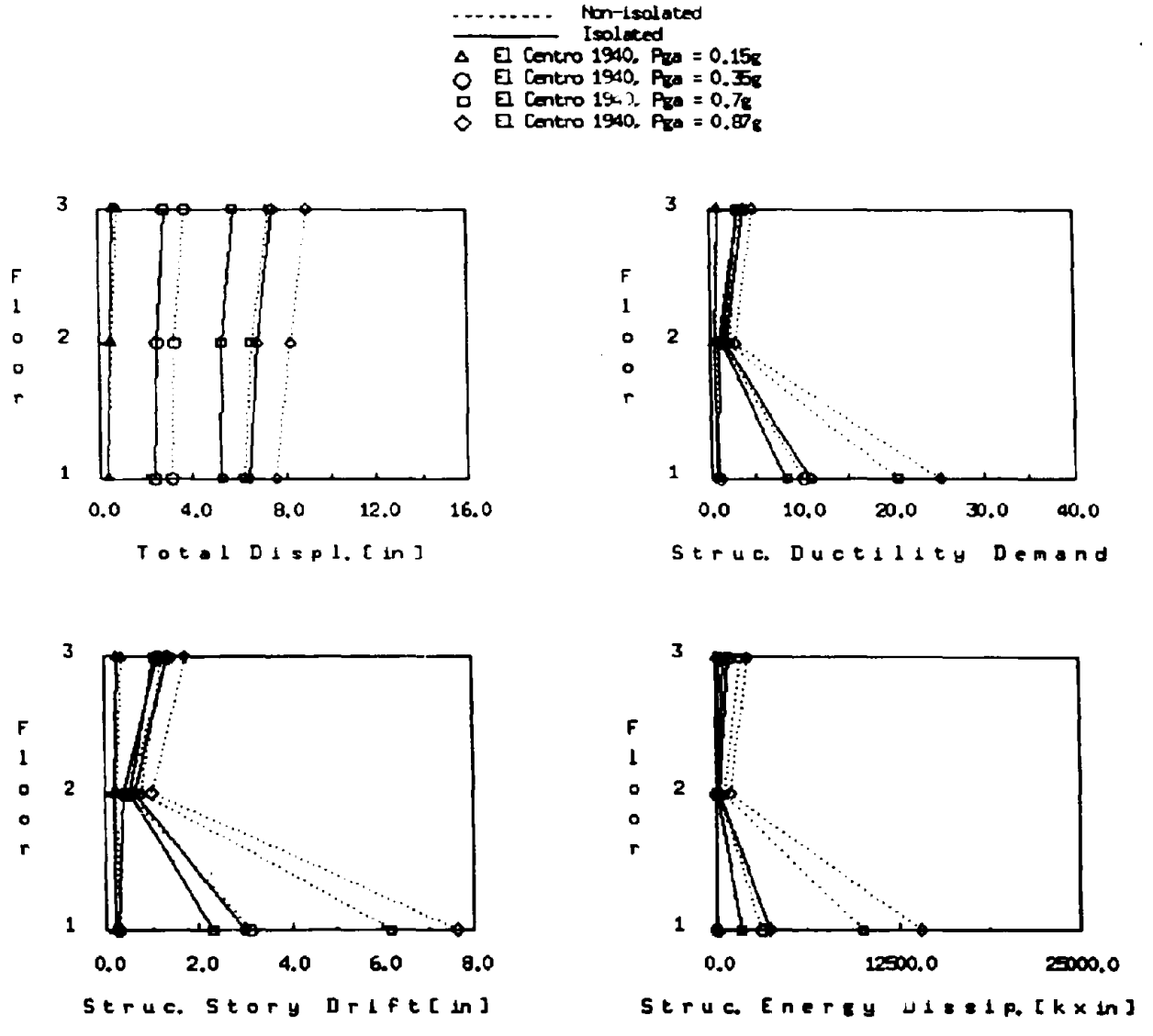

Fig. 7.7 Response Envelopes for Case IV Structure

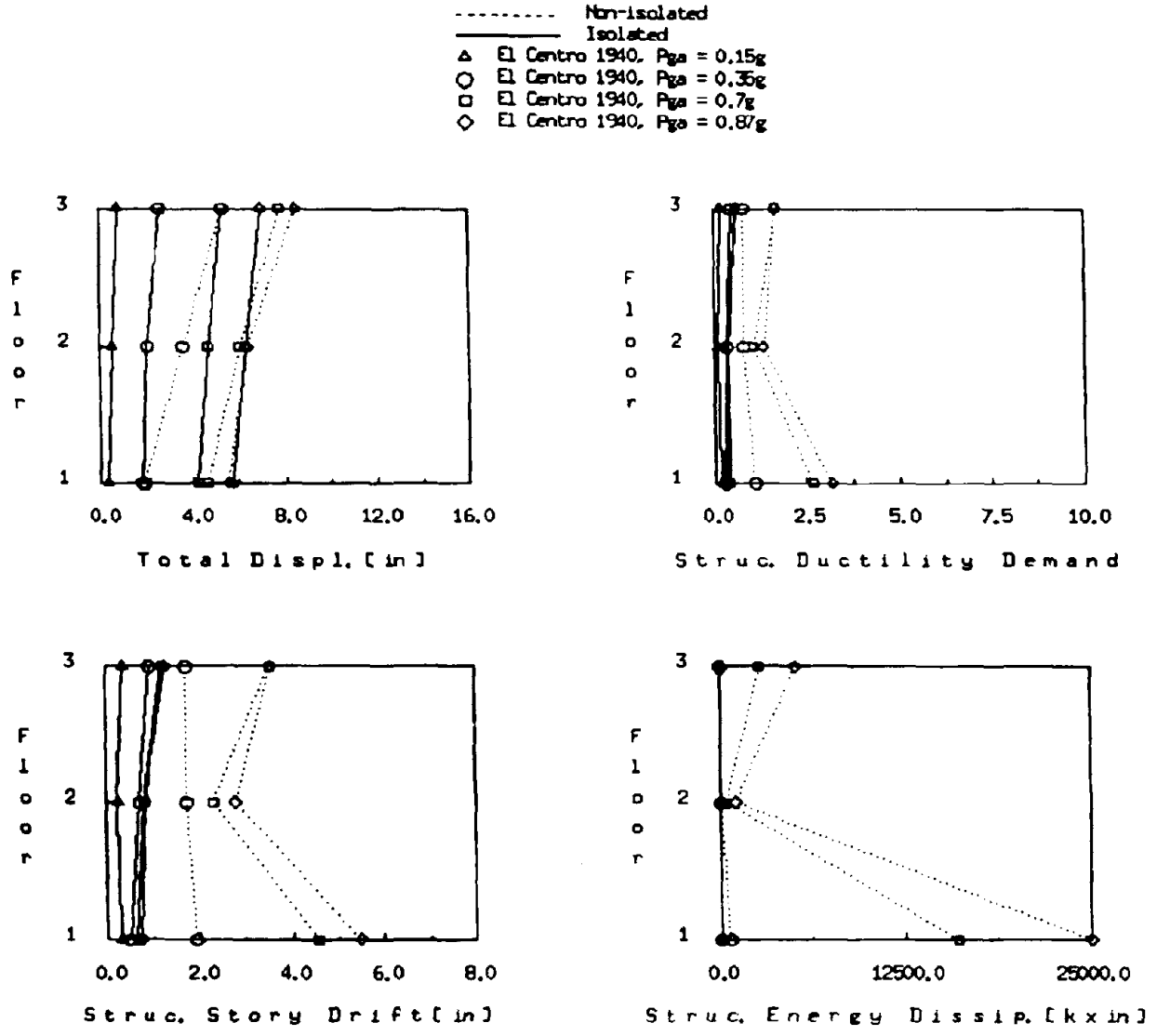

Fig. 7.8 Response Envelopes for Case VI Structure

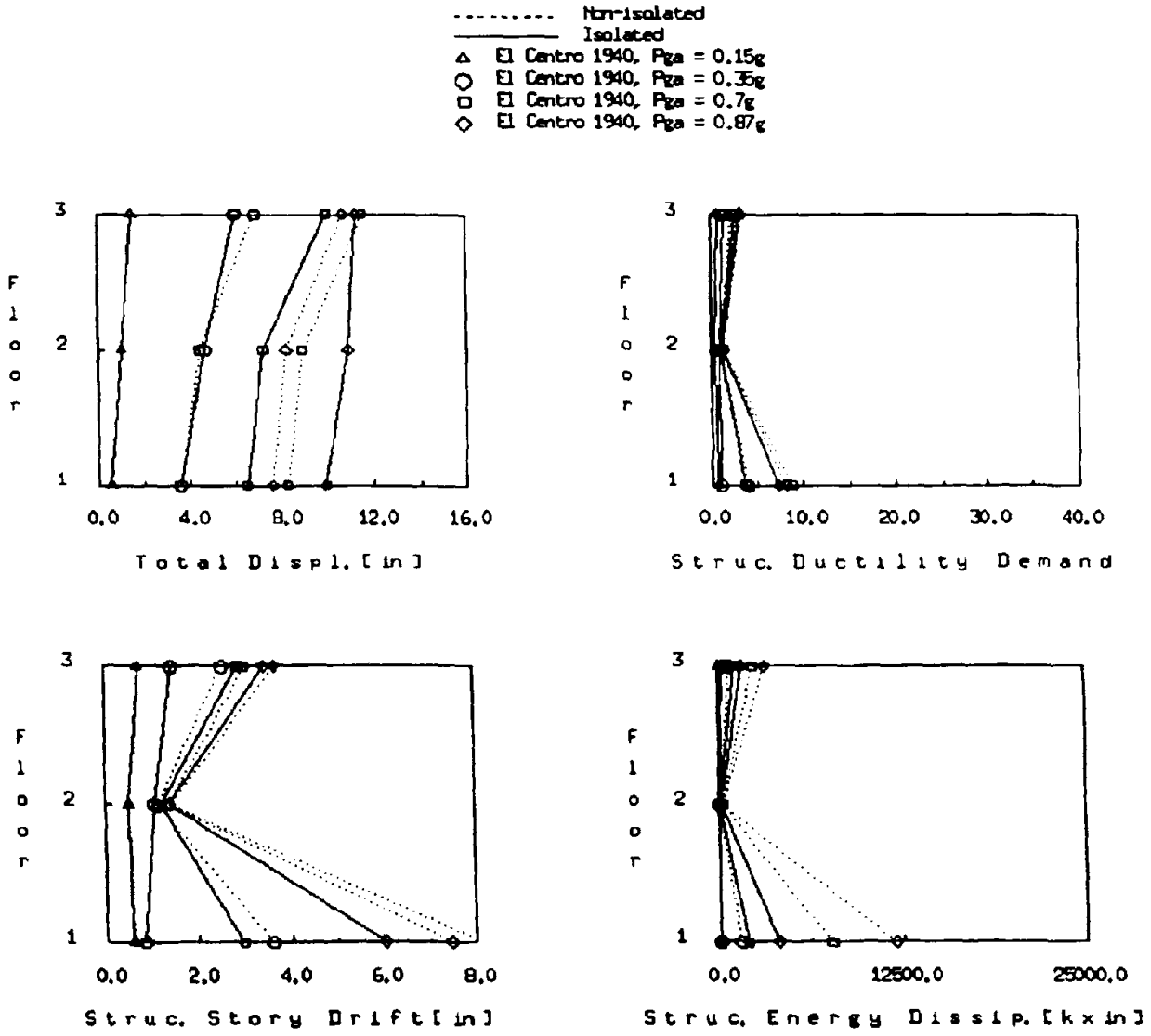

Fig. 7.9 Response Envelopes for Case VII Structure

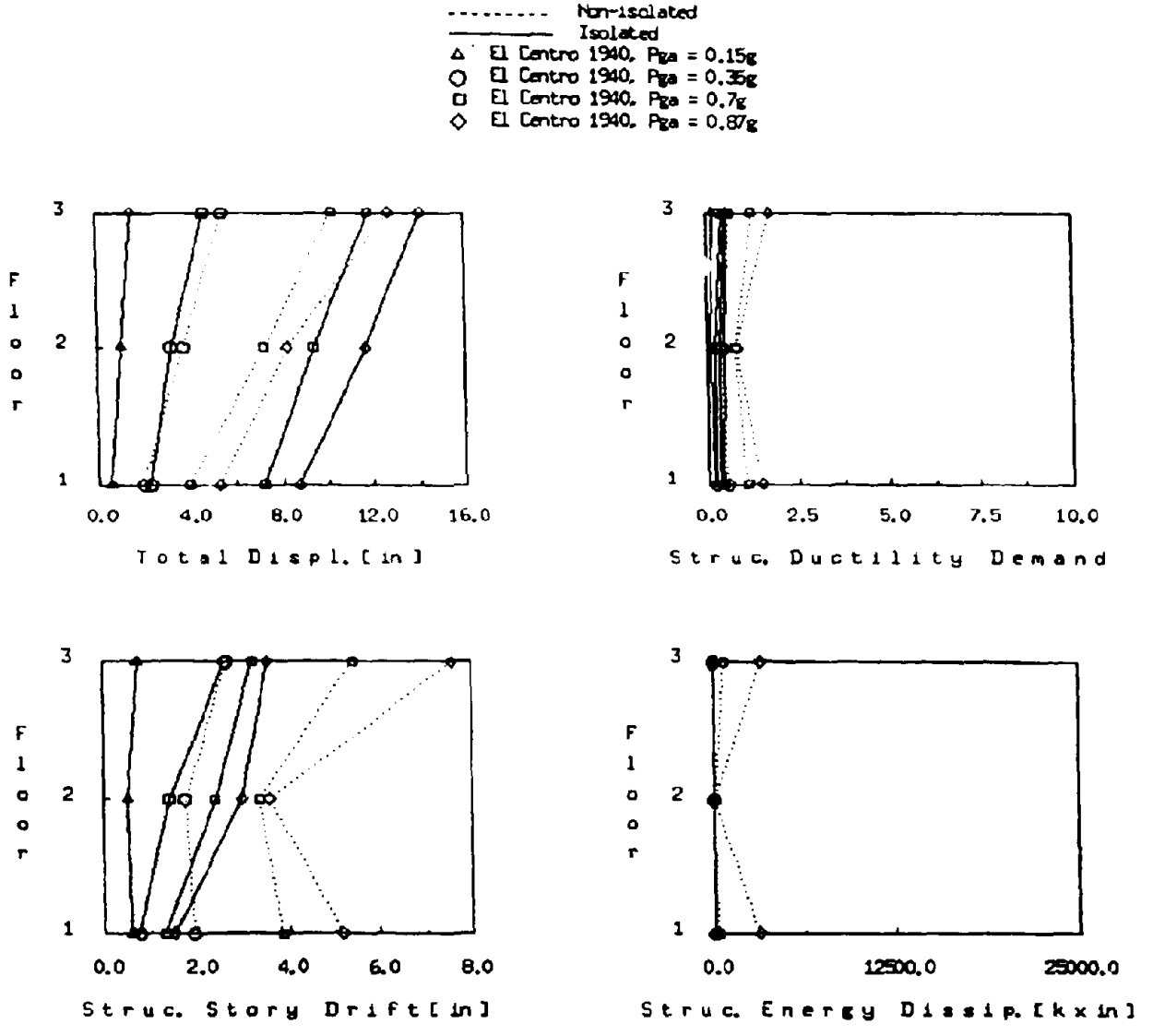

Fig. 7.10 Response Envelopes for Case VIII Structure

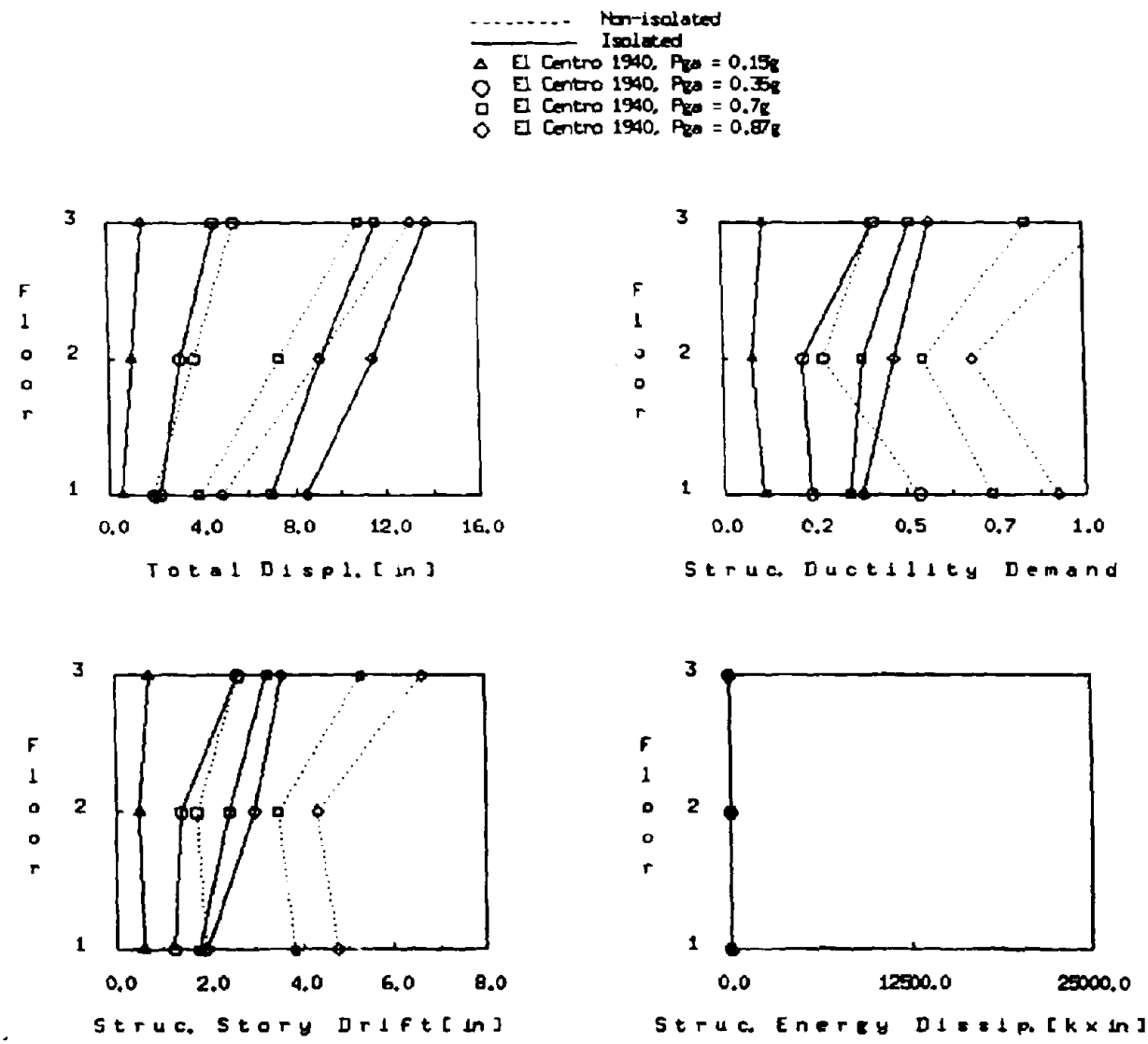

Fig. 7.11 Response Envelopes for Case IX Structure

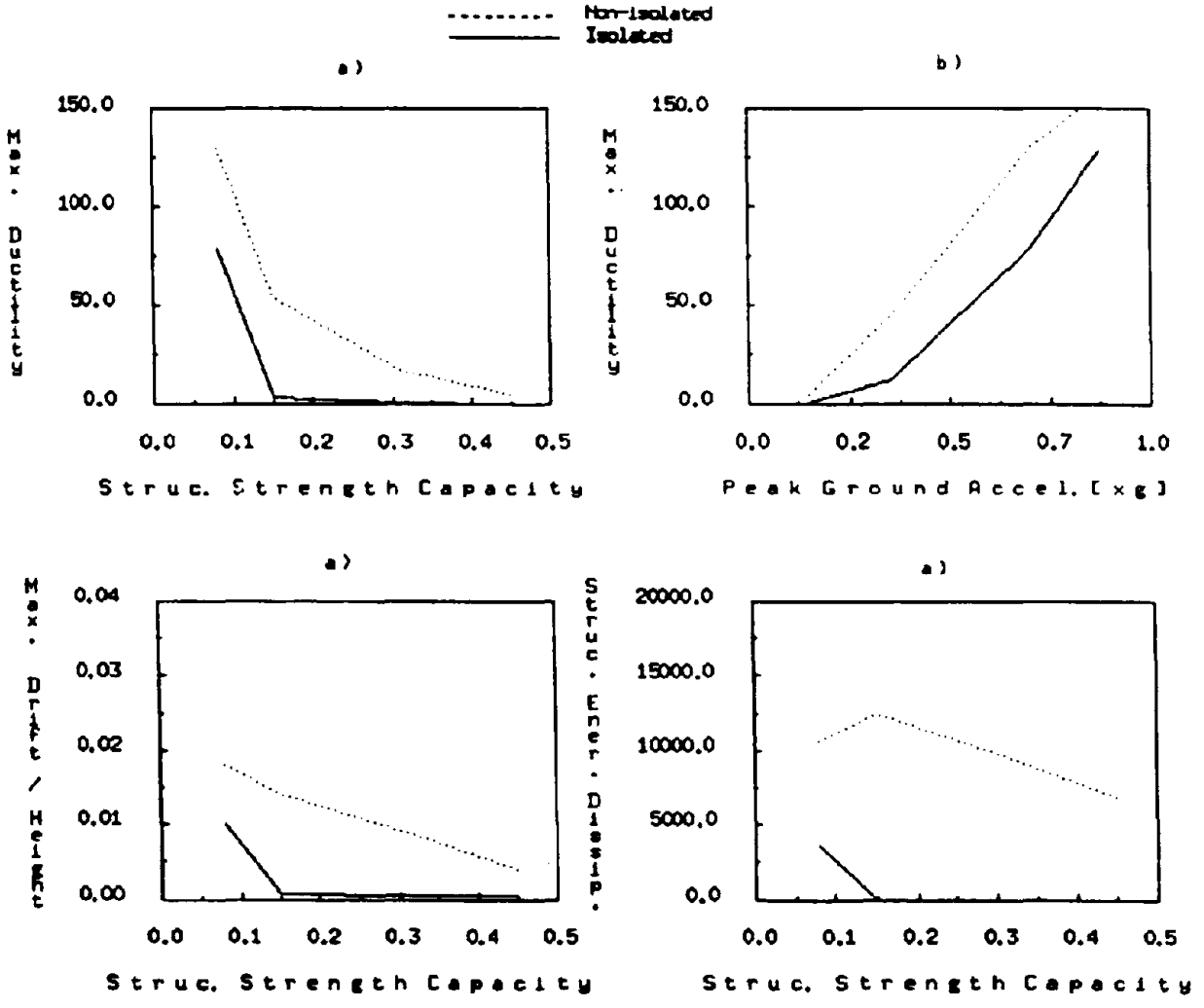

Fig. 7.12 Response Envelopes. Structural Period = 0.25sec

a) El Centro 1940, NS Comp., Pga = 0.7g, ξ=5%

b) El Centro 1940, NS Comp., η_{sr} = 0.08, ξ=5%

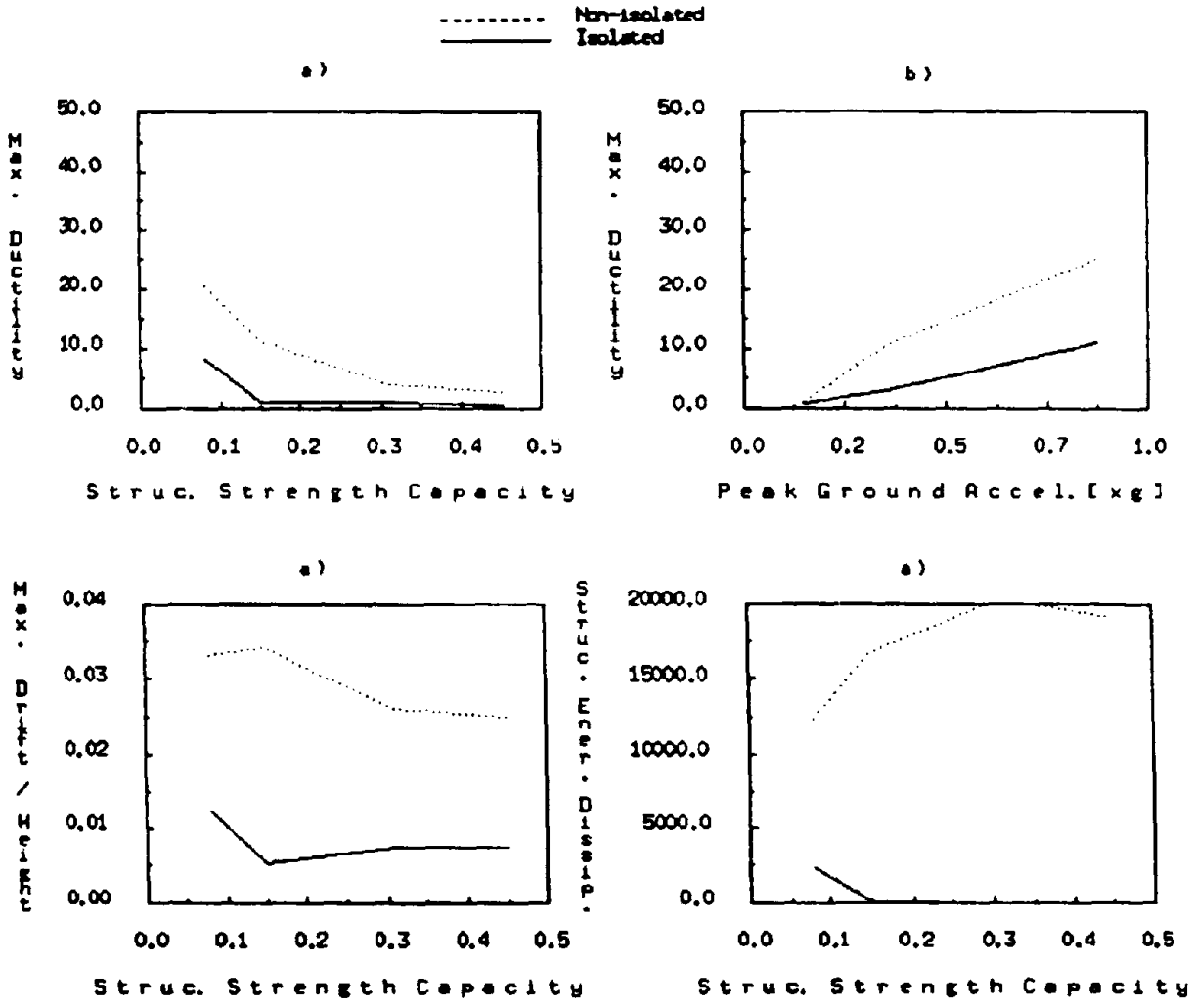

Fig. 7.13 Response Envelopes. Structural Period = 0.86sec

a) El Centro 1940, NS Comp., Pga = 0.7g, ξ=5%

b) El Centro 1940, NS Comp., η_{st} = 0.08, ξ=5%

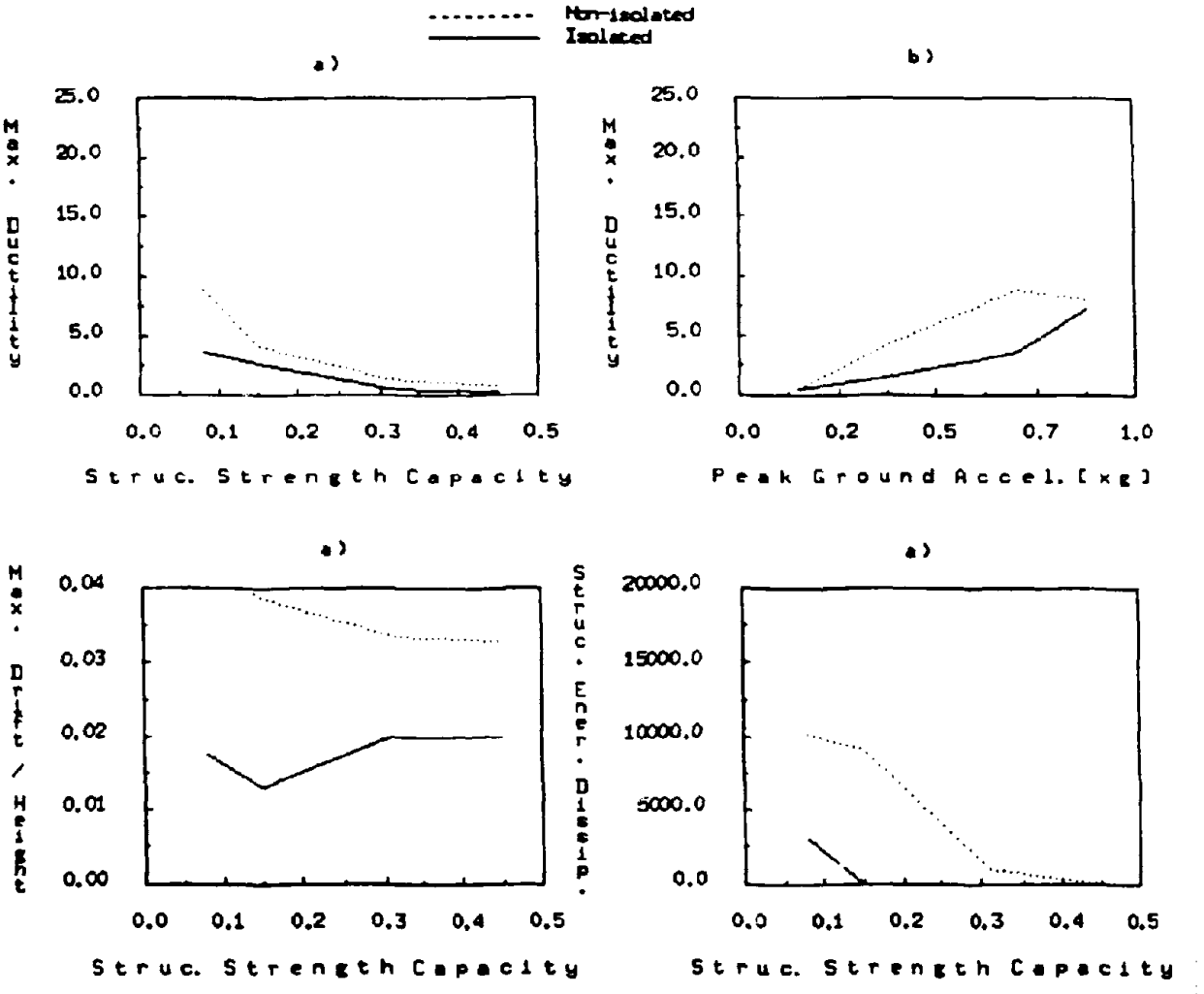

Fig. 7.14 Response Envelopes. Structural Period = 1.5sec

a) El Centro 1940, NS Comp., Pga = 0.7g, ξ=5%

b) El Centro 1940, NS Comp., η_{st} = 0.08, ξ=5%

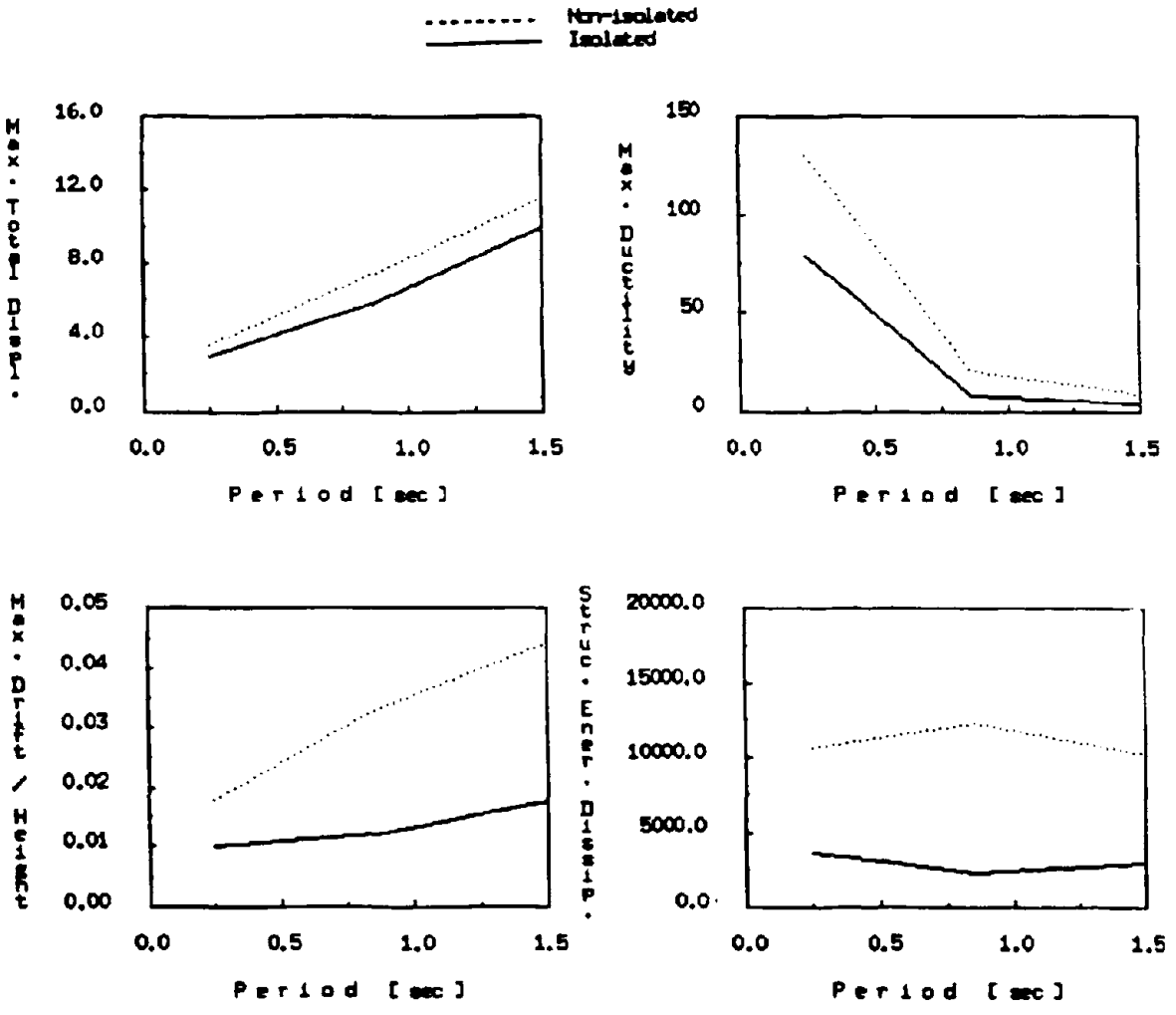

Fig. 7.15 Response Envelopes, Structural Strength Coefficient = 0.08, El Centro 1940 NS Comp., Pga = 0.7g, ξ=5%

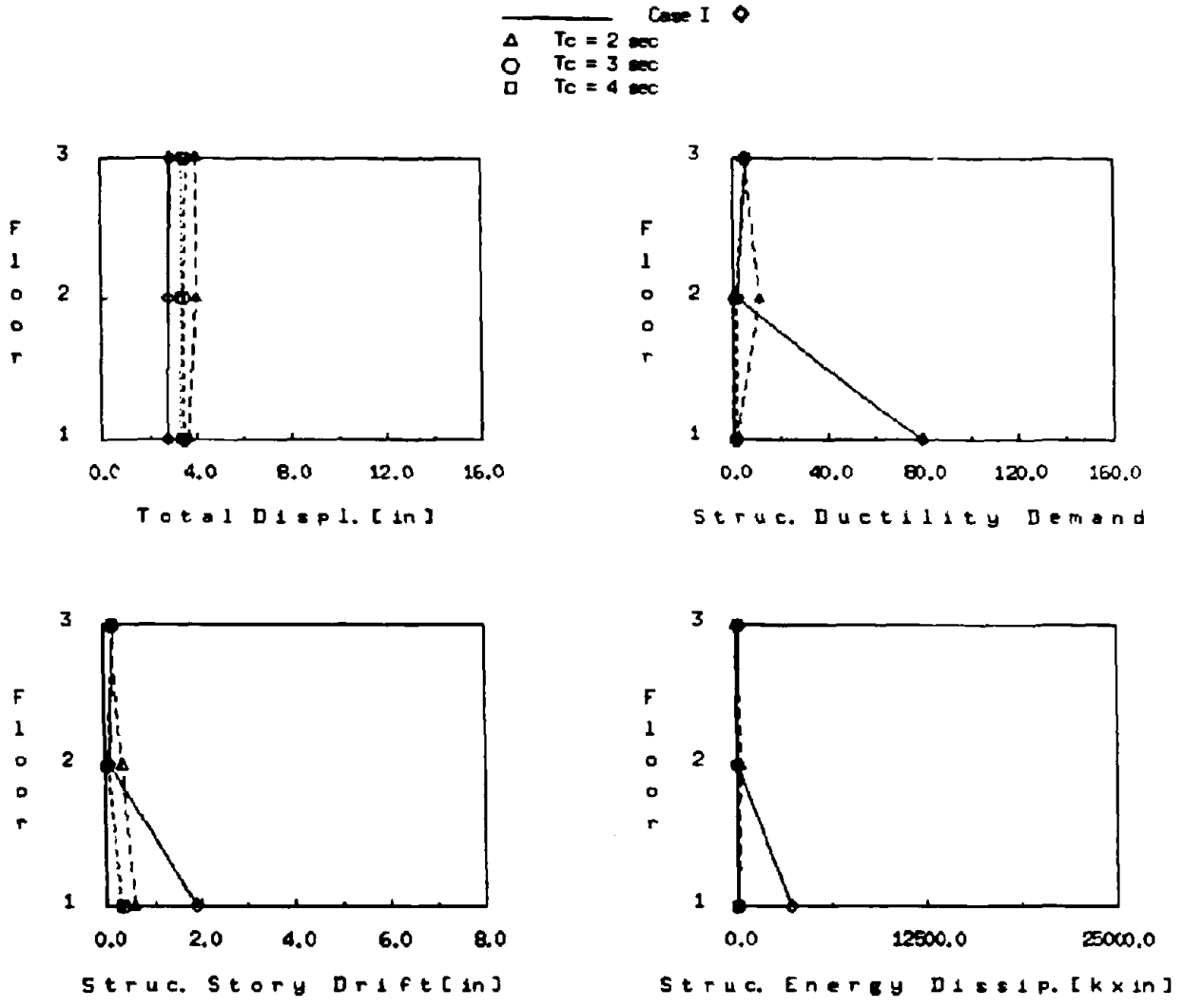

Fig. 7.16 Response Envelopes Case I, Variation of Tc and Yielding Strength for first level columns.

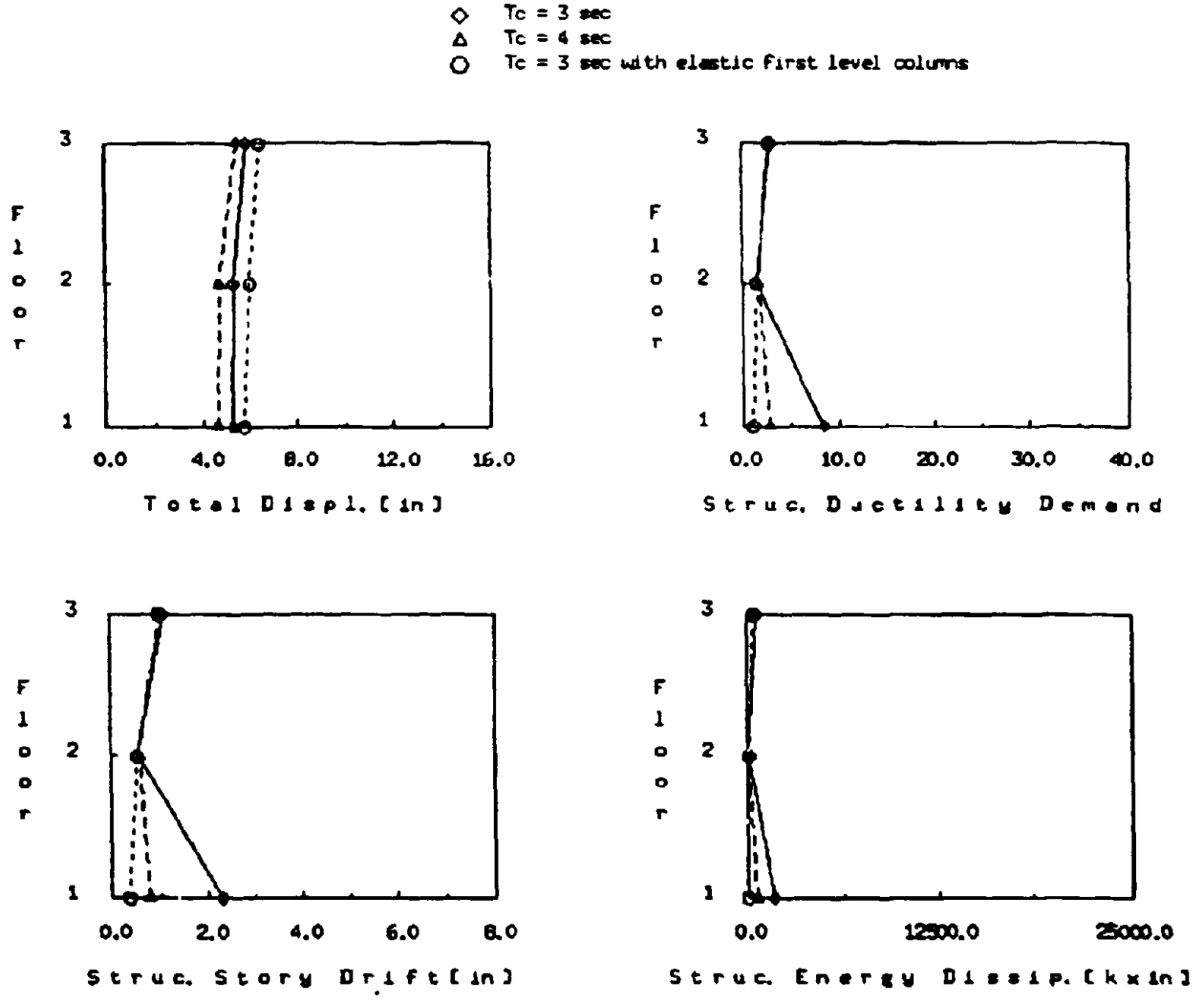

Fig. 7.17 Response Envelopes Case IV, Variation of Tc and Yielding Strength for first level columns.

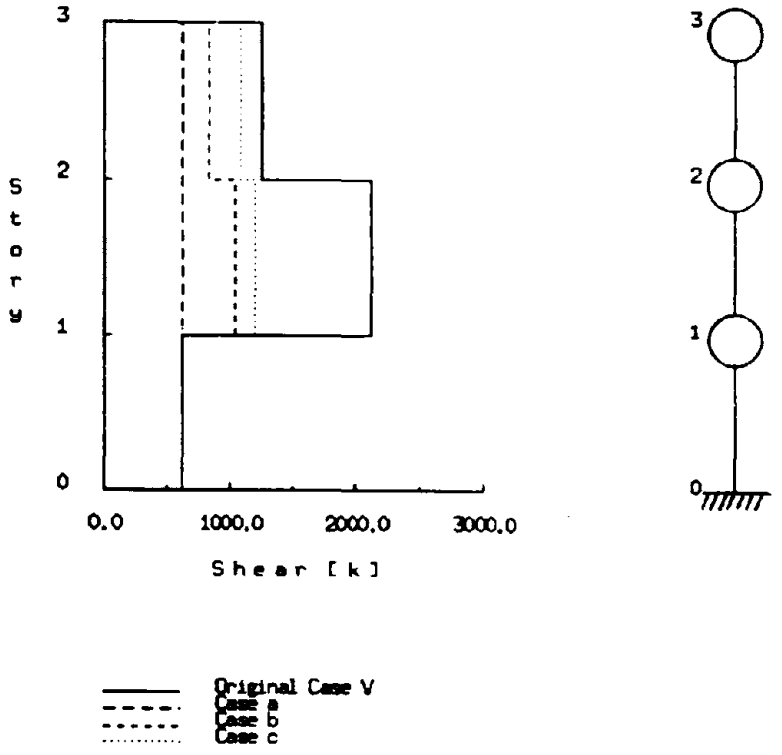

Fig. 7.18 Variation of Story Shear Capacities and Structural Model for Case V

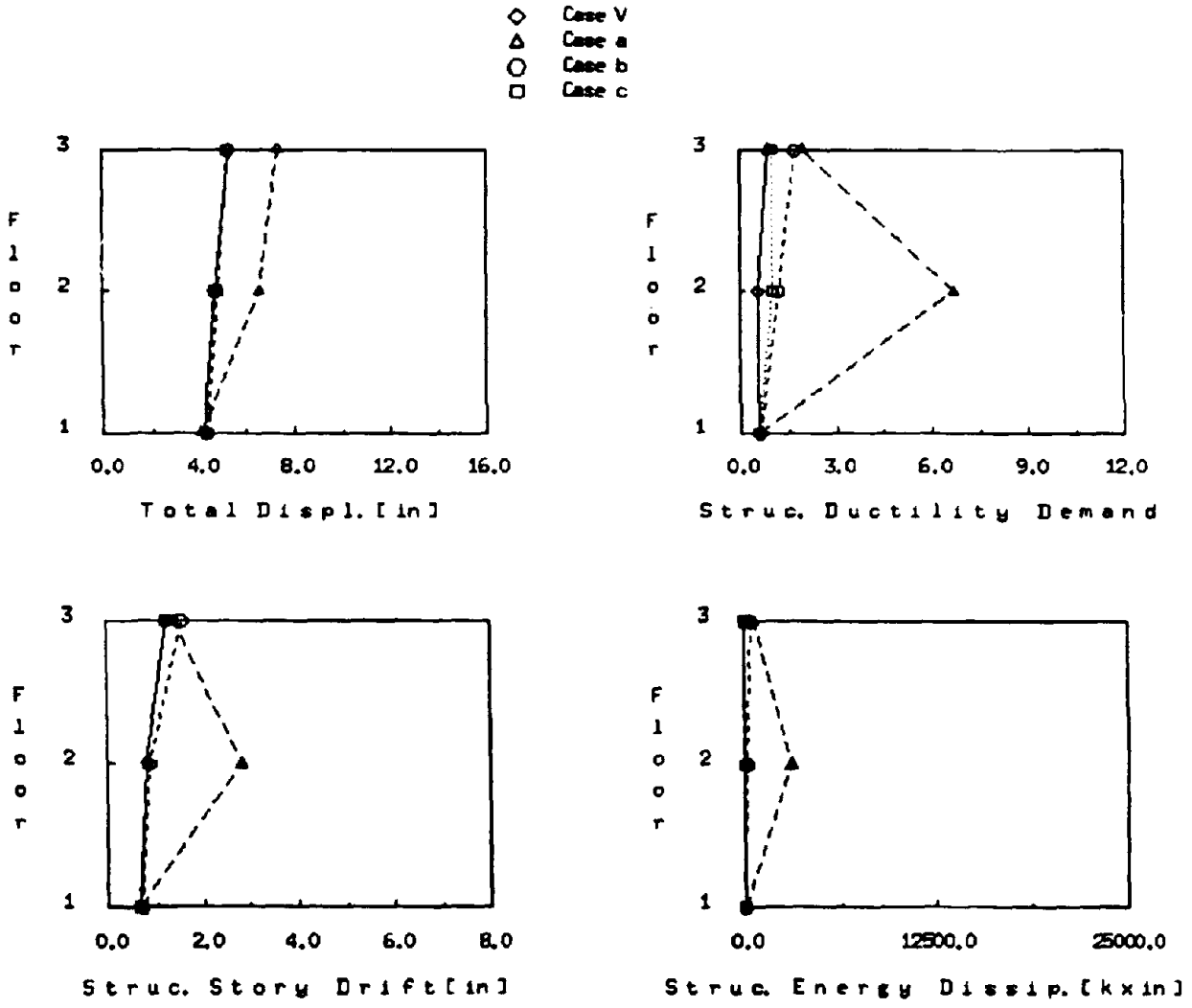

Fig. 7.19 Response Envelopes Case V, Variation of Yielding Strength. El Centro 1940, Pga = 0.7g.

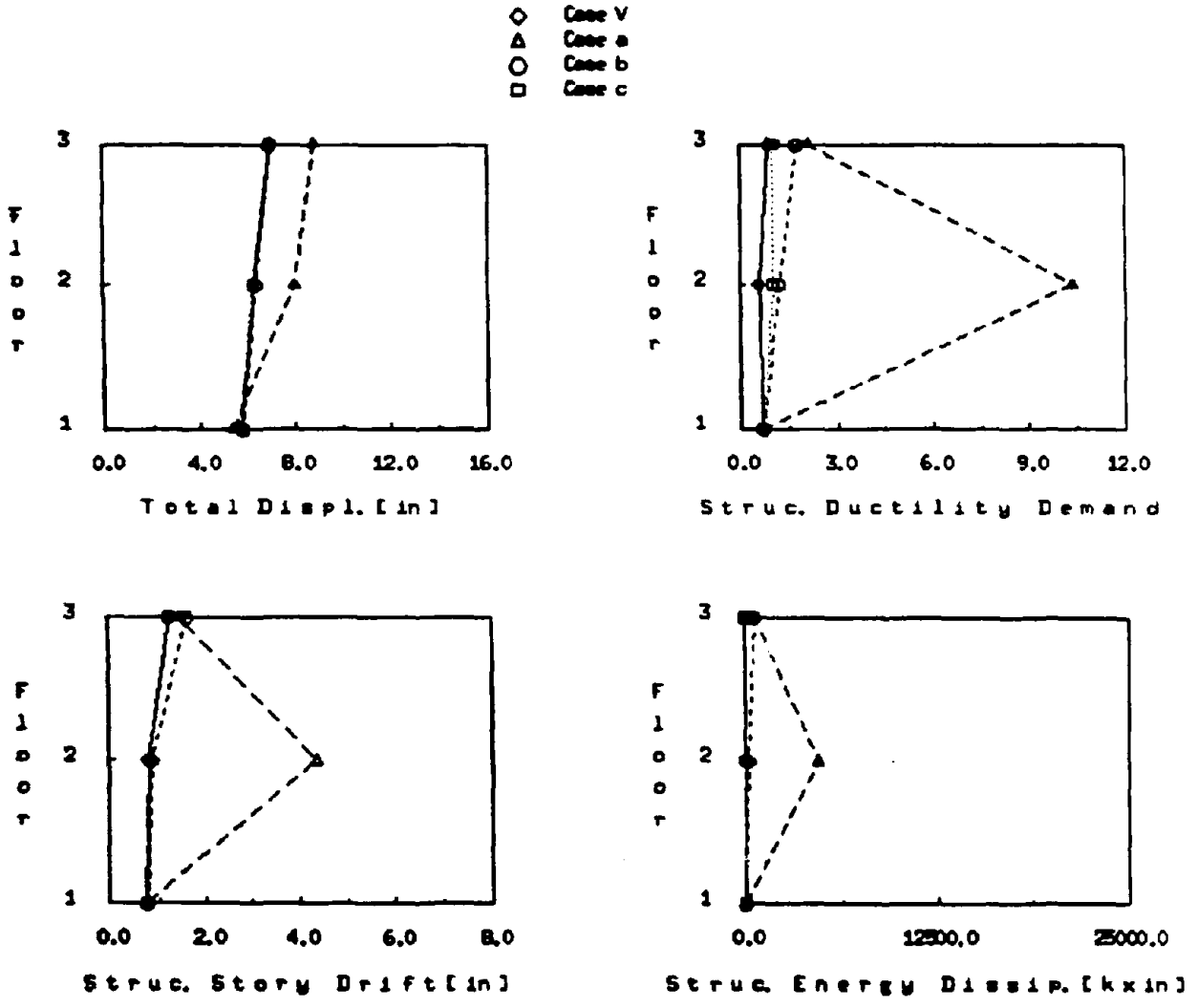

Fig. 7.20 Response Envelopes Case V, Variation of Yielding Strength. El Centro 1940, Pga = 0.87g.

CHAPTER 8

RESPONSE OF ELASTIC SINGLE DEGREE OF FREEDOM SYSTEMS SUPPORTED ON FPS CONNECTIONS

by

Luis Bozzo

and

Stephen Mahin

SECTIONS

CHAPTER 8

SECTION 1 - INTRODUCTION

A systematic study is presented in this Chapter to identify the influence of various structural, connector and earthquake parameters on response. To clearly identify the controlling parameters this study is limited to single degree of freedom elastic structures supported on ideal F.P.S. connectors.

For preliminary design purposes many response parameters, such as total displacements and base shears, can be estimated satisfactorily using single degree of freedom idealizations. Thus, while the result are based on simple structural idealizations, it is expected that many of the results will be applicable to regular multiple degree of freedom systems.

Simulations will be performed for different earthquake ground motions, friction coefficients and connection periods in order to understand the interrelation between the different parameters that influence response. When appropriate, comparisons between the response of elastic structures supported on F.P.S. connections and elastic structures without the F.P.S. connections will be made. An important goal of this report is to test analytically the trends identified in previous Chapters.

Section 2 describes a convenient way to model a single degree of freedom structure supported on F.P.S. connections. In this section an equivalent single degree of freedom nonlinear structure is used to model the system. The equation of motion and the force-displacement relationships for the structure and the connection (See Fig. 1.1) are also studied.

Section 3 derives relations between the response of the equivalent model derived in Section 2 and the response of the actual structure. Expressions are presented for the structural drift, sliding and residual connection displacements, the minimum strength coefficient for the structure to remain elastic, total acceleration, and so on. The expressions are normalized to make the results applicable to as wide a range of structures as possible and to facilitate the construction of nonlinear response spectra.

In Section 4, the response for different parameters, like total displacement, structural displacement, ratio of structural to total displacement, residual displacements, maximum acceleration, minimum strength coefficient for the structure to remain elastic, etc. is presented. Plots containing the individual responses for ten different earthquakes and the mean and coefficient of variation of these responses are presented in this section. Important interrelationships are described and trends are identified.

Finally, in Section 5, conclusions are offered and recommendations for future research are presented.

CHAPTER 8

SECTION 2 - EQUATIONS OF MOTION

2.1 Introduction

In general, a single degree of freedom structure supported on F.P.S. connections should be modeled as a two degree of freedom system, as shown in Fig 2.1. In most cases, however, the mass associated with the connection degree of freedom will be negligible in comparison with the mass of the supported structure. Consequently, it is desirable to eliminate this degree of freedom from the subsequent analytical studies. Formulation of an equivalent single degree of freedom model would result in significant computational savings and allow existing single degree of freedom nonlinear dynamic analysis computer programs to be utilized. Moreover, it would facilitate identification of the interrelationships between design and response parameters and development of preliminary design aids.

There are several difficulties in formulating this simplified model. For example, the damping characteristics for the structure and for the sliding surface are different. Structural damping is most likely to be represented as being viscous and F.P.S. connections exhibit frictional or Coulomb damping.

Before deriving the equations of motion for the equivalent system, it is convenient to initially consider the force-deformation relations and the damping characteristics of each portion of the structure. The form of the simplified equations of motion and their limitations are then examined.

2.2 Idealization of the F.P.S. Connection

The basic response characteristics of an ideal F.P.S. connection have been described in Section 1. Hysteretic characteristics are essentially rigid-plastic with the initial strength governed by the friction coefficient (ν) and the deformation hardening slope governed by the curvature (r) of the sliding surface. In reality, behavior will be somewhat different. For example, while the F.P.S. connection will begin sliding when the applied shear force equals the static frictional resistance, once sliding commences the shear transmitted will be a function not only of the curvature of the slider, but of differences in the dynamic and static friction coefficients, variations in sliding velocity, dynamic fluctuations in vertical loads and so on. Fortunately, experimental evidence (1,2) and analytical results (3,4,5) on structures supported on multiple connections indicate that the general shape of the hysteretic loops in actual structures remain essentially rigid-plastic with the slope of the linear deformation hardening still governed by the curvature of the sliding surface.

Consequently, it is possible to consider, at least for the sake of these preliminary analysis, the simple hysteretic idealization shown in Fig. 1.1 where an effective value is used for the friction coefficient.

This resistance of the connection while sliding can be mathematically represented by:

$$V \approx \nu W \frac{\dot{u}_{sl}}{|\dot{u}_{sl}|} + W \frac{u_{sl}}{r} \qquad (2.1)$$

or

$$V \approx \nu W \frac{\dot{u}_{sl}}{|\dot{u}_{sl}|} + k_c u_{sl} \qquad (2.2)$$

where W is the total weight of the structure above the connection and $\dot{u}_{sl}$ is the sliding velocity.

Damping associated with the connection is primarily related to friction or Coulomb forces. The area within the hysteretic loops (Fig. 1.1) represents the energy being dissipated.

2.3 Structural Idealization

As indicated in Section 1, only a simple single degree of freedom system will be considered herein. Moreover, the structure will be assumed to respond in the elastic range. As such, its resistance can be idealized as:

$$V = k\ (u - u_{sl}) \qquad (2.3)$$

in which k is the elastic lateral stiffness of the idealized structure.

Damping in structures is often characterized as being viscous; i.e., proportional to velocity. Due to the high elastic stiffness of the structure compared with the deformation stiffness of the connection, and small mass of the connection degree of freedom, mass proportional viscous damping will be assumed in this study. This will substantially simplify subsequent derivations. It should be recognized that by using mass proportional viscous damping, the damping forces are not proportional to the structural velocities but to the combined velocity of the F.P.S. connection and structure.

2.4 Equation of Motion for the Equivalent System

The equation of motion for a single degree of freedom model representing an elastic structure supported on F.P.S. connections may be written as:

$$m\ \ddot{u}(t) + 2m\ w\ \xi\ \dot{u}(t) + V(t) = -m\ \ddot{u}_g(t) \qquad (2.4)$$

or by dividing through by m,

$$\ddot{u}(t) + 2w\ \xi\ \dot{u}(t) + \frac{V(t)}{m} = -\ddot{u}_g(t) \qquad (2.5)$$

where

V(t): Equivalent resisting force.

ξ : Equivalent viscous damping ratio ($c = 2\ \xi\ w\ m$)

For equilibrium it is required that the shear force between the F.P.S. connection and the structure be the same. Thus, their flexibilities can be combined in the model considering them as an equivalent serial spring (Fig. 2.2). The stiffnesses for this equivalent system are k for the initial branch and k_s for the sliding branch. Considering the F.P.S. connection to be rigid unless it is sliding, the initial stiffness for the equivalent system equals the lateral stiffness of the structure. For the

sliding system, the tangent stiffness of the sliding branch can be established using the serial spring analogy as:

$$k_e = \frac{k\ k_c}{k + k_c} \tag{2.6}$$

An equivalent period (T_e) for the combined system while the F.P.S. connectors are sliding can be simply derived to be:

$$T_e = 2\pi\sqrt{\frac{m}{k_e}} \tag{2.7}$$

and it can observed that this equivalent period is a function of the period of the structure as well as that of the connection (See Figs. 2.3 to 2.4).

An equivalent deformation hardening ratio (s) can be defined as $\frac{k_e}{k}$, or

$$s = \frac{k_c}{k + k_c} \tag{2.8}$$

or

$$s = \frac{1}{1 + (\frac{T_c}{T})^2} \tag{2.9}$$

The equivalent deformation hardening ratio is a function only of the ratio between the structural stiffness and the sliding stiffness of the connection. Generally, the ratio Tc/T would be expected to vary between 1.5 and 30. Therefore, the equivalent deformation hardening ratios generally vary from 0.0 to 0.3.

Figure 2.5 presents this equivalent deformation hardening ratio as a function of the stiffness of the connection and the stiffness of the structure. Similarly, Fig. 2.6 plots s as a function of the period of the connection and the period of the structure. Usually, the stiffness of the structure is much bigger than the sliding stiffness of the connection. In this case the equivalent stiffness of the sliding branch is nearly equal to the sliding stiffness of the connector. Consequently,

$$s \approx \frac{k_c}{k} \tag{2.10}$$

However, the exact expression will be used herein.

The value of V(t) in Eq. (2.5) can be computed based on these stiffness values and the physics of the F.P.S. connection. The resulting hysteretic loops are shown in Fig. 2.2.

A particularly interesting form of the equation of motion is when the friction coefficient is very small and it can be neglected. In this case, hysteretic energy dissipation is not present so that damping in the equivalent system is due just to the viscous structural damping. Moreover, in this case the lateral stiffness corresponds to the sliding branch of the combined system. The equation of motion for this extreme case becomes:

$$\ddot{u}(t) + 2w\xi\dot{u}(t) + \frac{k_e}{m}u(t) = -\ddot{u}_g(t) \tag{2.11}$$

An equivalent natural frequency (w_e) and a fictitious equivalent damping ξ^* can be defined for this system as follows :

$$w^2_e = \frac{k_e}{m} \approx \frac{k_c}{m} \tag{2.12}$$

and

$$\xi^* = \frac{w}{w_e}\,\xi \approx \frac{T_c}{T}\,\xi \tag{2.13}$$

Finally, it can be established that:

$$\ddot{u}(t) + 2\,w_e\,\xi^*\,\dot{u}(t) + w^2_e\,u(t) = -\ddot{u}_g(t) \tag{2.14}$$

From this expression it can be observed that, when the friction coefficient can be neglected, the structure tends to behave as an elastic structure with period equal to the period of the connection and with an equivalent damping coefficient which is inversely proportional to the period of the structure. Therefore, the F.P.S. connection tends to shift the period of the structural system to that of the connection far from the usual resonance range of most earthquakes. Moreover, for stiff structures, where $T << T_c$ the equivalent system behaves as a highly damped system.

2.5 Summary

It has been possible to represent a simple single degree of freedom elastic system supported on F.P.S. connections as an equivalent single degree of freedom system. It is important to observe that this equivalent system behaves as a well-defined bilinear elasto-plastic hysteretic system resembling an inelastic structure with yielding and deformation hardening. Thus, conventional nonlinear analysis programs may be used to simulate the seismic response of the combined system.

The equivalent system possesses full hysteretic loops, which should be effective in dissipating seismic input energy. Thus, it is expected that input energy will be dissipated mainly in the connection, and not in the structure. Since the supported structure remains elastic in this model, special procedures will have to be formulated to interpret the apparent inelastic deformation (ductility) demands computed for the equivalent system.

CHAPTER 8

SECTION 3 - RESPONSE CHARACTERIZATION

3.1 Introduction

As indicated in Section 2, a single degree of freedom elastic structure supported on F.P.S. connections can be modeled as an equivalent single degree of freedom inelastic system with equivalent stiffness and damping characteristics. The displacement computed for this equivalent system, however, corresponds to the total relative displacement of the structure, i.e, the structural plus sliding displacement. Apparent yielding of this system related to sliding of F.P.S. connections and not to structural ductility demands.

Usually, we are interested not only in the total displacement, but in the displacement and shear forces in the structure and the intensity of sliding in the F.P.S connection. Therefore, it would be desirable to develop direct relations between the equivalent system response and those of the actual structural system and F.P.S. connection.

In this section, some of the parameters that characterize these response will be discussed. Before doing this, the equation of motion will be normalized to facilitate interpretation and presentation of the analytical results. Procedures for computing various structural response quantities (e.g., drift, shear and acceleration) and F.P.S connection response values (sliding displacement) will then be derived.

3.2 Normalized Equation of Motion

There are many differents ways to normalize the equation of motion for single degree of freedom systems (6). However, a particularly convenient way for the purpose of this study is to normalize displacements with respect to the maximum ground acceleration. To do this, a new normalized response parameter $\lambda(t)$ is introduced:

$$\lambda(t) = \frac{u(t)}{\ddot{u}_{g_{max}}} \tag{3.1}$$

Thus, by dividing both sides of Eq. (2.5) by $\ddot{u}_{g_{max}}$ one obtains:

$$\ddot{\lambda}(t) + 2\omega\xi\dot{\lambda}(t) + \frac{V(t)}{m\ddot{u}_{g_{max}}} = \frac{\ddot{u}_g(t)}{\ddot{u}_{g_{max}}} \tag{3.2}$$

This equation can be further simplified by introducing another new parameter relating the characteristic intensity of the ground motion to the characteristic strength of the structure. This, sliding strength coefficient (η_{sl}) can be written as:

$$\eta_{sl} = \frac{V_{sl}}{m\ddot{u}_{g_{max}}} \tag{3.3}$$

where V_{sl} is the initial sliding force for the equivalent system($V_{sl} = \nu W$). Therefore, one can also write:

$$\eta_{sl} = \frac{\nu}{\frac{\ddot{u}_{g_{max}}}{g}} \tag{3.4}$$

The hysteretic loops can be normalized (Fig. 3.1) as:

$$\rho(t) = \frac{V(t)}{V_{st}} \tag{3.5}$$

or similarly

$$\rho(t) = \frac{V(t)}{\eta_{st} m \ddot{u}_{g_{max}}} \tag{3.6}$$

From these expressions a normalized equation of motion can be written:

$$\ddot{\lambda}(t) + 2 w \xi \dot{\lambda}(t) + \eta_{st} \rho(t) = \frac{\ddot{u}_g(t)}{\ddot{u}_{g_{max}}} \tag{3.7}$$

Therefore, any system with the same structural period, damping coefficient, strength coefficient, and hysteretic loop shape subjected to the same earthquake record, will have the same normalized response so long as the sliding strength coefficient is the same. The influence of the connection period, T_c , on the response is accounted for in the sliding slope of the normalized hysteretic loops. To maintain the same hysteretic loop shape the value of $\frac{T_c}{T}$ must be kept constant in any comparison.

Normalizing the equation of motion in this way permits one to plot the response for many different systems in a efficient way. In general, normalized charts can be prepared for a variety of normalized response quantities. For example, plots of maximum normalized structural displacements (λ_{st}), normalized structural shears (η_{st}) and accelerations ($\ddot{\lambda}$) can be easily generated for any structure with a given period of the connection, damping coefficient and sliding strength coefficient subjected to a particular ground motion.

Examples of such normalized response spectra plots are shown in Figs. 3.4 and 3.5. Before looking at these plots in detail consider first, for example, the response of a structure such as that of Fig. 3.2 supported on F.P.S. connections with a period of 3 seconds and a friction coefficient equal to 0.04. The equivalent damping coefficient is 0.05 and the structural period is taken to be 0.5 sec. This system will be excited by the NS component of the 1940 El Centro earthquake scaled to 0.4 g.

The displacement and accelerations time histories and the hysteretic loop for this structure subjected to this particular earthquake are showed in Fig. 3.3. This shows a predominant displacement oscillation at about 0.5 sec with intermittent large displacement cycles with much longer apparent periods. The accelerations in the structure are effectively limited by sliding of the F.P.S. connectors. The hysteretic loops are bilinear and indicate substantial numbers and magnitudes of sliding excursions.

The normalized equations can be used to assess peak response values for other structures as well. To do this the sliding strength coefficient for this system must be first computed:

$$\eta_{st} = \frac{\nu}{\frac{\ddot{u}_{g_{max}}}{g}} = \frac{0.04}{0.4} = 0.1$$

Using the normalized plots of Figs 3.4 and 3.5, prepared for ranges of T between 0.1 and 2 sec., sliding strength coefficients ranging from 0.1 to 0.3 and damping of 0.05 of critical, it can directly be establish that the maximum total displacement and acceleration for the mass of the example structure is:

$$u_{max} = \lambda_{max} \ddot{u}_{g_{max}} = 0.018 * 392.4$$

$$u_{max} = 7\ cms.$$

This is in agreement with Fig. 3.3. Furthermore, Fig. 3.5 can be used to estimate maximum acceleration:

$$\ddot{u}_{max} = \lambda_{max}\ \ddot{u}_g max = 0.23 * 394.4 cm/sec/sec$$

$$\ddot{u}_{max} = 90\ cm/sec/sec$$

which is again in agreement with the results in Fig. 3.3.

It must be observed that the maximum total displacement for a similar elastic structure but without the F.P.S. connections will be similar. However, the maximum total accelerations sustained will be increased 11 times.

If the friction coefficient and the maximum ground acceleration are both increased by a factor of two so that the sliding strength coefficient (η_{sl}) remains constant, the normalized response values originally obtained would still remain the same. However, the actual total displacement and acceleration of the mass will be twice the original ones.

3.3 Shear Force and Structural Displacement

The maximum structural displacement and shear force can be obtained considering that the force on the structure, the force on the connection and also the force on the equivalent system are the same. Moreover, for the maximum response it can be established:

$$u_{max} = u_{st_{max}} + u_{sl} \tag{3.8}$$

So long as the structure remains elastic the maximum structural displacement is given by:

$$u_{st_{max}} = \frac{V_{max}}{k} \tag{3.9}$$

where V_{max} is the maximum shear in the structure. The sliding displacement is thus given by:

$$u_{sl} = \frac{V_{max} - \nu W}{\frac{W}{r}} \tag{3.10}$$

Therefore, the maximum total displacement is:

$$u_{max} = \frac{V_{max}}{k} + \frac{r V_{max}}{W} - \nu r \tag{3.11}$$

or similarly

$$V_{max} = kW\frac{u_{max} + \nu r}{W + k\ r} = k\frac{u_{max} + \nu r}{1 + \frac{k\ r}{W}} \tag{3.12}$$

Dividing both sides by the maximum acceleration and taking into account that $r = g(\frac{T_c}{2\pi})^2$ it can be established that:

$$\frac{V_{max}}{\ddot{u}_{g_{max}}} = \frac{[\lambda_{max} + \frac{\nu g}{\ddot{u}_{g_{max}}}\frac{(T_c)^2}{(2\pi)^2}]k}{1 + \frac{kr}{W}} \tag{3.13}$$

or

$$\frac{V_{max}}{\ddot{u}_{g_{max}}} = \frac{[\lambda_{max}+\eta_{st}(\frac{T_c}{2\pi})^2]k}{1+(\frac{T_c}{T})^2} \tag{3.14}$$

Similarly,

$$\frac{V_{max}}{\ddot{u}_{g_{max}}} = \frac{k\lambda_{max}+\eta_{st}(\frac{T_c}{T})^2 m}{1+(\frac{T_c}{T})^2} \tag{3.15}$$

A convenient form of this expression is:

$$\eta_{st} = \frac{\lambda_{max}(2\pi)^2 + \eta_{st}\ T_c^2}{T^2+T_c^2} \tag{3.16}$$

Where ($\eta_{st} = \frac{V_{max}}{W}$) is the minimum strength coefficient required for the structure to remain elastic.

The importance of this expression is that it directly relates the minimum strength coefficient for the structure to remain elastic with the maximum total displacement for the combined system. This equation will permit some general observations to be developed regarding the behavior of this simple system. For example, Newmark and Hall (8) have noted that, with the exception of short period structures, maximum lateral displacements of elastic and inelastic systems are similar and tend to increase with increasing structural period. If we accept these observations, Eq. 3.16 will indicate that for a system with a given period for the connection, period of the structure and damping coefficient, the minimum strength coefficient required in order to maintain the structure in the elastic range will be reduced if the sliding strength coefficient decreases(or similarly the friction coefficient is reduced). On the other hand, for a system with a given connection period and sliding strength coefficient, if the period of the structure is increased usually the maximum total displacement will increase. In this case, however, the shear force can either increase or decrease. This is because the numerator and denominator of Eq. 3.14 both increase. From Eq. 3.14 the maximum structural displacement can be written by dividing by k as:

$$\lambda_{st_{max}} = \frac{\lambda_{max}+\eta_{st}(\frac{Tc}{2\pi})^2}{1+(\frac{Tc}{T})^2} \tag{3.17}$$

It is interesting to observe that if the friction coefficient is small in this equation, the term $\eta_{st}(\frac{T_c}{2\pi})^2$ can be neglected compared with the normalized maximum total displacement and the maximum structural displacement can be simply written as:

$$\lambda_{st_{max}} = \frac{\lambda_{max}}{1+(\frac{Tc}{T})^2} \tag{3.18}$$

From this expression it can be directly observed that if for a given structure the period of the connection is increased, the structural displacements will be reduced. This is true because λ_{max} does not change too much with T_c and $\frac{Tc}{T}$ is increased.

On the other hand, it must be observed that, the maximum structural displacement is always smaller or at most equal to the maximum total displacement. The latter case tends to occur as the period of the structure is increased.

3.4 Summary

In this section the equations of motion have been normalized with respect to the maximum ground acceleration. This is a convenient way to present and interpret the analytical results. It should be noted that not only accelerations but displacements or forces were normalized using the maximum ground acceleration.

Expressions have also been established that directly relate the maximum total displacement for the equivalent system and the maximum structural displacements for the real structure. These are important relations because permit the interpretation of the structural response through the behavior of the nonlinear equivalent system. Expressions that directly relate the minimum strength coefficient required for the structure to remain elastic and the normalized maximum total displacement have also been derived.

CHAPTER 6

SECTION 4 - ANALYSIS OF THE RESPONSE

4.1 Introduction

In this section the principal response parameters of a single degree of freedom elastic structure supported on F.P.S. connections will be considered. Charts containing normalized maximum total displacements, maximum structural displacements, ratios of structural to total displacements, maximum total accelerations, minimum structural strength coefficients necessary for the structure to remain elastic, and residual displacements will be presented.

These charts will be presented for different periods of the connection and ten different earthquake records. Elastic structures with periods ranging between 0.1 and 2.0 sec were considered. Mass proportional viscous damping equal to 5 % of critical was assumed for all the analysis. Connection periods of 2 and 3 secs were considered. The earthquakes selected for the simulation were: El Centro (1934), El Centro (1940), Helene, Olympia and Taft events. Two horizontal components from each event are used in the analysis. These records were considered as representative of typical moderate earthquakes ground motions on firm soil conditions. Mean values and coefficients of variation for each response parameter are also plotted and evaluated. For comparison purposes, results for similar elastic structures not supported on F.P.S. connectors are plotted were possible on the figures as solid lines .As discussed later, the EW component of the 1940 El Centro record produced anomalous results and was not considered in the statistical evaluation.

4.2 Maximum Total Displacements

The total displacements of the equivalent single degree of freedom system correspond to the structural displacement plus the slidding displacement. They do not include the ground displacement. Plots of maximum displacement normalized by peak ground acceleration are shown in Figs. 4.1 to 4.20 for connection periods of 2 and 3 secs and ten earthquake records. According to Newmark and Hall (8), the total displacement of a nonlinear system, regardless of strength, tends to approximate the elastic relative displacement response of an elastic system provided the period of the structure is relatively long. This tendency is observed in Figs 4.1 to 4.20 for structures with a period greater than about 0.5 secs.

In general, the total displacements are observed to increase with period. If one only considers periods greater than about 0.5 secs, the sliding strength coefficient - at least for the range of values considered in this study - does not influence the total displacements too much either. Thus, for preliminary design purposes it may be possible to estimate conservatively the total displacements of an F.P.S. elastic system with a period greater than about 1/2 seconds from an elastic displacement spectrum.

As was established in Eq. 2.9, there is a direct relation between the period of the connection and the equivalent strain hardening of the system; if the period of the connection is increased the strain hardening is reduced. The results shown in Figs. 4.1 through 4.20 show that the influence of the strain hardening (or the period of the connection) on the total maximum displacement is not too important, at least for the range of values considered.

It can also be observed from Figs. 4.1 to 4.20 that there is a total displacement amplification region corresponding to short period structures. This region varies according to the record, but it corresponds generally to periods less than 0.5 secs. In this region, if the strength coefficient (or the friction coefficient) is decreased, the total displacement is increased. This is consistent with Newmark and Hall's observations which suggest that for elastic-perfectly plastic systems the displacements in this period range increase according to:

$$u = u_y \sqrt{2\mu - 1} \tag{4.1}$$

Where

u : Corresponding displacement of a completely elastic system

u_y : Yielding displacement

μ : Ductility ratio ($\frac{u_{max}}{u_y}$)

The effective yielding displacement for the equivalent system considered here in can be defined as:

$$\frac{u_y}{\ddot{u}_{g_{max}}} = \eta_{st} \left(\frac{T}{2\pi} \right)^2 \tag{4.2}$$

Equation 4.1 is based on equal energy absorption for the elastic and inelastic systems. A similar expression but for a bilinear model with deformation hardening can be obtained as:

$$u = u_y \sqrt{2\mu - 1 + (\mu - 1)^2 s} \tag{4.3}$$

The maximum displacement of the system can be estimated by noting $u_{max} = \mu u_y$. It is convenient to note that if this expression is divided by $\ddot{u}_{g_{max}}$ normalized quantities can be used instead of particular ones.

Consider, for example, a structure with a structural period equal to 0.25 sec supported on F.P.S. connections with a period of 2 sec. and a sliding strength coefficient equal to 0.1. The equivalent strain hardening for this system is, according to Fig. 2.6 or Eq. 2.9 equal to 0.0154. When this structure is subjected to the NS component of the 1940 El Centro earthquake, the normalized maximum elastic displacement can be obtain from Fig. 4.11. It is equal to .003 sec^2. The normalized yielding displacement according to Eq. 4.2 is equal to .000158 sec^2. Therefore, a quadratic expression resalting from Eq. 4.3 can be solved for the normalized ductility ratio. This expression would predict an apparent ductility (μ) equal to $\mu = 102$ Therefore,

$$\frac{u_{max}}{\ddot{u}_{g_{max}}} \approx 102 * .000158 = .016 sec^2$$

From Fig. 4.11 the exact value is 0.015 sec^2. As can be observed, for this case, this expression provides a good estimate; however, the quality of this result varies according to the particular earthquake. Nevertheless, this expression provides a reasonable way to estimate the maximum total displacement for stiff structures.

The mean values of maximum total displacement for the nine records considered are shown in Figs 4.21 and 4.22. The trends observed for mean values are very similar to the responses for individual records. There is an initial amplification region and afterward total displacements increase linearly with structural period. The responses for T_c = 2 sec and 3 sec are, in general, very similar.

The coefficients of variation are always smaller than 0.45. They are nearly the same for T_c =2sec. and 3 sec. (see Figs 4.23 and 4.24).

4.3 Maximum Structural Displacements

From Figs 4.25 to 4.44 can be observed that the maximum computed structural displacement tends to vary like a parabolic function of the period of the structure. In general, its shape is smooth and similar for the different earthquake records considered. For short period structures the maximum structural displacement is very small and always increases with the period of the structure. The maximum structural displacement for a system supported on F.P.S. connections is always smaller than the maximum structural displacement for a similar structure but without the connection. The structural displacements tend to approach the displacement response of an elastic structure at large structural periods.

It is important to note that if the sliding strength coefficient (or the friction coefficient) is reduced the structural displacements are reduced. This is nearly a general observation. However, it is not observed for the EW component for the 1940 El Centro earthquake (Fig. 4.33). For this earthquake the maximum structural displacements tend to be similar for different sliding strength coefficients. Moreover, sometimes they are bigger for the smaller sliding strength coefficient. This anomalous result seems to be caused by the presence of an initial long pulse in the earthquake record. Nonlinear structures in general are particularly sensitive to this type of loading (7).

If the period of the connection is increased (or the equivalent strain hardening is reduced) the structural displacements will be reduced. This means that the flatter the sliding surface the smaller the structural displacements, and the larger the magnitude of sliding.

As long as the structure remains elastic, there is a direct relation between the shear force in the structure and the structural displacements. Therefore, the trends for these two response parameters are related as shown subsequently.

Mean values and coefficients of variation for the maximum structural displacements are plotted in Figs 4.45 and 4.46. They show the same trends noted above for the individual records.

Mean values and coefficients of variation for normalized sliding displacements are also shown in Fig. 4.47 and 4.48. As would be expected from the previous information these values increase initially with period, but remain practically constant for structural periods greater than 0.5 sec. Sliding displacements are inversely proportional to the friction coefficient and slightly proportional to the connection period.

4.4 Ratio of Structural to Total Displacements

The ratio of structural to total displacements indicates how much of the total displacements are sustain by the structure. The smaller the value of this ratio the more effective is the F.P.S. connection in isolating the structure from the earthquake. For structures with a natural period greater than about 0.5 seconds this ratio also indicates the reduction in response relative to that of an elastic nonisolated structure.

From Figs. 4.49 to 4.68 can be observed that this ratio tends to vary like a increasing linear function of the structural period. This ratio is of course always

equal or smaller than one. If the structure does not slide this ratio is equal to one. It should be noted that for the ground motions considered the total displacement of short period structures is mainly due to the sliding displacement while that of long period structures is mainly due to the structural displacement. Therefore, energy is dissipated most effectively at least for the ground motions considered here by the connection mainly for short period structures.

These charts are plotted for constant strength of the connectors. Thus, one would expect long period structures to require weaker connectors (lower friction coefficients) to develop the same degree of sliding. If the sliding strength coefficient is reduced this ratio of structural to total displacement is reduced and its shape becomes more smooth (Fig. 4.49 to 4.68).

If the period of the connection is increased the ratio is always reduced. This is due to the fact that the total displacements are not considerably influenced in the long period range either by the period of the connection or by the sliding strength coefficient. Thus, by the physics of the connector behavior, the structural displacement must always be reduced, if the period of the connection is increased or the sliding strength coefficient is reduced.

Mean values and coefficients of variation are plotted in Figs. 4.69 to 4.72.

4.5 Residual Displacements

The residual displacement in the F.P.S. connection is an important parameter because it provides information on the offset present after the earthquake. The structure will have zero residual displacement due to its elastic behavior. Figures 4.73 to 4.94 represent the absolute value of this residual displacement for ten different earthquakes.

As expected, the residual displacements vary considerably between records. It should be noted that the sliding strength coefficient - at least for the range of values selected here - does not influence too much the maximum value of residual displacements. Moreover, they are reduced if the period of the connection is reduced.

The coefficient of variation is bigger for residual displacement than for the other response parameters. It is similar for periods of the connection of 2 and 3 secs (see Figs 4.95 to 4.96).

From Figs. 4.77 to 4.80 can be observed that a structure supported on F.P.S. connections with normalized sliding strength coefficients of 0.2 or 0.3 subjected to Helena earthquake will not have residual displacements. This is because the structure slides but after some cycles it stop near the zero offset position and continues to vibrate elastically around the neutral position.

4.6 Maximum Total Acceleration

Total acceleration is an important response quantity as it is an indication of the shear developed in the structure. It also relates to the forces that can be imparted to attached equipment.

As established in Eq. 2.14 when the friction coefficient is sufficiently small to be neglected, a structure supported on F.P.S. connections can be modeled as an elastic structure with modified damping and stiffness coefficients. The structural period is shifted to the period of the connection. The total acceleration response for this

case could then be obtained from an elastic response spectrum for the modified amount of damping, $\xi^* = \frac{T_c}{T}\xi$.

From plots 4.97 to 4.116 it can be observed that the maximum total acceleration tends to be a smooth decreasing function of structural period. For T greater or equal to 0.6 sec the total acceleration is almost constant. For a sliding strength coefficient equal to 0.1 this constant value is close to the maximum total acceleration of an elastic structure with a period equal to the period of the connection.

If the sliding strength coefficient is reduced the maximum total acceleration is always reduced. It is important to observe that if the period of the connection is increased the total maximum acceleration always decreases. It is also important to note that the maximum total acceleration for a structure supported on F.P.S. connections is considerably reduced with respect to the maximum total acceleration for the same structure but without the F.P.S. connections.

It is convenient to observe that if the sliding strength coefficient is increased the variation of acceleration tends to be more jagged. On the other hand, if the sliding strength coefficient is increased the differences in the maximum total acceleration for connections with periods of 2 and 3 sec. are smaller. This is predictable because by increasing η_{st} the system tends to behave as an elastic one, i.e the period of the connection has less influence.

The mean values for connection periods of 2 and 3 sec. can be observed in Figs. 4.117 and 4.118. They have similar trends as for the individual records. The coefficients of variation (Figs. 4.119 and 4.120) is not considerably affected by the sliding strength coefficients and varies from 0.1 to 0.3.

4.7 Structural Strength Coefficient

The structural strength coefficient η_{st} is an important parameter because it directly provides the design forces required for the structure to remain elastic. From Figs. 4.121 to 4.140 can be observed that the structural strength coefficient initially increases with period and afterward is nearly constant with period.

Like trends for maximum total acceleration, increasing the period of the connection always reduces the structural strength coefficient. This means that the flatter the sliding surface, the smaller the design forces in the structure. Moreover, if the sliding strength coefficient (or the friction coefficient) is reduced, η_{st} is also reduced.

Figures 4.141 and 4.142 present the mean structural strength coefficient. These are plotted along with the equivalent 1985 U.B.C. requirements (9). Here,

$$\eta_{st} = \alpha\, Z\, I\, C\, S\, K\, \frac{g}{\ddot{u}_{g_{max}}}$$

where Z = 1 (location # 4), I = 1 (normal occupancy), K = 0.67 (ductile moment resisting frame), S = 1 (soil profile S_1). Furthermore, the factor α = 1.5 is taken as to account for likely overstrength of U.B.C. designed structures and the difference between working stresses and ultimate strengths. The maximum acceleration level select for this comparison was $\ddot{u}_{g_{max}} = 0.4g$. It can be observed that for short period structures the forces develop on a structure supported on F.P.S. connections are smaller than the forces required by the U.B.C. For longer period structures this is not the case. However, it should be recognized that while the forces required by the U.B.C. are based on reduction due to ductility (damage) the forces required herein for the F.P.S. supported structures correspond to no

yielding in the structure. Moreover, structures designed according to the U.B.C. are often substantially stronger than required. Thus, the strength of structures need no necessarily be increased over conventional design values if can be demonstrated that the structure has adequate strength. Even weaker structures may be constructed provided yielding is acceptable in the structure and details to provide the required ductility can be employed.

It is interesting to note that if the sliding strength coefficient is increased the differences between the structural strength coefficient, for connection periods of 2 and 3 secs are smaller. In the other hand, if the connection period is increased, as expected, the coefficient of variation will be reduced (Figs 4.143 and 4.144). This is because in the limiting case of a flat sliding surface the maximum force that can be transmitted is the friction force and therefore the coefficient of variation would be in this case equal to zero. It should also be noted that as far as there is a direct relation between the structural displacement and the shear force the coefficient of variation is the same.

CHAPTER 8

SECTION 5 - SUMMARY AND CONCLUSIONS

Analytical studies for a single degree of freedom elastic structure supported on F.P.S. connections were carried out. Simulation for different earthquake ground motions, friction coefficients and periods of the connection were done in order to understand the interrelation between the different parameters that characterize the response. When appropriate, comparisons between the response of elastic structures supported on F.P.S. connections and elastic structures without the F.P.S. connection were made.

A single degree of freedom elastic structure supported on F.P.S. connections was modeled as an equivalent single degree of freedom nonlinear structure. The fundamental period for this isolated structure while sliding was shown to be similar to be the period of the connection. The equivalent damping coefficient for systems with very low friction coefficients was shown to be directly proportional to the original stiffness of the structure.

The response for this equivalent system was related to the response of the original structure. Expressions were derived that directly relate the structural drift or the minimum strength coefficient for the structure to remain elastic to the maximum total displacement of the equivalent structure.

The total displacements of F.P.S. isolated elastic structures were observed to increase with structural period. Total displacements are very similar to (or slightly smaller than) the displacements for an elastic structure without the connections, except for short period structures. A simple expression that permits evaluation of the expected total displacements in this short period amplification region was also derived. In general, total displacement is not influenced by the friction coefficient or by the period of the connection in the moderate and long period range, whereas both of these parameters are important for short period structures.

The maximum structural displacement for a system supported on F.P.S. connections is always smaller than the maximum structural displacement for a similar structure without the connection. In fact, as the experimental report (1) also showed previously, they tend to be equal as the structural period tends toward the period of the connection. If the friction coefficient is reduced, structural displacements are also generally reduced. Moreover, if the period of the connection is increased, the structural displacements are reduced.

For structures with a period greater than about 0.5 sec. the maximum sliding displacement tends to be constant with the structural period. For periods less than about 0.5 sec, the sliding displacement is observed to usually increase with period. If the friction coefficient is reduced, this sliding displacement is increased. Moreover, in general if the period of the connection is increased, the sliding displacement is increased.

The ratio of structural displacement to total displacement is reduced, if the sliding strength coefficient is reduced. If the period of the connection is increased, this ratio is always reduced. It should be noted that the ratio for elastic structural systems increases with period in the long period range when the strength of the connectors is kept constant. Thus, one would expect long period structures to require weaker connectors (lower friction coefficients) to develop the same degree of sliding.

The residual displacements are, at least for the range of values considered in this study, constant with the friction coefficient. However, in general, they are reduced, if the period of the connection is reduced.

The maximum total acceleration tends to be a smoothly varying function of the structural period, and it always decreases with it. It is almost constant for periods greater than about 0.6 sec. For small friction coefficients, this constant value tends to equal the maximum total acceleration for an elastic structure with a period equal to the period of the connection. If the period of the connection is increased the total maximum acceleration always decreases. Moreover, if the sliding strength coefficient is reduced, the maximum total acceleration is always reduced.

It is important to observe that, if the period of the connection is increased, the minimum structural strength coefficient for the structure in order to remains elastic is always reduced. If the sliding strength coefficient , or the friction coefficient, is reduced this structural strength coefficient is also reduced

It is apparent that there are a variety of interrelationships between response and design parameters. Consequently, single optimal design will not likely be applicable to all situations. For example, if limits on sliding displacements need be imposed, this can be achieved by utilizing lower period connectors or connectors with higher friction coefficients. However, in this case higher shear and accelerations would result. These relations and the consequences of such tradeoffs are clearly shown in this report.

Additional research is needed to extent this work by incorporating more realistic damping models and particularly accounting for the effects of structural yielding. Extensions to multiple degree of freedom systems would be especially useful.

CHAPTER 8

SECTION 6 - REFERENCES

(1) Zayas, Victor., Low, Stanley., and Mahin, Stephen., " The FPS Earthquake Resisting System, Experimental Report " EERC Report 87-01, Earthquake Engineering Research Center, University of California, Berkeley, 1987

(2) Hisano, Masayoshi., Kawamura, Soichi., Kitazawa, Koji., Nagashima, Ichiro., " Study on a Sliding-Type Base Isolation System - Tri-axial Shaking Table Test and its Simulation - " Technology Research Center, Taisei Corporation, Yokohama, Japan

(3) Kawamura, Soichi., Kitazawa, Koji., Hisano, Masayoshi., Nagashima, Ichiro., " Study on a Sliding-Type Base Isolation System - System Composition and Element Properties - " Technology Research Center, Taisei Corporation, Totsuka-ku, Yokohama, Japan

(4) Nagashima, Ichiro., Kawamura, Soichi., Kitazawa, Koji., Hisano, Masayoshi., " Study on a Sliding-Type Base Isolation System - Multi-Dimensional Response Analysis - " Technology Research Center, Taisei Corporation, Totsuka-ku, Yokohama, Japan

(5) Nagashima, S. Kawamura, K. Kitazawa & M. Hisano " Study on a Base Isolation System " Presented at 3rd Conference on Soil Dynamics and Earthquake Engineering 1987.06.22 - 24 at Princeton Univ. U.S.A. Technology Research Center, Taisei Corporation, Japan

(6) Mahin, S., Lin, J., " Construction of Inelastic Response Spectra for Single Degree of Freedom Systems, Computer program and applications " EERC Report 83-17, Earthquake Engineering Research Center, University of California, Berkeley, 1983.

(7) Lin, J., Mahin, S., " Effect of Inelastic Behavior on the Analysis and Design of Earthquake Resistant Structures " EERC Report 85-08, Earthquake Engineering Research Center, University of California, Berkeley, 1985.

(8) Newmark, N., Hall, W., " Earthquake Spectra and Design " EERI, 1982, Engineering Monographs on Earthquake Criteria, Structural Design, and Strong Motion Records., v-3.

(9) U.B.C. Uniform building code, 1985.

CHAPTER 8

SECTION 7 - NOTATION

g : Acceleration of Gravity.

k : Lateral Stiffness of the Structure.

k_c : Stiffness of the Connection (W / r).

k_e : Equivalent Stiffness.

r : Radio of Curvature.

s : Equivalent Deformation Hardening Ratio.

T : Period of the Structure.

T_e : Equivalent Period ($T_e = 2\pi\sqrt{\frac{m}{k_e}}$)

T_c : Period of the Connection ($T_c = 2\pi\sqrt{\frac{r}{g}}$).

$u(t)$: Total Displacement

$\dot{u}(t)$: Total Velocity.

$\ddot{u}(t)$: Total Acceleration.

$u_{sl}(t)$: Sliding Displacement.

$\dot{u}_{sl}(t)$: Sliding Velocity.

$u_{st}(t)$: Structural Displacement.

u_r : Residual Displacement.

$\ddot{u}_g(t)$: Ground Acceleration.

$\ddot{u}_{g_{max}}$: Peak Ground Acceleration.

$V(t)$: Shear force.

V_{sl} : Sliding force (νW).

W : Total Weigth of the Structure.

w : Natural frequency of Vibration (Hz).

w_e : Equivalent Natural frequency of Vibration (Hz).

λ : Normalized Displacement ($\frac{u(t)}{\ddot{u}_{g_{max}}}$).

λ_{st} : Normalized Structural Displacement ($\frac{u_{st}(t)}{\ddot{u}_{g_{max}}}$).

λ_{sl} : Normalized Sliding Displacement ($\frac{u_{sl}(t)}{\ddot{u}_{g_{max}}}$).

λ_r : Normalized Residual Displacement ($\frac{u_r}{\ddot{u}_{g_{max}}}$).

$\ddot{\lambda}$: Normalized Total Acceleration ($\frac{\ddot{u}(t)}{\ddot{u}_{g_{max}}}$).

ν : Friction Coefficient.

ξ : Damping Coefficient.

η_{sl} : Sliding Strength Coefficient ($\eta_{sl} = \frac{\nu}{\frac{\ddot{u}_{g_{max}}}{g}}$).

η_{st} : Structural Strength Coefficient ($\frac{V_{max}}{W}$).

$\rho(t)$: Normalized resisting Force ($\frac{V(t)}{V_{sl}}$)

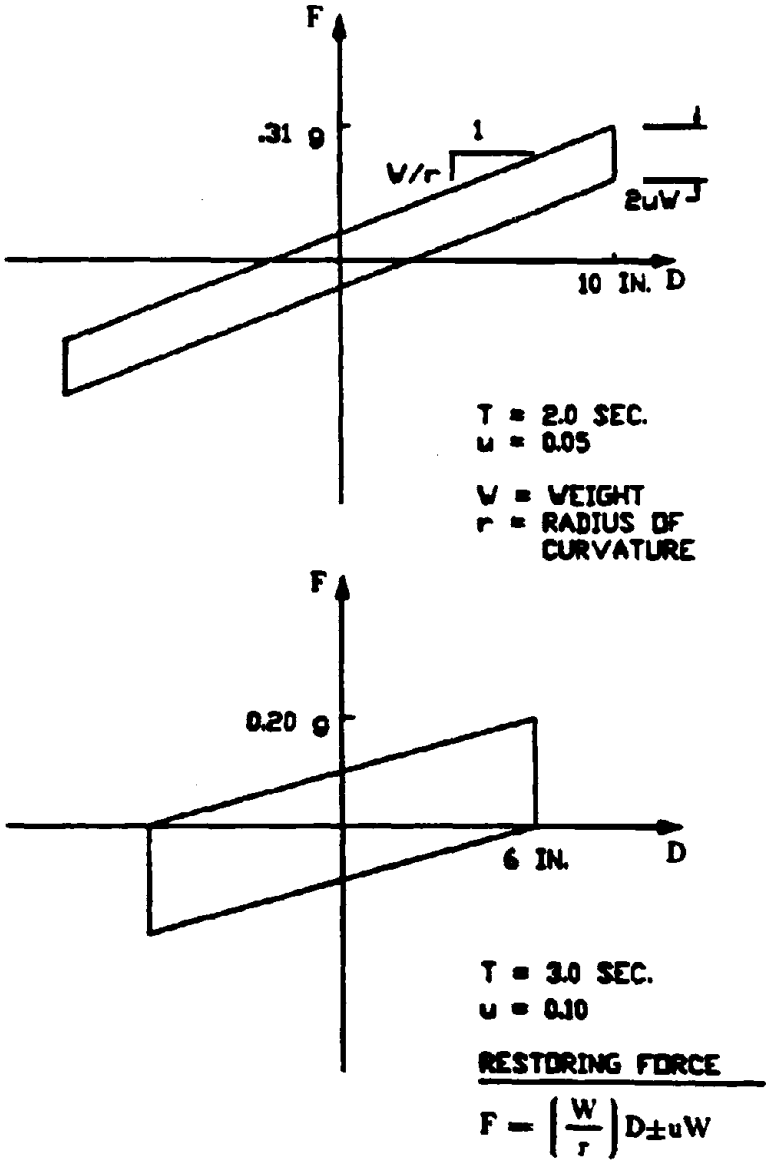

FIG. 1.1 Examples of FPS Hysteretic Loops

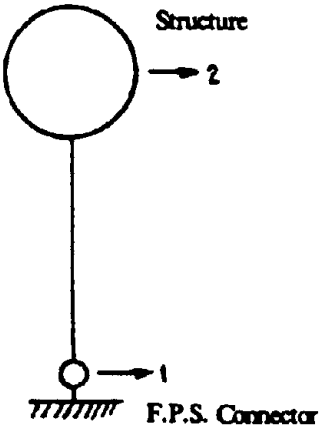

Fig. 2.1 Two degree of freedom model of simple structure supported on F.P.S. connectors.

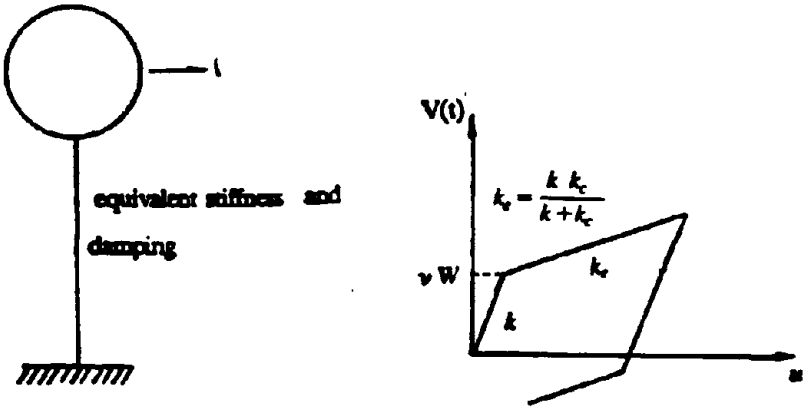

Fig 2.2 Equivalent single degree of freedom system.

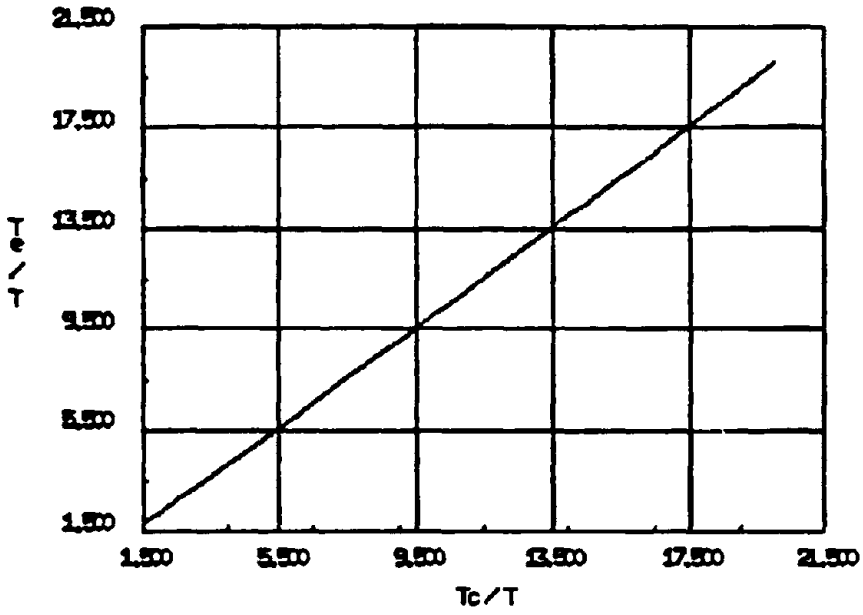

Fig. 2.3 Equivalent period as function of Connection and Structural period.

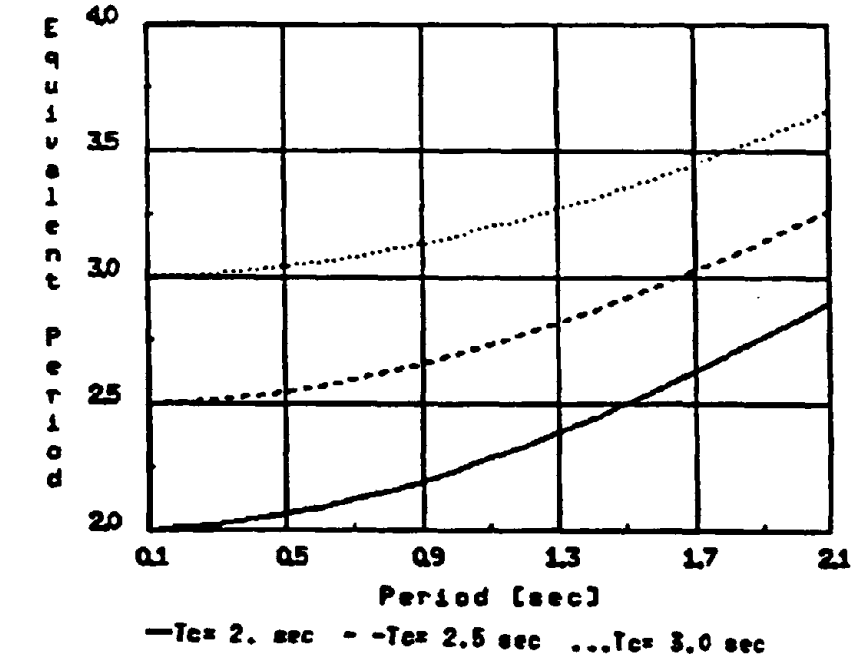

Fig. 2.4 Equivalent period as function of Structural period.

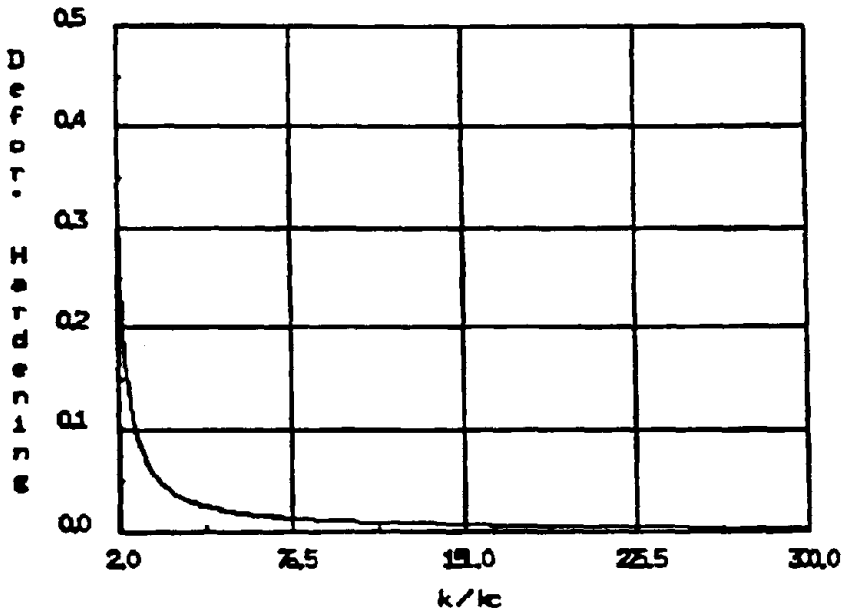

Fig. 2.5 Equivalent Deformation Hardening Ratio as function of k / k_c

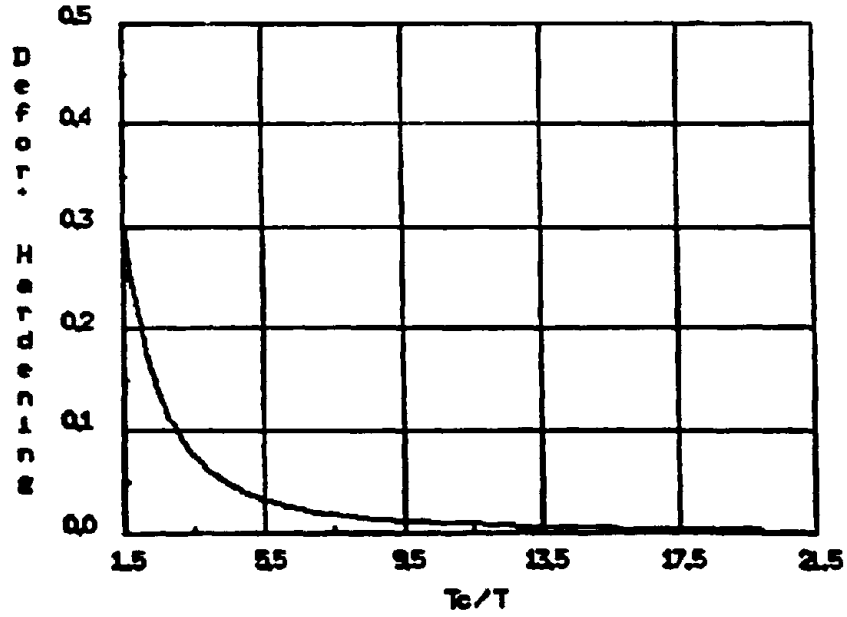

Fig. 2.6 Equivalent Deformation Hardening Ratio as function of T_e / T

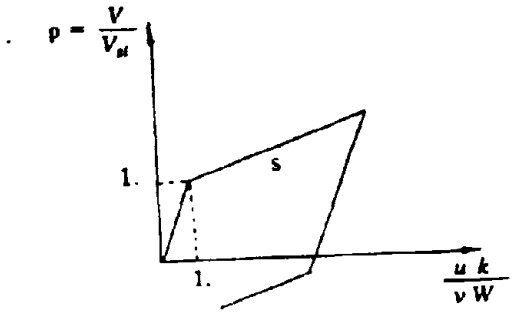

s : Equivalent Deformation Hardening

k : Structural Stiffness

V_{si} : Sliding Force (νW)

Fig. 3.1 Normalized Hysteretic Loop

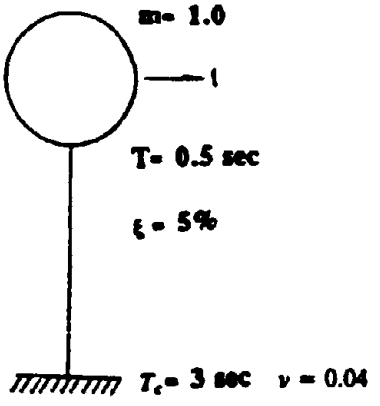

Fig. 3.2 Example Structure.

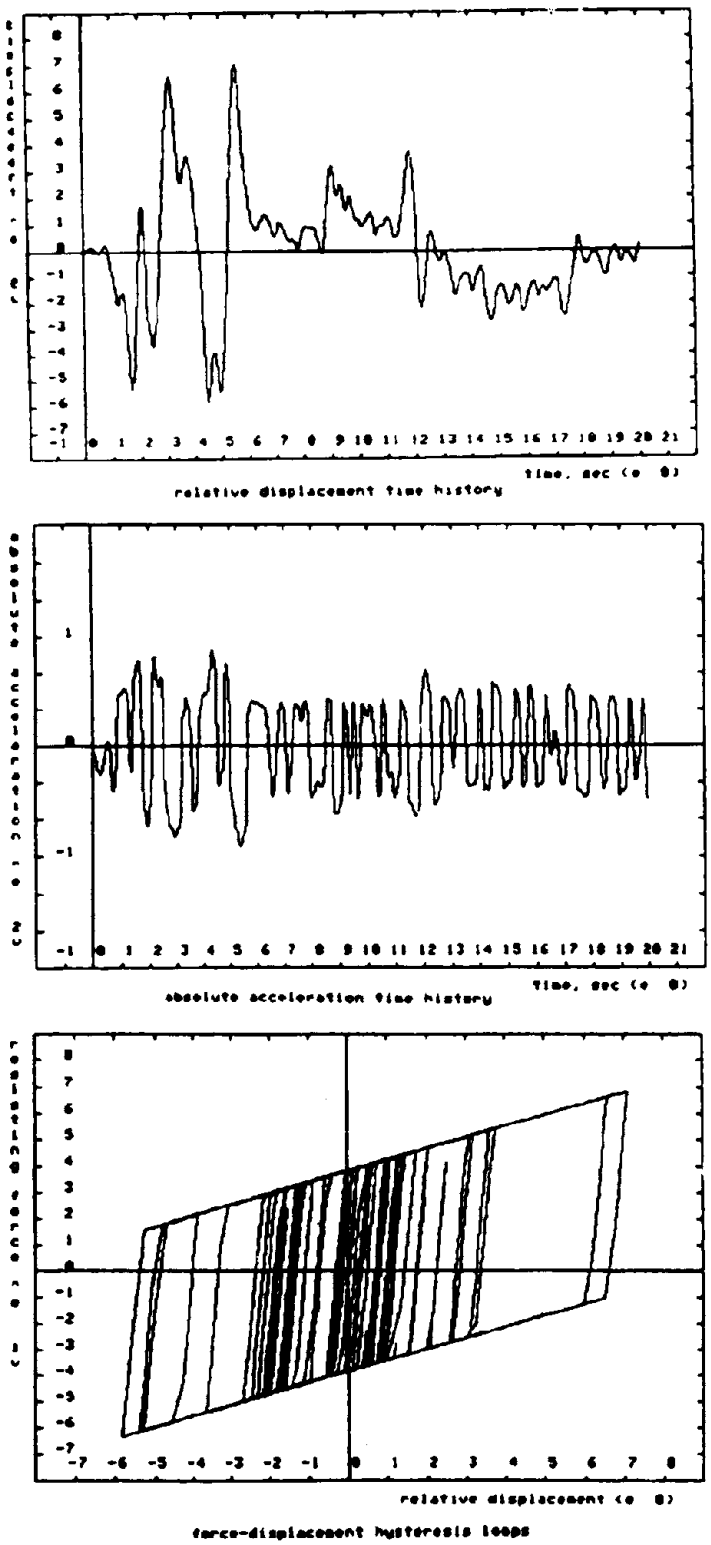

Fig. 3.3 Displacement and Acceleration Time History, and Force Displacement Hysteretic Loop corresponding to example Fig. 3.2. El Centro 1940, NS Comp.

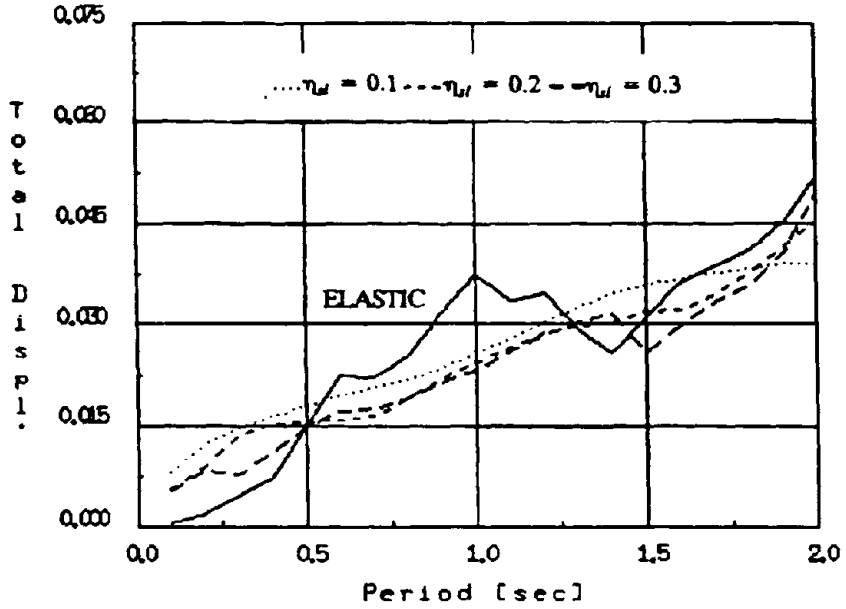

Fig. 3.4 Max. Normalized Displacement [sec^2] for the El Centro(NS) record with ξ=5%

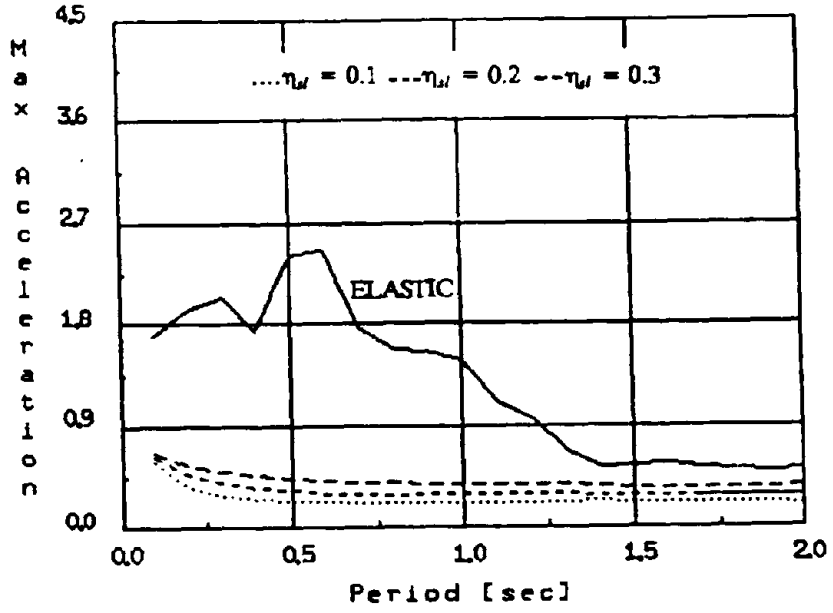

Fig. 3.5 Max. Normalized Acceleration for the El Centro(NS) record with ξ = 5%

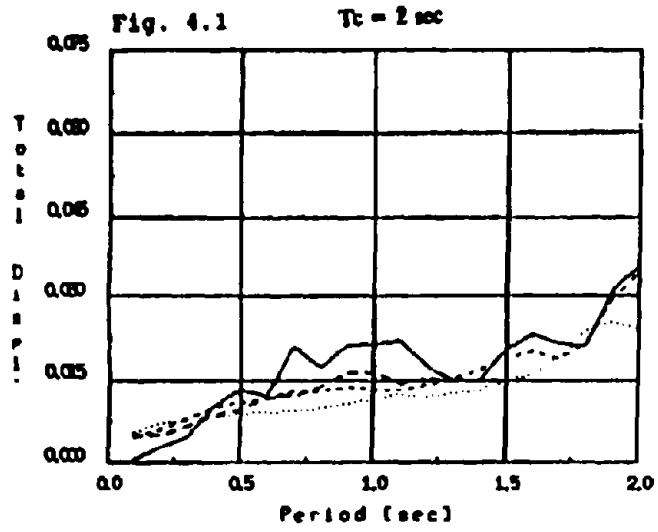

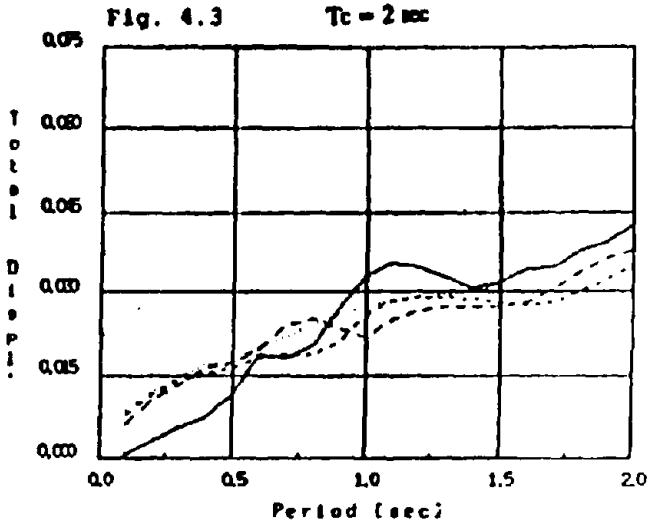

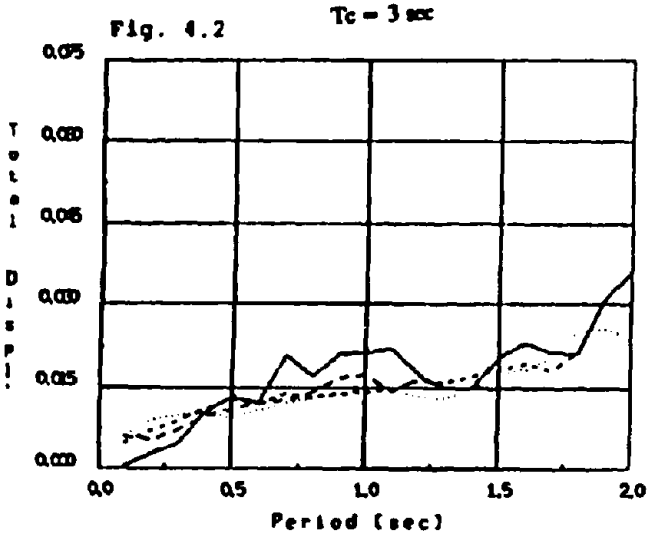

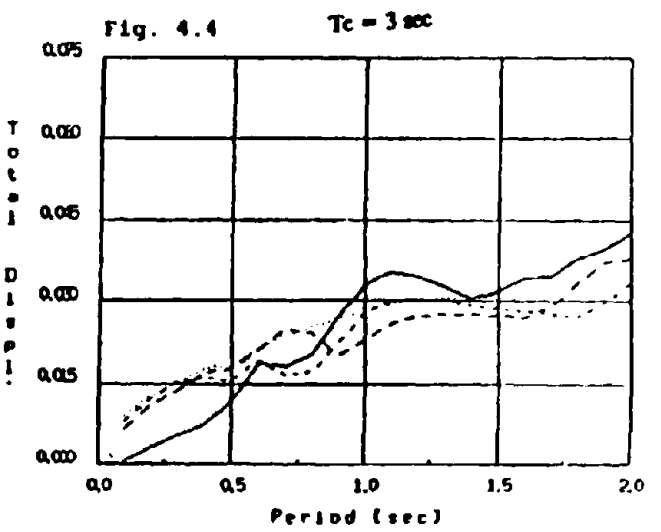

Figs. 4.1 to 4.4 Normalized Max. Total Displacement [sec^2] - El Centro 1934, ξ = 5 % ....η_M = 0.1 ... η_M = 0.2 _ _ η_M = 0.3

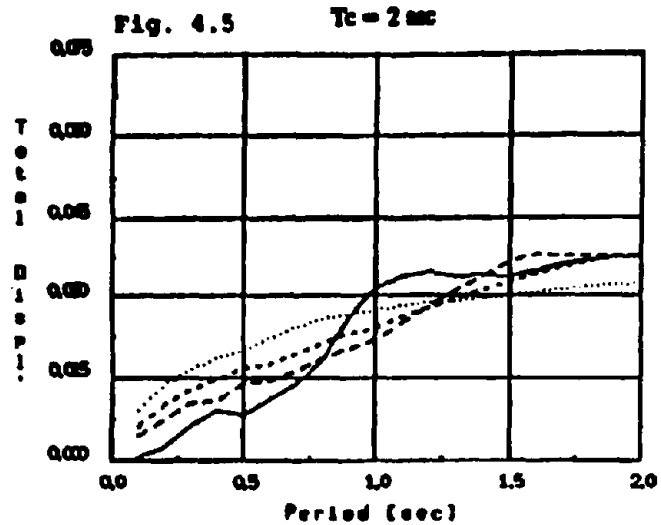

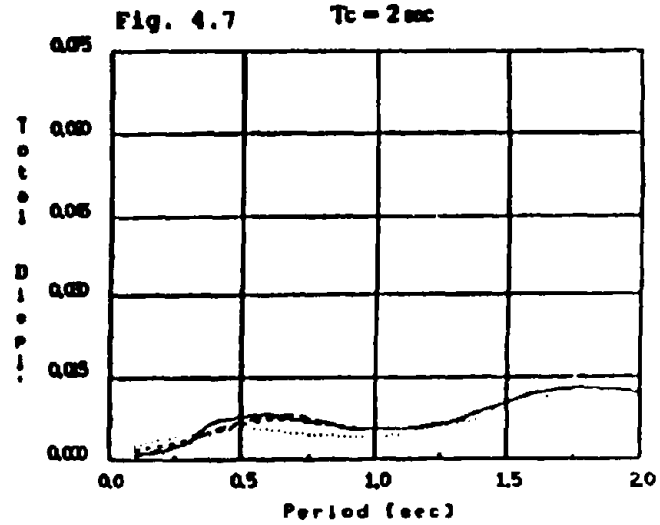

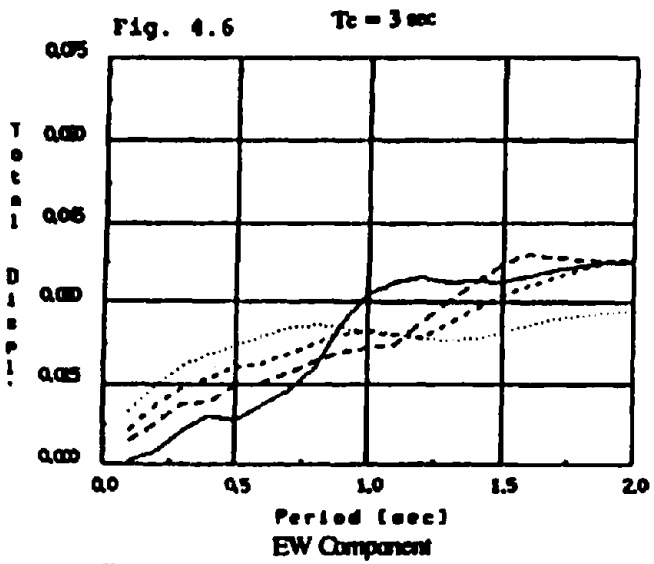

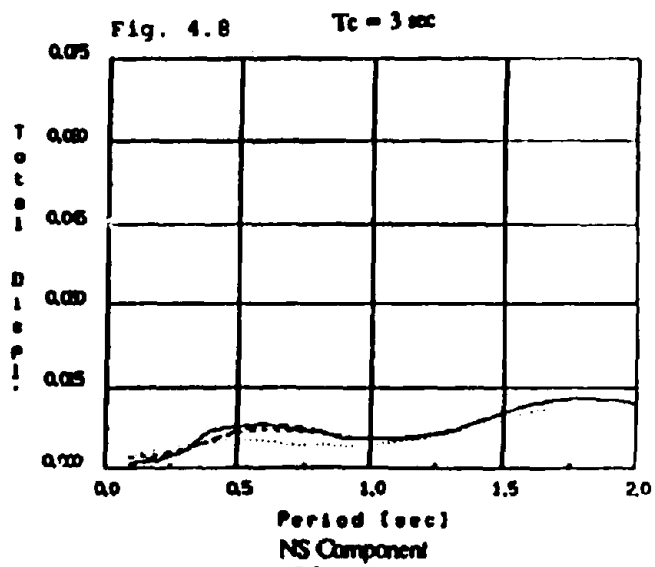

Figs. 4.5 to 4.8 Normalized Max. Total Displacement [sec^2] , Helena 1935, ξ = 5 % ....η_M = 0.1 ... η_M = 0.2 -- η_M = 0.3

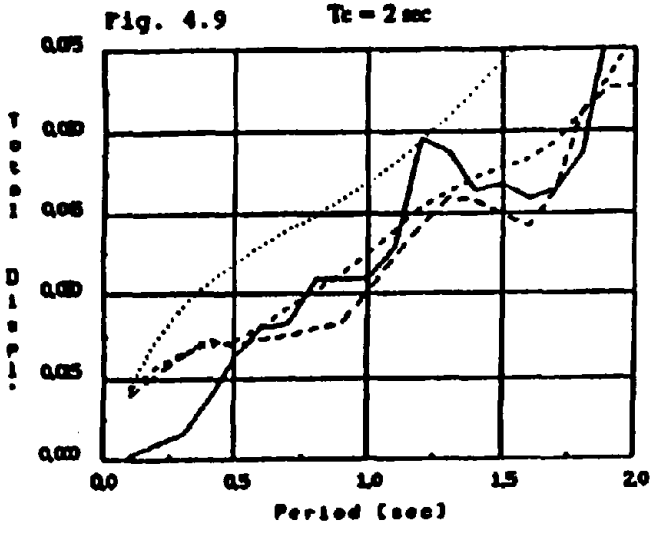

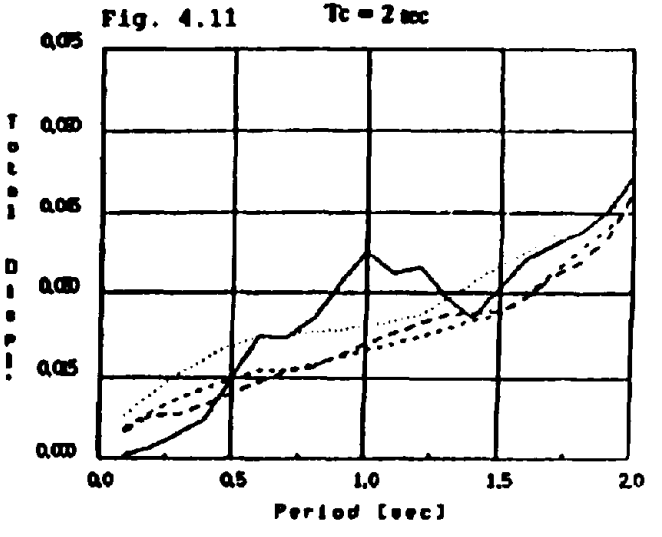

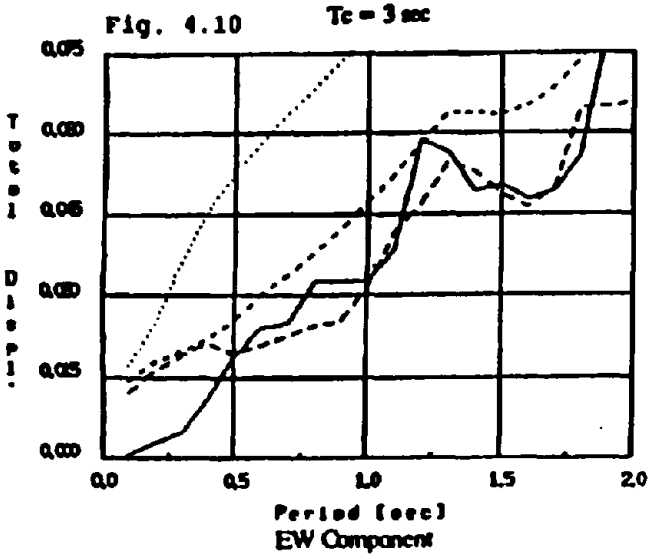

EW Component

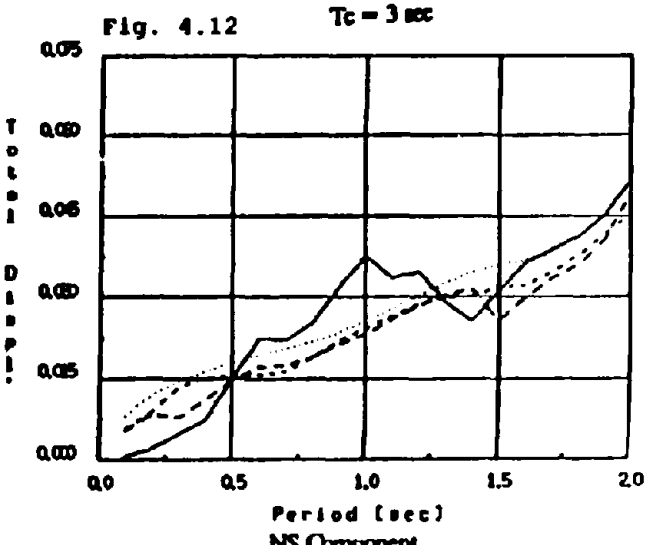

NS Component

Figs. 4.9 to 4.12 Normalized Max. Total Displacement [sec^2] , El Centro 1940, ξ = 5 % ....η_M = 0.1 ... η_M = 0.2 -- η_M = 0.3

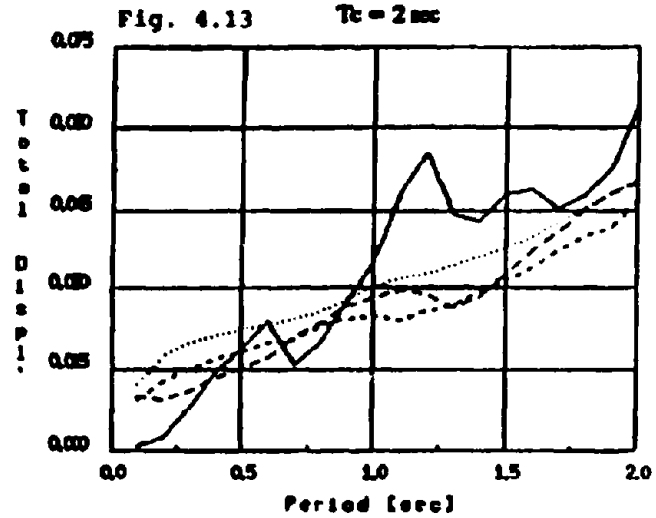

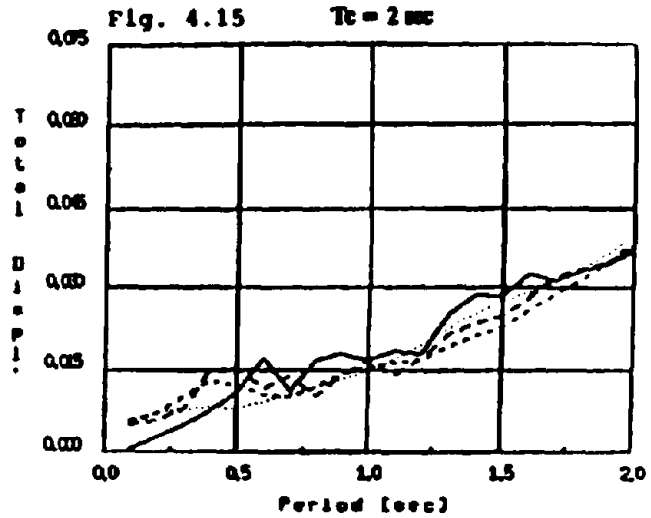

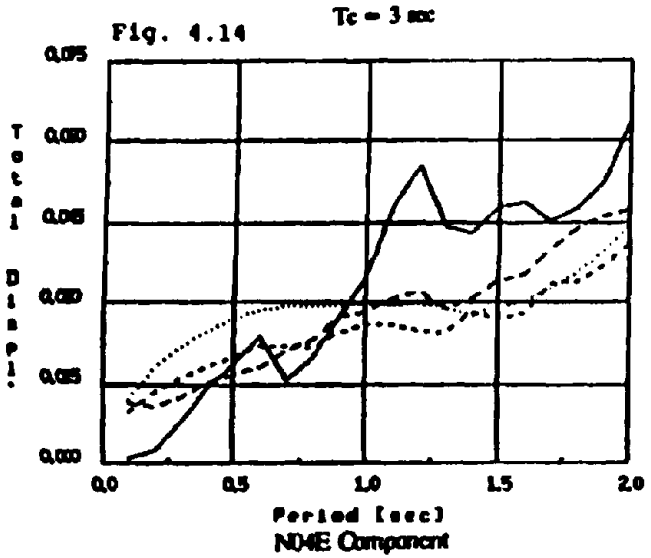

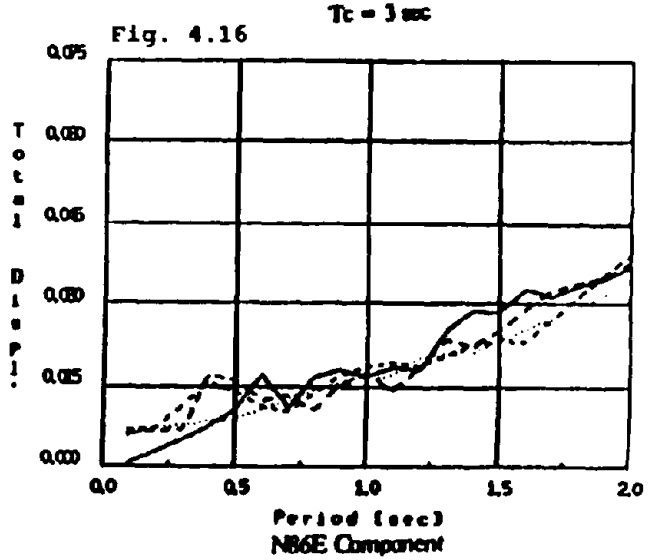

Figs. 4.13 to 4.16 Normalized Max. Total Displacement [sec^2], Olympia 1949, ξ = 5 % ....η_M = 0.1 ---η_M = 0.2 – –η_M = 0.3

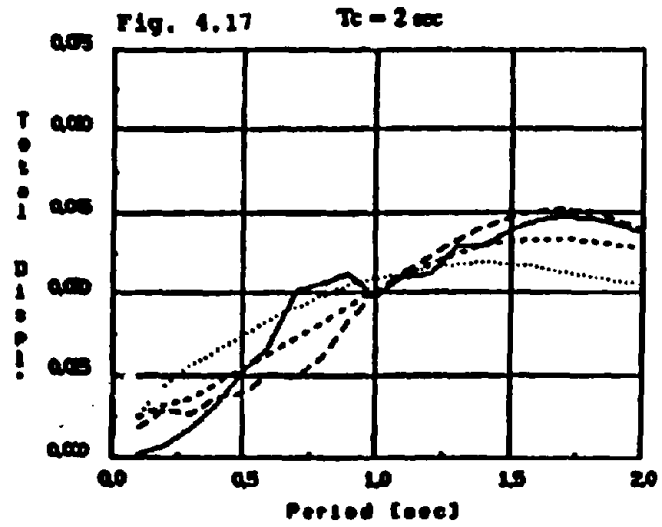

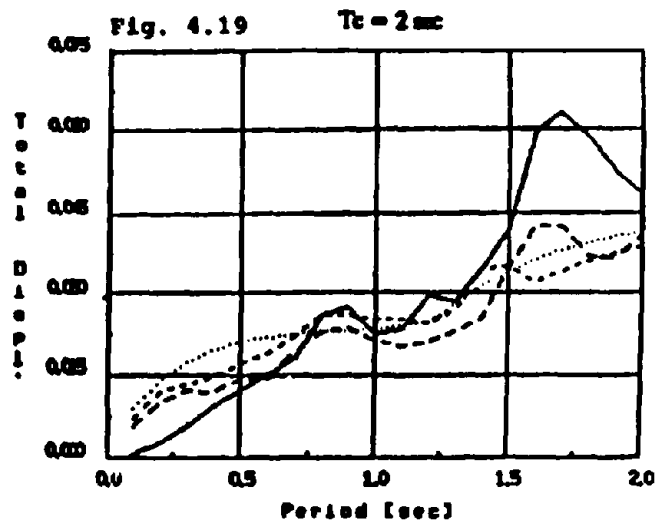

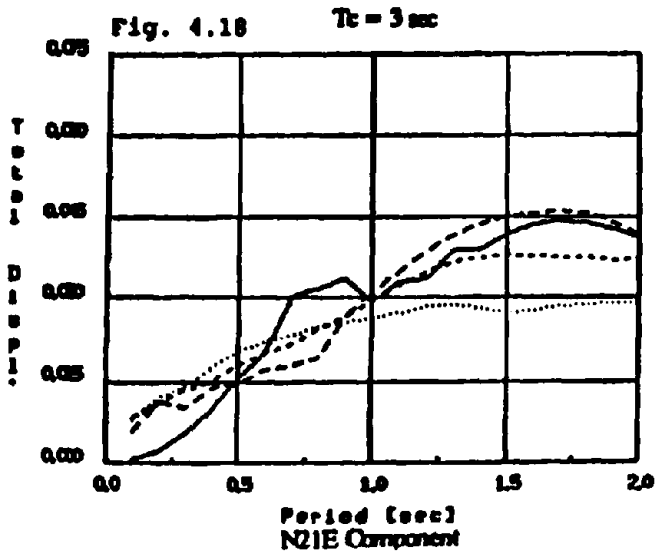

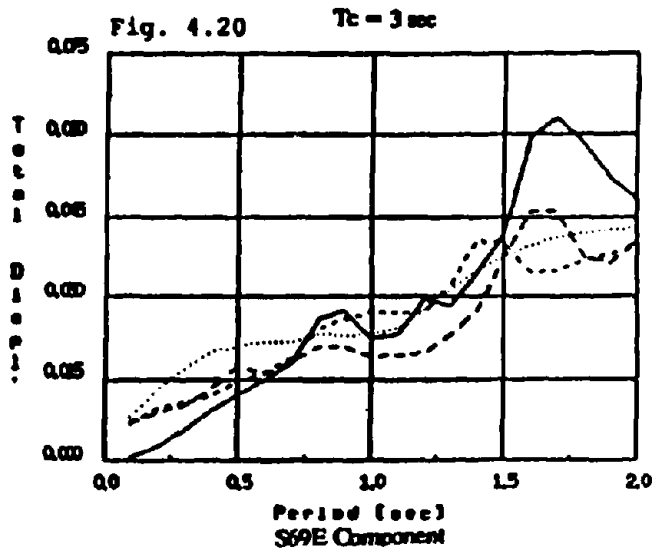

Figs. 4.17 to 4.20 Normalized Max. Total Displacement [sec^2] , Taft 1952, ξ = 5 % ....η_M = 0.1 ---η_M = 0.2 – –η_M = 0.3

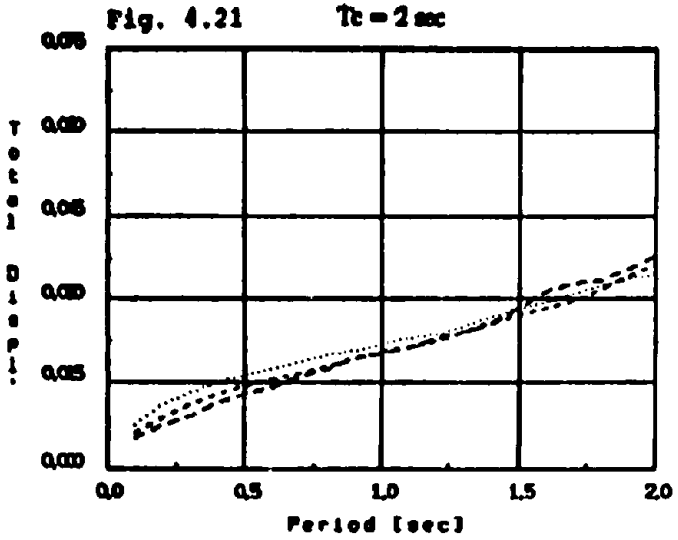

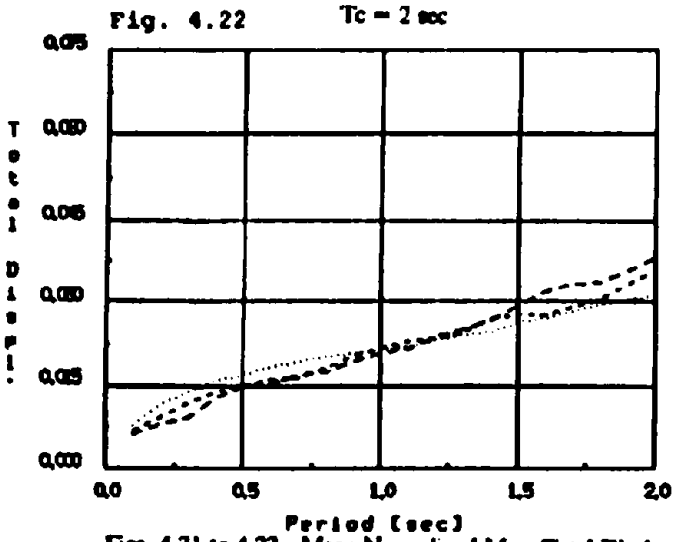

Figs. 4.21 to 4.22 Mean Normalized Max. Total Displacement [sec^2]

$\cdots \eta_{bl} = 0.1 \; \ldots \eta_{bl} = 0.2 \; \_ \_ \; \eta_{bl} = 0.3$

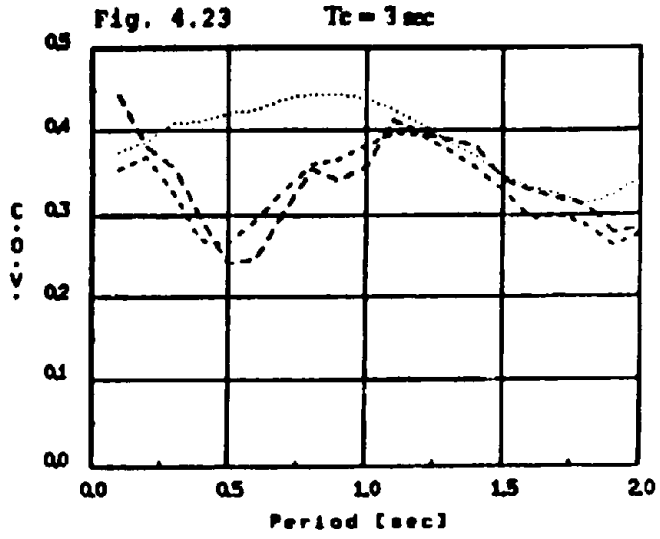

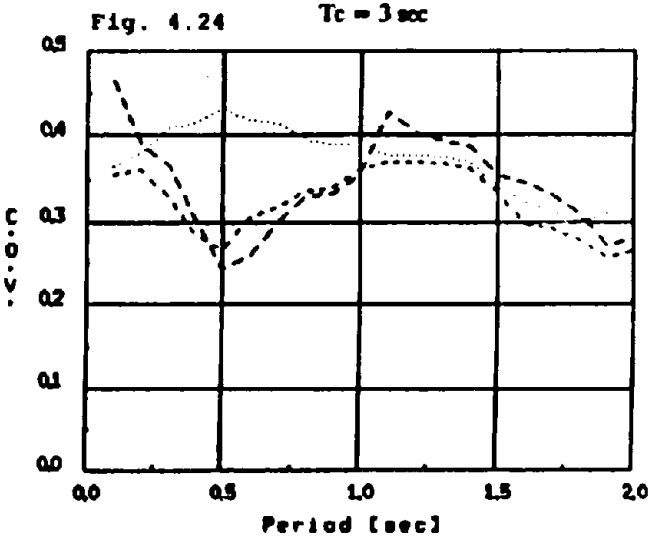

Figs. 4.23 to 4.24 Coefficient of variation

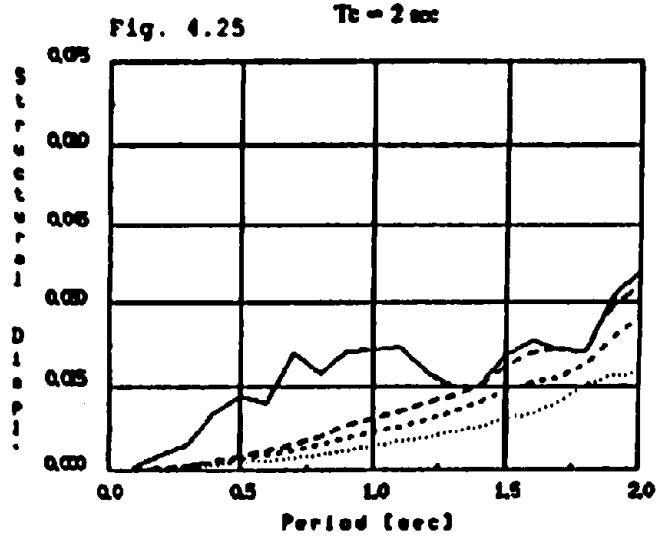

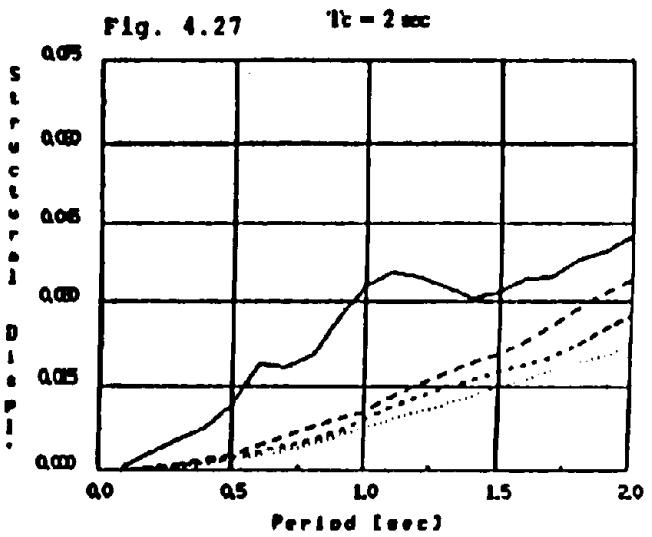

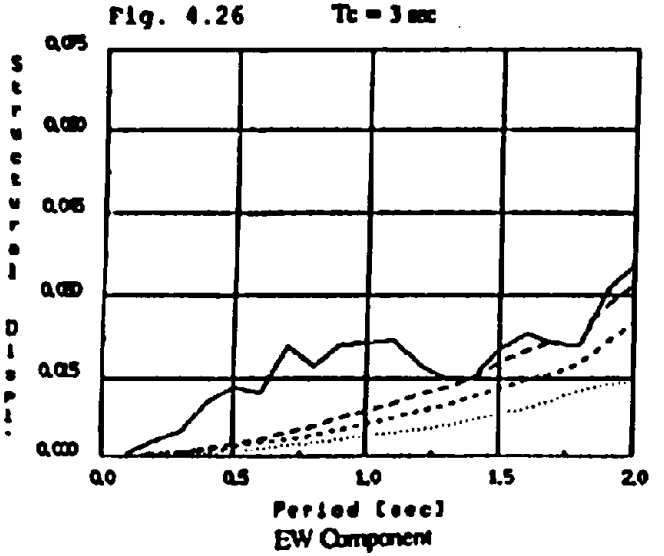

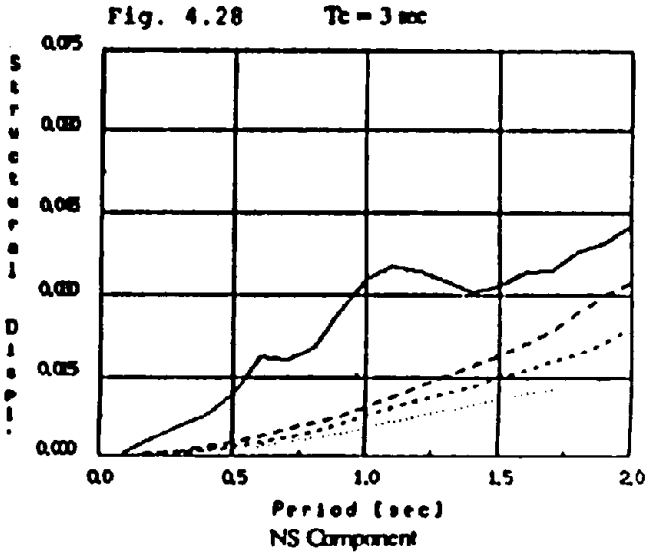

Figs. 4.25 to 4.28 Max. Structural Displacement [sec^2], El Centro 1934, ξ = 5 % ....η_w = 0.1 ... η_w = 0.2 -- η_w = 0.3

Fig. 4.29 Tc = 2 sec

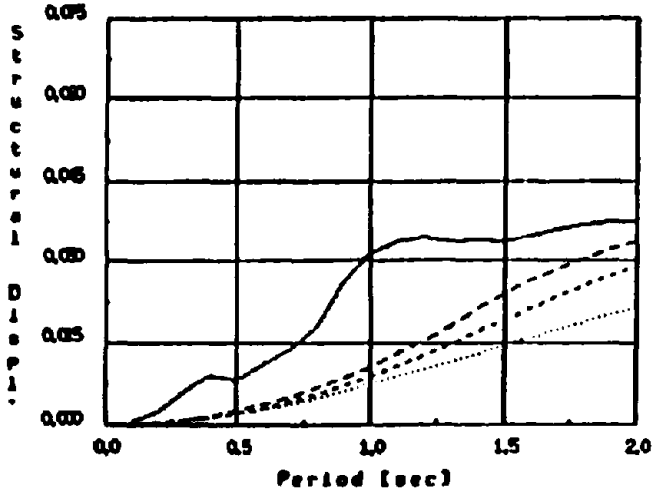

Fig. 4.30 Tc = 3 sec

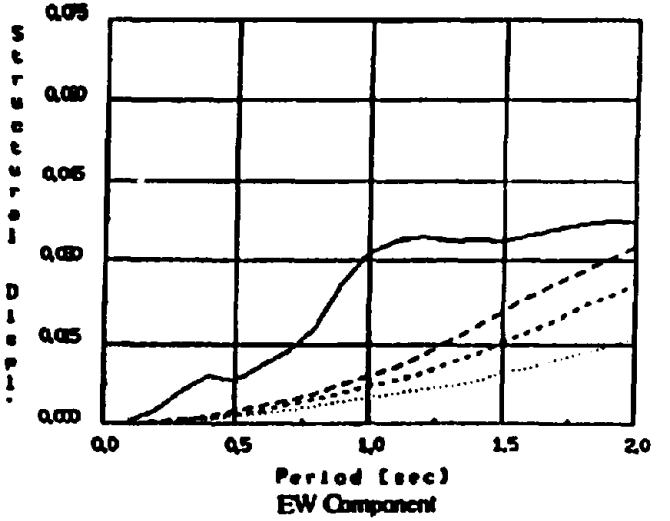

EW Component

Fig. 4.31 Tc = 2 sec

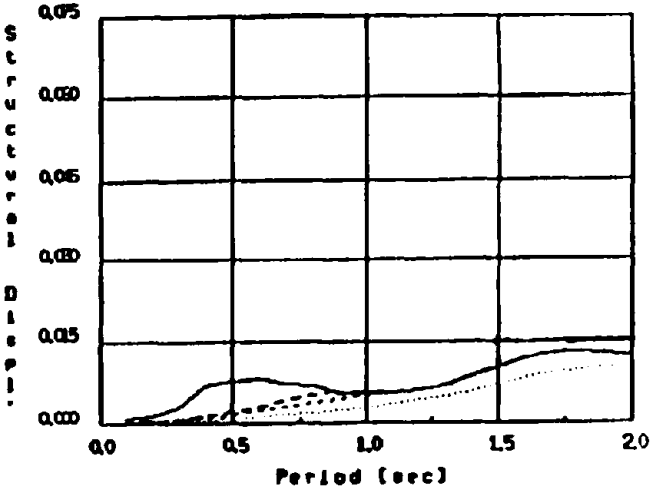

Fig. 4.32 Tc = 3 sec

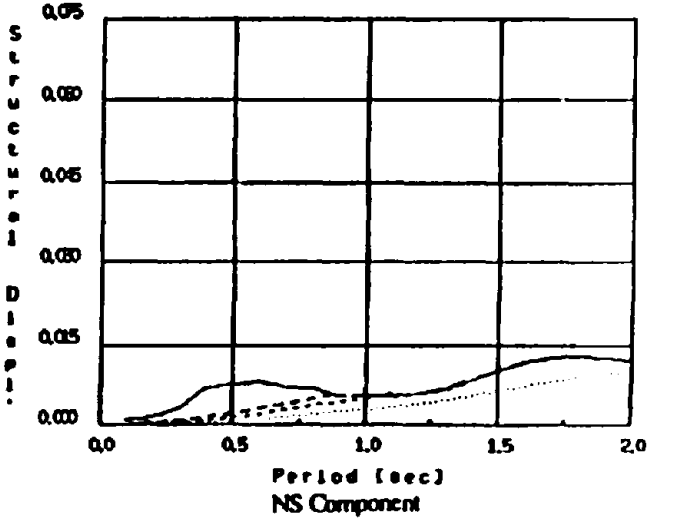

NS Component

Figs. 4.29 to 4.32 Max. Structural Displacement [sec^2], Helena 1935, ξ = 5 % ....η_M = 0.1 ---η_M = 0.2 – –η_M = 0.3

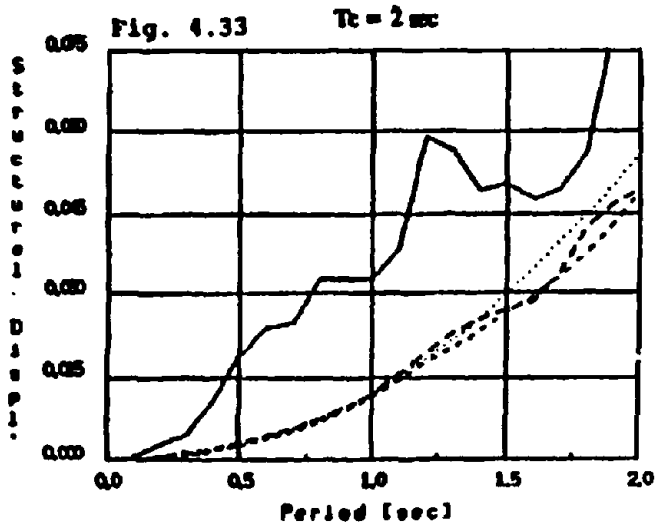

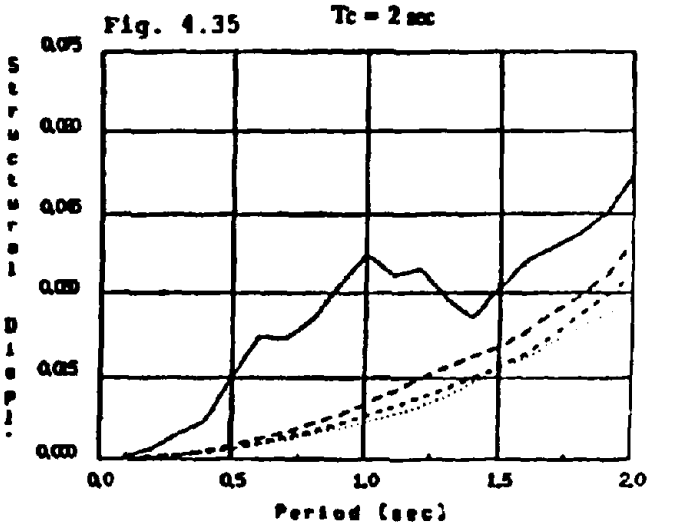

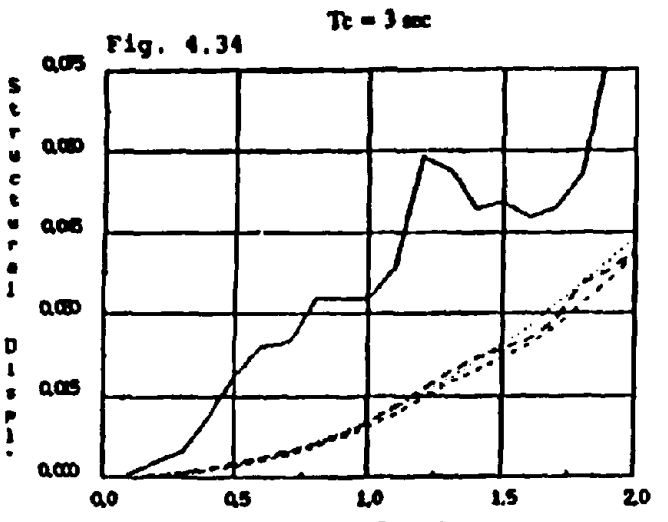

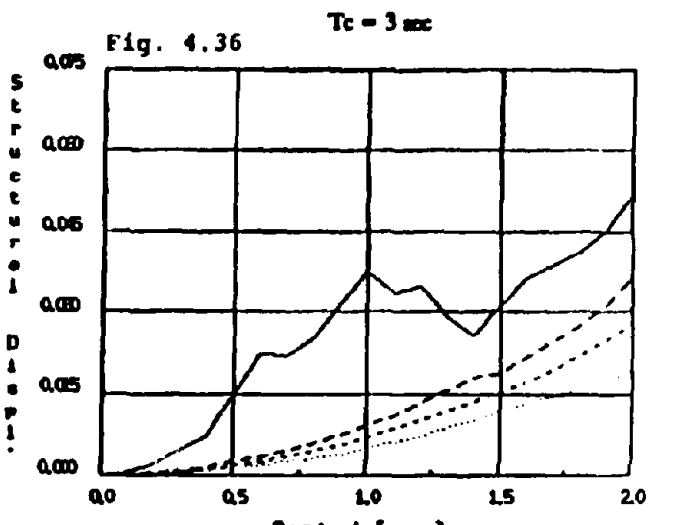

Figs. 4.33 to 4.36 Max. Structural Displacement [sec^2] , El Centro 1940, ξ = 5 % ....η_{sl} = 0.1 - - - η_{sl} = 0.2 - - η_{sl} = 0.3

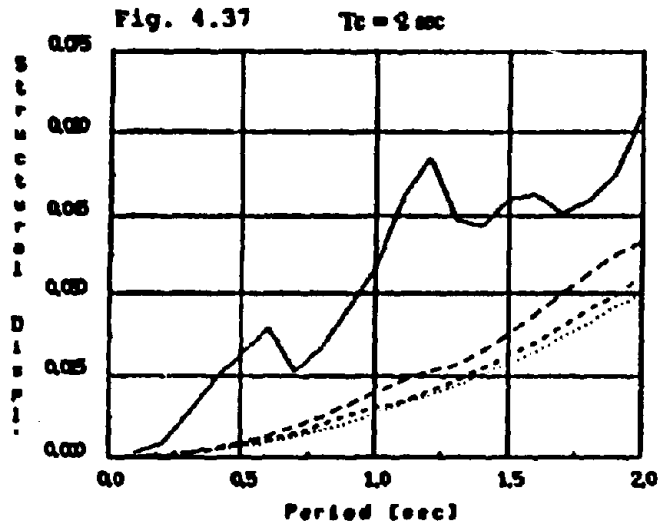

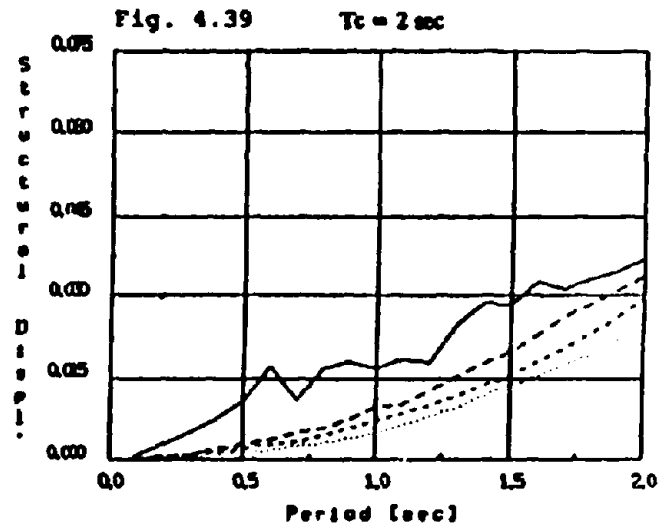

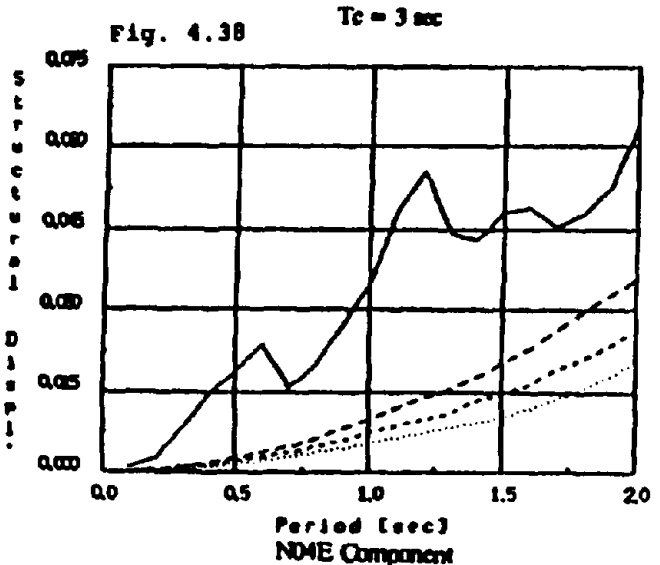

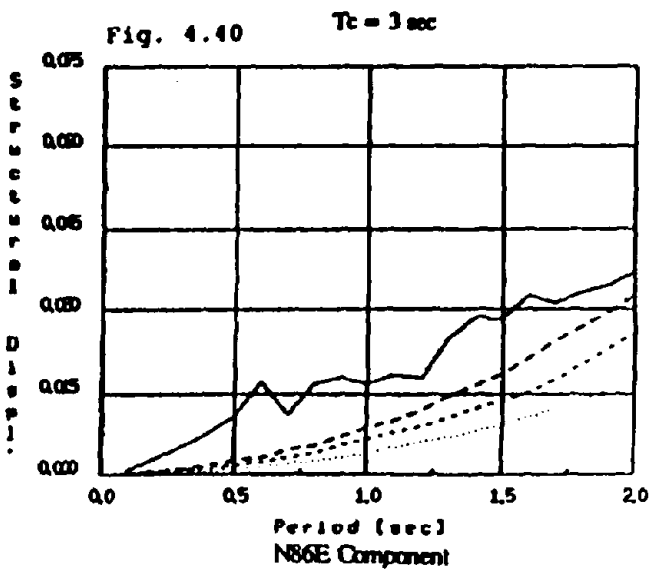

Figs. 4.37 to 4.40 Max. Structural Displacement [sec^2], Olympia 1949, $\xi = 5\%$ ....$\eta_M = 0.1$ ---$\eta_M = 0.2$ – –$\eta_M = 0.3$

Fig. 4.41 Tc = 2 sec

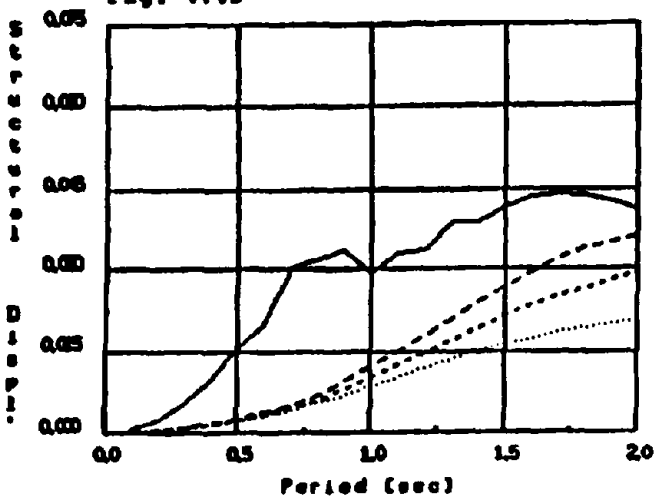

Fig. 4.42 Tc = 3 sec

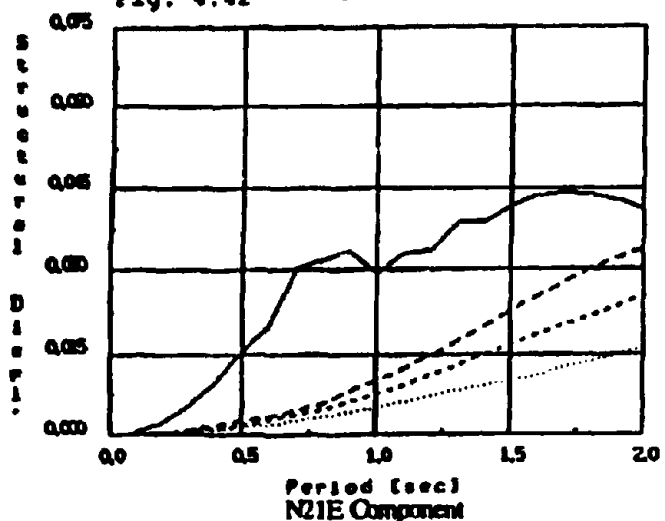

N21E Component

Fig. 4.43 Tc = 2 sec

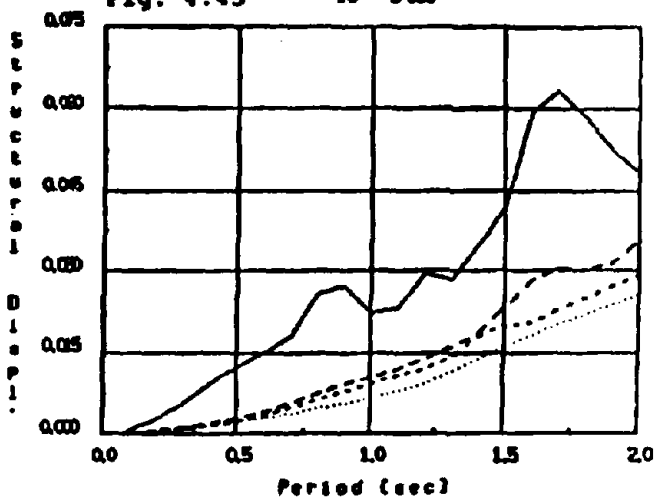

Fig. 4.44 Tc = 3 sec

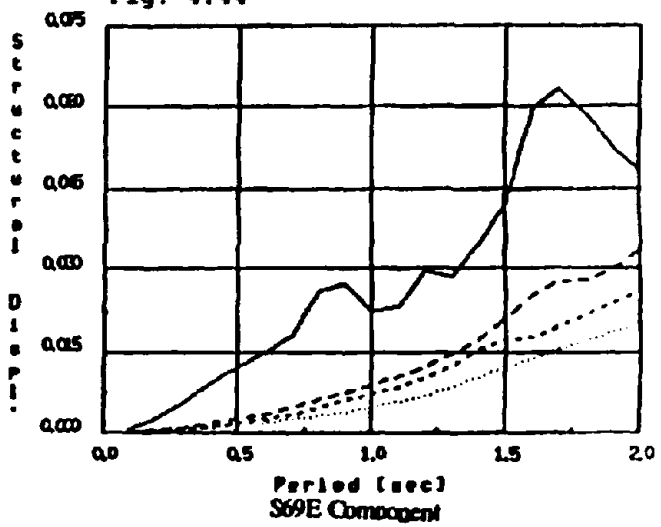

S69E Component

Figs. 4.41 to 4.44 Max. Structural Displacement [sec^2], Taft 1952, $\xi = 5\%$ ....$\eta_M = 0.1$ ...$\eta_M = 0.2$ --$\eta_M = 0.3$

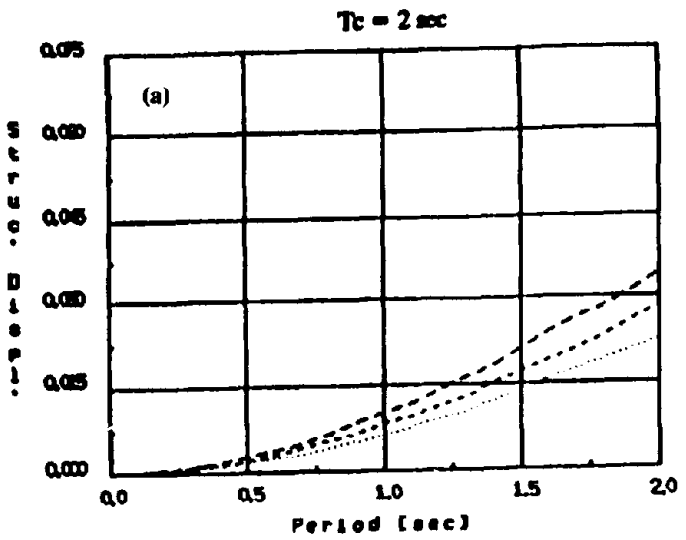

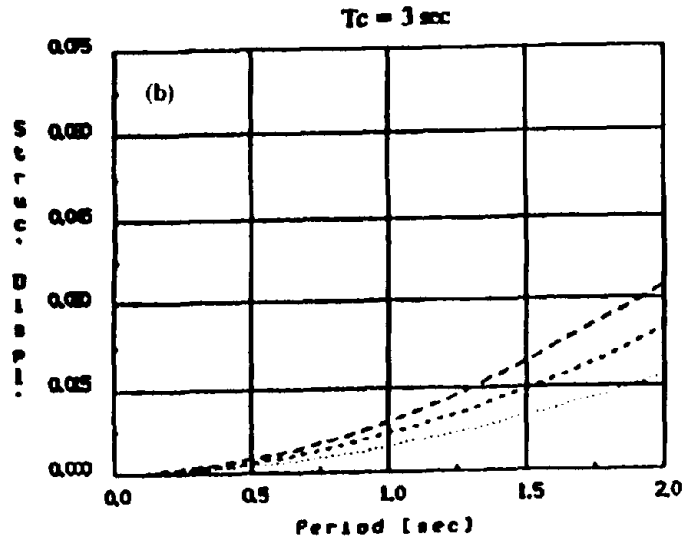

Fig . 4.45 Mean Normalized Max. Structural Displacement [sec^{1}]

....η_{bl} = 0.1 ---η_{bl} = 0.2 -- η_{bl} = 0.3

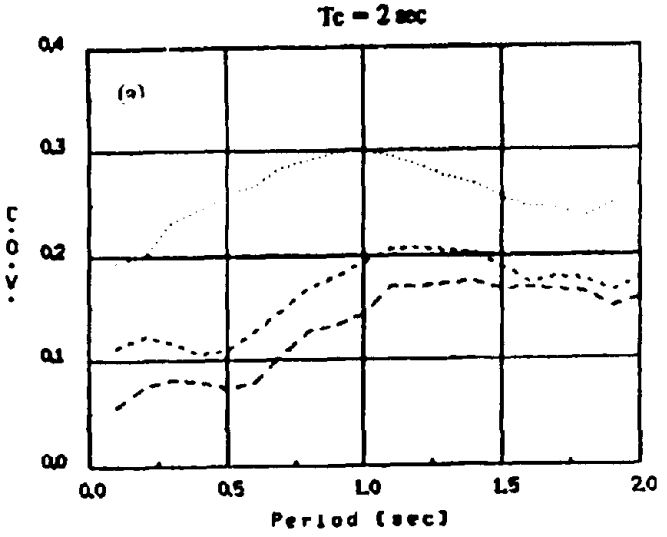

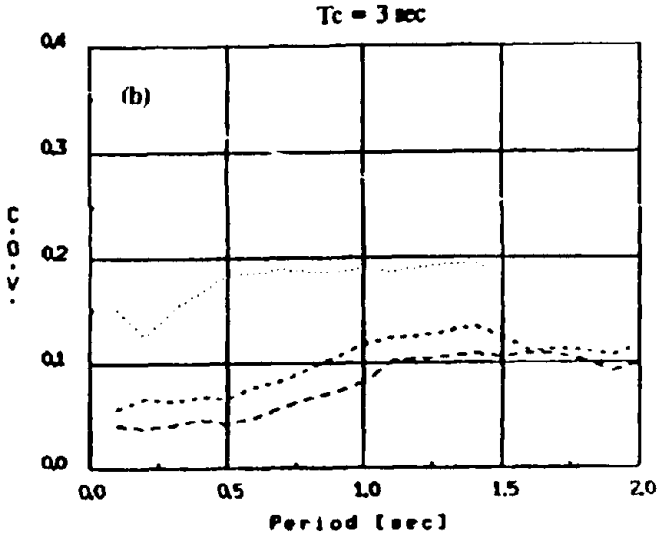

Fig . 4.46 Coefficient of variation

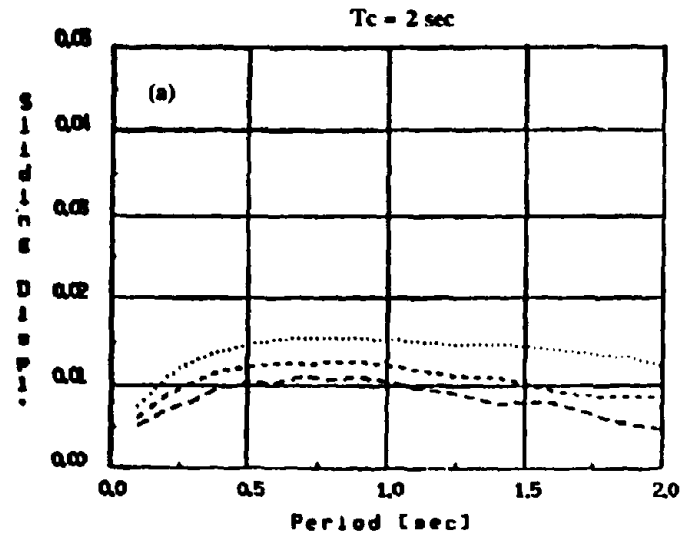

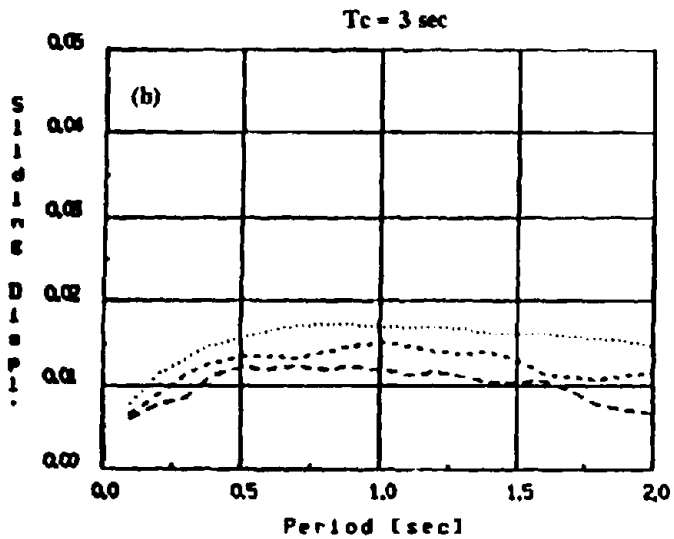

Fig. 4.47 Mean Normalized Max. Sliding Displacement [sec^2]

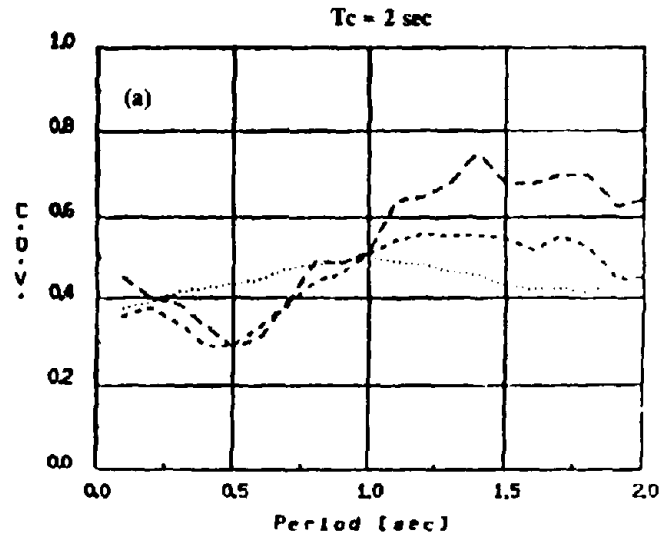

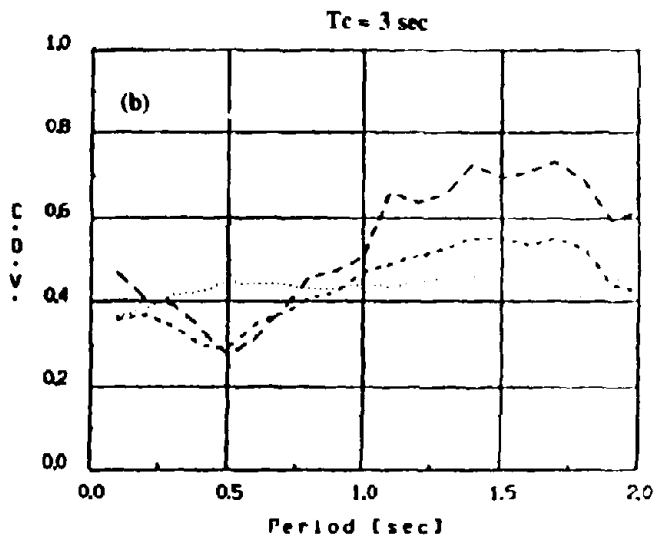

Fig. 4.48 Coefficient of variation

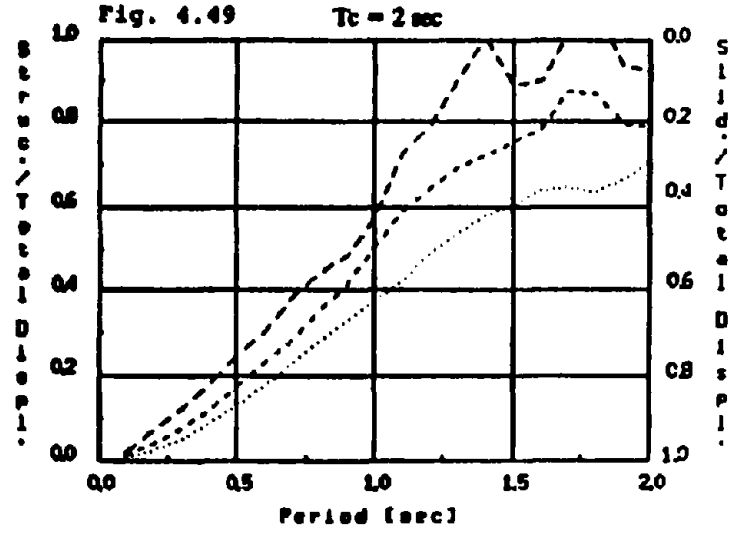

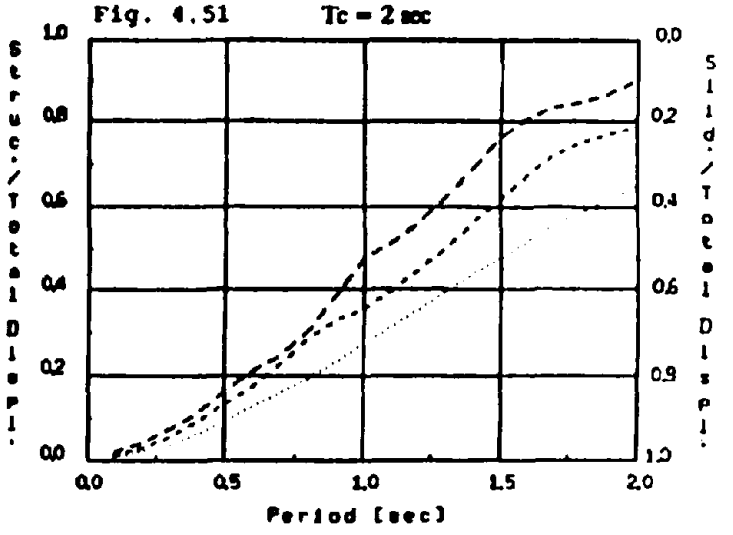

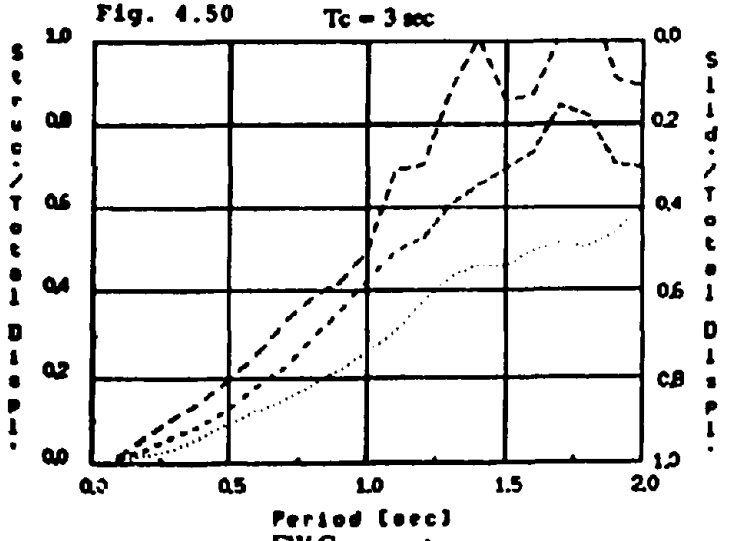

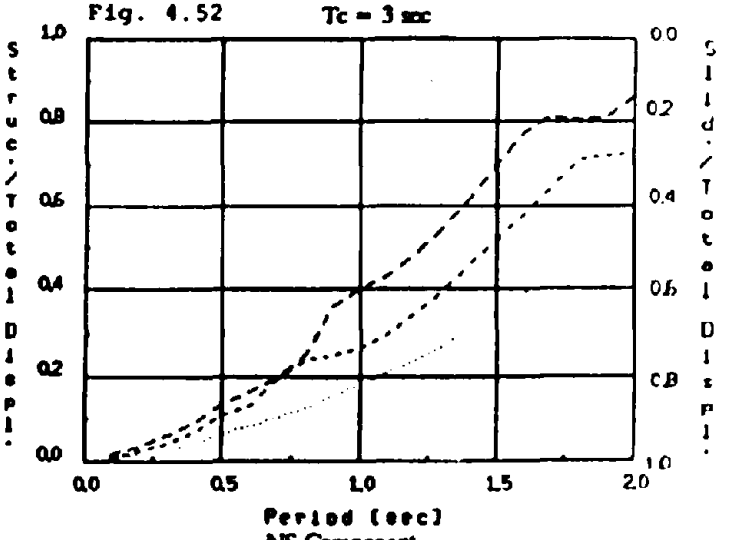

Figs. 4.49 to 4.52 Structural Displacement Total Displacements Ratio [sec^2], El Centro 1934, ξ = 5 % ....η_M = 0.1 ...η_M = 0.2 _ _ η_M = 0.3

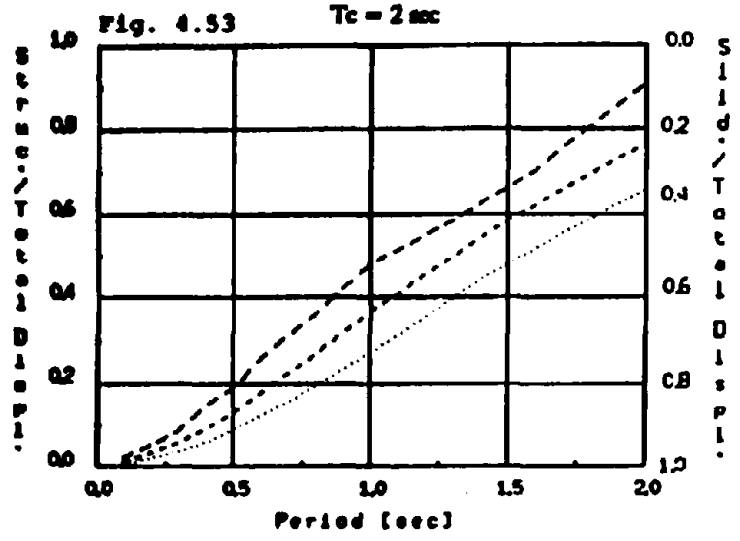

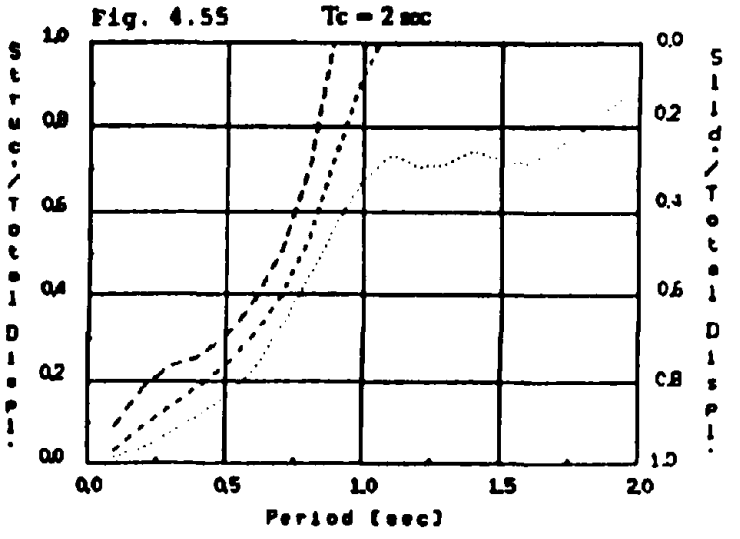

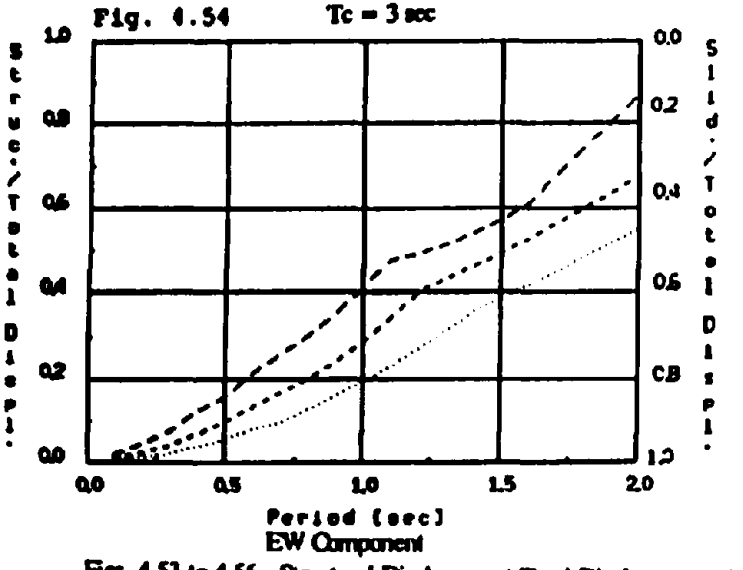

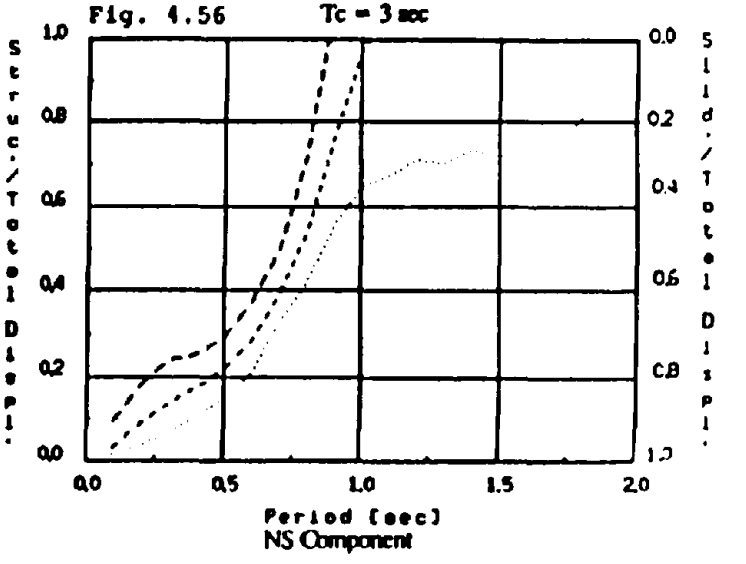

Figs. 4.53 to 4.56 Structural Displacement Total Displacements Ratio [sec^2], Helena 1935, ξ = 5 % ....η_d = 0.1 ... η_d = 0.2 _ _ η_d = 0.3

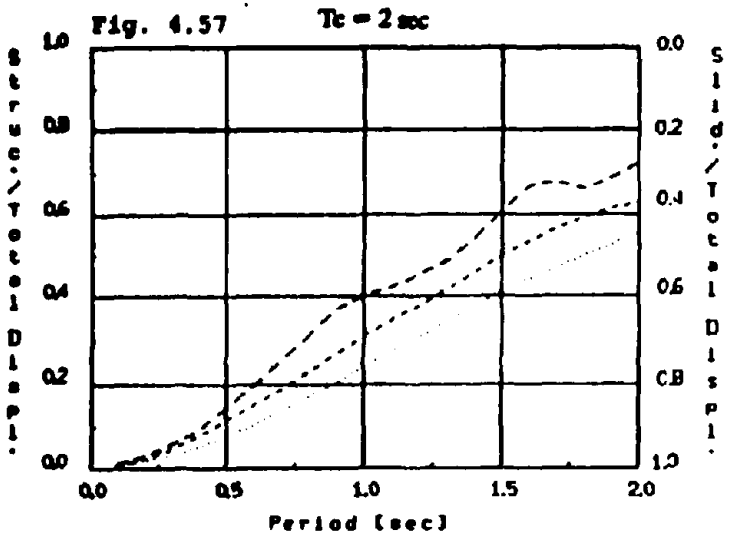

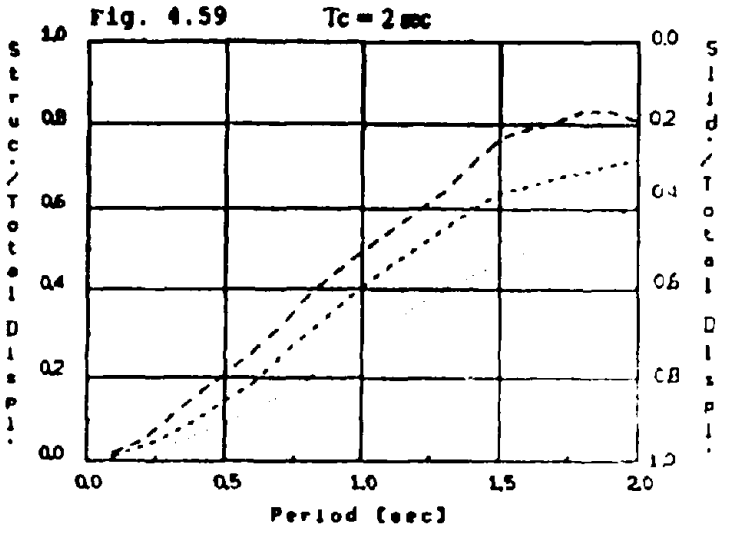

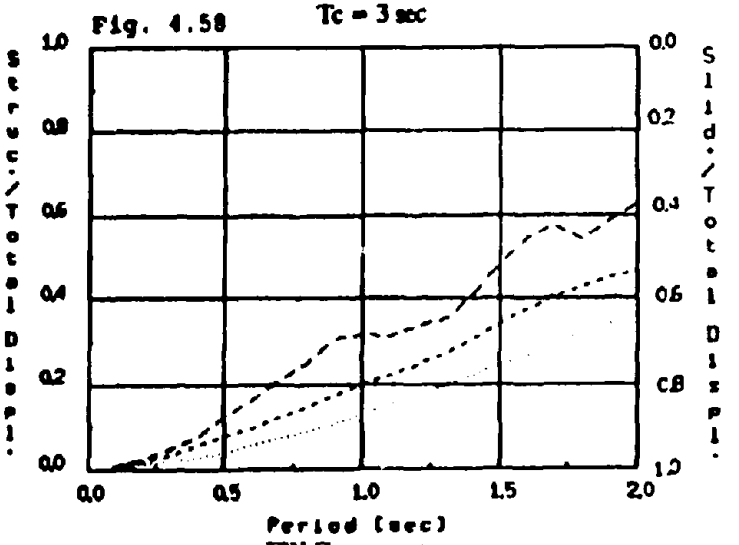

EW Component

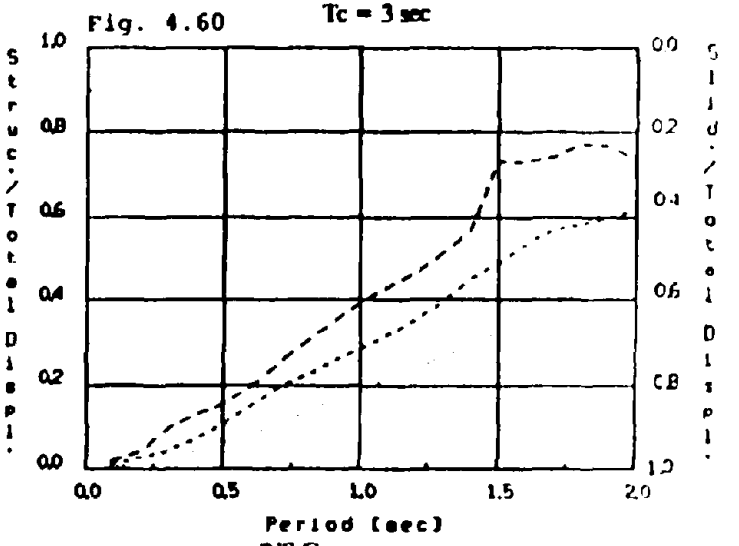

NS Component

Figs. 4.57 to 4.60 Structural Displacement Total Displacements Ratio [sec^2], El Centro 1940, ξ = 5 % .... η_{sl} = 0.1 ... η_{sl} = 0.2 _ _ η_{sl} = 0.3

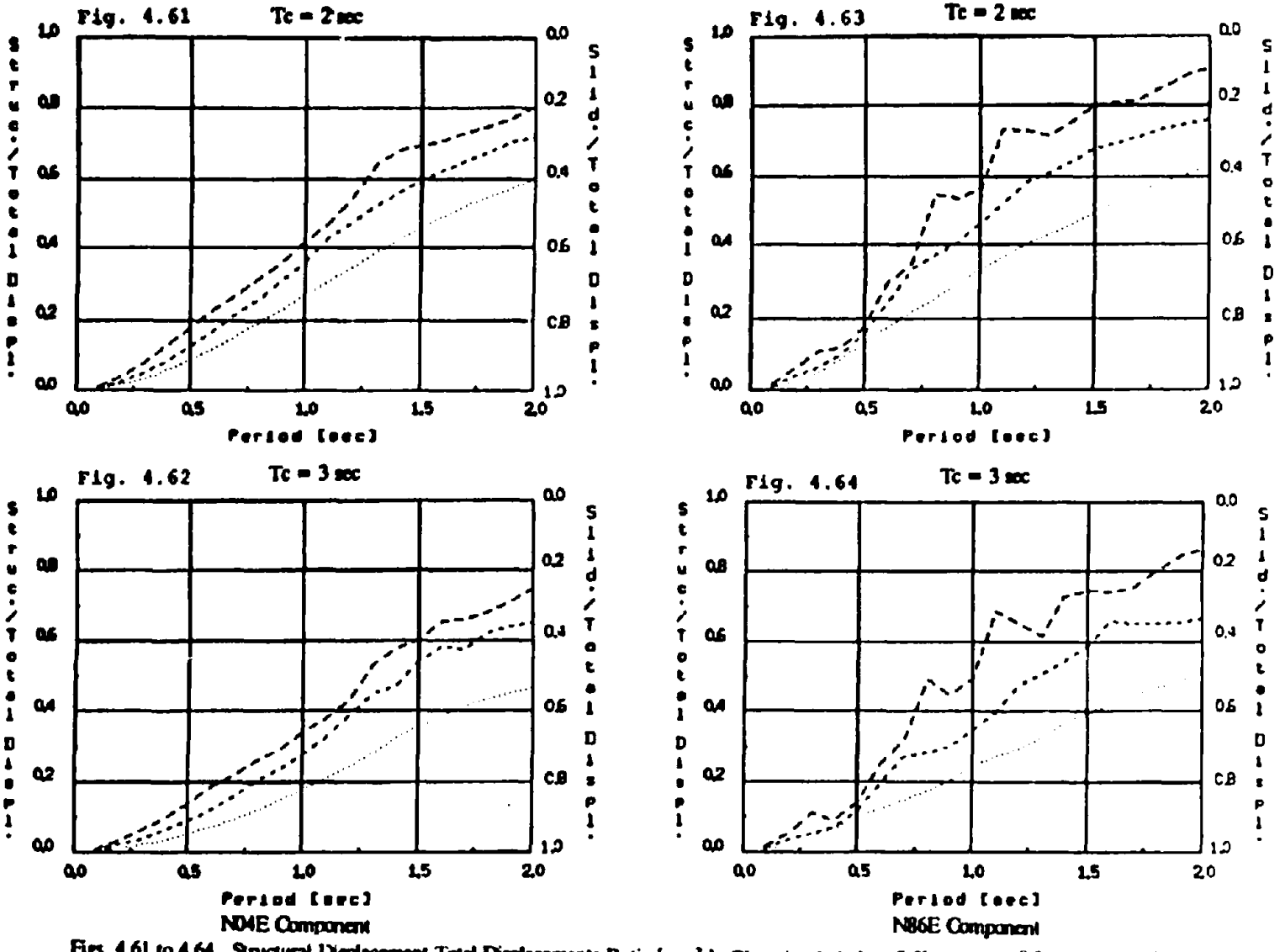

Figs. 4.61 to 4.64 Structural Displacement Total Displacements Ratio [sec^2], Olympia 1949. ξ = 5 % ....η_{sl} = 0.1 - - -η_{sl} = 0.2 – –η_{sl} = 0.3

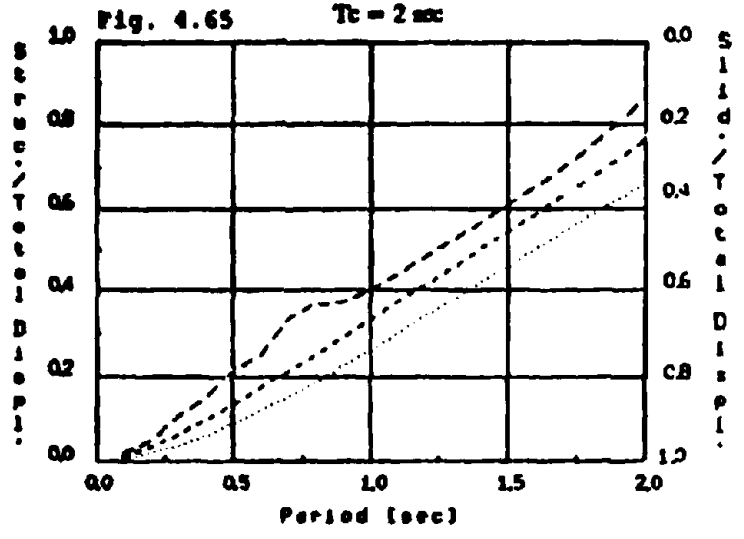

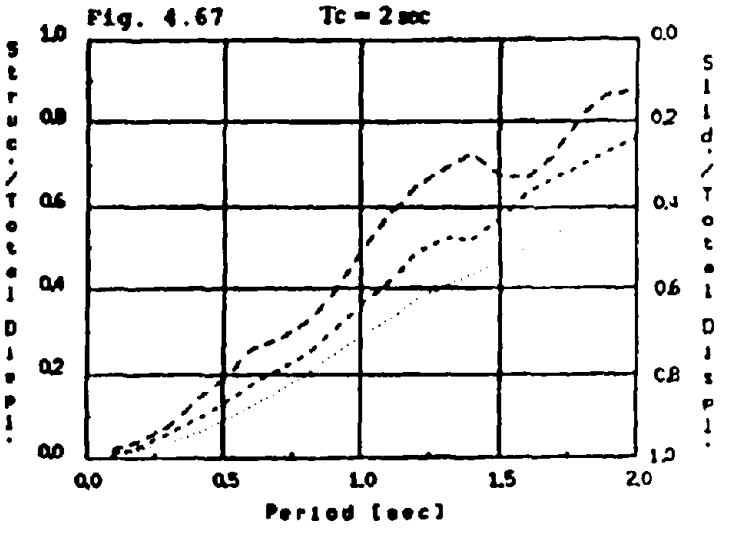

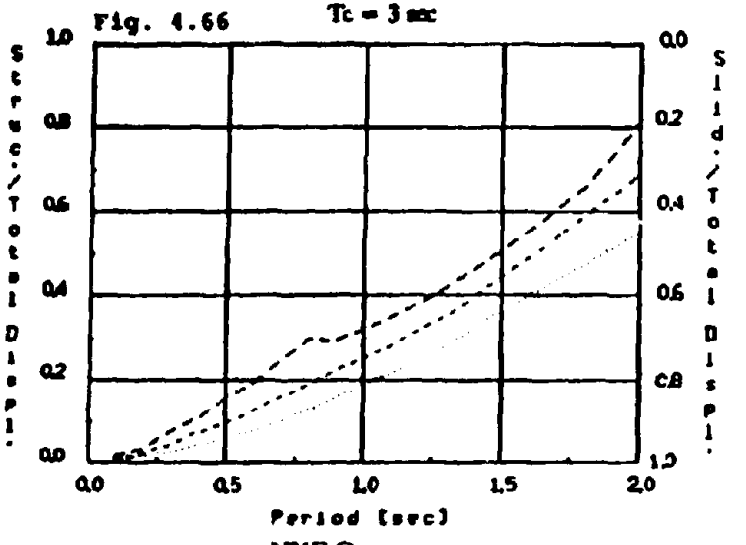

N21E Component

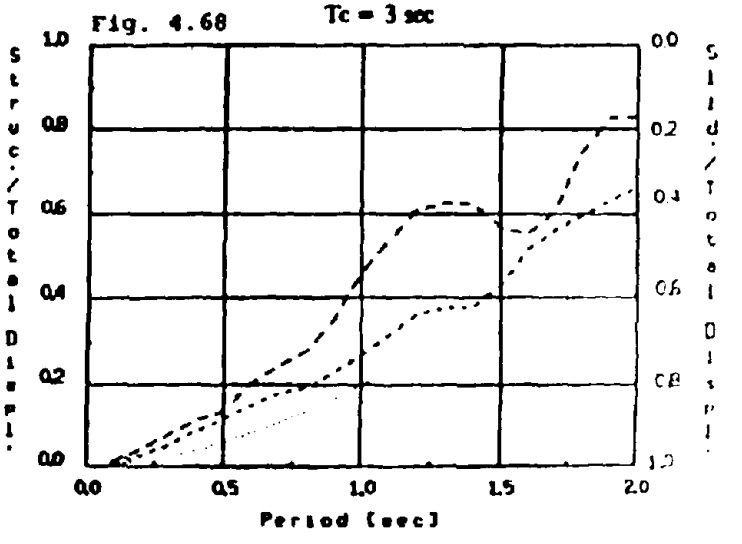

S69E Component

Figs. 4.65 to 4.68 Structural Displacement Total Displacements Ratio [sec^2] , Taft 1952, ξ = 5 % ....η_{sd} = 0.1 . . . η_{sd} = 0.2 _ _ η_{sd} = 0.3

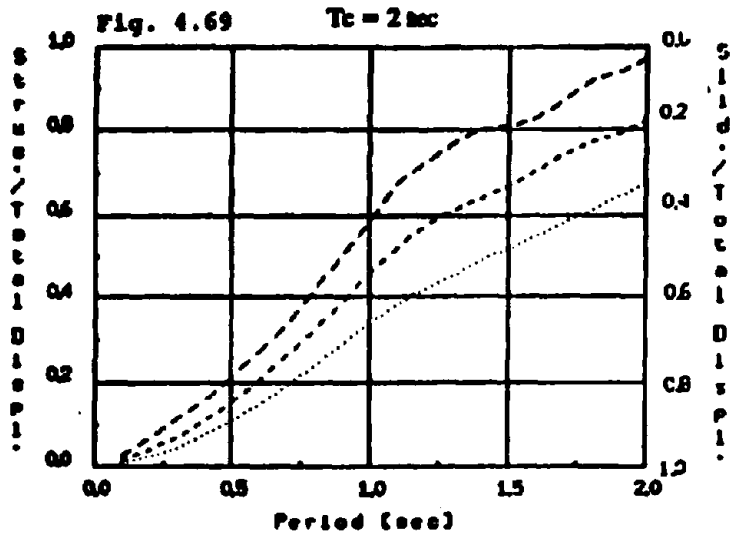

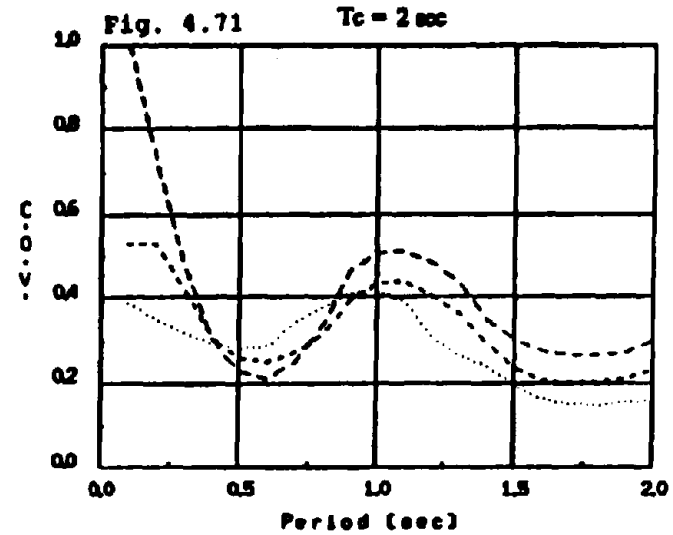

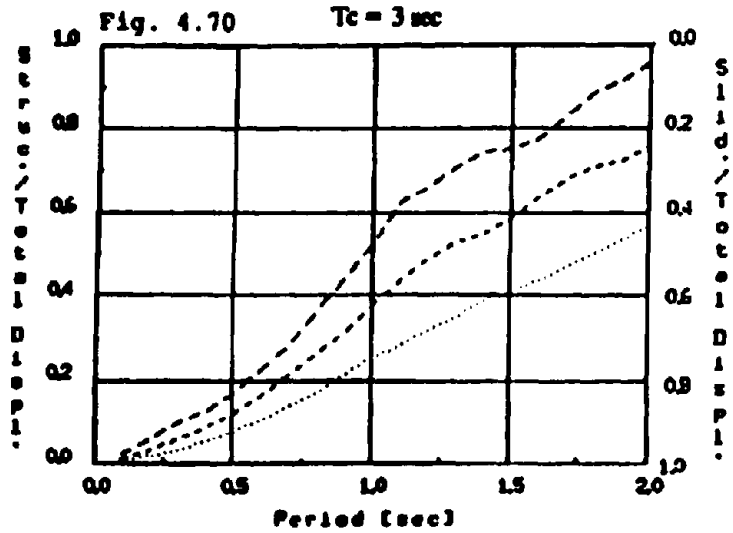

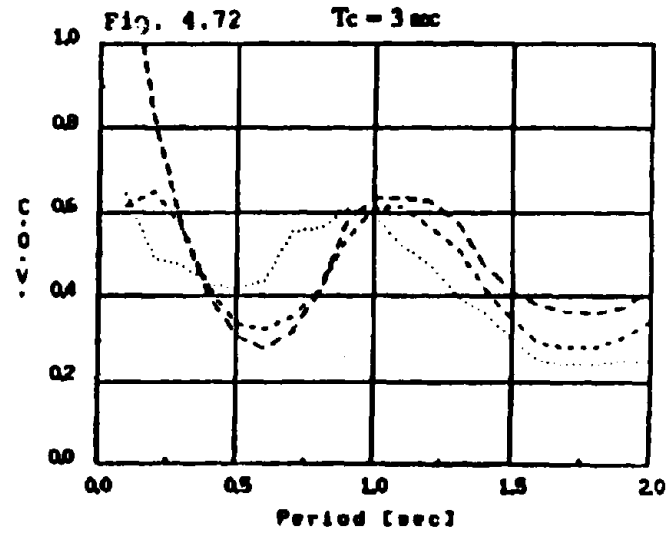

Figs. 4.69 to 4.70 Mean Structural Displacement Total Displacement Ratio [sec^2]

Figs. 4.71 to 4.72 Coefficient of variation

....$\eta_M = 0.1$ $\eta_M = 0.2$ $\eta_M = 0.3$

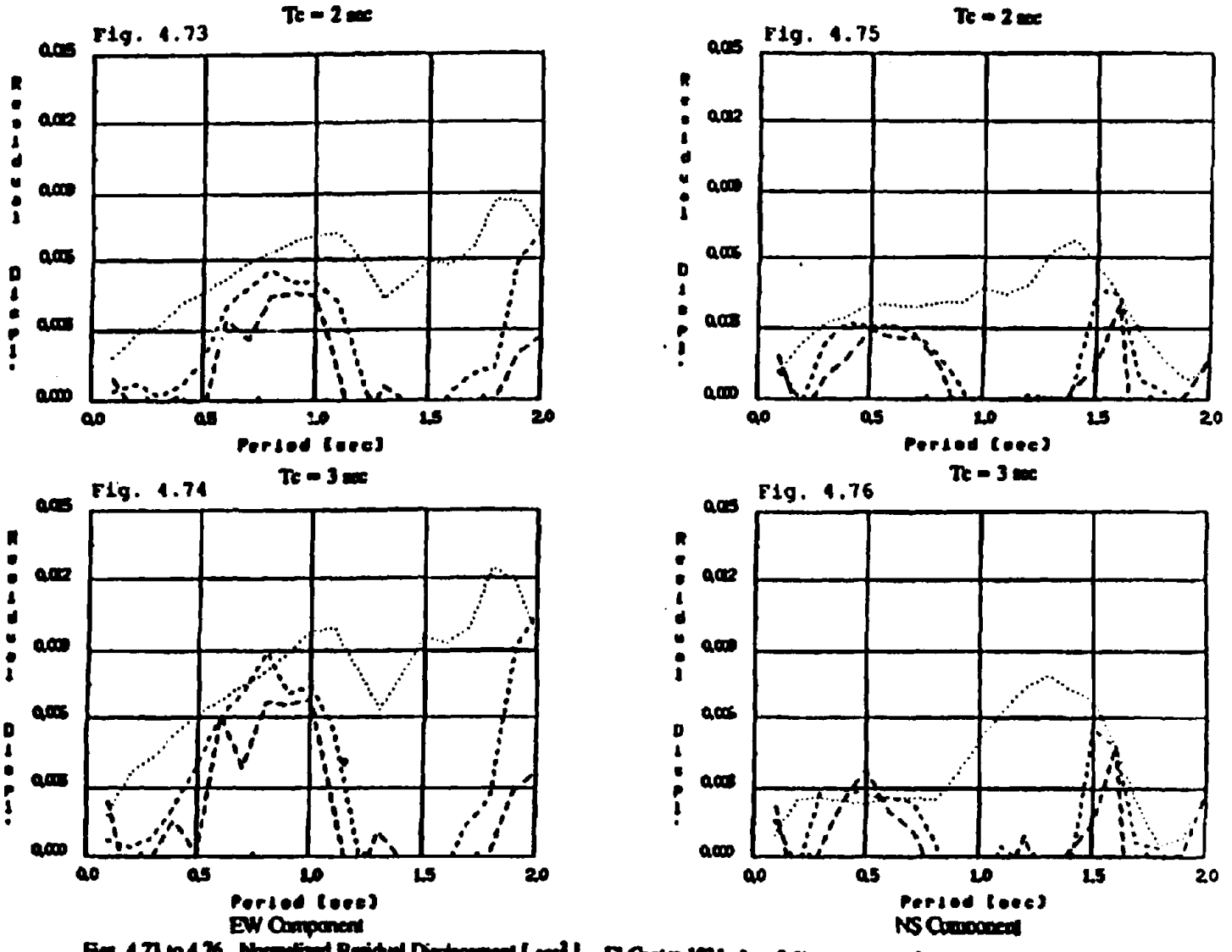

Figs. 4.73 to 4.76 Normalized Residual Displacement [sec^2], El Centro 1934, $\xi = 5\%$ ....$\eta_M = 0.1$ ---$\eta_M = 0.2$ - -$\eta_M = 0.3$

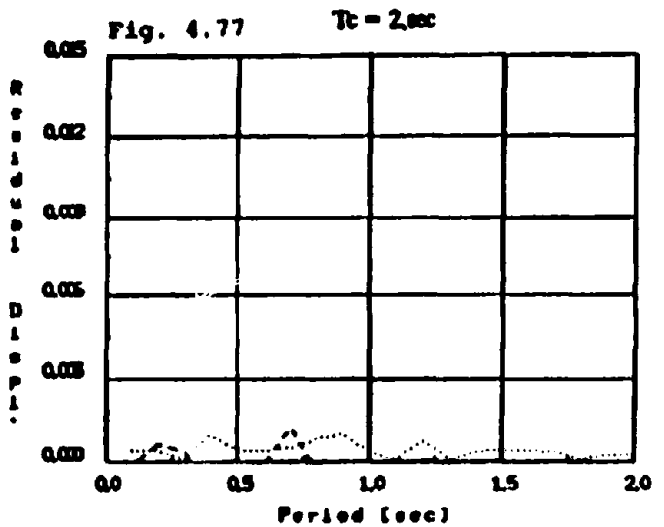

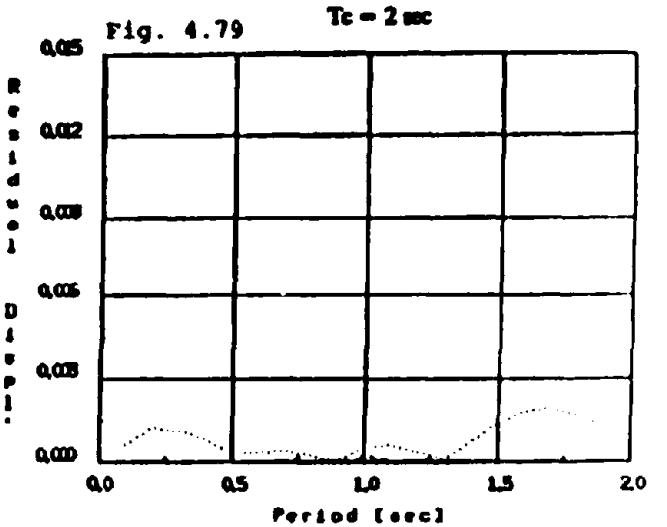

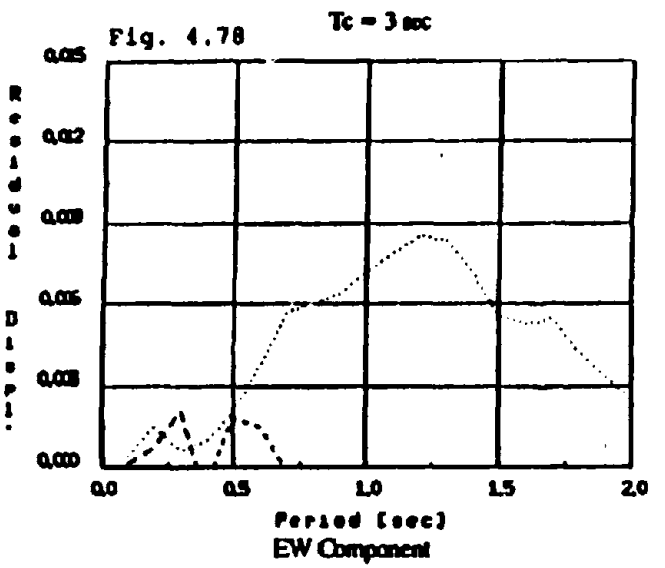

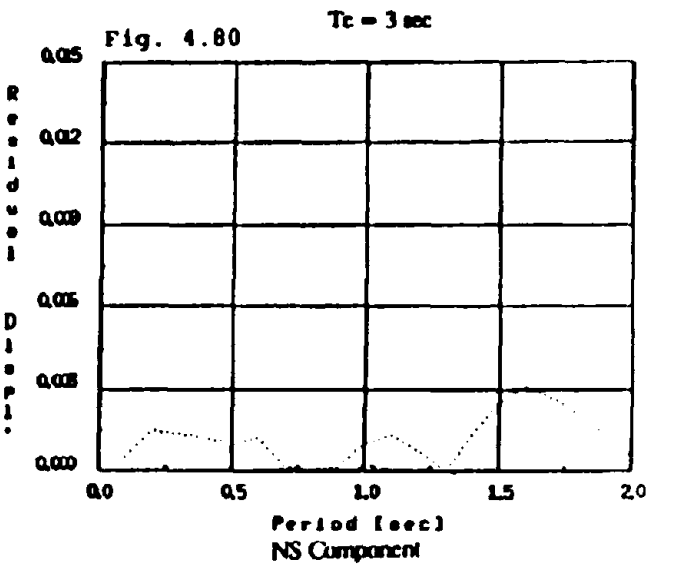

Figs. 4.77 to 4.80 Normalized Residual Displacement [sec^2], Helena 1935, $\xi = 5\%$ .... $\eta_M = 0.1$ ... $\eta_M = 0.2$ -- $\eta_M = 0.3$

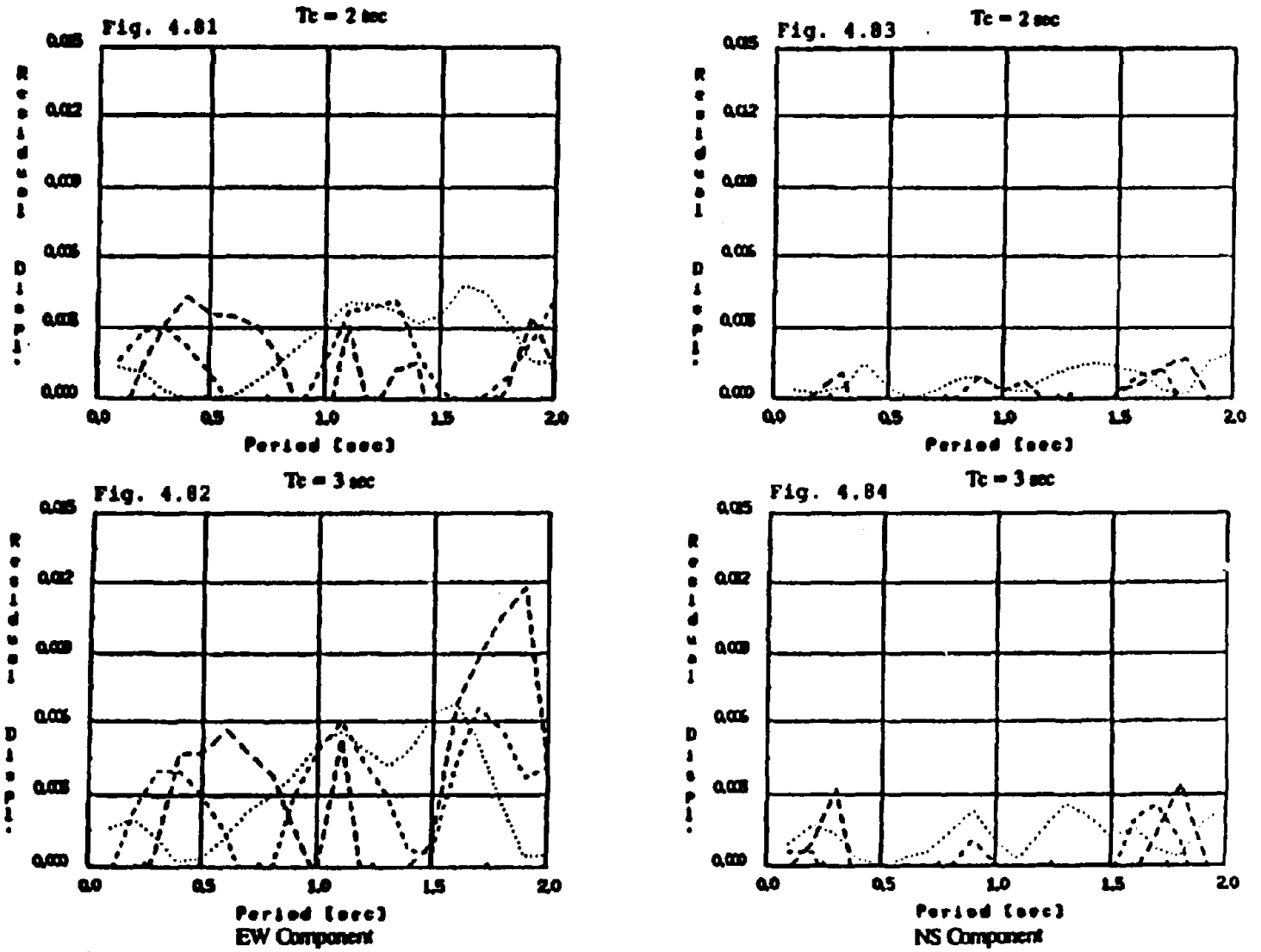

Figs. 4.81 to 4.84 Normalized Residual Displacement [sec^2] , El Centro 1940, $\xi = 5\ \%$ ....$\eta_{sf} = 0.1$ ... $\eta_{sf} = 0.2$ _ _ $\eta_{sf} = 0.3$

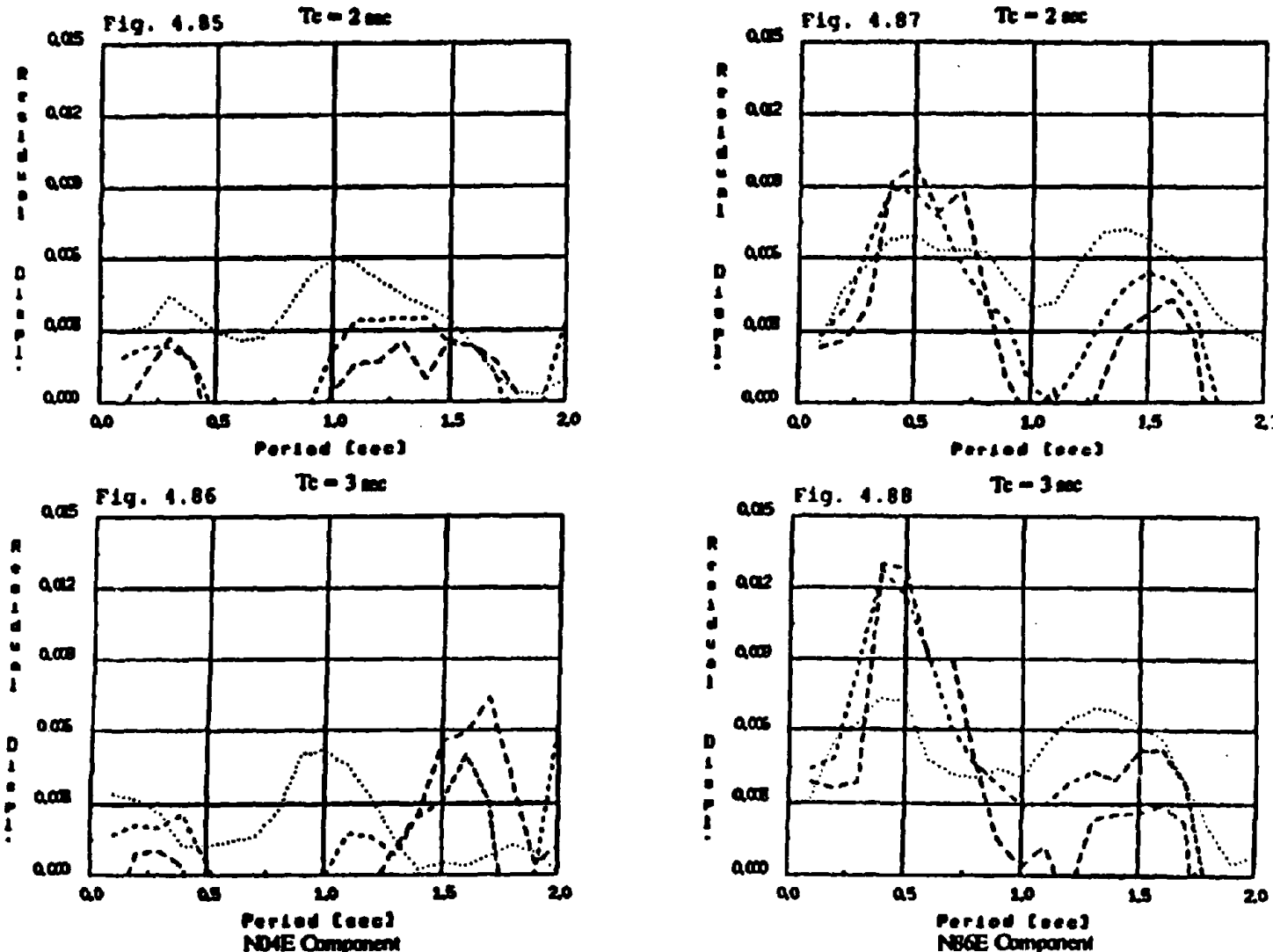

Figs. 4.85 to 4.88 Normalized Residual Displacement [sec^2] , Olympia 1949, $\xi = 5\%$ ....$\eta_M = 0.1$ ---$\eta_M = 0.2$ _ _ $\eta_M = 0.3$

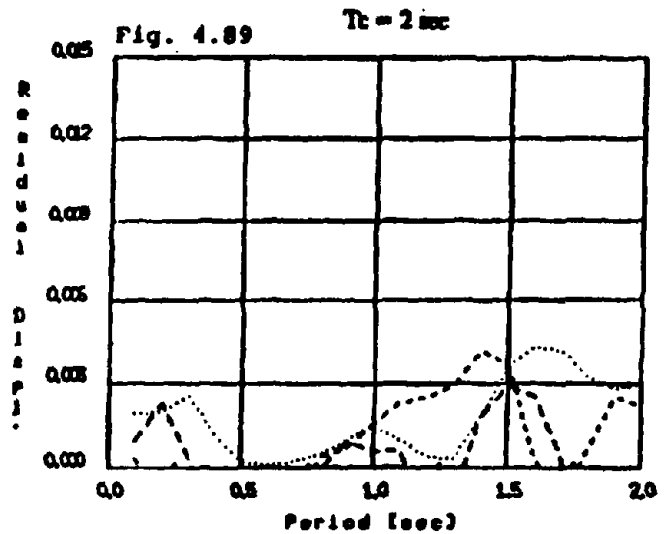

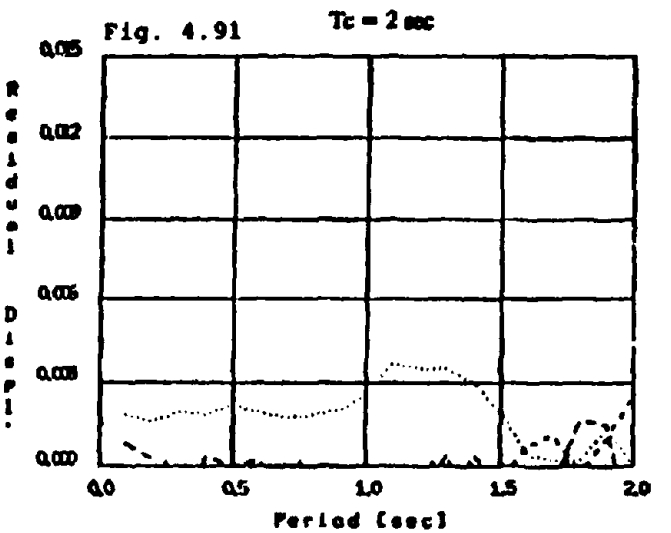

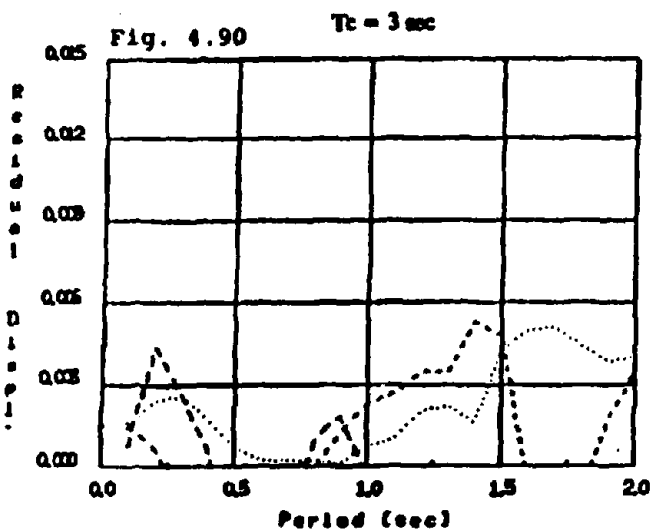

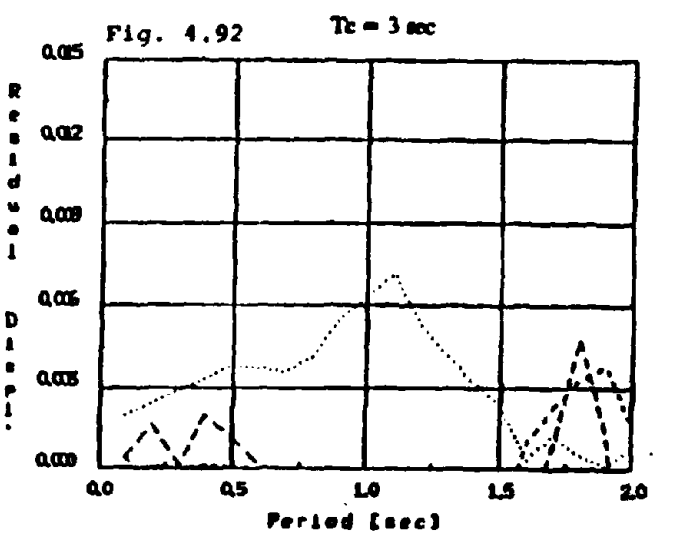

Figs. 4.89 to 4.92 Normalized Residual Displacement [sec^2], Taft 1952, $\xi = 5\%$ ....$\eta_M = 0.1$ ...$\eta_M = 0.2$ _ _ $\eta_M = 0.3$

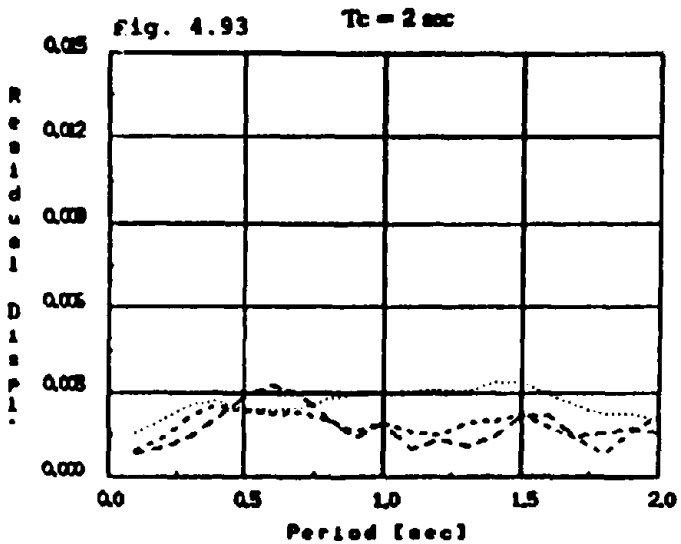

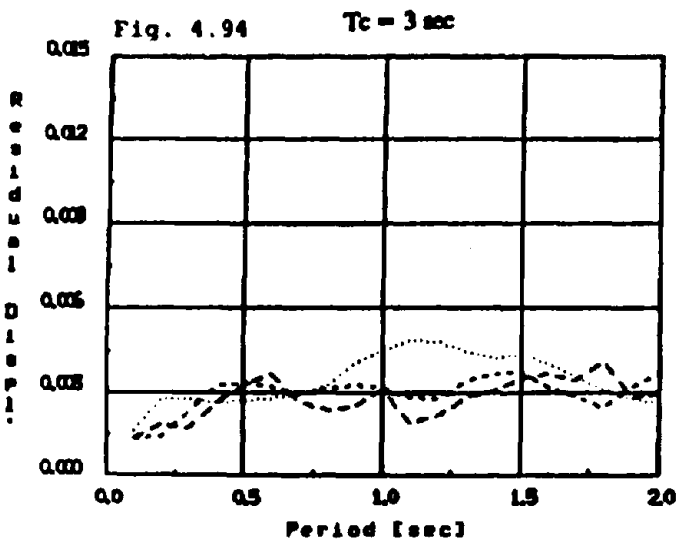

Figs. 4.93 to 4.94 Mean Normalized Residual Displacement [sec^2]

....η_d = 0.1 ...η_d = 0.2 _ _ η_d = 0.3

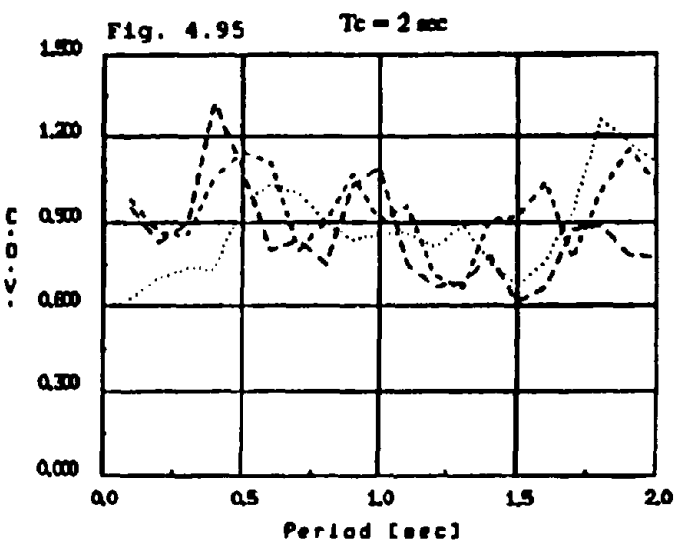

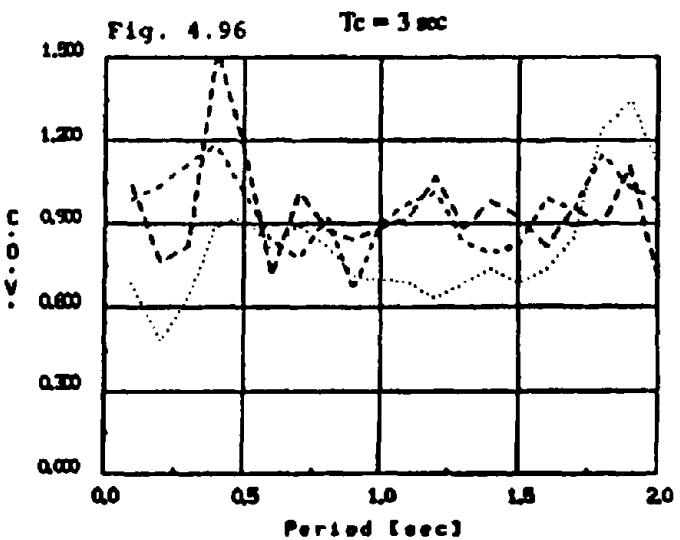

Figs. 4.95 to 4.96 Coefficient of variation

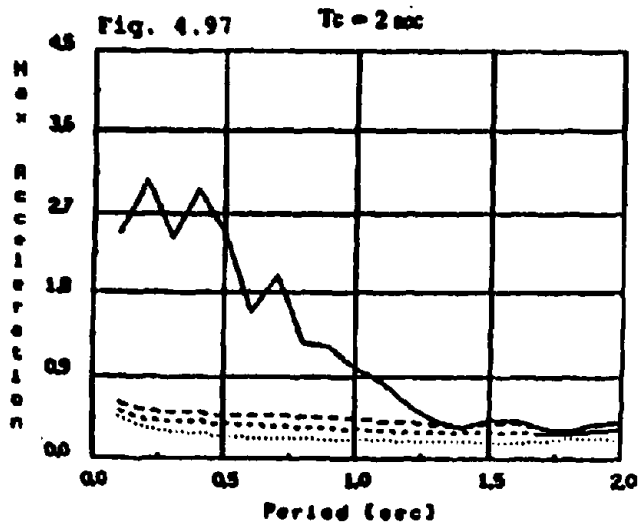

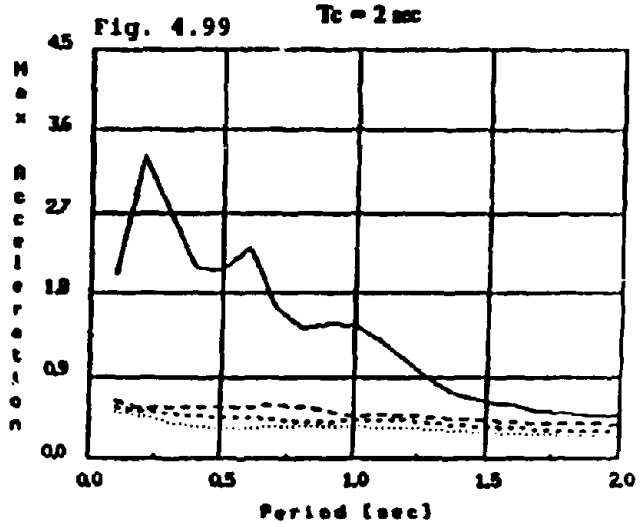

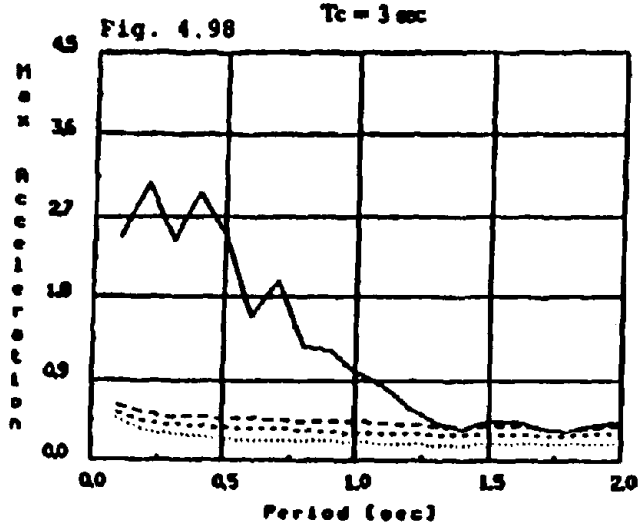

EW Component

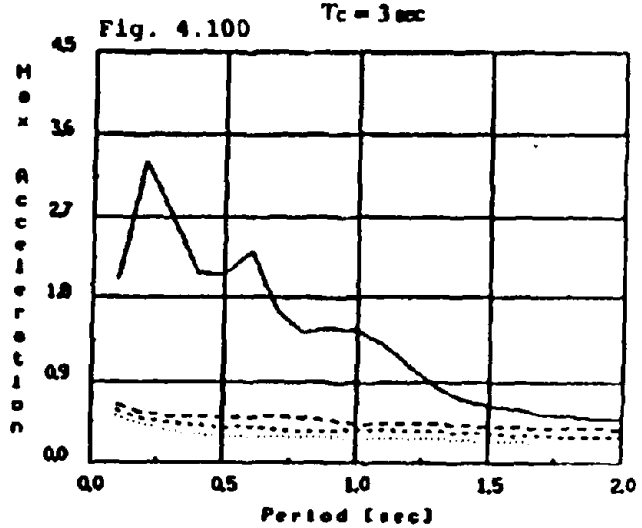

NS Component

Figs. 4.97 to 4.100 Normalized Max. Acceleration, El Centro 1934, $\xi = 5\%$ ....$\eta_M = 0.1$ ---$\eta_M = 0.2$ – –$\eta_M = 0.3$

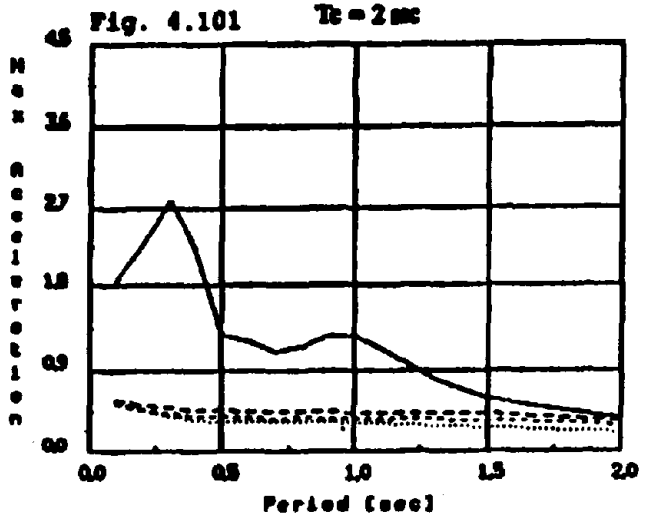

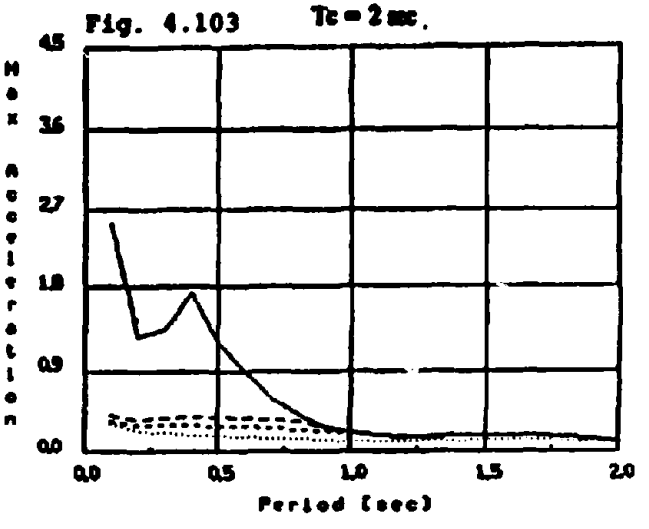

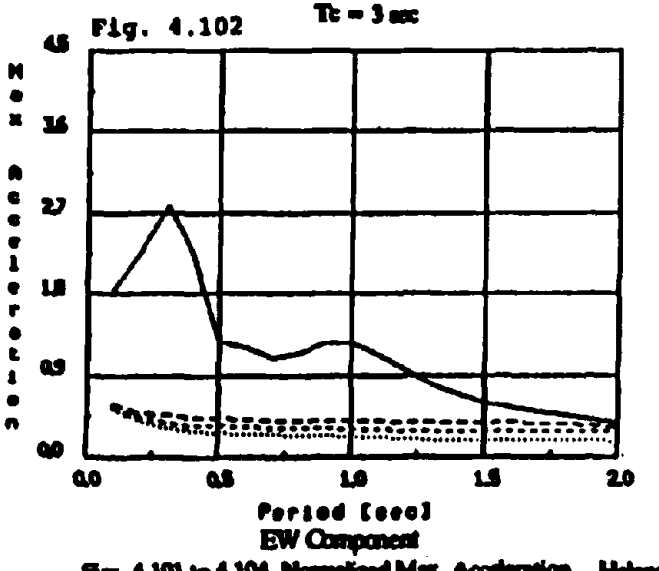

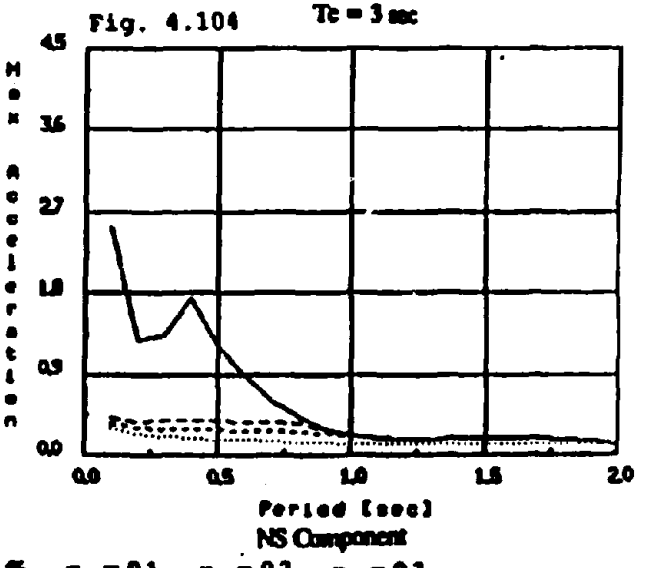

Figs. 4.101 to 4.104 Normalized Max. Acceleration , Helena 1935, $\xi = 5\%$ ....$\eta_M = 0.1$ ---$\eta_M = 0.2$ – –$\eta_M = 0.3$

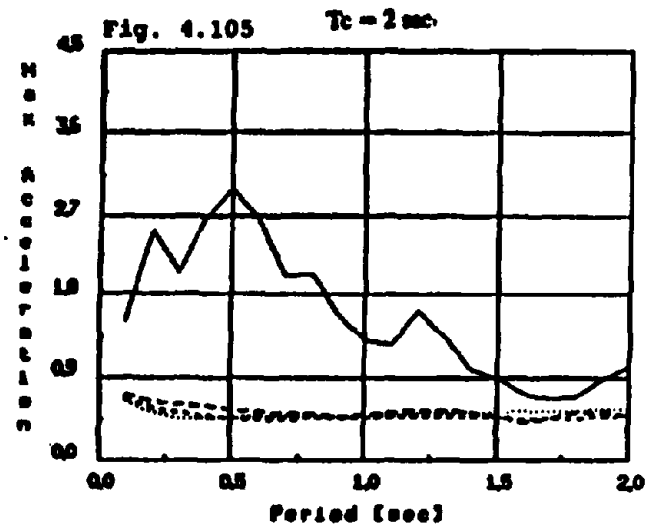

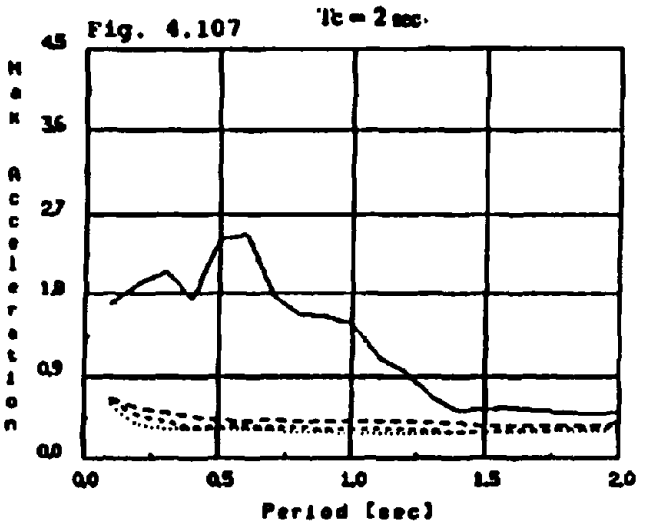

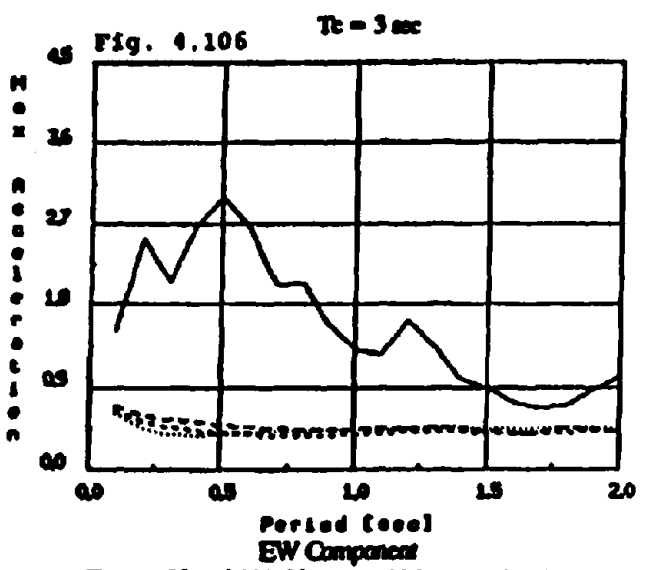

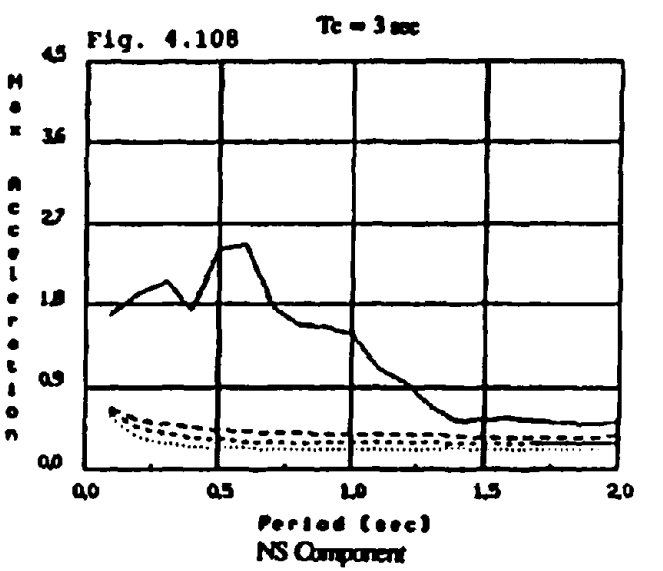

Figs. 4.105 to 4.108 Normalized Max. Acceleration , El Centro 1940, $\xi = 5\%$ ....$\eta_M = 0.1$ ...$\eta_M = 0.2$ --$\eta_M = 0.3$

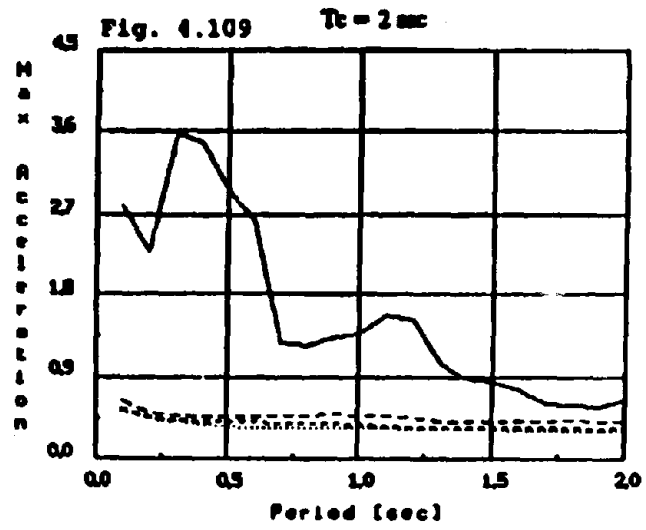

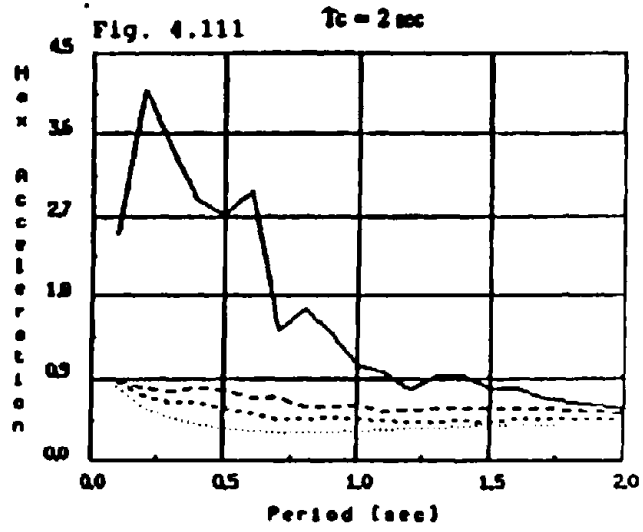

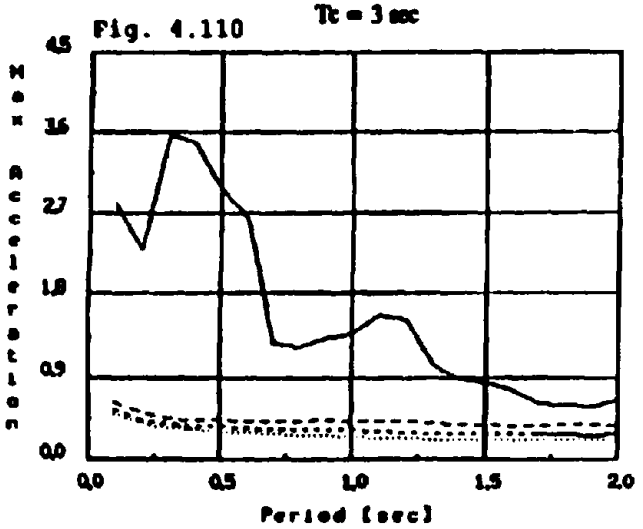

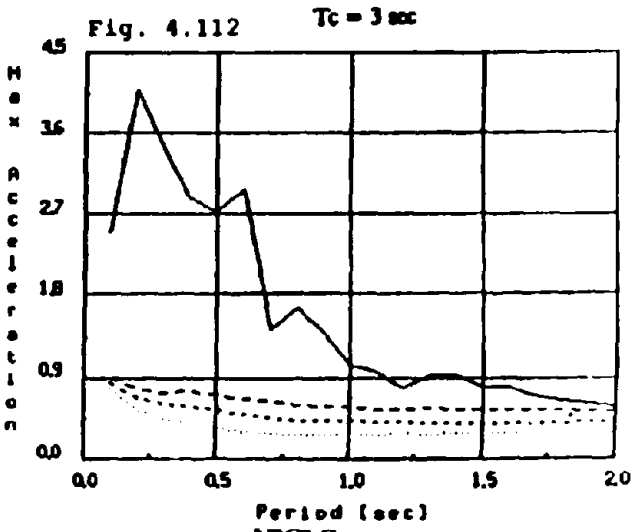

Figs. 4.109 to 4.112 Normalized Max. Acceleration , Olympia 1949, $\xi = 5\%$ ....$\eta_M = 0.1$ ...$\eta_M = 0.2$ --$\eta_M = 0.3$

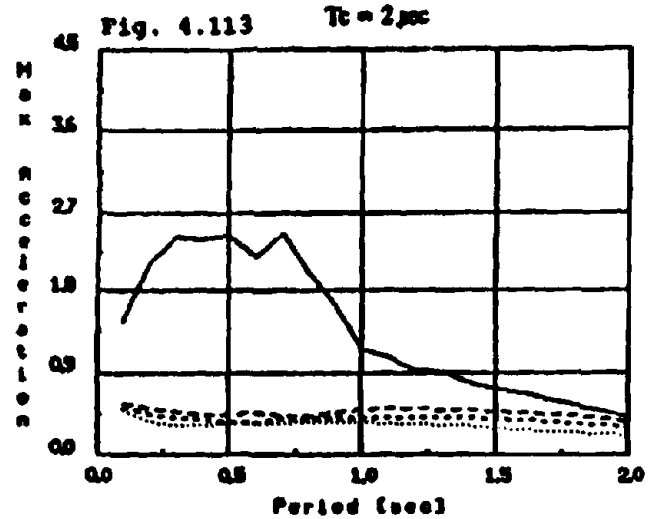

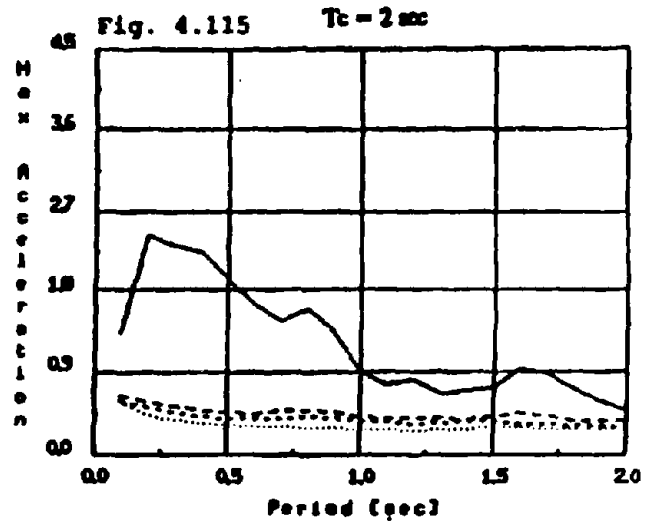

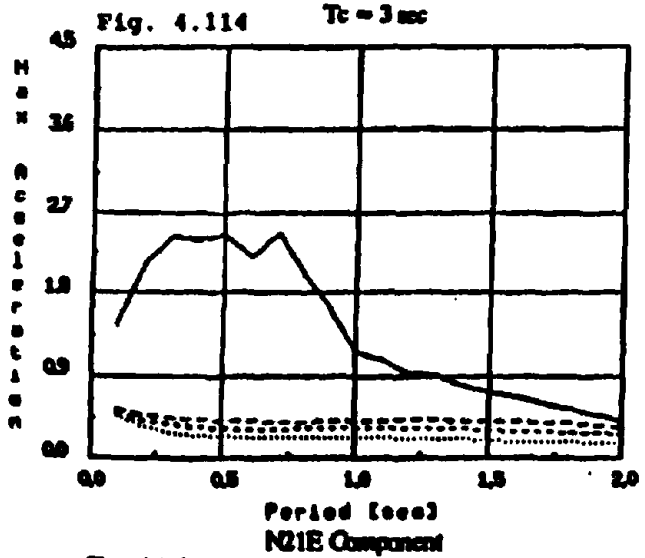

N21E Component

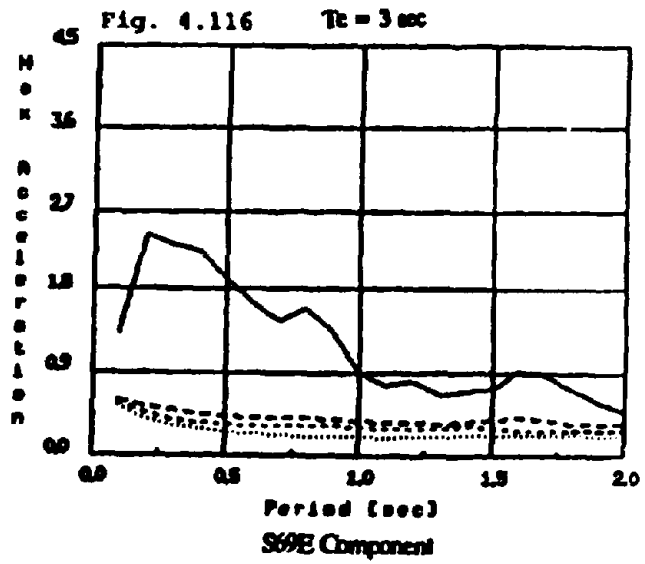

S69E Component

Figs. 4.113 to 4.116 Normalized Max. Acceleration, Taft 1952, ξ = 5 % ....η_d = 0.1 ...η_d = 0.2 --η_d = 0.3

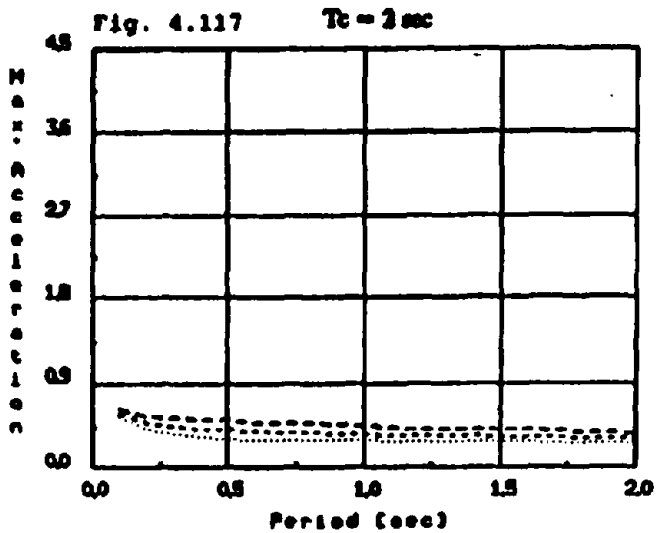

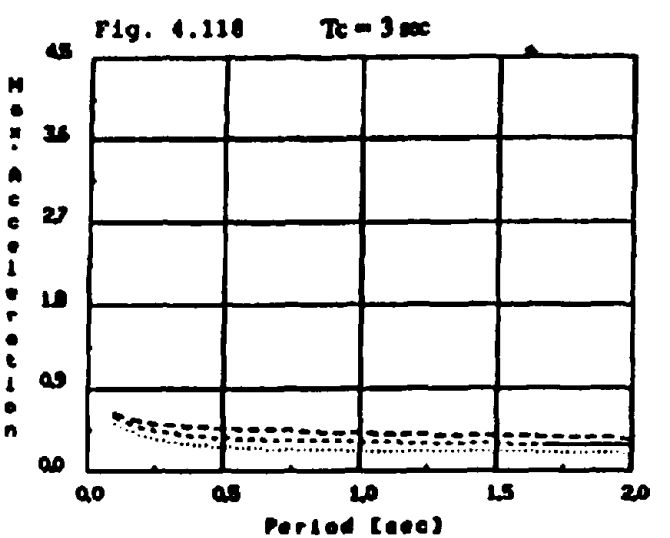

Figs. 4.117 to 4.118 Mean Normalized Max. Acceleration

$....\eta_{sf} = 0.1 \ldots \eta_{sf} = 0.2 \_\_ \eta_{sf} = 0.3$

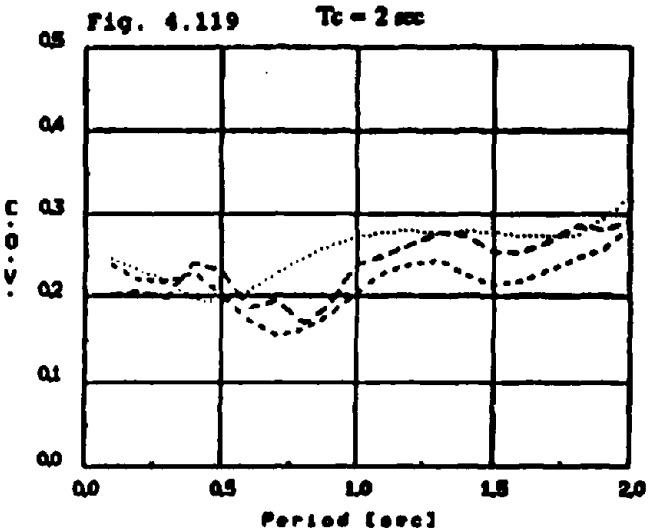

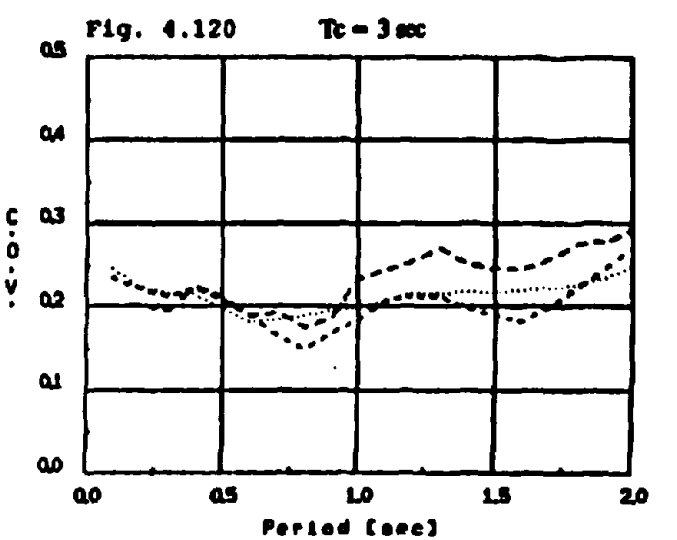

Figs. 4.119 to 4.120 Coefficient of variation

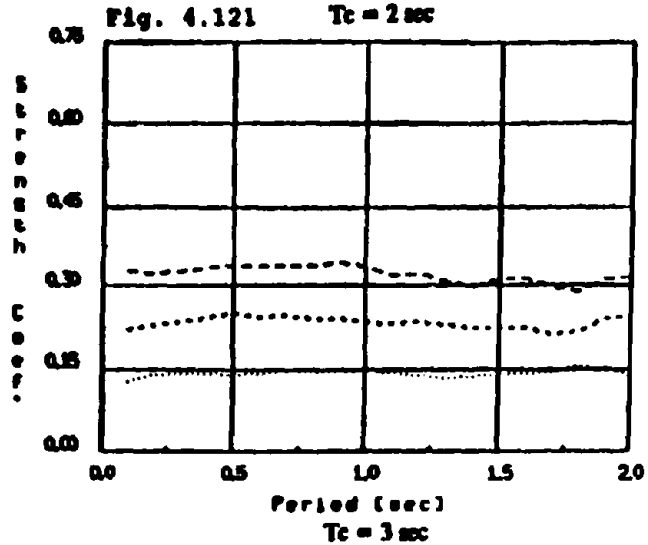

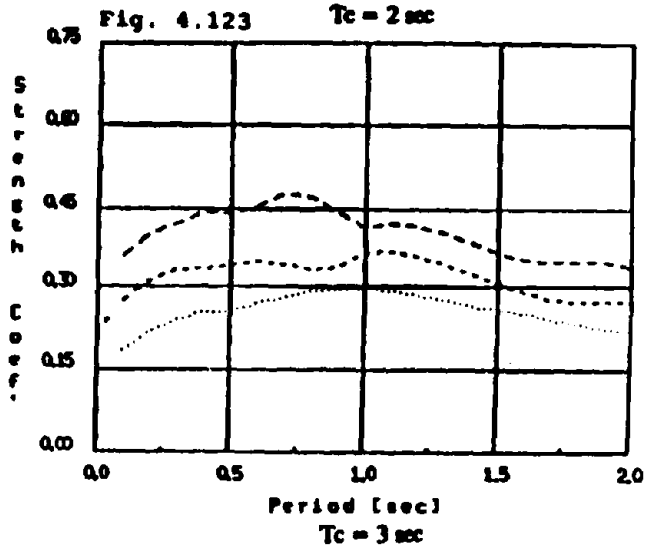

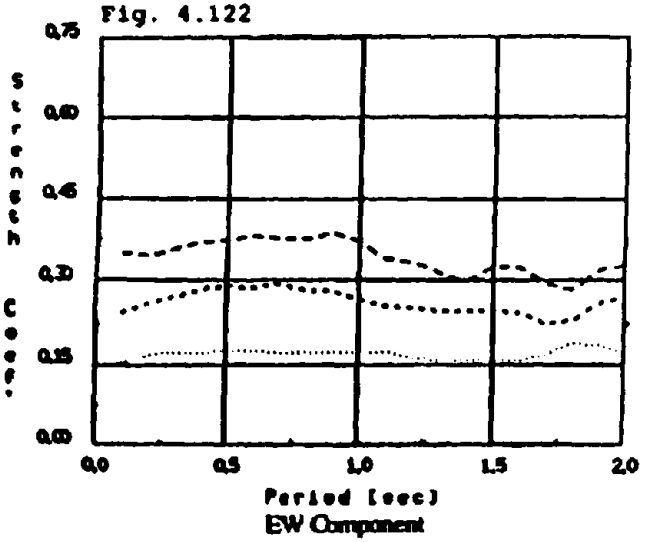

EW Component

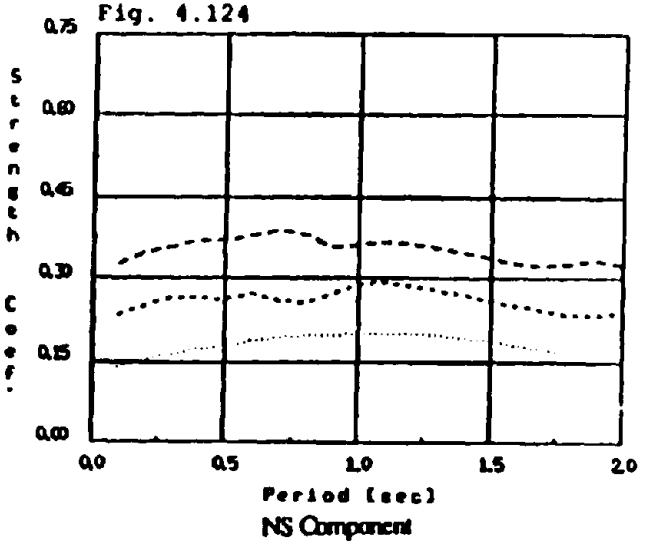

NS Component

Figs. 4.121 to 4.124 Structural Strength Coefficient , El Centro 1934, ξ = 5 % ....η_{el} = 0.1 ...η_{el} = 0.2 _ _ η_{el} = 0.3

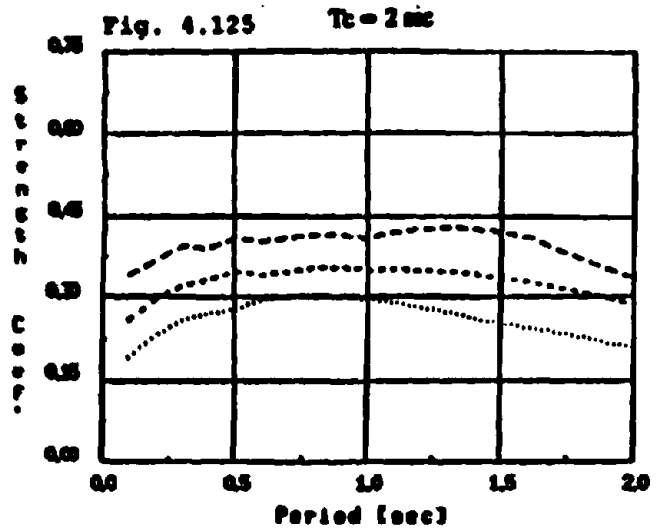

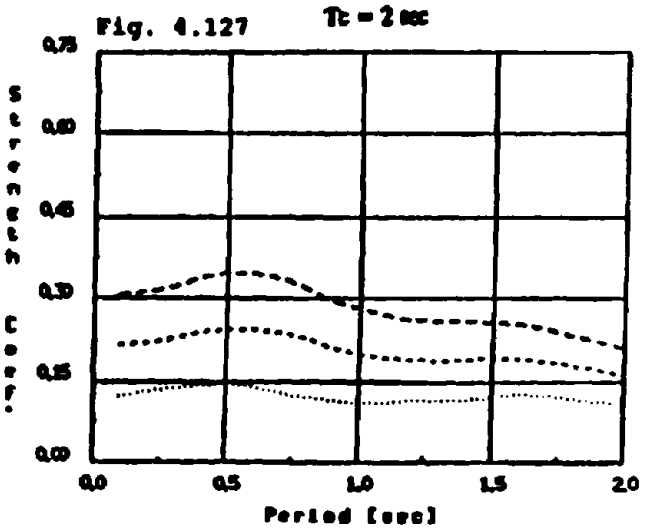

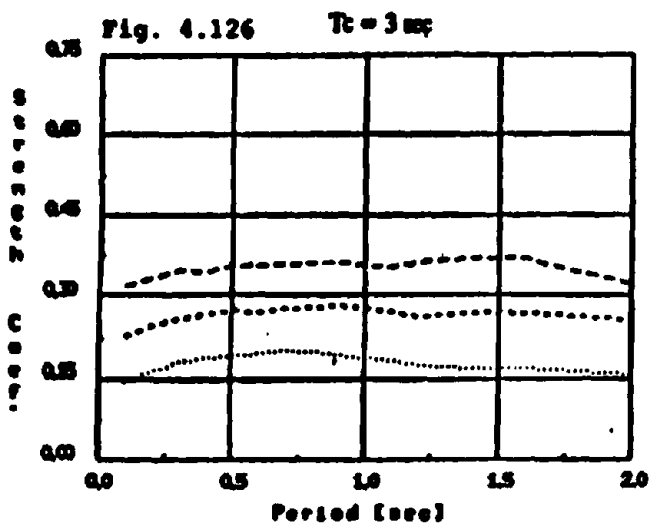

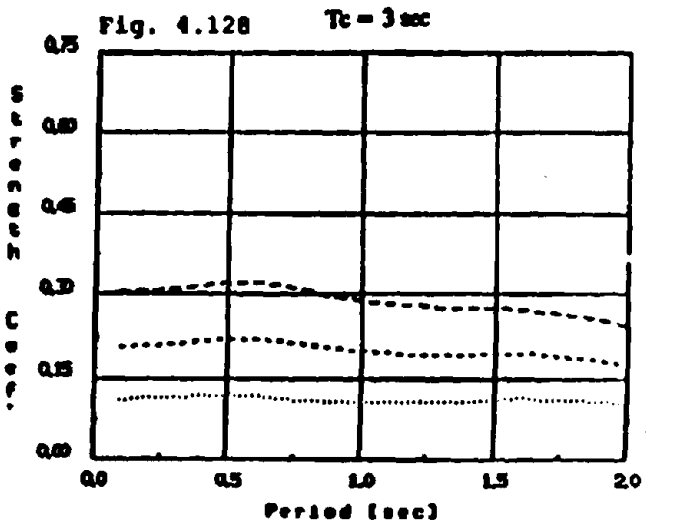

Figs. 4.125 to 4.128 Structural Strength Coefficient, Helena 1935, $\xi = 5\%$ ....$\eta_M = 0.1$ ---$\eta_M = 0.2$ --$\eta_M = 0.3$

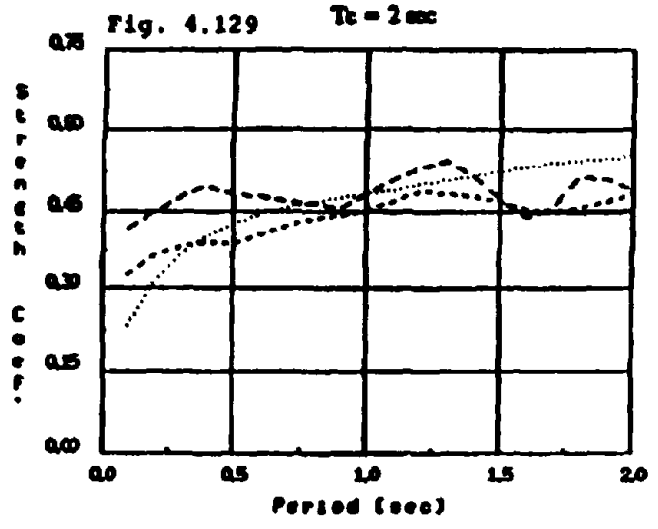

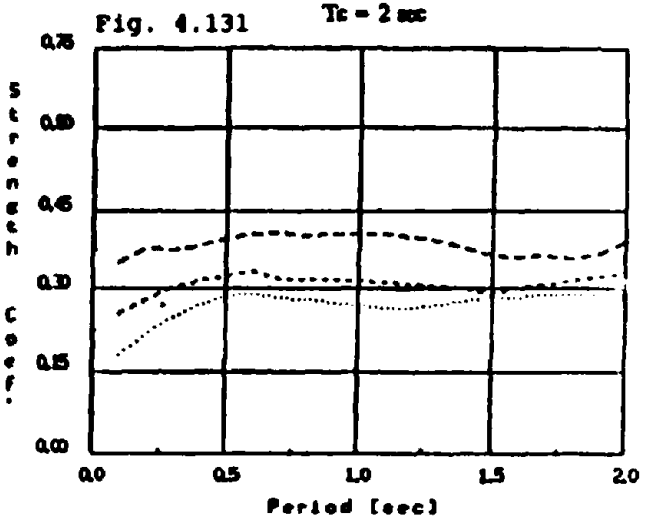

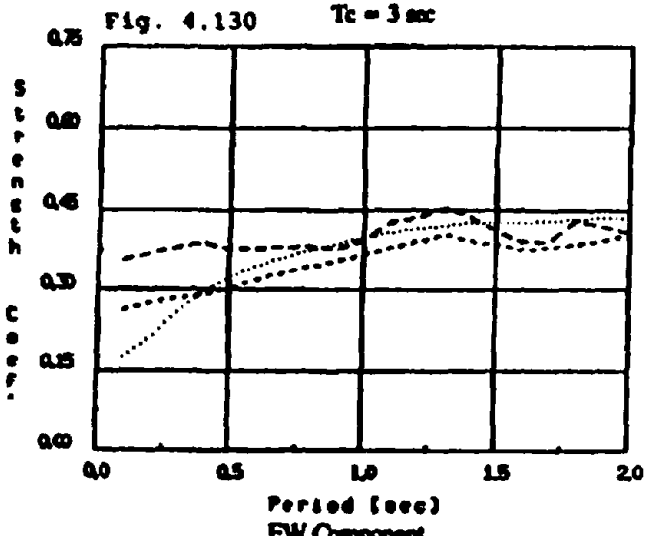

EW Component

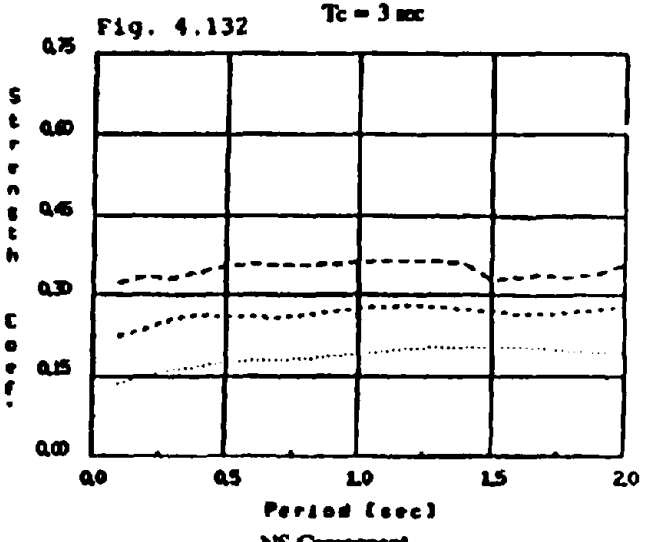

NS Component

Figs. 4.129 to 4.132 Structural Strength Coefficient , El Centro 1940, ξ = 5 % ....η_M = 0.1 ...η_M = 0.2 --η_M = 0.3

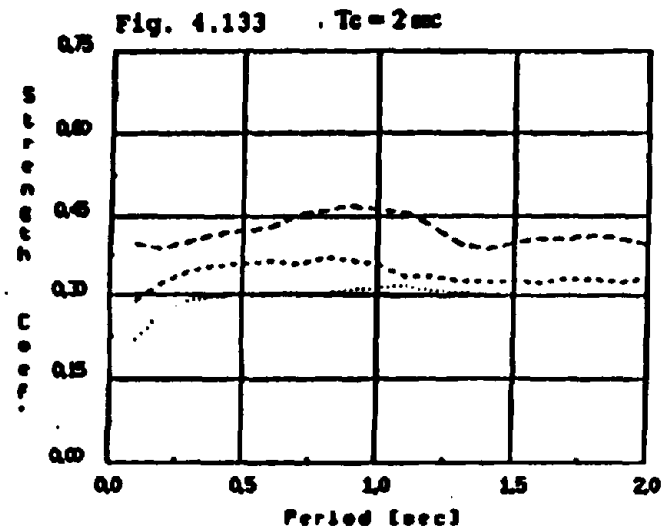

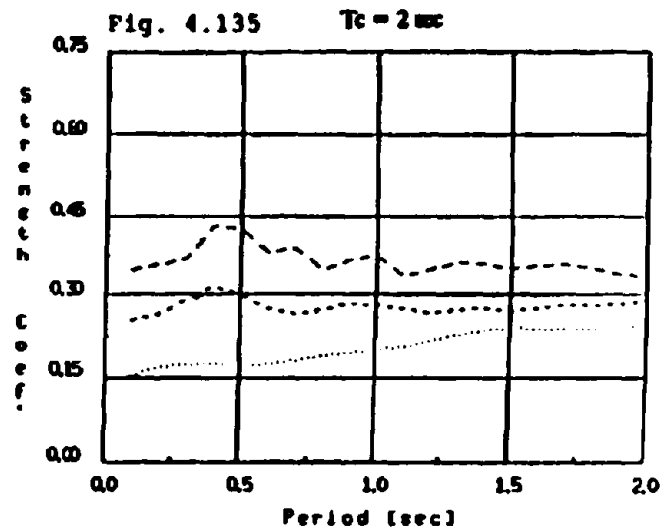

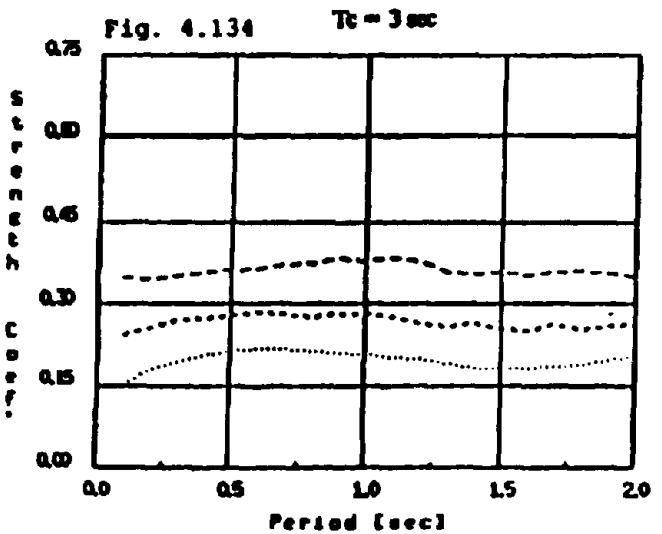

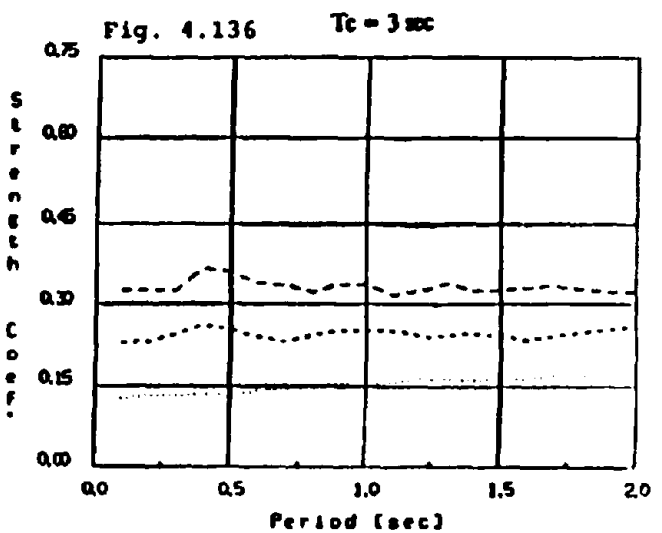

Figs. 4.133 to 4.136 Structural Strength Coefficient , Olympia 1949, $\xi = 5\ \%$ ....$\eta_M = 0.1$ ...$\eta_M = 0.2$ _ _$\eta_M = 0.3$

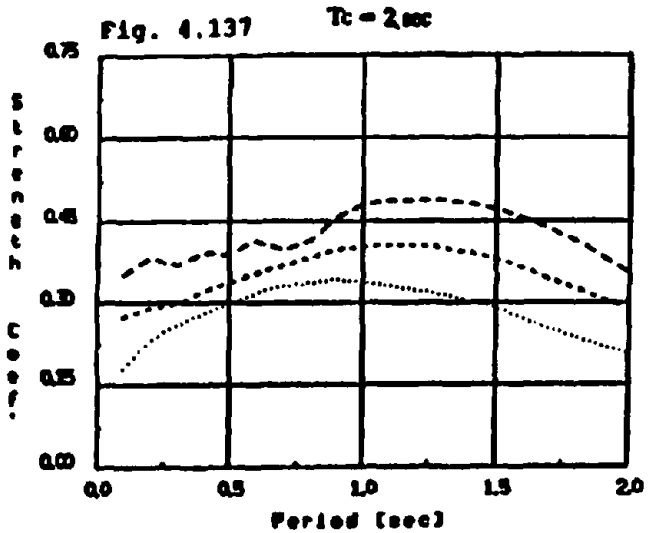

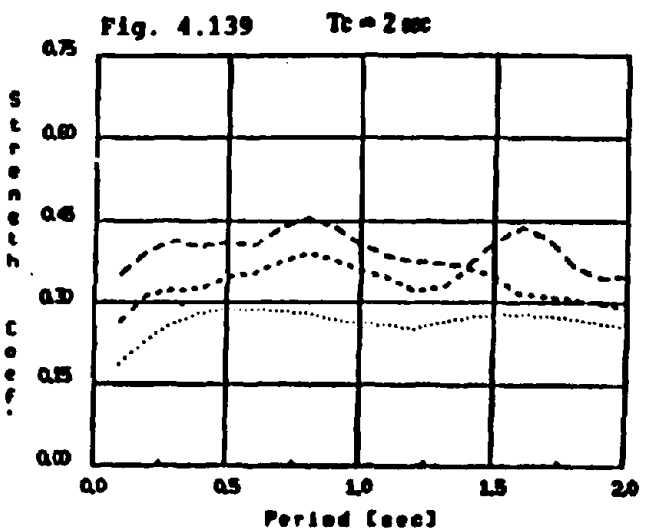

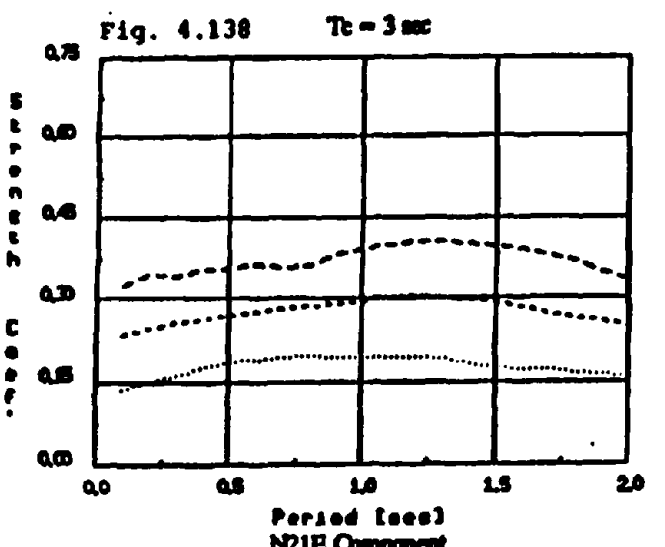

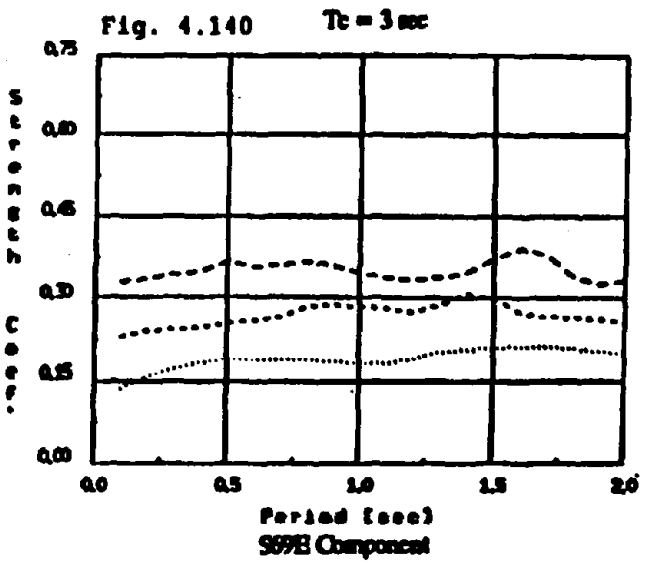

Figs. 4.137 to 4.140 Structural Strength Coefficient, Taft 1952, $\xi = 5\%$ ....$\eta_{sf} = 0.1$ ...$\eta_{sf} = 0.2$ __$\eta_{sf} = 0.3$

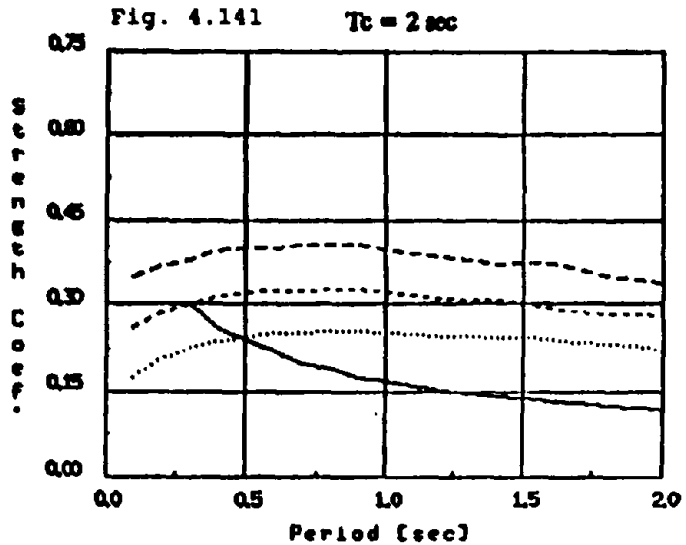

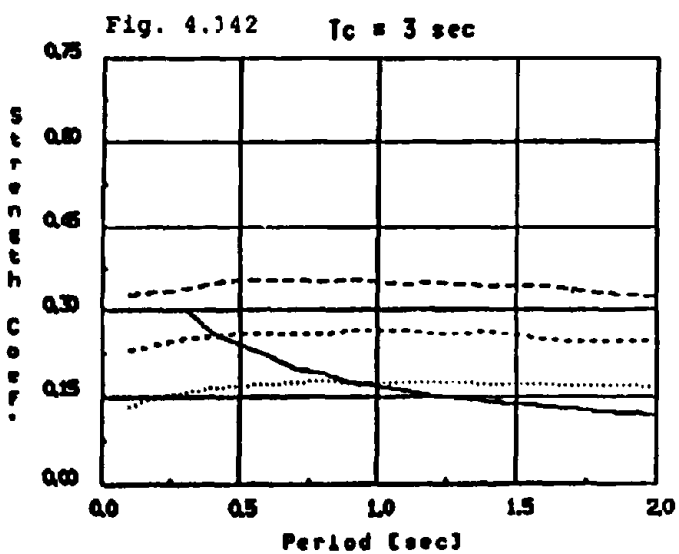

Fig. 4.141 to 4.142 Mean Structural Strength Coefficient

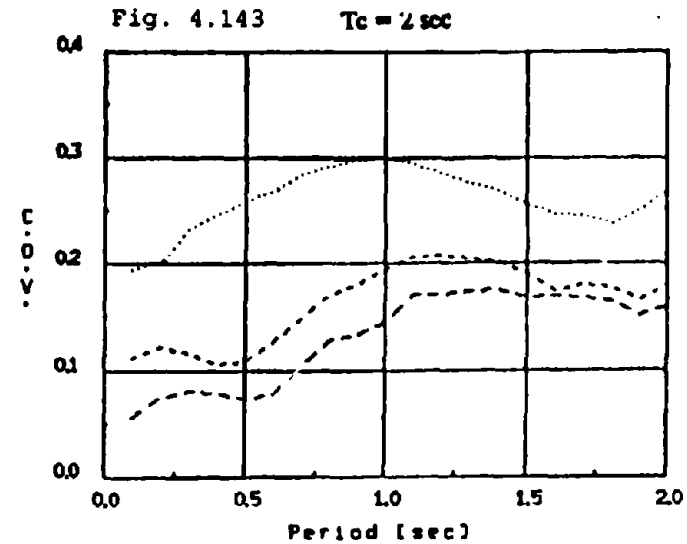

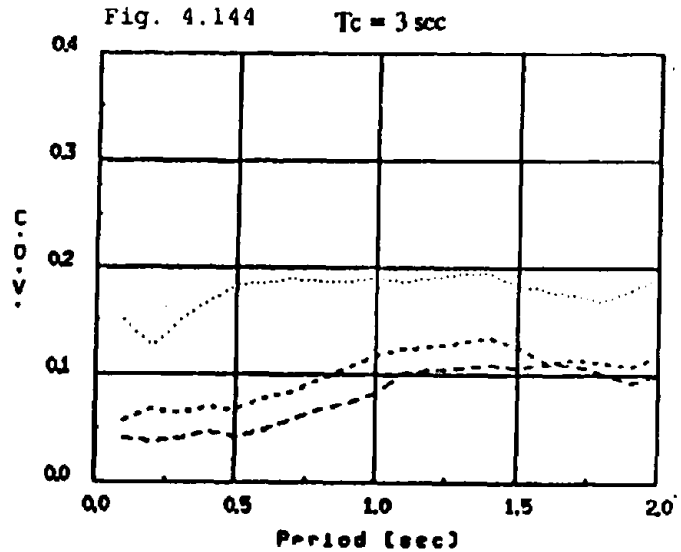

Fig. 4.143 to 4.144 Coefficient of variation

Appendix A

Design and Analysis Calculations, and Analytical Models for the Example Building

Sections

1. Check Original Design
2. Redesign for Isolated Structure
3. Check SEAONC Isolation Guidelines
4. Cost Estimates
5. Dynin Model of Non-Isolated and Isolated Buildings
6. Response to Magnitude 5 Earthquake
7. Response to Magnitude 6 Earthquake
8. Response to Magnitude 7 Earthquake
9. Damage Estimates

Section 1: Check Original Design

CHECK ORIGINAL DESIGN OF OPERATIONS BUILDING

DESIGN OF THE NON-ISOLATED STRUCTURE

DESIGN CRITERIA - UBC 1985

$V = ZIKCSW$ $\quad Z=1.0 \quad K=0.67$
$I=1.5 \quad CS=0.14$

$V = 1.0[1.5][0.67][0.14]W = 0.14W$

DESIGN OF MOMENT FRAME

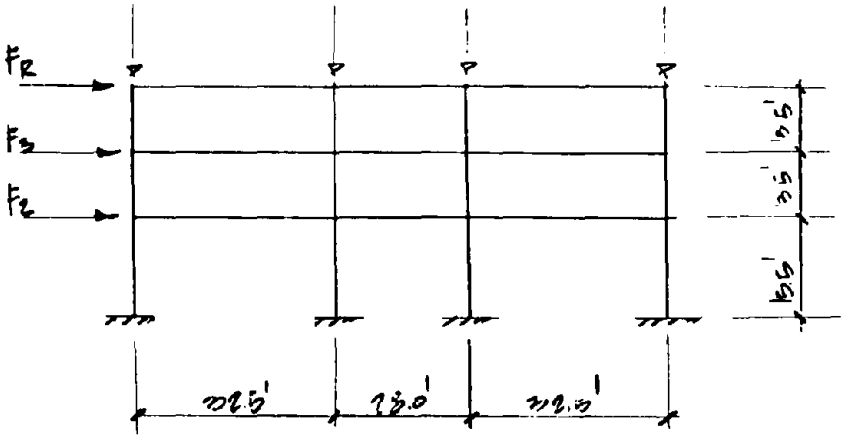

TRIBUTARY AREA PER FLOOR = 5700^{ft^2}/FRAME

$$\text{ROOF} = 98[5700] = 558^k$$
$$3^{RD} = 103[5700] = 587$$
$$2^{ND} = 103[5700] = \underline{587}$$
$$1732$$

$V = 0.14[1732] = 243^k$

$F_i = \frac{VwH}{\Sigma wH}$

$F_2 = \frac{243[558][15.5]}{50620} = 42^k$

$F_3 = \frac{243[587][27]}{50620} = 76^k$

$F_R = \frac{243[587][42.5]}{50620} = 119^k$

Design Moment Frame

BEAM W30-116 $I_b = 4930\ in^4$

COLUMN W24x146 $I_{c_1} = 5630\ in^4$

WEAK COLUMN W8x18x3/4 $I_{c_2} = 2[15(0.75)][9]^2 + \frac{8^3(1.50)}{12} = 2916\ in^4$

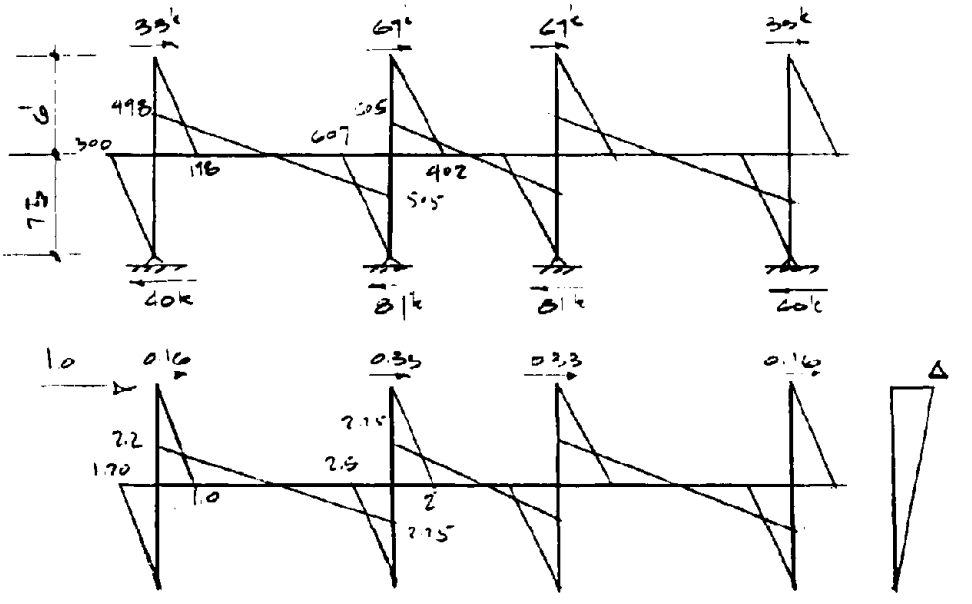

$$\Delta = 2\left[\frac{\Sigma M_m}{EI_c} + \frac{\Sigma M_n}{EI_b}\right]$$

$$= 2\left[\frac{300[7.5]}{2EI_{c_2}}[0.80] + \frac{198[6]}{2EI_{c_2}}[0.67] + \frac{607[7.5]}{2EI_{c_1}}[1.67] + \frac{402[6]}{2EI_{c_1}}[1.33]\right.$$

$$\left. + \frac{498[16.5]}{2EI_b}[1.47] + \frac{505[16.5]}{2EI_b}[1.5] + \frac{515[9]}{2EI_b}[1.5]\right]$$

$$= 2\left[\frac{1298}{EI_{c_2}} + \frac{5405}{EI_{c_1}} + \frac{17591}{EI_b}\right]\left[\frac{1}{29000}\right]$$

$$= 2\left[\frac{1298}{2916} + \frac{5405}{5630} + \frac{17591}{4930}\right]\left[\frac{1}{29000}\right] = 0.593''.$$

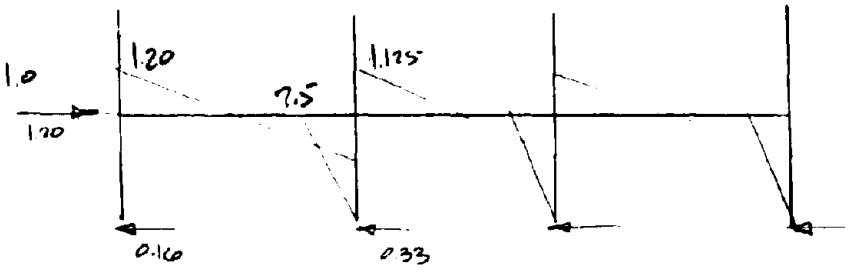

$$\Delta = 2\left[\frac{300[7.5]}{2EI_{c_2}}[0.80] + \frac{600[7.5]}{2EI_{c_1}}[1.67] + \frac{505[16.5]}{2EI_b}[0.75][2] + \frac{505[14.0]}{2EI_b}[0.15]\right]$$

$$= 2\left[\frac{900}{EI_{c_2}} + \frac{3801}{EI_{c_1}} + \frac{8700.}{EI_b}\right]$$

$$= \frac{2}{29000}\left[\frac{900}{2916} + \frac{3801}{5690} + \frac{8980}{4930}\right][1728] = 0.33''$$

FIRST LEVEL

$\Delta_1 = 0.33[2] = 0.66''$ $\quad \simeq 0.005 H_k = 0.005[15][0.67][12]$

$= 0.61''$ UBC Allowable Drift

ok

SECOND LEVEL

$\Delta_2 = [\Delta - \Delta_1] \times 2 = [0.513 - 0.33] \times 2 = 0.52''$

$\simeq 0.005 H_k = 0.005[13][0.67][12]$

$= 0.52''$ UBC Allowable Drift

ok

Check capacity of beam

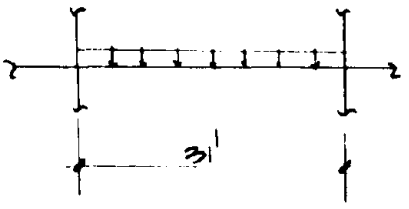

w = 1750 #/'
L 1155 #/'
2905 #/'

$M = \frac{wL^2}{12} = \frac{2905[31]^2}{12} = 233^{k'}$

$M_{beam} = 505^{k'}$

$M_{total} = 233 + 505 = 738^{k'}$

$S = \frac{M}{S} = \frac{738[12]}{1.33[0.66][36]} = 280^{in^3}$

W30x116 $S = 329 in^3$ ok

Section 2: Redesign for FPS Isolated Structure

RE-DESIGN OPERATIONS BUILDING FOR REDUCED STRUCTURAL STRENGTH REQUIREMENTS FOR ISOLATED STRUCTURE

REQUIRED BASE SHEAR WITH FPS

$V = ZIKCSW$ $\quad Z = 1.0$ $\quad I = 1.5$ $\quad K = 0.67$ $\quad S = 1.5$ $\quad T = 2.29 sec.$

$$C = \frac{1}{15\sqrt{T}} = \frac{1}{15\sqrt{2.29}} = 0.0444$$

$$V = 1.0[1.5][0.67][0.044][1.5] = 0.067W$$

Design of Moment Frame

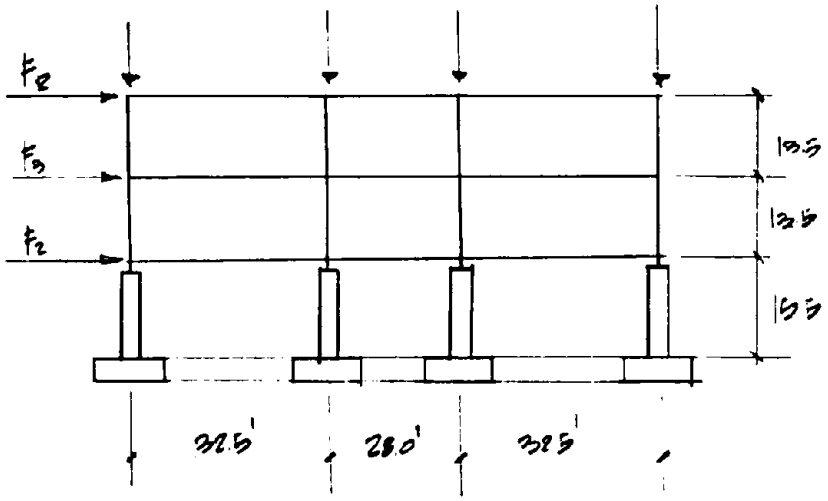

$V = 0.067W$ AREA PER FLOOR = $60 \times 95 = 5700\ ft^2$ / FRAME

ROOF = 98 [5700] = 558
3RD = 103 [5700] = 587
2ND = 103 [5700] = 587
1732

$V = 0.067 [1732] = 116^k$

$F_i = \frac{V w_i h_i}{\Sigma w_i h_i}$ $\Sigma w_i h_i = 50620$

$F_2 = \frac{116 [558][15.5]}{50620} = 20^k$

$F_3 = \frac{116 [587][29]}{50620} = 39^k$

$F_R = \frac{116 [587][42.5]}{50620} = 57^k$

DESIGN MOMENT FRAME PORTAL FRAME ANALYSIS (SHORT DIRECTION)

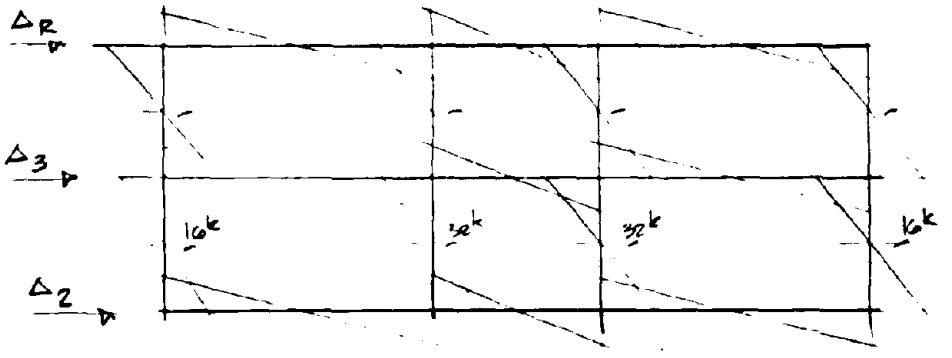

BEAMS W21×84 $I_b = 2850\ in^4$

COLUMN W21×111 $I_c = 2670\ in^4$

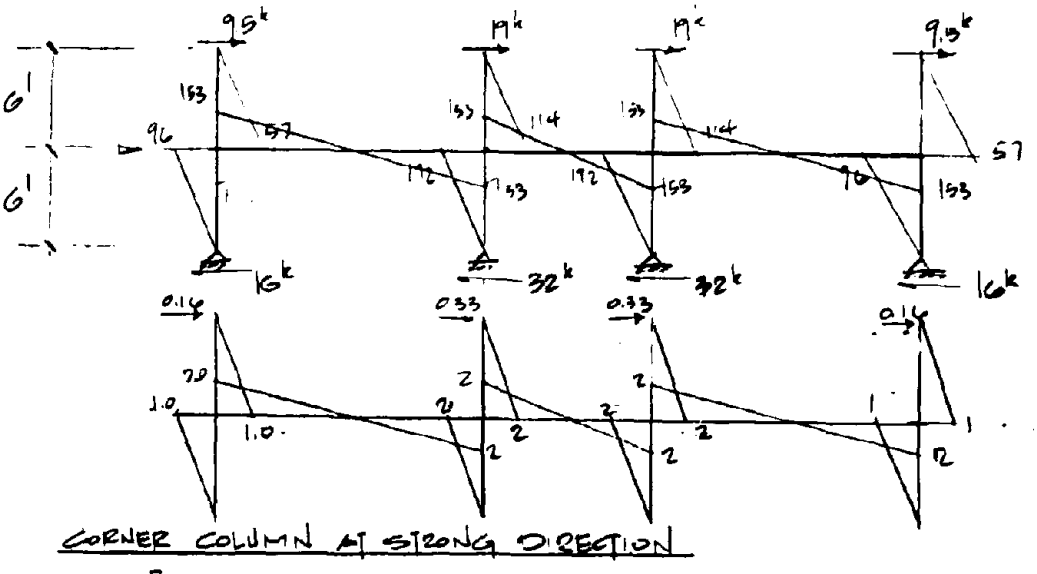

CORNER COLUMN AT STRONG DIRECTION

$$\Delta_3 = 2\left[\frac{\Sigma M_m}{EI_c} + \frac{\Sigma M_m}{EI_b}\right] \quad \text{(DRIFT AT 3RD FLOOR)}$$

$$= \frac{2}{E}\left[\frac{1}{I_c}\left[\frac{57[6]}{2}[0.66] + \frac{114[6]}{2}[1.32] + \frac{96[6]}{2}[0.66] + \frac{192[6]}{2}[1.32]\right]\right.$$

$$\left. + \frac{1}{I_b}\left[\frac{153[165]}{2}[132] + \frac{153[16.5]}{2}[1.32] + \frac{153[14]}{2}[1.32]\right]\right]$$

$$= \frac{2}{E}\left[\frac{1515}{I_c} + \frac{4745}{I_b}\right][1728] = \frac{2}{29000}\left[\frac{1515}{2670} + \frac{4745}{2850}\right][1728]$$

$\Delta_3 = 0.26\text{IN} < 0.005HK = 0.005[15][12][0.6] = 0.52$ IN. ok

DESIGN OF MOMENT FRAME (LONG DIRECTION)

SOME COLUMNS ARE ORIENTED IN THE WEAK DIRECTION

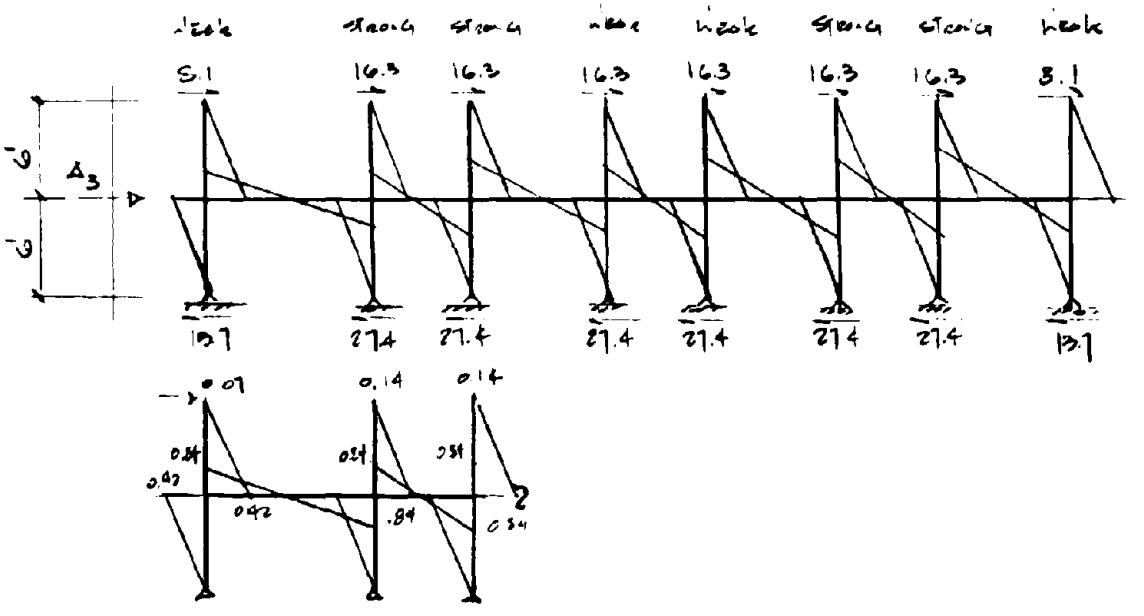

$$\Delta_3 = \left[2\left[\frac{48.6[6]}{2EI_{cy}}[0.28] + \frac{82.2[6]}{2EI_{cy}}[0.28]\right] + 2\left[\frac{97.2[6]}{2EI_{cy}}[0.56] + \frac{[164][6]}{2EI_{cy}}[0.56]\right.\right.$$

$$\left. + 4\left[\frac{97.2[6]}{2EI_{cx}}[0.56] + \frac{164[6]}{2EI_{cx}}[0.56]\right] + 8\left[\frac{131[16.5]}{2EI_b}[0.56]\right]\right.$$

$$\left. + 6\left[\frac{131[14]}{2EI_b}[0.56]\right]\right]$$

$$= \left[\frac{1097}{I_{cy}} + \frac{1755}{I_{cx}} + \frac{7923}{I_b}\right]\frac{[1728]}{E}$$

$$\Delta_3 = \left[\frac{1097}{274} + \frac{1755}{2670} + \frac{7923}{2850}\right]\frac{[1728]}{27000} = 0.44 \text{ IN}$$

$$< 0.005 H_t = 0.005[12][0.67]$$

$$= 0.52 \text{ IN.}$$

Check capacity of beam

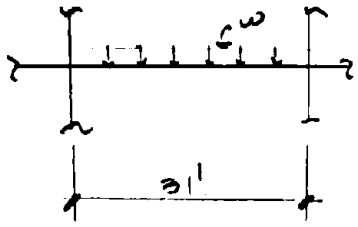

w D [103][16.5] + 100 = 1760 #/'
L [100][16.5] 0.70 = 1155 #/'
2905 #/'

$M = \frac{wL^2}{12} = \frac{2905[31]^2}{12} = 233^{k'}$

$M_{SEISMIC} = 164^{k'}$

$M_{TOTAL} = 233 + 164 = 397^{k'}$

$S = \frac{M_I}{f_b} = \frac{397[12]}{1.33[0.66][36]} = 150^{IN^3}$

W27 x 84 $S = 196^{IN^3}$ ok

CHECK CONCRETE COLUMN (INTERIOR COLUMN)

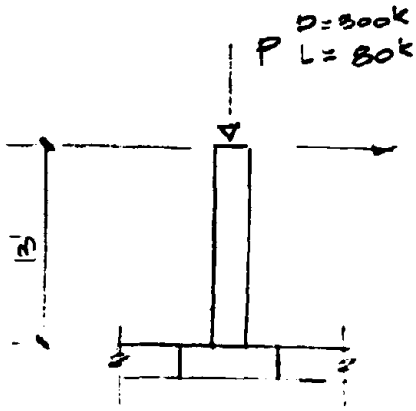

2 x BOLSTER REQUIRED

$F = 0.133[300] = 40^k$

$M = 40[13] = 520^{k'} \Rightarrow 6240^{k''}$

$e = \frac{6240}{300} = 20.8''$

USE 30" x 30" CONCRETE COLUMN

$e = 20''$ $\phi P_n = P_u = 710^k$

$f'_c = 4000$ psi 12-#11 $P_D = \frac{710}{1.4} = 507^k > 300^k$ ok

$P_{D+L} = \frac{710}{1.5} = 473^k > 380^k$ ok

CHECK SLENDERNESS

$M_c = S_b M_{2b} + S_s M_{2s}$

$P = 1.4[D] = 1.4[300] = 420^k$
$0.75[1.4D + 1.7L + 1.6E] > 417^k$

$P_c = \frac{\pi^2 EI}{[kl_u]^2} = \frac{\pi^2[3000][615000]}{[2[13-12]]^2[3.5]}$ $EI = \frac{E_c I_g/2.5}{1+\beta_d}$

$= 5868^k$

$S_s = \frac{1}{1 - \frac{\Sigma P_u}{\phi \Sigma P_c}} = \frac{1}{1 - \frac{420}{0.70[5868]}} = 1.11$

$M_c = S_s M_{2s} = 1.11[1.4[6240]] = 9696$

$e = \frac{M}{P} = \frac{9696}{420} = 23''$

FOR 30" x 30" CONC. COL $f'_c = 4000$ psi 12-#11 EA FACE

$e = 24''$ $\phi P_n = P_u = 579^k > 420^k$ ok

CHECK CONCRETE COLUMN ST SIDE

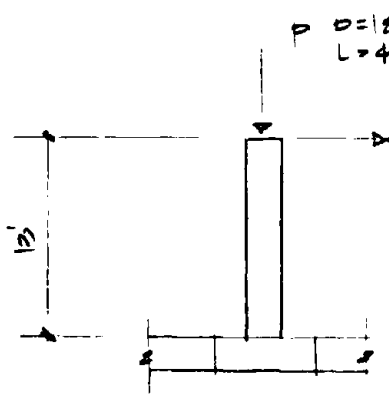

$F = 0.133[180] = 24^k$

$M = [24][13] = 312^{k'} \Rightarrow 3744^{k''}$

$e = \frac{M}{P} = \frac{3744}{180} = 21''$

USE 26" x 26" REINFORCED CONC. COLUMN

$f'_c = 4000$ psi $e = 25''$ $\phi P_n = 317^k$

$\frac{\phi P_n}{1.4} = \frac{317}{1.4} = 222^k > 180^k$

OK

DESIGN GRODE BM.

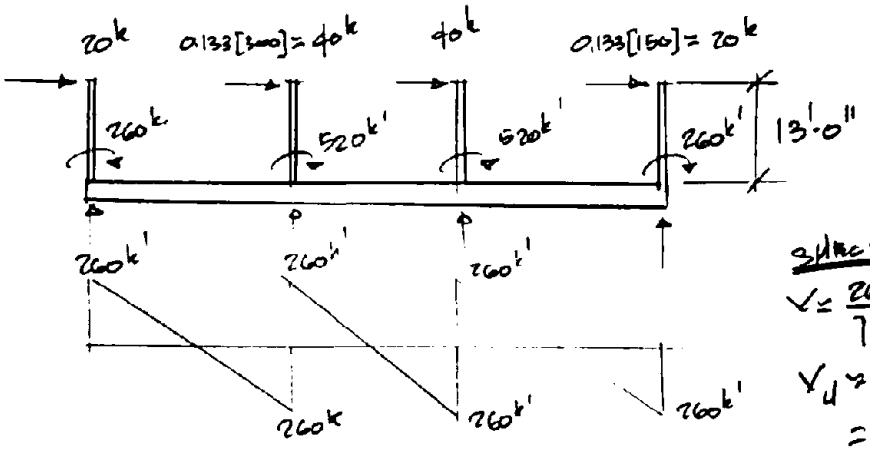

SHEAR

$V = \frac{260}{12} = 22^k$

$V_u = [1.4][22]$

$= 30.8^k$

$V_c = 2\sqrt{f'_c}\, b w d \phi$

$= 0.85(2)\sqrt{4000}\,[24][27]$

$= 69^k$

USE #3 STIRRUP @ 24" o.c.

DESIGN GROOE BM => USE 2'-0" x 2'-6"

$U = 0.75[1.4D + 1.7L + 1.87E]$

$M_u = 1.4E$

$M'_u = 1.4[760] = 364^{k'} \Rightarrow 4368^{k''}$

$\frac{M_u}{\phi} = A_s f_y \left[d - \frac{0.59 A_s f_y}{b f'_c}\right]$

$\frac{4368}{0.9} = [27][60]A_s - \frac{0.59[60]^2 A_s^2}{[24][3]}$

$5964 = 1620 - 29.5 A_s^2$

$29.5A_s^2 - 1620 + 5964 = 0$

$x = \frac{-b \pm \sqrt{b^2 - 4ac}}{2a}$

$A_s = \frac{1620 \pm \sqrt{[1620]^2 - 4[29.5][5964]}}{2[29.5]} = 3.97\ in^2$

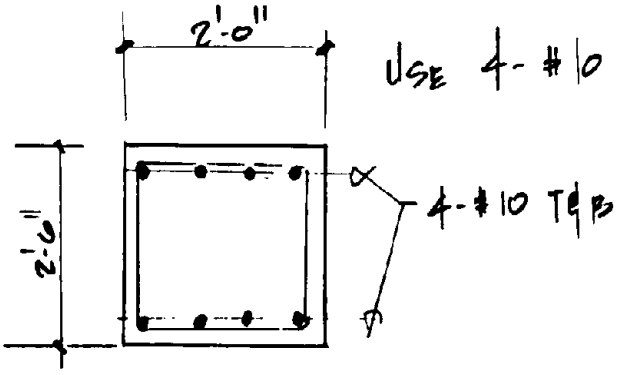

USE 4-#10 $A_s = 5.08\ in^2$

Check Deflection of Grade Bm & Column

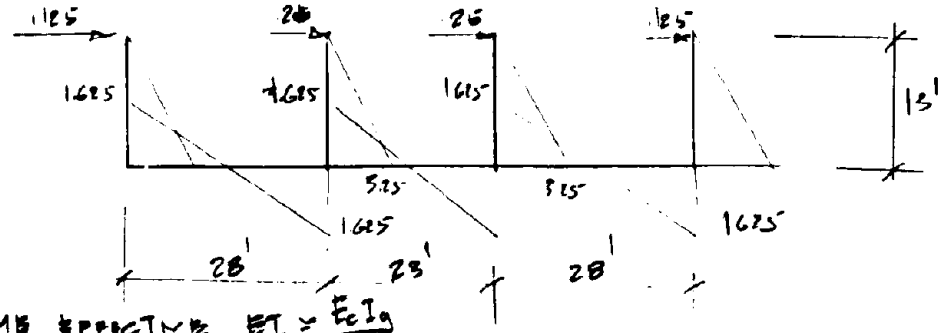

Assume effective $EI = \frac{E_c I_g}{2}$

EI column $C_1 = 3000\left[\frac{26[26]^3}{12}\right]^{1/2} = 37{,}122{,}000\ in^4$ EI_1

EI column $C_2 = 3000\left[\frac{30[30]^3}{12}\right]^{1/2} = 101{,}250{,}000\ in^4$ EI_2

EI Grade Bm $= 3000\left[\frac{24[30]^3}{12}\right]^{1/2} = 81{,}000{,}000\ in^4$ EI_3

$$\Delta = 2\left[\frac{260[13]}{2EI_1}[1.08] + \frac{260[14]}{2EI_3}[1.08][12] + \frac{260[11.5]}{2EI_3}[1.08] + \frac{[520][13]}{2EI_2}[2.16]\right][1728]$$

$= 0.5872^{11} \approx 0.005H = 0.005[13][12][0.67] = 0.523^{11}$

ok

Section 3: Check SEAONC Isolation Guidelines

CHECK REQUIREMENTS OF SEAONC
1990 TENTATIVE SEISMIC ISOLATION GUIDELINES

Location of PG&E Building

Assume Soil Type S1

Fault	Distance	Magnitude	MM
San Andreas Fault	8.0 Miles	8.3	XII
Hayward Fault		7.0	

Using Tentative Seismic Isolation Design Requirement

SECTION 3

$T_{structure} = 0.40$ sec.

Site Coeff.	$S = 1.0$
Near Field Response	$N = 1.0$
Seismic Zone	$Z = 0.4$
Weight	$W = 6126^k$

$k = \frac{W}{T} = \frac{W}{41.5} = 0.02W$

Assume $D = 5.0''$ $V = 0.20W$

$k_{eff} = \frac{0.20W}{5} = 0.04W$

$T = 2\pi\sqrt{\frac{W}{k_{eff}\,g}} = 1.60$ sec.

$\beta = \frac{\text{Area Hys}}{2\pi k_{eff}[D]^2} = \frac{4[0.1][5.0]W}{2\pi[0.04]W[5.0]^2} = 0.32$ $\quad B = 1.7$

$b = \frac{10ZNST}{B} = \frac{10[0.4][1.0][1.0][1.6]}{1.7} = 3.76''$

Try $D = 4.0''$ $V = 0.18W$ $k_{eff} = 0.045$ $T = 2\pi\sqrt{\frac{W}{0.045W386}} = 1.50$ sec.

$b = \frac{10[0.4][1.0][1.0][1.50]}{1.7} = 3.60'' \doteq 4.0''$ ok.

Design Data for Structure

$$V_s = \frac{2L_{max}}{F_H} = \frac{\pi[0.05][4]}{2} = 0.45.1$$

Torsional Deflection

$$\rightarrow D_t = 1200\frac{1}{[1+D/C]} = 12[0.05]40\frac{1}{[1+[0.05]^2/12]} = 0.20''$$

Use $D + D_t = 4.00 + 0.20 = 4.20''$

For Torsion Equation See Torsion Section

Result: Design Parameters for FMS Isolator.

$T_{FMS} = 2.25$ sec. Coefficient of Friction = 0.045W

Travel = 4.20 in.

Estimated Construction Cost of Non-Isolated Building $6.5 million

Savings In Steel (Isolated Building)

STEEL REQUIRED WITHOUT FPS

COLUMNS

16 - W24×146 @ 46.5'	=	108624#
8 - 18" dia × 3/4" - 86#/' @ 46.5'	=	69192
8 - W14×90 @ 42.5'	=	30600
		208416#

BEAMS

24 - W30×116 @ 30'	=	83520
16 - W30×116 @ 25'	=	46400
12 W24×76 @ 30'	=	27360
8 W24×76 @ 25'	=	15200
		172480#

TOTAL = 380896#

STEEL REQUIRED WITH FPS

COLUMNS

24 - W21×111 @ 29'	=	77256
8 - W14×68 @ 29'	=	15776
		93032#

BEAMS

24 - W27×84 @ 30'	=	60480
16 - W27×84 @ 25'	=	33600
12 - W24×62 @ 30'	=	22320
8 - W24×62 @ 25'	=	12400
		128800#

TOTAL = 221832#

SAVINGS = 380896 − 221832 = 159064#

70,000# FROM ELIMINATING 1ST LEVEL COLUMNS

Cost Estimates

Prices from National Construction Estimator 1988

Cost Saving in Steel

Erect. steel = $0.80 per pound => $1600/ton Material

Total savings = $0.80[159064] = $127,251 Material

Addition cost of

12 - 30" x 30" x 13'-0" concrete col.
20 - 24" x 24" x 13'-0" concrete col.

Assume cost of $600 cu. yd. - Installation cost. [Material, Labor]

Vol. concrete = $[2.5]^2[13][12] = 975$ cu ft.
$[2.0]^2[13][20] = 1040$ cu. ft.
2015 cu ft = 75 cu yd

Total cost = 600[75] = $45,000

Cost of FPS Isolators

Cost per Isolator = $2000

32 Isolator.

Cost = 32 [2000] = $64,000

GRADE BM & TIE BMS & FOUNDATION.

WITHOUT FPS

GRADE BMS.

$4 - 2'-6'' \times 3'-6'' \times 79'-0'' = 2765$ cu. ft.
$2 - 2'-6'' \times 3'-6'' \times 100'-0'' = 2800$
5565

TIE BMS.

$4 - 2'-0'' \times 2'-0'' \times 77'-0'' = 1232$
$2 - 2'-0'' \times 2'-0'' \times 179'-0'' = 1432$
2664

TOTAL = 8229 cu ft.

WITH FPS

GRADE BMS

$8 - 2'-0'' \times 2'-6'' \times 78'-0'' = 3120$ cu. ft.
$4 - 2'-0'' \times 2'-6'' \times 170'-0'' = 3400$
6520

SAVINGS = 8229 - 6520 = 1709 cu ft

⇒ 63.3 cu. yd @ $400 cu. yd

SAVING. = $400 [63.3] = $25318

BOSNG . THE DEEP PILE CAP AT MOMENT FRAME.

DEEP PILE CAP

$24 - 2'-0'' \times 6'-0'' \times 2'-0'' = 576$ cu ft.

⇒ 21.3 cu yd @ $400 cu. yd.

SAVINGS = $400 [21.3] = $8432

ADDITIONAL ARCHITECTURAL COST

BRACING AT TOP OF COLUMNS TO LATERALLY SUPPORT EXTERIOR ARCHITECTURAL PANEL

2 - C12×30 @ 90' = 5400

2 - C12×30 @ 100' = 12000

17400

STEEL @ $1600/Ton

COST = 0.80 [17,400] = $13,920

USE $15,000

STRUCTURAL COST SUMMARY

SAVINGS

	COST
1. ELIMINATION OF FIRST LEVEL STEEL COLUMNS.	$56,000
2. REDUCE STEEL SIZE DUE TO REDUCTION IN LATERAL LOAD	$71,250
3. REDUCING SIZE OF PERIMETER GRADE BM, ELIMINATING TIE BM AND REPLACING THEM WITH GRADE BM	$25,318
4. RESIZING PILE CAPS AT MOMENT FRAME	$8,432
	$161,000

COST

1. 32 - FPS ISOLATORS	$64,000
2. 12 - 30" x 30" x 15'-0" CONC. COL. 20 - 24" x 24" x 15'-0" CONC. COL.	$45,000
3. 1ST LEVEL BRACING FOR EXTERIOR ARCHITECTURAL PANEL.	$15,000
	$124,000

NET STRUCTURAL SAVINGS

$161,000 - $124,000 = **$37,000**

SUMMARY OF SAVINGS

1. ELIMINATION OF STEEL COLUMN AT FIRST LEVEL
2. REDUCTION IN LATERAL FORCES REDUCE MEMBER SIZES OF MOMENT FRAME
3. REDUCE SIZE OF INTERIOR STEEL COLUMN BY ELIMINATING ONE LEVEL OF LOADING
4. ELIMINATED THE SPECIAL 18×18×3/4 STEEL COLUMN.
5. ELIMINATE THE FIXED BASE STEEL COL. TO CONCRETE CONNECTION.
6. SWITCHING FROM PRESENT GRADE BM @ TIE BM TO ALL GRADE BM.
7. RAISING IN DEEP PILE CAP AT THE MOMENT FRAME.

SUMMARY OF ADDITIONAL COST

1. 34 FPS ISOLATORS
2. NEW 30"×30" & 24"×24" CONC COL.
3. SEISMIC ISOLATION JOINT AT TOP OF FIRST LEVEL
4. ELEVATOR AND STAIR DETAIL TO ACCOMMODATE 6" TO 8" OF MOVEMENT
5. CEILING, PARTITION, ARCHITECTURAL FACIAL CONNECTION, FLEXIBLE PIPES.

ARCHITECTURAL COST SUMMARY

1. ELEVATOR - 2- W8x15 - 9'-6" ($1.60/lb) — $400
4- 3"SQ THKNG x 18'-0" ($1.60/lb) — 870
ADDITION HOTEL STUD — 400
DEEPER FOUNDATION ($400/cu yd) — 800
$2530

2. STAIRS. - THREE STAIRS.
- 6-3"ϕ THKNG x 15'-0" ($1.60/lb) — $1090
- 3-C12x20.7 x 6'-0" ($1.60/lb) — 600
$1690

3. EXPANSION GAP MATERIAL AROUND BUILDING
NEOPRENE GASKET 1/2"x8"
650 FT ($6.00/FT) — $3900

4. BRACING FOR INTERIOR PARTITIONS — $4000

5. MOULDING FOR HUNG CEILING.
($3/FT) - 1000 FT — $3000

7. FLEXIBLE PIPES & CONDUIT — $1000

8. SEISMIC GAP
ELEVATOR-STEEL ANGLE @ $20/FT. — $880
(44 FT)
$17000

NET SAVING STRUCTURAL & ARCHITECTURAL
$37,000 - $17,000 = $20,000

ASSUMING CONTINGENCY & MISCELLANEOUS COST
≈ $20,000

Net Savings / Cost $0

DYNIN MODEL OF OPERATIONS BUILDING (NON-ISOLATED & ISOLATED)

FULL STRENGTH BUILDING

BUILDING WEIGHT (AREA = 97' x 217') = 21049 ft²

ROOF	TYPICAL ROOF	87[21049] =	1831 k
	MECHANICAL	=	95 k
	EXTERIOR FACIAL	=	71 k
			1997 k
3RD FLR	TYPICAL FLOOR	95(21049) =	1999
	EXTERIOR FACIAL	=	92
			2091 k
2ND FLR	TYPICAL FLOOR	=	1999
	EXTERIOR FACIAL		92
			2091 k
	TOTAL		6179 k

4088

STRUCTURAL MODEL

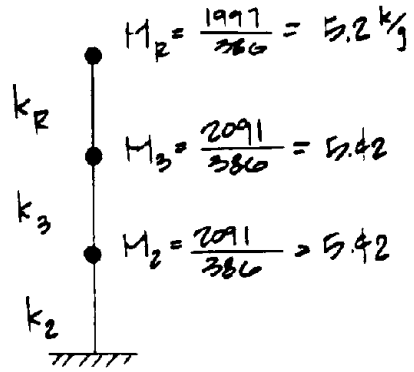

$V_R = 1376^k$ $\quad k_R = 1333$ k/in

$V_3 = 2324^k$ $\quad k_3 = 1544$ k/in

$V_2 = 2804^k$ $\quad k_2 = 1472$ k/in

DETERMINE THE STIFFNESS

NON-ISOLATED

$k_2 = \frac{243}{0.66} = 368$ k/in $\times 4 = 1472$ k/in [SEE CALCULATIONS]

$\Delta_3 = 0.52$

$k_3 = \frac{201}{0.52} = 386\ ^k/_{IN} \times 4 = 1544\ ^k/_{IN}$

ESTIMATE STIFFNESS OF ROOF

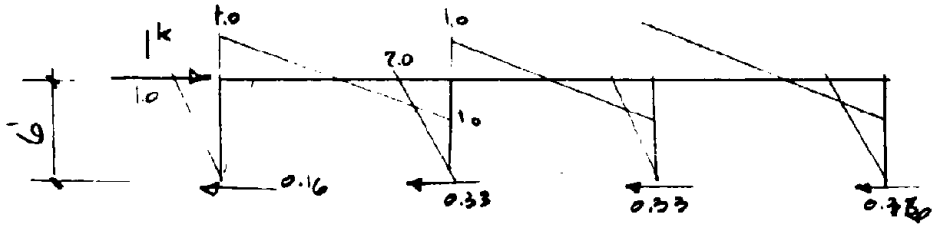

COLUMN W24×146 $I = 5630^{IN^4}$
18.18×3/4" $I = 7916^{IN^4}$

BEAM W24×76 $I = 2100$

$$\Delta = 2\left[\frac{1.0[6]}{2EI_{c_1}}[0.67] + \frac{2.0[6]}{2EI_{c_2}}[1.34] + \frac{2[1.0][16.5]}{2EI_b}[0.67] + \frac{1.0[14]}{2EI_b}[0.67]\right]$$

$$= \frac{2}{29000}\left[\frac{2.01}{7916} + \frac{8.04}{5630} + \frac{15.74}{2100}\right][1728] = 0.0015$$

$\Delta_R = 2\Delta = 2[0.0015] = 0.0030$

$K = \frac{1}{\Delta_R} 2 \frac{1}{0.0030} \times 4 = 1333\ ^k/_{IN.}$

DETERMINE STRENGHT CAPACITY OF MOMENT FRAME

CHECK ONE MECHANISM

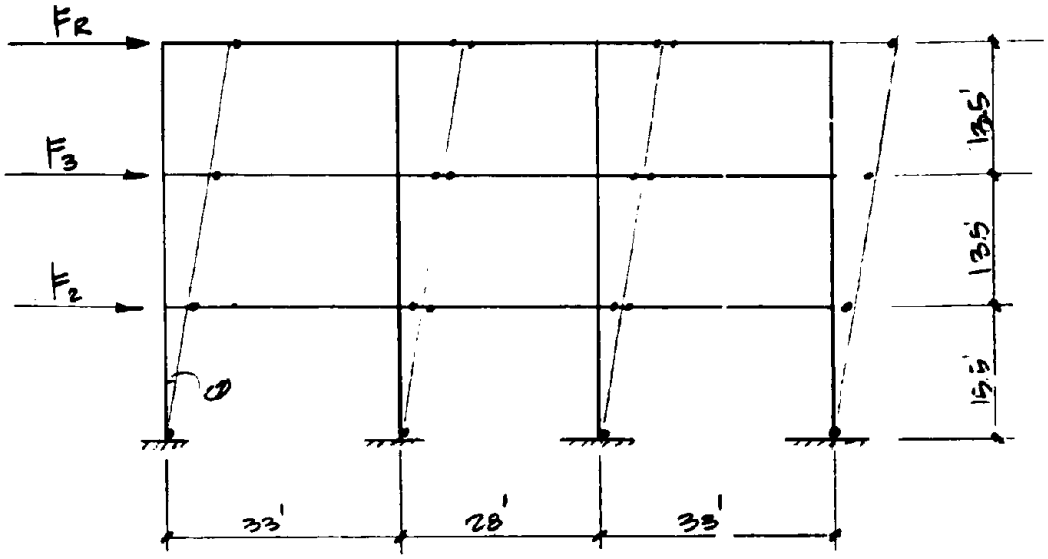

BEAM W30×116 $M_p = 1130^{k'}$
W24×76 $M_p = 600^{k'}$

COLUMN W24×146 $M_p = 1250^{k'}$
18×18×3/4 $Z' = \frac{[18]^3}{4} - \frac{[16.5]^3}{4} = 335^{in^4}$ $M_p = 1005^{k'}$

STEEL $F_y = 36^{ksi}$

$F_3 = 0.69 F_R$ $F_2 = 0.35 F_R$ => BASE ON. $F_i = \frac{\sum w_i H_i}{\sum_i w H}$

$$F_2[15]\phi + F_3[27](\phi) + F_R[39](\phi) = \left[2M_{pc_1} + 2M_{pc_2} + 6M_{pb_1} + 12M_{pb_2}\right]$$

$$\left[0.35[15] + 0.69[27] + 39\right] F_R = \left[2[1005] + 2[1250] + 6[600] + 12[1130]\right]$$

$$62.88 F_R = 21670^{k'}$$

$$F_R = \frac{21670}{62.88} = 344^{k}$$

Story Shear Loads (Mechanism Loads)

		# of Frame	
$V_2 = 344^k$	$= 344$	$\times 4$	$= 1376^k$
$V_3 = 344 + 0.69[344] = 581$		$\times 4$	$= 2324^k$
$V_2 = 581 + 0.35[344] = 701$		$\times 4$	$= 2804^k$

Plastic Strength of Non-Isolated Building

BASESHEAR CAPACITY $= \frac{2804}{6179} = \boxed{0.45W}$

ISOLATOR PROPERTY

SLIDING PERIOD: 2.25sec

$r = 49.5''$

$k_{FPS} = \frac{W}{r} = \frac{6126}{49.5} = 124^k/IN.$

ESTIMATE THE ELASTIC STRENGTH OF THE NON-ISOLATED BUILDING.

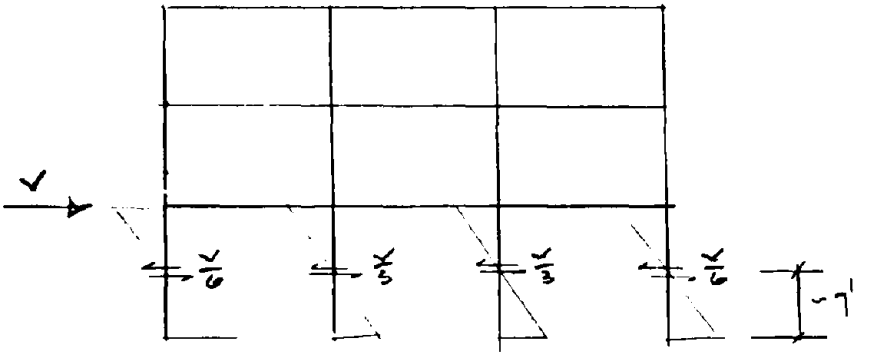

COLUMNS STEEL = ksi

W24×146 $S = 371\ in^3$ $M_y = 371[36] = 13{,}356^{k''} \Rightarrow 1113^{k'}$

18×18×3/4 $S = \frac{[18]^3}{6} - \frac{[16.5]^3}{6} = 223^{in^3}$ $M_y = 223[36] = 8028^{k''} \Rightarrow 669^{k'}$

$\frac{V}{3}[7] = 1113^{k'}$

$V = 477^k \times 4 = 1908^k$

(4 = # of Frame)

$$V = \frac{1908}{6179} = 0.31W$$

DYN'J MODEL OF THE ISOLATED OPERATIONS BUILDING FOR

Cost Equivalent Isolated Design

BUILDING WEIGHT

Roof 1997^k

3RD FLR 2091^k

2ND FLR 2091^k

6179^k

ISOLATOR

SLIDING PERIOD = 2.25 sec

$r = 49.5"$

$K_{FPS} = \frac{W}{r} = \frac{6126}{49.5} = 124^{k/IN}$

$a = \frac{124}{1635} = 0.0758$

TRAVEL DISP = 6.5 IN.

STRUCTURAL MODEL

USE (SHORT DIRECTION)

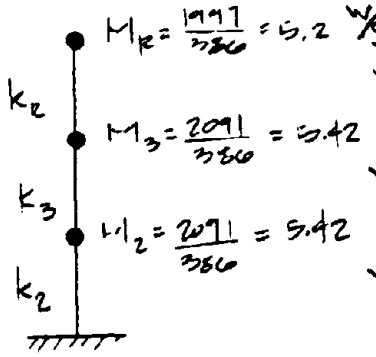

$V_R = 1252^k$ $\quad k_2 = 877^{k/IN}$

$V_3 = 2116^k$ $\quad k_3 = 1477^{k/IN}$

$V_2 = 1970^k$ $\quad k_2 = 1635^{k/IN}$

DETERMINE THE STIFFNESS (ISOLATED) (SHORT DIRECTION)

$k_2 = \frac{120}{0.587} = 204^{k/IN} \times 8 = 1635^{k/IN}$ (SEE CALCULATIONS)

$k_3 = \frac{96}{0.26} = 369^{k/IN} \times 4 = 1477^{k/IN}$

$k_R = \frac{57}{0.26} = 219^{k/IN} \times 4 = 877^{k/IN}$

(LONG DIRECTION)

$k_2 = \frac{120}{0.587} = 204^{k/IN} \times 8 = 1635^{k/IN}$

$k_3 = \frac{192}{0.44} = 436^{k/IN} \times 2 = 871^{k/IN}$

$k_R = \frac{114}{0.44} = 259^{k/IN} \times 2 = 519^{k/IN}$

Plastic Strength Capacity - Cost Equivalent Isolated Design

(LONG DIRECTION)

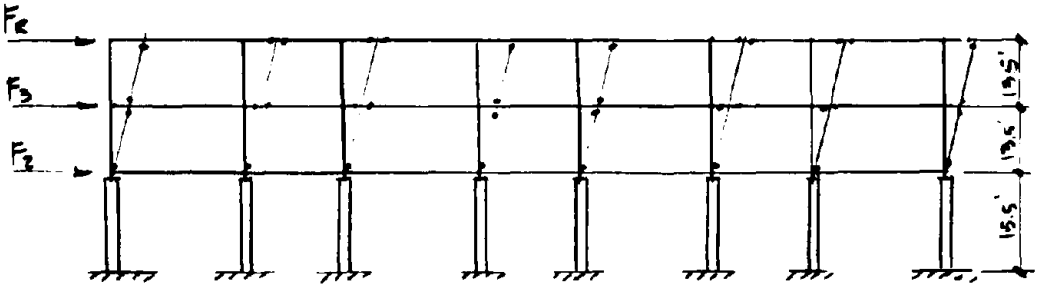

DETERMINE BASE SHEAR CAPACITY OF LOWER CONC. COLUMN.

12 - 30"x30" Conc. Col. $P = 300^k$ $M_n = 481[28] - 300[6]$
12 - #11 Ea. Face $= 11668\ k''$

P =

20 - 26"x26" Conc. Col. $P = 150^k$ $M_n = 317[28] - 150[6]$
12 - #10 Ea. Face $= 7976\ k''$

$$\text{CAPACITY} = \frac{[12[11668] + 20[7976]}{12[13]} = 1920^k$$

$$V = \frac{1920}{6179} = 0.31W$$

LONG DIRECTION FRAME

COLUMN W21x111 STRONG $M_p = 837^{k'}$
WEAK $\ell = 68.2$ $M_p = 68.2[30] = 205^{k'}$

BEAM W27x84 $M_p = 732^{k'}$
W24x62 $M_p = 459^{k'}$

$F_3 = 0.69 F_R$ BASE on $F_i = \frac{\sum w_i h_i}{\sum wH}$

$[0.69F_R][12] + F_R[24] = 8M_{pb_2} + 8M_{pb_1} + 16M_{pc_1} + 4M_{pc_2}$

$32.3F_R = 8[456] + 8[732] + 16[205] + 4[397]$

$F_R = 499^k$

Story Shears (Mechanism Loads)

$V_R = 499^k \quad = 499^k \times 2 = 998^k$

$V_3 = 499 + 0.69[499] \quad = 843^k \times 2 = 1686^k$

$V_2 = \quad = 1920^k$

Plastic Strength

BASE SHEAR CAPACITY $= \frac{1920}{6179} = 0.31W$

STRENGTH CAPACITY (SHORT DIRECTION)

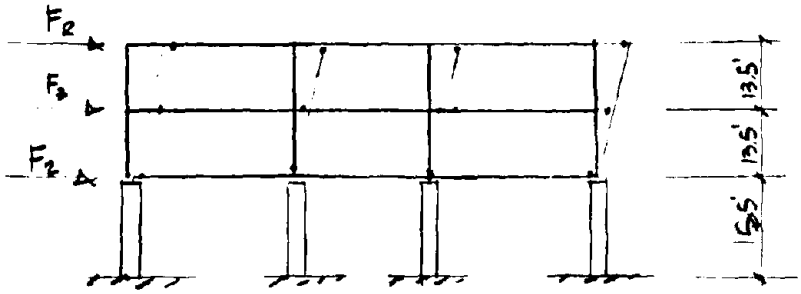

BEAM W 27×84 $M_p = 732^{k'}$
W 24×62 $M_p = 456^{k'}$

COLUMN W 21×111 $M_p = 837^{k'}$

$F_3 = 0.67 F_R$ BASED ON $F_i = \frac{\sum w_i H_i}{\sum w H}$

$$[0.67F_R][12] + F_R[24] = 4M_{pc_1} + 8M_{pb_1} + 2M_{pb_2}$$
$$= 4[837] + 8[732] + 2[456]$$
$$32.3F_R = 10116$$
$$F_R = 313^k$$

SHEAR CAPACITY (SHORT DIRECTION)

		# OF FRAMES	
$V_R = 313$	$= 313$	$\times 4 =$	1252^k
$V_3 = 313 + 0.67[313] =$	529	$\times 4 =$	2116^k
V_2			1920^k

ESTIMATE THE ELASTIC STRENGTH OF THE COST EQUIVALENT

ISOLATED DESIGN

COLUMN

W21 x 111 STRONG $S = 249\ in^3$ $M_y = 8856^{k''} \Rightarrow 738^{k'}$

WEAK $S = 49.5\ in^3$ $M_y = 1602^{k''} \Rightarrow 134^{k'}$

$\frac{V}{12}[5,5] = 134^k$ LONG DIRECTION - 2ND FLOOR

$V = 292^k \times 2 = 584^k$

↑ # OF FRAME

$V = \frac{584}{1997 + 2091} = 0.14W$

$V = 0.14W$	LONG DIRECTION SECOND LEVEL.

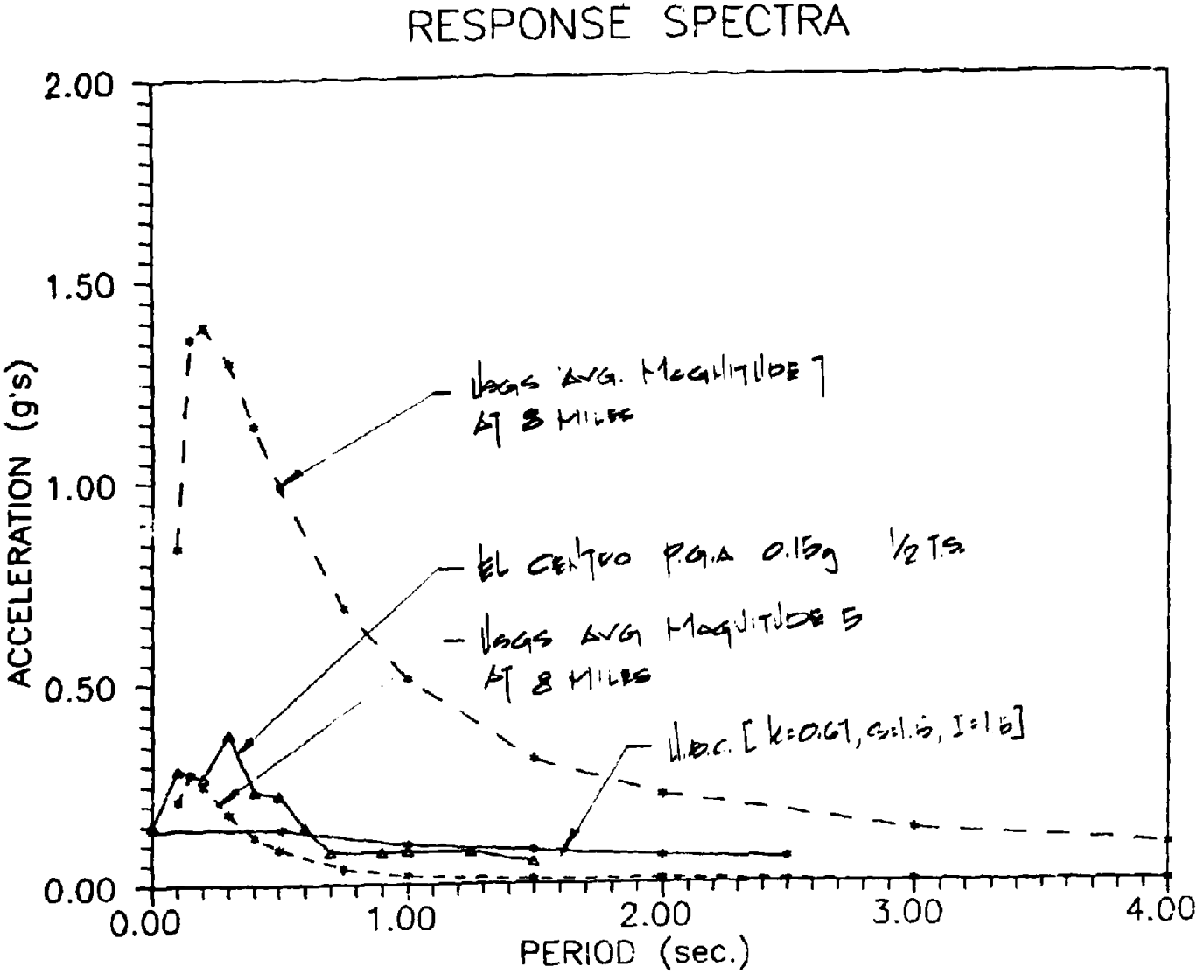
RESPONSE SPECTRA
ACCELERATION (g's)
2.00
1.50
1.00
0.50
0.00
0.00
1.00
2.00
3.00
4.00
PERIOD (sec.)
USGS AVG. MAGNITUDE 7 AT 8 MILES
EL CENTRO P.G.A 0.15g 1/2 T.S.
USGS AVG MAGNITUDE 5 AT 8 MILES
U.B.C. [k=0.67, S=1.5, I=1.5]

RESPONSE OF MAGNITUDE 5 EARTHQUAKE AT 8 MILES

EARTHQUAKE LOADING: EL CENTRO SCALED TO PGA 0.15g AT 1/2 TIME SCALE

COMPARISON OF STORY SHEAR - ISOLATED & NON-ISOLATED

	FULL STRENGTH BUILDING		REDUCED STRENGTH BUILDING ISOLATED	STORY SHEAR REDUCTION RATIO *
	NON-ISOLATED	ISOLATED		
1ST STORY	0.08W	0.08W	0.08W	1.00
2ND STORY	0.09W	0.09W	0.09W	1.00
3RD STORY	0.12W	0.12W	0.10W	1.00

* RATIO OF NON-ISOLATED TO ISOLATED - CYGNIA DESIGN

COMPARISON OF STORY DRIFT - ISOLATED & NON ISOLATED

	FULL STRENGTH BUILDING		REDUCED STRENGTH BUILDING ISOLATED	STORY DRIFT REDUCTION RATIO *
	NON-ISOLATED	ISOLATED		
FPS	—	0	0	
1ST STORY FRAME	0.336 IN.	0.336 IN.	0.306	1.00
2ND STORY FRAME	0.233 IN.	0.233 IN.	0.245	1.00
3RD STORY FRAME	0.202 IN.	0.202 IN.	0.360	1.00

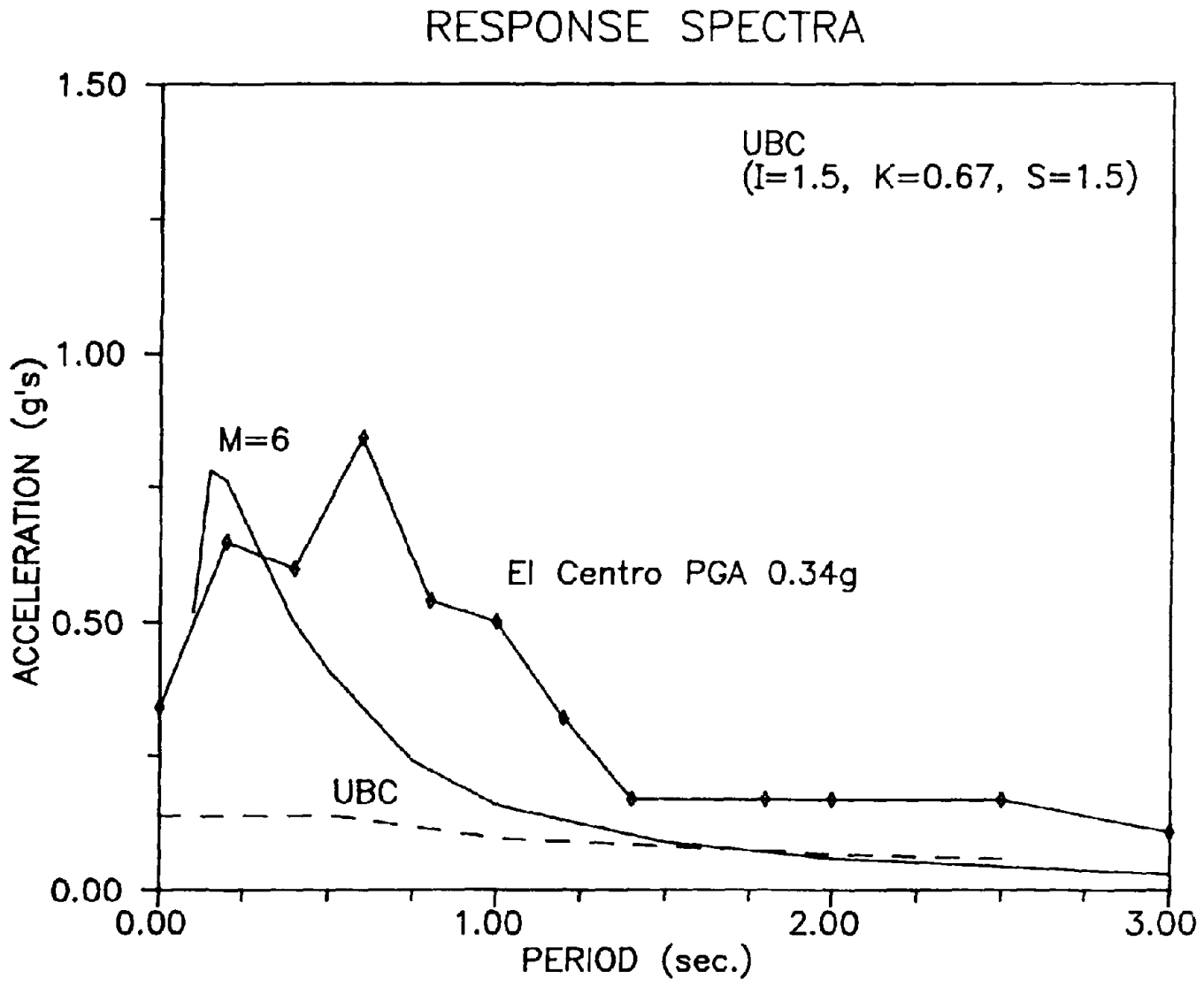
RESPONSE SPECTRA
UBC
(I=1.5, K=0.67, S=1.5)
M=6
El Centro PGA 0.34g
UBC
ACCELERATION (g's)
PERIOD (sec.)
1.50
1.00
0.50
0.00
0.00
1.00
2.00
3.00

RESPONSE OF MAGNITUDE 6 EARTHQUAKE AT 8 MILES

EARTHQUAKE LOADING: EL CENTRO SCALED TO PGA. 0.34g

COMPARISON OF STORY SHEAR - ISOLATED & NON-ISOLATED

	FULL STRENGTH BUILDING		REDUCED STRENGTH BUILDING ISOLATED	STORY SHEAR REDUCTION RATIO *
	NON-ISOLATED	ISOLATED		
1ST STORY	0.54W	0.15W	0.14W	3.6
2ND STORY	0.67W	0.20W	0.22W	3.4
3RD STORY	0.77W	0.32W	0.38W	2.4

* RATIO OF NON-ISOLATED TO ISOLATED
- CYGNIA DESIGN

COMPARISON OF STORY DRIFT - ISOLATED & NON-ISOLATED

	FULL STRENGTH BUILDING		REDUCED STRENGTH BUILDING ISOLATED	STORY DRIFT REDUCTION RATIO *
	NON-ISOLATED	ISOLATED		
FPS	—	1.73 IN.	1.64 IN	
1ST STORY FRAME	2.28 IN	0.62 IN.	0.54 IN	3.6
2ND STORY FRAME	1.77 IN	0.52 IN.	0.60 IN	3.4
3RD STORY FRAME	1.15 IN	0.48 IN.	0.35 IN.	2.4

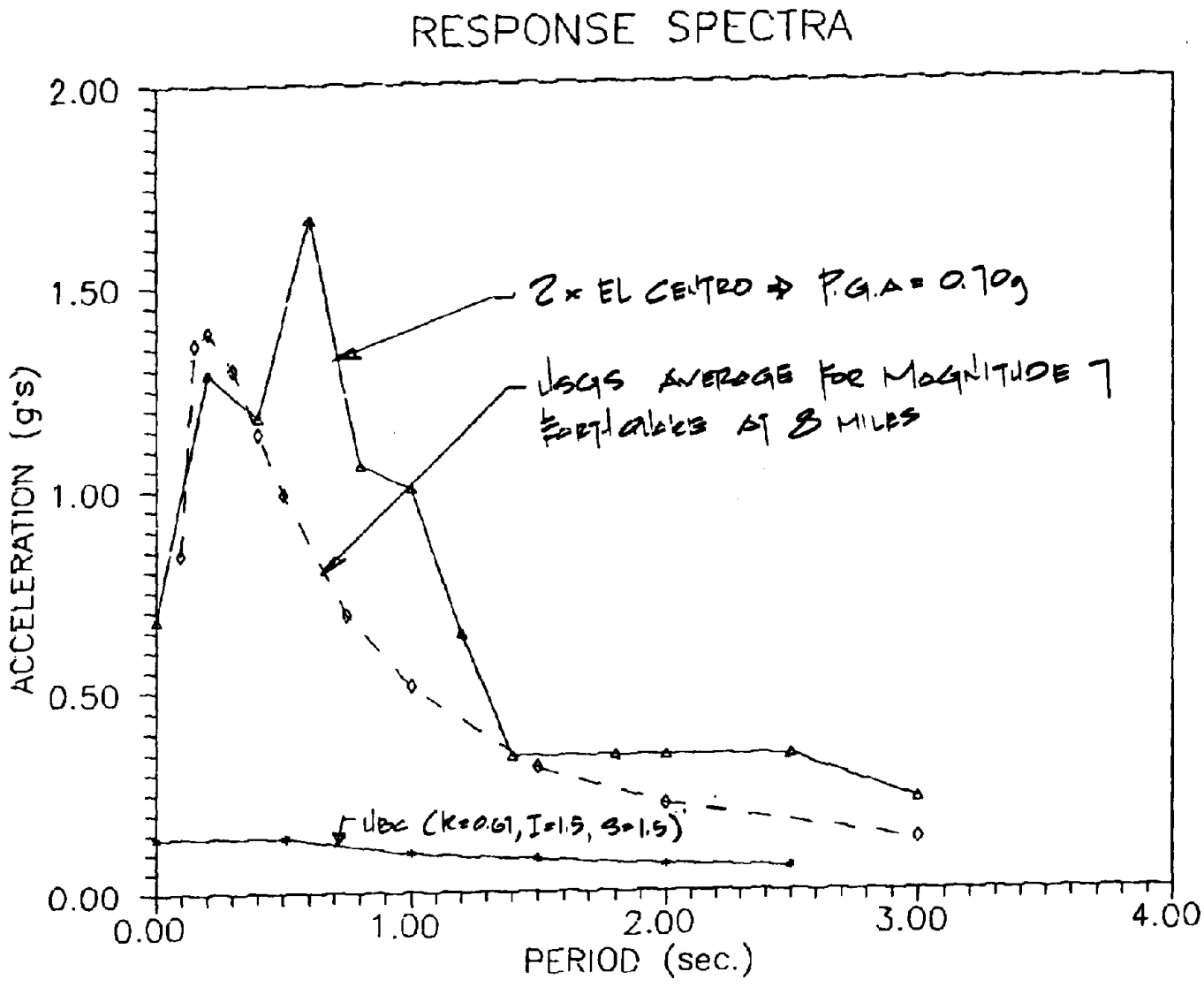
RESPONSE SPECTRA
2.00
1.50
1.00
0.50
0.00
ACCELERATION (g's)
0.00
1.00
2.00
3.00
4.00
PERIOD (sec.)
2 x EL CENTRO → P.G.A = 0.70g
USGS AVERAGE FOR MAGNITUDE 7 EARTHQUAKES AT 8 MILES
UBC (Ck=0.61, I=1.5, S=1.5)

RESPONSE OF MAGNITUDE 7 EARTHQUAKE AT 8 MILES

EARTHQUAKE LOADING: EL CENTRO SCALED TO PGA 0.70g

COMPARISON OF STORY SHEAR - ISOLATED & NON-ISOLATED

	FULL STRENGTH BUILDING		REDUCED STRENGTH BUILDING ISOLATED	STORY SHEAR REDUCTION RATIO *
	NON-ISOLATED	ISOLATED		
1ST STORY	1.11 W	0.20 W	0.21 W	5.6
2ND STORY	1.37 W	0.26 W	0.25 W	5.3
3RD STORY	1.57 W	0.40 W	0.45 W	3.9

* RATIO OF NON-ISOLATED TO ISOLATED - CYCLIC DESIGN.

COMPARISON OF STORY DRIFT - ISOLATED & NON-ISOLATED

	FULL STRENGTH BUILDING		REDUCED STRENGTH BUILDING ISOLATED	STORY DRIFT REDUCTION RATIO *
	NON-ISOLATED	ISOLATED		
FPS	—	4.30 IN.	4.70 IN.	
1ST STORY FRAME	4.64 IN.	0.80 IN	0.74 IN.	5.8
2ND STORY FRAME	3.59 IN	0.67 IN.	0.66 IN.	5.4
3RD STORY FRAME	2.32 IN	0.56 IN.	0.99 IN.	4.1

Section 9: Damage Estimates

CORRELATE MMI (MODIFIED MERCALLI INTENSITY) WITH U.S.G.S. AVERAGE SITE SPECTRA.

$$MMI = \frac{\text{Log}_{10}(14 \cdot PGV)}{\text{Log}_{10} 2}$$

PGV $\left(\frac{cm}{s}\right)$ => WERE OBTAINED FROM THE SCALED EARTHQUAKE.

THE FOLLOWING DAMAGE ESTIMATE IS BASED ON THE ATC-13 "EARTHQUAKE DAMAGE EVALUATION DATA FOR CALIFORNIA" FOR LOW RISE PERIMETER MOMENT FRAME STRUCTURE.

INTENSITY MMI	DAMAGE LEVEL	PERCENTAGE OF BUILDING WITH THIS DAMAGE LEVEL	MAGNITUDE OF EARTHQUAKE AT 8 MILES FROM SITE
XII	45% 20%	54.7% 45.3%	
XI	45% 20%	130% 85.1%	
X	20% 5%	80.6% 19.3%	M=7
IX	20% 5%	12.9% 87.1%	
VIII	5% 0.5%	99.0% 0.4%	M=6
VII	5% 0.5%	72.3% 27.5%	
VI	5% 0.5%	24.3% 62.0%	M=5

ESTIMATE BUILDING DAMAGE BASED ON DRIFT

COMPARISON OF STORY DRIFT

		FULL STRENGTH BUILDING		REDUCED STRENGTH BUILDING ISOLATED
		NON-ISOLATED	ISOLATED	
M=7	1ST STORY	4.64 IN	0.80 IN	0.74 IN
	2ND STORY	3.59 IN	0.67 IN	0.605 IN
	3RD STORY	2.32 IN	0.56 IN	0.99 IN
M=6	1ST STORY	2.28 IN	0.62 IN	0.54 IN
	2ND STORY	1.77 IN	0.52 IN	0.60 IN
	3RD STORY	1.15 IN	0.48 IN	0.85 IN
M=5	1ST STORY	0.336 IN	0.336 IN	0.336 IN
	2ND STORY	0.233 IN	0.233 IN	0.225 IN
	3RD STORY	0.202 IN	0.202 IN	0.360 IN

UBC Allowable Drift: 1ST Story = 0.61" 2ND/3RD Stories 0.52"

BUILDING DAMAGE BASED ON TOTAL DRIFT

FULL STRENGTH ISOLATED CASE:

M=7 $\%\ \text{DAMAGE} = \left[\frac{2.03 - 0.771}{5.70 - 0.771}\right][4.5] + 0.5 = 1.78$

M=6 No Damage: Drift < UBC Allowable

M=5 No Damage: Drift < UBC Allowable

REDUCED STRENGTH ISOLATED CASE:

M=7 $\%\ \text{DAMAGE} = \left[\frac{2.36 - 0.771}{5.70 - 0.771}\right][4.5] + 0.5 = 2.13$

M=6 $\%\ \text{DAMAGE} = \left[\frac{1.99 - 0.771}{5.70 - 0.771}\right][4.5] + 0.5 = 1.73$

M=5 No Damage: Drift < UBC Allowable

ESTIMATE BUILDING DAMAGE BASED ON DRIFT

CONSTRUCTION COST OF BUILDING = $0.5 MILLION

DAMAGE ESTIMATE

	FULL STRENGTH BUILDING		REDUCED STRENGTH BUILDING ISOLATED
	NON-ISOLATED	ISOLATED	
M=7	% DAMAGE = 20 $1,300,000	% DAMAGE = 1.78 $115,700	% DAMAGE = 2.13 $138,450
M=6	% DAMAGE = 5 $325,000	No Damage	% DAMAGE = 1.73 $112,450

EARTHQUAKE ENGINEERING RESEARCH CENTER REPORT SERIES

EERC reports are available from the National Information Service for Earthquake Engineering(NISEE) and from the National Technical Information Service(NTIS). Numbers in parentheses are Accession Numbers assigned by the National Technical Information Service; these are followed by a price code. Contact NTIS, 5285 Port Royal Road, Springfield Virginia, 22161 for more information. Reports without Accession Numbers were not available from NTIS at the time of printing. For a current complete list of EERC reports (from EERC 67-1) and availability information, please contact University of California, EERC, NISEE, 1301 South 46th Street, Richmond, California 94804.

UCB/EERC-80/01 "Earthquake Response of Concrete Gravity Dams Including Hydrodynamic and Foundation Interaction Effects," by Chopra, A.K., Chakrabarti, P. and Gupta, S., January 1980, (AD-A087297)A10.

UCB/EERC-80/02 "Rocking Response of Rigid Blocks to Earthquakes," by Yim, C.S., Chopra, A.K. and Penzien, J., January 1980, (PB80 166 002)A04.

UCB/EERC-80/03 "Optimum Inelastic Design of Seismic-Resistant Reinforced Concrete Frame Structures," by Zagajeski, S.W. and Bertero, V.V., January 1980, (PB80 164 635)A06.

UCB/EERC-80/04 "Effects of Amount and Arrangement of Wall-Panel Reinforcement on Hysteretic Behavior of Reinforced Concrete Walls," by Iliya, R. and Bertero, V.V., February 1980, (PB81 122 525)A09.

UCB/EERC-80/05 "Shaking Table Research on Concrete Dam Models," by Niwa, A. and Clough, R.W., September 1980, (PB81 122 368)A06.

UCB/EERC-80/06 "The Design of Steel Energy-Absorbing Restrainers and their Incorporation into Nuclear Power Plants for Enhanced Safety (Vol 1a): Piping with Energy Absorbing Restrainers: Parameter Study on Small Systems," by Powell, G.H., Oughourlian, C. and Simons, J., June 1980.

UCB/EERC-80/07 "Inelastic Torsional Response of Structures Subjected to Earthquake Ground Motions," by Yamazaki, Y., April 1980, (PB81 122 327)A08.

UCB/EERC-80/08 "Study of X-Braced Steel Frame Structures under Earthquake Simulation," by Ghanaat, Y., April 1980, (PB81 122 335)A11.

UCB/EERC-80/09 "Hybrid Modelling of Soil-Structure Interaction," by Gupta, S., Lin, T.W. and Penzien, J., May 1980, (PB81 122 319)A07.

UCB/EERC-80/10 "General Applicability of a Nonlinear Model of a One Story Steel Frame," by Sveinsson, B.I. and McNiven, H.D., May 1980, (PB81 124 877)A06.

UCB/EERC-80/11 "A Green-Function Method for Wave Interaction with a Submerged Body," by Kioka, W., April 1980, (PB81 122 269)A07.

UCB/EERC-80/12 "Hydrodynamic Pressure and Added Mass for Axisymmetric Bodies," by Nilrat, F., May 1980, (PB81 122 343)A08.

UCB/EERC-80/13 "Treatment of Non-Linear Drag Forces Acting on Offshore Platforms," by Dao, B.V. and Penzien, J., May 1980, (PB81 153 413)A07.

UCB/EERC-80/14 "2D Plane/Axisymmetric Solid Element (Type 3-Elastic or Elastic-Perfectly Plastic)for the ANSR-II Program," by Mondkar, D.P. and Powell, G.H., July 1980, (PB81 122 350)A03.

UCB/EERC-80/15 "A Response Spectrum Method for Random Vibrations," by Der Kiureghian, A., June 1981, (PB81 122 301)A03.

UCB/EERC-80/16 "Cyclic Inelastic Buckling of Tubular Steel Braces," by Zayas, V.A., Popov, E.P. and Mahin, S.A., June 198., (PB81 124 885)A10.

UCB/EERC-80/17 "Dynamic Response of Simple Arch Dams Including Hydrodynamic Interaction," by Porter, C.S. and Chopra, A.K., July 1981, (PB81 124 000)A13.

UCB/EERC-80/18 "Experimental Testing of a Friction Damped Aseismic Base Isolation System with Fail-Safe Characteristics," by Kelly, J.M., Beucke, K.E. and Skinner, M.S., July 1980, (PB81 148 595)A04.

UCB/EERC-80/19 "The Design of Steel Energy-Absorbing Restrainers and their Incorporation into Nuclear Power Plants for Enhanced Safety (Vol.1B): Stochastic Seismic Analyses of Nuclear Power Plant Structures and Piping Systems Subjected to Multiple Supported Excitations," by Lee, M.C. and Penzien, J., June 1980, (PB82 201 872)A08.

UCB/EERC-80/20 "The Design of Steel Energy-Absorbing Restrainers and their Incorporation into Nuclear Power Plants for Enhanced Safety (Vol 1C): Numerical Method for Dynamic Substructure Analysis," by Dickens, J.M. and Wilson, E.L., June 1980.

UCB/EERC-80/21 "The Design of Steel Energy-Absorbing Restrainers and their Incorporation into Nuclear Power Plants for Enhanced Safety (Vol 2): Development and Testing of Restraints for Nuclear Piping Systems," by Kelly, J.M. and Skinner, M.S., June 1980.

UCB/EERC-80/22 "3D Solid Element (Type 4-Elastic or Elastic-Perfectly-Plastic) for the ANSR-II Program," by Mondkar, D.P. and Powell, G.H., July 1980, (PB81 123 242)A03.

UCB/EERC-80/23 "Gap-Friction Element (Type 5) for the Ansr-II Program," by Mondkar, D.P. and Powell, G.H., July 1980, (PB81 122 285)A03.

UCB/EERC-80/24 "U-Bar Restraint Element (Type 11) for the ANSR-II Program," by Oughourlian, C. and Powell, G.H., July 1980, (PB81 122 293)A03.

UCB/EERC-80/25 "Testing of a Natural Rubber Base Isolation System by an Explosively Simulated Earthquake," by Kelly, J.M., August 1980, (PB81 201 360)A04.

UCB/EERC-80/26 "Input Identification from Structural Vibrational Response," by Hu, Y., August 1980, (PB81 152 308)A05.

UCB/EERC-80/27 "Cyclic Inelastic Behavior of Steel Offshore Structures," by Zayas, V.A., Mahin, S.A. and Popov, E.P., August 1980, (PB81 196 180)A15.

UCB/EERC-80/28 "Shaking Table Testing of a Reinforced Concrete Frame with Biaxial Response," by Oliva, M.G., October 1980, (PB81 154 304)A10.

UCB/EERC-80/29 "Dynamic Properties of a Twelve-Story Prefabricated Panel Building," by Bouwkamp, J.G., Kollegger, J.P. and Stephen, R.M., October 1980, (PB82 138 777)A07.

UCB/EERC-80/30 "Dynamic Properties of an Eight-Story Prefabricated Panel Building," by Bouwkamp, J.G., Kollegger, J.P. and Stephen, R.M., October 1980, (PB81 200 313)A05.

UCB/EERC-80/31 "Predictive Dynamic Response of Panel Type Structures under Earthquakes," by Kollegger, J.P. and Bouwkamp, J.G., October 1980, (PB81 152 316)A04.

UCB/EERC-80/32 "The Design of Steel Energy-Absorbing Restrainers and their Incorporation into Nuclear Power Plants for Enhanced Safety (Vol 3): Testing of Commercial Steels in Low-Cycle Torsional Fatigue," by Spanner, P., Parker, E.R., Jongewaard, E. and Dory, M., 1980.

UCB/EERC-80/33 "The Design of Steel Energy-Absorbing Restrainers and their Incorporation into Nuclear Power Plants for Enhanced Safety (Vol 4): Shaking Table Tests of Piping Systems with Energy-Absorbing Restrainers," by Stiemer, S.F. and Godden, W.G., September 1980, (PB82 201 880)A05.

UCB/EERC-80/34 "The Design of Steel Energy-Absorbing Restrainers and their Incorporation into Nuclear Power Plants for Enhanced Safety (Vol 5): Summary Report," by Spencer, P., 1980.

UCB/EERC-80/35 "Experimental Testing of an Energy-Absorbing Base Isolation System," by Kelly, J.M., Skinner, M.S. and Beucke, K.E., October 1980, (PB81 154 072)A04.

UCB/EERC-80/36 "Simulating and Analyzing Artificial Non-Stationary Earth Ground Motions," by Nau, R.F., Oliver, R.M. and Pister, K.S., October 1980, (PB81 153 397)A04.

UCB/EERC-80/37 "Earthquake Engineering at Berkeley - 1980," by , September 1980, (PB81 205 674)A09.

UCB/EERC-80/38 "Inelastic Seismic Analysis of Large Panel Buildings," by Schricker, V. and Powell, G.H., September 1980, (PB81 154 338)A13.

UCB/EERC-80/39 "Dynamic Response of Embankment, Concrete-Gravity and Arch Dams Including Hydrodynamic Interation," by Hall, J.F. and Chopra, A.K., October 1980, (PB81 152 324)A11.

UCB/EERC-80/40 "Inelastic Buckling of Steel Struts under Cyclic Load Reversal," by Black, R.G., Wenger, W.A. and Popov, E.P., October 1980, (PB81 154 312)A08.

UCB/EERC-80/41 "Influence of Site Characteristics on Buildings Damage during the October 3,1974 Lima Earthquake," by Repetto, P., Arango, I. and Seed, H.B., September 1980, (PB81 161 739)A05.

UCB/EERC-80/42 "Evaluation of a Shaking Table Test Program on Response Behavior of a Two Story Reinforced Concrete Frame," by Blondet, J.M., Clough, R.W. and Mahin, S.A., December 1980, (PB82 196 544)A11.

UCB/EERC-80/43 "Modelling of Soil-Structure Interaction by Finite and Infinite Elements," by Medina, F., December 1980, (PB81 229 270)A04.

UCB/EERC-81/01 "Control of Seismic Response of Piping Systems and Other Structures by Base Isolation," by Kelly, J.M., January 1981, (PB81 200 735)A05.

UCB/EERC-81/02 "OPTNSR- An Interactive Software System for Optimal Design of Statically and Dynamically Loaded Structures with Nonlinear Response," by Bhatti, M.A., Ciampi, V. and Pister, K.S., January 1981, (PB81 218 851)A09.

UCB/EERC-81/03 "Analysis of Local Variations in Free Field Seismic Ground Motions," by Chen, J.-C., Lysmer, J. and Seed, H.B., January 1981, (AD-A099508)A13.

UCB/EERC-81/04 "Inelastic Structural Modeling of Braced Offshore Platforms for Seismic Loading," by Zayas, V.A., Shing, P.-S.B., Mahin, S.A. and Popov, E.P., January 1981, (PB82 138 777)A07.

UCB/EERC-81/05 "Dynamic Response of Light Equipment in Structures," by Der Kiureghian, A., Sackman, J.L. and Nour-Omid, B., April 1981, (PB81 218 497)A04.

UCB/EERC-81/06 "Preliminary Experimental Investigation of a Broad Base Liquid Storage Tank," by Bouwkamp, J.G., Kollegger, J.P. and Stephen, R.M., May 1981, (PB82 140 385)A03.

UCB/EERC-81/07 "The Seismic Resistant Design of Reinforced Concrete Coupled Structural Walls," by Aktan, A.E. and Bertero, V.V., June 1981, (PB82 113 358)A11.

UCB/EERC-81/08 "Unassigned," by Unassigned, 1981.

UCB/EERC-81/09 "Experimental Behavior of a Spatial Piping System with Steel Energy Absorbers Subjected to a Simulated Differential Seismic Input," by Stiemer, S.F., Godden, W.G. and Kelly, J.M., July 1981, (PB82 201 898)A04.

UCB/EERC-81/10 "Evaluation of Seismic Design Provisions for Masonry in the United States," by Sveinsson, B.I., Mayes, R.L. and McNiven, H.D., August 1981, (PB82 166 075)A08.

UCB/EERC-81/11 "Two-Dimensional Hybrid Modelling of Soil-Structure Interaction," by Tzong, T.-J., Gupta, S. and Penzien, J., August 1981, (PB82 142 118)A04.

UCB/EERC-81/12 "Studies on Effects of Infills in Seismic Resistant R/C Construction," by Brokken, S. and Bertero, V.V., October 1981, (PB82 166 190)A09.

UCB/EERC-81/13 "Linear Models to Predict the Nonlinear Seismic Behavior of a One-Story Steel Frame," by Valdimarsson, H., Shah, A.H. and McNiven, H.D., September 1981, (PB82 138 793)A07.

UCB/EERC-81/14 "TLUSH: A Computer Program for the Three-Dimensional Dynamic Analysis of Earth Dams," by Kagawa, T., Mejia, L.H., Seed, H.B. and Lysmer, J., September 1981, (PB82 139 940)A06.

UCB/EERC-81/15 "Three Dimensional Dynamic Response Analysis of Earth Dams," by Mejia, L.H. and Seed, H.B., September 1981, (PB82 137 274)A12.

UCB/EERC-81/16 "Experimental Study of Lead and Elastomeric Dampers for Base Isolation Systems," by Kelly, J.M. and Hodder, S.B., October 1981, (PB82 166 182)A05.

UCB/EERC-81/17 "The Influence of Base Isolation on the Seismic Response of Light Secondary Equipment," by Kelly, J.M., April 1981, (PB82 255 266)A04.

UCB/EERC-81/18 "Studies on Evaluation of Shaking Table Response Analysis Procedures," by Blondet, J. M., November 1981, (PB82 197 278)A10.

UCB/EERC-81/19 "DELIGHT.STRUCT: A Computer-Aided Design Environment for Structural Engineering," by Balling, R.J., Pister, K.S. and Polak, E., December 1981, (PB82 218 496)A07.

UCB/EERC-81/20 "Optimal Design of Seismic-Resistant Planar Steel Frames," by Balling, R.J., Ciampi, V. and Pister, K.S., December 1981, (PB82 220 179)A07.

UCB/EERC-82/01 "Dynamic Behavior of Ground for Seismic Analysis of Lifeline Systems," by Sato, T. and Der Kiureghian, A., January 1982, (PB82 218 926)A05.

UCB/EERC-82/02 "Shaking Table Tests of a Tubular Steel Frame Model," by Ghanaat, Y. and Clough, R.W., January 1982, (PB82 220 161)A07.

UCB/EERC-82/03 "Behavior of a Piping System under Seismic Excitation: Experimental Investigations of a Spatial Piping System supported by Mechanical Shock Arrestors," by Schneider, S., Lee, H.-M. and Godden, W. G., May 1982, (PB83 172 544)A09.

UCB/EERC-82/04 "New Approaches for the Dynamic Analysis of Large Structural Systems," by Wilson, E. L., June 1982, (PB83 148 080)A05.

UCB/EERC-82/05 "Model Study of Effects of Damage on the Vibration Properties of Steel Offshore Platforms," by Shahrivar, F. and Bouwkamp, J.G., June 1982, (PB83 148 742)A10.

UCB/EERC-82/06 "States of the Art and Pratice in the Optimum Seismic Design and Analytical Response Prediction of R/C Frame Wall Structures," by Aktan, A.E. and Bertero, V.V., July 1982, (PB83 147 736)A05.

UCB/EERC-82/07 "Further Study of the Earthquake Response of a Broad Cylindrical Liquid-Storage Tank Model," by Manos, G.C. and Clough, R.W., July 1982, (PB83 147 744)A11.

UCB/EERC-82/08 "An Evaluation of the Design and Analytical Seismic Response of a Seven Story Reinforced Concrete Frame," by Charney, F.A. and Bertero, V.V., July 1982, (PB83 157 628)A09.

UCB/EERC-82/09 "Fluid-Structure Interactions: Added Mass Computations for Incompressible Fluid," by Kuo, J.S.-H., August 1982, (PB83 156 281)A07.

UCB/EERC-82/10 "Joint-Opening Nonlinear Mechanism: Interface Smeared Crack Model," by Kuo, J.S.-H., August 1982, (PB83 149 195)A05.

UCB/EERC-82/11 "Dynamic Response Analysis of Techi Dam," by Clough, R.W., Stephen, R.M. and Kuo, J.S.-H., August 1982, (PB83 147 496)A06.

UCB/EERC-82/12 "Prediction of the Seismic Response of R/C Frame-Coupled Wall Structures," by Aktan, A.E., Bertero, V.V. and Piazzo, M., August 1982, (PB83 149 203)A09.

UCB/EERC-82/13 "Preliminary Report on the Smart 1 Strong Motion Array in Taiwan," by Bolt, B.A., Loh, C.H., Penzien, J. and Tsai, Y.B., August 1982, (PB83 159 400)A10.

UCB/EERC-82/14 "Shaking-Table Studies of an Eccentrically X-Braced Steel Structure," by Yang, M.S., September 1982, (PB83 260 778)A12.

UCB/EERC-82/15 "The Performance of Stairways in Earthquakes," by Roha, C., Axley, J.W. and Bertero, V.V., September 1982, (PB83 157 693)A07.

UCB/EERC-82/16 "The Behavior of Submerged Multiple Bodies in Earthquakes," by Liao, W.-G., September 1982, (PB83 158 709)A07.

UCB/EERC-82/17 "Effects of Concrete Types and Loading Conditions on Local Bond-Slip Relationships," by Cowell, A.D., Popov, E.P. and Bertero, V.V., September 1982, (PB83 153 577)A04.

UCB/EERC-82/18 "Mechanical Behavior of Shear Wall Vertical Boundary Members: An Experimental Investigation," by Wagner, M.T. and Bertero, V.V., October 1982, (PB83 159 764)A05.

UCB/EERC-82/19 "Experimental Studies of Multi-support Seismic Loading on Piping Systems," by Kelly, J.M. and Cowell, A.D., November 1982.

UCB/EERC-82/20 "Generalized Plastic Hinge Concepts for 3D Beam-Column Elements," by Chen, P. F.-S. and Powell, G.H., November 1982, (PB83 247 981)A13.

UCB/EERC-82/21 "ANSR-II: General Computer Program for Nonlinear Structural Analysis," by Oughourlian, C.V. and Powell, G.H., November 1982, (PB83 251 330)A12.

UCB/EERC-82/22 "Solution Strategies for Statically Loaded Nonlinear Structures," by Simons, J.W. and Powell, G.H., November 1982, (PB83 197 970)A06.

UCB/EERC-82/23 "Analytical Model of Deformed Bar Anchorages under Generalized Excitations," by Ciampi, V., Eligehausen, R., Bertero, V.V. and Popov, E.P., November 1982, (PB83 169 532)A06.

UCB/EERC-82/24 "A Mathematical Model for the Response of Masonry Walls to Dynamic Excitations," by Sucuoglu, H., Mengi, Y. and McNiven, H.D., November 1982, (PB83 169 011)A07.

UCB/EERC-82/25 "Earthquake Response Considerations of Broad Liquid Storage Tanks," by Cambra, F.J., November 1982, (PB83 251 215)A09.

UCB/EERC-82/26 "Computational Models for Cyclic Plasticity, Rate Dependence and Creep," by Mosaddad, B. and Powell, G.H., November 1982, (PB83 245 829)A08.

UCB/EERC-82/27 "Inelastic Analysis of Piping and Tubular Structures," by Mahasuverachai, M. and Powell, G.H., November 1982, (PB83 249 987)A07.

UCB/EERC-83/01 "The Economic Feasibility of Seismic Rehabilitation of Buildings by Base Isolation," by Kelly, J.M., January 1983, (PB83 197 988)A05.

UCB/EERC-83/02 "Seismic Moment Connections for Moment-Resisting Steel Frames.," by Popov, E.P., January 1983, (PB83 195 412)A04.

UCB/EERC-83/03 "Design of Links and Beam-to-Column Connections for Eccentrically Braced Steel Frames," by Popov, E.P. and Malley, J.O., January 1983, (PB83 194 811)A04.

UCB/EERC-83/04 "Numerical Techniques for the Evaluation of Soil-Structure Interaction Effects in the Time Domain," by Bayo, E. and Wilson, E.L., February 1983, (PB83 245 605)A09.

UCB/EERC-83/05 "A Transducer for Measuring the Internal Forces in the Columns of a Frame-Wall Reinforced Concrete Structure," by Sause, R. and Bertero, V.V., May 1983, (PB84 119 494)A06.

UCB/EERC-83/06 "Dynamic Interactions Between Floating Ice and Offshore Structures," by Croteau, P., May 1983, (PB84 119 486)A16.

UCB/EERC-83/07 "Dynamic Analysis of Multiply Tuned and Arbitrarily Supported Secondary Systems," by Igusa, T. and Der Kiureghian, A., July 1983, (PB84 118 272)A11.

UCB/EERC-83/08 "A Laboratory Study of Submerged Multi-body Systems in Earthquakes," by Ansari, G.R., June 1983, (PB83 261 842)A17.

UCB/EERC-83/09 "Effects of Transient Foundation Uplift on Earthquake Response of Structures" by Yim, C.-S. and Chopra, A.K., June 1983, (PB83 261 396)A07.

UCB/EERC-83/10 "Optimal Design of Friction-Braced Frames under Seismic Loading," by Austin, M.A. and Pister, K.S., June 1983, (PB84 119 288)A06.

UCB/EERC-83/11 "Shaking Table Study of Single-Story Masonry Houses: Dynamic Performance under Three Component Seismic Input and Recommendations," by Manos, G.C., Clough, R.W. and Mayes, R.L., July 1983, (UCB/EERC-83/11)A08.

UCB/EERC-83/12 "Experimental Error Propagation in Pseudodynamic Testing," by Shiing, P.B. and Mahin, S.A., June 1983, (PB84 119 270)A09.

UCB/EERC-83/13 "Experimental and Analytical Predictions of the Mechanical Characteristics of a 1/5-scale Model of a 7-story R/C Frame-Wall Building Structure," by Aktan, A.E., Bertero, V.V., Chowdhury, A.A. and Nagashima, T., June 1983, (PB84 119 213)A07.

UCB/EERC-83/14 "Shaking Table Tests of Large-Panel Precast Concrete Building System Assemblages," by Oliva, M.G. and Clough, R.W., June 1983, (PB86 110 210/AS)A11

UCB/EERC-83/15 "Seismic Behavior of Active Beam Links in Eccentrically Braced Frames," by Hjelmstad, K.D. and Popov, E.P., July 1983, (PB84 119 676)A09.

UCB/EERC-83/16 "System Identification of Structures with Joint Rotation," by Dimsdale, J.S., July 1983, (PB84 192 210)A06.

UCB/EERC-83/17 "Construction of Inelastic Response Spectra for Single-Degree-of-Freedom Systems," by Mahin, S. and Lin, J., June 1983, (PB84 208 834)A05.

UCB/EERC-83/18 "Interactive Computer Analysis Methods for Predicting the Inelastic Cyclic Behaviour of Structural Sections," by Kaba, S. and Mahin, S., July 1983, (PB84 192 012)A06.

UCB/EERC-83/19 "Effects of Bond Deterioration on Hysteretic Behavior of Reinforced Concrete Joints," by Filippou, F.C., Popov, E.P. and Bertero, V.V., August 1983, (PB84 192 020)A10.

UCB/EERC-83/20 "Correlation of Analytical and Experimental Responses of Large-Panel Precast Building Systems," by Oliva, M.G., Clough, R.W., Velkov, M. and Gavrilovic, P., May 1988.

UCB/EERC-83/21 "Mechanical Characteristics of Materials Used in a 1/5 Scale Model of a 7-Story Reinforced Concrete Test Structure," by Bertero, V.V., Aktan, A.E., Harris, H.G. and Chowdhury, A.A., October 1983, (PB84 193 697)A05.

UCB/EERC-83/22 "Hybrid Modelling of Soil Structure Interaction in Layered Media," by Tzong, T.-J. and Penzien, J., October 1983, (PB84 192 178)A08.

UCB/EERC-83/23 "Local Bond Stress-Slip Relationships of Deformed Bars under Generalized Excitations," by Eligehausen, R., Popov, E.P. and Bertero, V.V., October 1983, (PB84 192 848)A09.

UCB/EERC-83/24 "Design Considerations for Shear Links in Eccentrically Braced Frames," by Malley, J.O. and Popov, E.P., November 1983, (PB84 192 186)A07.

UCB/EERC-84/01 "Pseudodynamic Test Method for Seismic Performance Evaluation: Theory and Implementation," by Shing, P.-S.B. and Mahin, S.A., January 1984, (PB84 190 644)A08.

UCB/EERC-84/02 "Dynamic Response Behavior of Kiang Hong Dian Dam," by Clough, R.W., Chang, K.-T., Chen, H.-Q. and Stephen, R.M., April 1984, (PB84 209 402)A08.

UCB/EERC-84/03 "Refined Modelling of Reinforced Concrete Columns for Seismic Analysis," by Kaba, S.A. and Mahin, S.A., April 1984, (PB84 234 384)A06.

UCB/EERC-84/04 "A New Floor Response Spectrum Method for Seismic Analysis of Multiply Supported Secondary Systems," by Asfura, A. and Der Kiureghian, A., June 1984, (PB84 239 417)A06.

UCB/EERC-84/05 "Earthquake Simulation Tests and Associated Studies of a 1/5th-scale Model of a 7-Story R/C Frame-Wall Test Structure," by Bertero, V.V., Aktan, A.E., Charney, F.A. and Sause, R., June 1984, (PB84 239 409)A09.

UCB/EERC-84/06 "R/C Structural Walls: Seismic Design for Shear," by Aktan, A.E. and Bertero, V.V., 1984.

UCB/EERC-84/07 "Behavior of Interior and Exterior Flat-Plate Connections subjected to Inelastic Load Reversals," by Zee, H.L. and Moehle, J.P., August 1984, (PB86 117 629/AS)A07.

UCB/EERC-84/08 "Experimental Study of the Seismic Behavior of a Two-Story Flat-Plate Structure," by Moehle, J.P. and Diebold, J.W., August 1984, (PB86 122 553/AS)A12.

UCB/EERC-84/09 "Phenomenological Modeling of Steel Braces under Cyclic Loading," by Ikeda, K., Mahin, S.A. and Dermitzakis, S.N., May 1984, (PB86 132 198/AS)A08.

UCB/EERC-84/10 "Earthquake Analysis and Response of Concrete Gravity Dams," by Fenves, G. and Chopra, A.K., August 1984, (PB85 193 902/AS)A11.

UCB/EERC-84/11 "EAGD-84: A Computer Program for Earthquake Analysis of Concrete Gravity Dams," by Fenves, G. and Chopra, A.K., August 1984, (PB85 193 613/AS)A05.

UCB/EERC-84/12 "A Refined Physical Theory Model for Predicting the Seismic Behavior of Braced Steel Frames," by Ikeda, K. and Mahin, S.A., July 1984, (PB85 191 450/AS)A09.

UCB/EERC-84/13 "Earthquake Engineering Research at Berkeley - 1984," by , August 1984, (PB85 197 341/AS)A10.

UCB/EERC-84/14 "Moduli and Damping Factors for Dynamic Analyses of Cohesionless Soils," by Seed, H.B., Wong, R.T., Idriss, I.M. and Tokimatsu, K., September 1984, (PB85 191 468/AS)A04.

UCB/EERC-84/15 "The Influence of SPT Procedures in Soil Liquefaction Resistance Evaluations," by Seed, H.B., Tokimatsu, K., Harder, L.F. and Chung, R.M., October 1984, (PB85 191 732/AS)A04.

UCB/EERC-84/16 "Simplified Procedures for the Evaluation of Settlements in Sands Due to Earthquake Shaking," by Tokimatsu, K. and Seed, H.B., October 1984, (PB85 197 887/AS)A03.

UCB/EERC-84/17 "Evaluation of Energy Absorption Characteristics of Bridges under Seismic Conditions," by Imbsen, R.A. and Penzien, J., November 1984.

UCB/EERC-84/18 "Structure-Foundation Interactions under Dynamic Loads," by Liu, W.D. and Penzien, J., November 1984, (PB87 124 889/AS)A11.

UCB/EERC-84/19 "Seismic Modelling of Deep Foundations," by Chen, C.-H. and Penzien, J., November 1984, (PB87 124 798/AS)A07.

UCB/EERC-84/20 "Dynamic Response Behavior of Quan Shui Dam," by Clough, R.W., Chang, K.-T., Chen, H.-Q., Stephen, R.M., Ghanaat, Y. and Qi, J.-H., November 1984, (PB86 115177/AS)A07.

UCB/EERC-85/01 "Simplified Methods of Analysis for Earthquake Resistant Design of Buildings," by Cruz, E.F. and Chopra, A.K., February 1985, (PB86 112299/AS)A12.

UCB/EERC-85/02 "Estimation of Seismic Wave Coherency and Rupture Velocity using the SMART 1 Strong-Motion Array Recordings," by Abrahamson, N.A., March 1985, (PB86 214 343)A07.

UCB/EERC-85/03 "Dynamic Properties of a Thirty Story Condominium Tower Building," by Stephen, R.M., Wilson, E.L. and Stander, N., April 1985, (PB86 118965/AS)A06.

UCB/EERC-85/04 "Development of Substructuring Techniques for On-Line Computer Controlled Seismic Performance Testing," by Dermitzakis, S. and Mahin, S., February 1985, (PB86 132941/AS)A08

UCB/EERC-85/05 "A Simple Model for Reinforcing Bar Anchorages under Cyclic Excitations," by Filippou, F.C., March 1985, (PB86 112 919/AS)A05.

UCB/EERC-85/06 "Racking Behavior of Wood-framed Gypsum Panels under Dynamic Load," by Oliva, M.G., June 1985.

UCB/EERC-85/07 "Earthquake Analysis and Response of Concrete Arch Dams," by Fok, K.-L. and Chopra, A.K., June 1985, (PB86 139672/AS)A10.

UCB/EERC-85/08 "Effect of Inelastic Behavior on the Analysis and Design of Earthquake Resistant Structures," by Lin, J.P. and Mahin, S.A., June 1985, (PB86 135340/AS)A08

UCB/EERC-85/09 "Earthquake Simulator Testing of a Base-Isolated Bridge Deck," by Kelly, J.M., Buckle, I.G. and Tsai, H.-C., January 1986, (PB87 124 152/AS)A06.

UCB/EERC-85/10 "Simplified Analysis for Earthquake Resistant Design of Concrete Gravity Dams," by Fenves, G. and Chopra, A.K., June 1986, (PB87 124 160/AS)A08

UCB/EERC-85/11 "Dynamic Interaction Effects in Arch Dams," by Clough, R.W., Chang, K.-T., Chen, H.-Q. and Ghanaat, Y., October 1985, (PB86 135027/AS)A05.

UCB/EERC-85/12 "Dynamic Response of Long Valley Dam in the Mammoth Lake Earthquake Series of May 25-27, 1980," by Lai, S. and Seed, H.B., November 1985, (PB86 142304/AS)A05

UCB/EERC-85/13 "A Methodology for Computer-Aided Design of Earthquake-Resistant Steel Structures," by Austin, M.A., Pister, K.S. and Mahin, S.A., December 1985, (PB86 159480/AS)A10.

UCB/EERC-85/14 "Response of Tension-Leg Platforms to Vertical Seismic Excitations," by Liou, G.-S., Penzien, J. and Yeung, R.W., December 1985, (PB87 124 871/AS)A08

UCB/EERC-85/15 "Cyclic Loading Tests of Masonry Single Piers: Volume 4 - Additional Tests with Height to Width Ratio of 1," by Sveinsson, B., McNiven, H.D. and Sucuoglu, H., December 1985.

UCB/EERC-85/16 "An Experimental Program for Studying the Dynamic Response of a Steel Frame with a Variety of Infill Partitions," by Yanev, B. and McNiven, H.D., December 1985.

UCB/EERC-86/01 "A Study of Seismically Resistant Eccentrically Braced Steel Frame Systems," by Kasai, K. and Popov, E.P., January 1986, (PB87 124 178/AS)A14.

UCB/EERC-86/02 "Design Problems in Soil Liquefaction," by Seed, H.B., February 1986, (PB87 124 186/AS)A03.

UCB/EERC-86/03 "Implications of Recent Earthquakes and Research on Earthquake-Resistant Design and Construction of Buildings," by Bertero, V.V., March 1986, (PB87 124 194/AS)A05.

UCB/EERC-86/04 "The Use of Load Dependent Vectors for Dynamic and Earthquake Analyses," by Leger, P., Wilson, E.L. and Clough, R.W., March 1986, (PB87 124 202/AS)A12.

UCB/EERC-86/05 "Two Beam-To-Column Web Connections," by Tsai, K.-C. and Popov, E.P., April 1986, (PB87 124 301/AS)A04.

UCB/EERC-86/06 "Determination of Penetration Resistance for Coarse-Grained Soils using the Becker Hammer Drill," by Harder, L.F. and Seed, H.B., May 1986, (PB87 124 210/AS)A07.

UCB/EERC-86/07 "A Mathematical Model for Predicting the Nonlinear Response of Unreinforced Masonry Walls to In-Plane Earthquake Excitations," by Mengi, Y. and McNiven, H.D., May 1986, (PB87 124 780/AS)A06.

UCB/EERC-86/08 "The 19 September 1985 Mexico Earthquake: Building Behavior," by Bertero, V.V., July 1986.

UCB/EERC-86/09 "EACD-3D: A Computer Program for Three Dimensional Earthquake Analysis of Concrete Dams," by Fok, K.-L., Hall, J.F. and Chopra, A.K., July 1986, (PB87 124 228/AS)A08.

UCB/EERC-86/10 "Earthquake Simulation Tests and Associated Studies of a 0.3-Scale Model of a Six-Story Concentrically Braced Steel Structure," by Uang, C.-M. and Bertero, V.V., December 1986, (PB87 163 564/AS)A17.

UCB/EERC-86/11 "Mechanical Characteristics of Base Isolation Bearings for a Bridge Deck Model Test," by Kelly, J.M., Buckle, I.G. and Koh, C.-G., November 1987.

UCB/EERC-86/12 "Effects of Axial Load on Elastomeric Isolation Bearings," by Koh, C.-G. and Kelly, J.M., November 1987.

UCB/EERC-87/01 "The FPS Earthquake Resisting System: Experimental Report," by Zayas, V.A., Low, S.S. and Mahin, S.A., June 1987.

UCB/EERC-87/02 "Earthquake Simulator Tests and Associated Studies of a 0.3-Scale Model of a Six-Story Eccentrically Braced Steel Structure," by Whittaker, A., Uang, C.-M. and Bertero, V.V., July 1987.

UCB/EERC-87/03 "A Displacement Control and Uplift Restraint Device for Base-Isolated Structures," by Kelly, J.M., Griffith, M.C. and Aiken, I.D., April 1987.

UCB/EERC-87/04 "Earthquake Simulator Testing of a Combined Sliding Bearing and Rubber Bearing Isolation System," by Kelly, J.M. and Chalhoub, M.S., 1987.

UCB/EERC-87/05 "Three-Dimensional Inelastic Analysis of Reinforced Concrete Frame-Wall Structures," by Moazzami, S. and Bertero, V.V., May 1987.

UCB/EERC-87/06 "Experiments on Eccentrically Braced Frames with Composite Floors," by Ricles, J. and Popov, E., June 1987.

UCB/EERC-87/07 "Dynamic Analysis of Seismically Resistant Eccentrically Braced Frames," by Ricles, J. and Popov, E., June 1987.

UCB/EERC-87/08 "Undrained Cyclic Triaxial Testing of Gravels-The Effect of Membrane Compliance," by Evans, M.D. and Seed, H.B., July 1987.

UCB/EERC-87/09 "Hybrid Solution Techniques for Generalized Pseudo-Dynamic Testing," by Thewalt, C. and Mahin, S.A., July 1987.

UCB/EERC-87/10 "Ultimate Behavior of Butt Welded Splices in Heavy Rolled Steel Sections," by Bruneau, M., Mahin, S.A. and Popov, E.P., July 1987.

UCB/EERC-87/11 "Residual Strength of Sand from Dam Failures in the Chilean Earthquake of March 3, 1985," by De Alba, P., Seed, H.B., Retamal, E. and Seed, R.B., September 1987.

UCB/EERC-87/12 "Inelastic Seismic Response of Structures with Mass or Stiffness Eccentricities in Plan," by Bruneau, M. and Mahin, S.A., September 1987.

UCB/EERC-87/13 "CSTRUCT: An Interactive Computer Environment for the Design and Analysis of Earthquake Resistant Steel Structures," by Austin, M.A., Mahin, S.A. and Pister, K.S., September 1987.

UCB/EERC-87/14 "Experimental Study of Reinforced Concrete Columns Subjected to Multi-Axial Loading," by Low, S.S. and Moehle, J.P., September 1987.

UCB/EERC-87/15 "Relationships between Soil Conditions and Earthquake Ground Motions in Mexico City in the Earthquake of Sept. 19, 1985," by Seed, H.B., Romo, M.P., Sun, J., Jaime, A. and Lysmer, J., October 1987.

UCB/EERC-87/16 "Experimental Study of Seismic Response of R. C. Setback Buildings," by Shahrooz, B.M. and Moehle, J.P., October 1987.

UCB/EERC-87/17 "The Effect of Slabs on the Flexural Behavior of Beams," by Pantazopoulou, S.J. and Moehle, J.P., October 1987.

UCB/EERC-87/18 "Design Procedure for R-FBI Bearings," by Mostaghel, N. and Kelly, J.M., November 1987.

UCB/EERC-87/19 "Analytical Models for Predicting the Lateral Response of R C Shear Walls: Evaluation of their Reliability," by Vulcano, A. and Bertero, V.V., November 1987.

UCB/EERC-87/20 "Earthquake Response of Torsionally-Coupled Buildings," by Hejal, R. and Chopra, A.K., December 1987.

UCB/EERC-87/21 "Dynamic Reservoir Interaction with Monticello Dam," by Clough, R.W., Ghanaat, Y. and Qiu, X-F., December 1987.

UCB/EERC-87/22 "Strength Evaluation of Coarse-Grained Soils," by Siddiqi, F.H., Seed, R.B., Chan, C.K., Seed, H.B. and Pyke, R.M., December 1987.

UCB/EERC-88/01 "Seismic Behavior of Concentrically Braced Steel Frames," by Khatib, I., Mahin, S.A. and Pister, K.S., January 1988.

UCB/EERC-88/02 "Experimental Evaluation of Seismic Isolation of Medium-Rise Structures Subject to Uplift," by Griffith, M.C., Kelly, J.M., Coveney, V.A. and Koh, C.G., January 1988.

UCB/EERC-88/03 "Cyclic Behavior of Steel Double Angle Connections," by Astaneh-Asl, A. and Nader, H.N., January 1988.

UCB/EERC-88/04 "Re-evaluation of the Slide in the Lower San Fernando Dam in the Earthquake of Feb. 9, 1971," by Seed, H.B., Seed, R.B., Harder, L.F. and Jong, H.-L., April 1988.

UCB/EERC-88/05 "Experimental Evaluation of Seismic Isolation of a Nine-Story Braced Steel Frame Subject to Uplift," by Griffith, M.C., Kelly, J.M. and Aiken, I.D., May 1988.

UCB/EERC-88/06 "DRAIN-2DX User Guide.," by Allahabadi, R. and Powell, G.H., March 1988.

UCB/EERC-88/07 "Cylindrical Fluid Containers in Base-Isolated Structures," by Chalhoub, M.S. and Kelly, J.M., April 1988.

UCB/EERC-88/08 "Analysis of Near-Source Waves: Separation of Wave Types using Strong Motion Array Recordings," by Darragh, R.B., June 1988.

UCB/EERC-88/09 "Alternatives to Standard Mode Superposition for Analysis of Non-Classically Damped Systems," by Kusainov, A.A. and Clough, R.W., June 1988.

UCB/EERC-88/10 "The Landslide at the Port of Nice on October 16, 1979," by Seed, H.B., Seed, R.B., Schlosser, F., Blondeau, F. and Juran, I., June 1988.

UCB/EERC-88/11 "Liquefaction Potential of Sand Deposits Under Low Levels of Excitation," by Carter, D.P. and Seed, H.B., August 1988.

UCB/EERC-88/12 "Nonlinear Analysis of Reinforced Concrete Frames Under Cyclic Load Reversals," by Filippou, F.C. and Issa, A., September 1988.

UCB/EERC-88/13 "Implications of Recorded Earthquake Ground Motions on Seismic Design of Building Structures," by Uang, C.-M. and Bertero, V.V., September 1988.

UCB/EERC-88/14 "An Experimental Study of the Behavior of Dual Steel Systems," by Whittaker, A.S., Uang, C.-M. and Bertero, V.V., September 1988.

UCB/EERC-88/15 "Dynamic Moduli and Damping Ratios for Cohesive Soils," by Sun, J.I., Golesorkhi, R. and Seed, H.B., August 1988.

UCB/EERC-88/16 "Reinforced Concrete Flat Plates Under Lateral Load: An Experimental Study Including Biaxial Effects," by Pan, A. and Moehle, J., November 1988.

UCB/EERC-88/17 "Earthquake Engineering Research at Berkeley - 1988," by EERC, November 1988.

UCB/EERC-88/18 "Use of Energy as a Design Criterion in Earthquake-Resistant Design," by Uang, C.-M. and Bertero, V.V., November 1988.

UCB/EERC-88/19 "Steel Beam-Column Joints in Seismic Moment Resisting Frames," by Tsai, K.-C. and Popov, E.P., September 1988.

UCB/EERC-88/20 "Base Isolation in Japan, 1988," by Kelly, J.M., December 1988.

UCB/EERC-89/01 "Behavior of Long Links in Eccentrically Braced Frames," by Engelhardt, M.D. and Popov, E.P., January 1989.

UCB/EERC-89/02 "Earthquake Simulator Testing of Steel Plate Added Damping and Stiffness Elements," by Whittaker, A., Bertero, V.V., Alonso, J. and Thompson, C., January 1989.

UCB/EERC-89/03 "Implications of Site Effects in the Mexico City Earthquake of Sept. 19, 1985 for Earthquake-Resistant Design Criteria in the San Francisco Bay Area of California," by Seed, H.B. and Sun, J.I., March 1989.

UCB/EERC-89/04 "Earthquake Analysis and Response of Intake-Outlet Towers," by Goyal, A. and Chopra, A.K., July 1989.

UCB/EERC-89/05 "The 1985 Chile Earthquake: An Evaluation of Structural Requirements for Bearing Wall Buildings," by Wallace, J.W. and Moehle, J.P., July 1989.

UCB/EERC-89/06 "Effects of Spatial Variation of Ground Motions on Large Multiply-Supported Structures," by Hao, H., July 1989.

UCB/EERC-89/07 "EADAP - Enhanced Arch Dam Analysis Program: Users's Manual," by Ghanaat, Y. and Clough, R.W., August 1989.

UCB/EERC-89/08 "Seismic Performance of Steel Moment Frames Plastically Designed by Least Squares Stress Fields," by Ohi, K. and Mahin, S.A., August 1989.

UCB/EERC-89/09 "Feasibility and Performance Studies on Improving the Earthquake Resistance of New and Existing Buildings Using the Friction Pendulum System," by Zayas, V., Low, S., Bozzo, L. and Mahin, S.A., September 1989.